WOODHEAD PUBLISHING SERIES IN COMPOSITES SCIENCE AND ENGINEERING

Fiber Technology for Fiber-Reinforced Composites

Edited by M. Özgür Seydibeyoğlu,
Amar K. Mohanty and Manjusri Misra

WP
WOODHEAD PUBLISHING

Fiber Technology for Fiber-Reinforced Composites

Related titles

Handbook of Natural Fibre Composites: Properties, Processes, Failure and Applications
(ISBN 978-0-85709-524-4)

Handbook of Natural Fibres Vol 2
(ISBN 978-1-84569-698-6)

Thermoplastics and Thermoplastic Composites
(ISBN 978-1-4557-7898-0)

Woodhead Publishing Series in Composites Science and Engineering

Fiber Technology for Fiber-Reinforced Composites

Edited by

M. Özgür Seydibeyoğlu

Amar K. Mohanty

Manjusri Misra

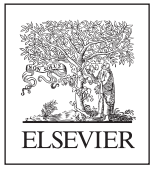

WP
WOODHEAD PUBLISHING
An imprint of Elsevier

Woodhead Publishing is an imprint of Elsevier
The Officers' Mess Business Centre, Royston Road, Duxford, CB22 4QH, United Kingdom
50 Hampshire Street, 5th Floor, Cambridge, MA 02139, United States
The Boulevard, Langford Lane, Kidlington, OX5 1GB, United Kingdom

Notices
Knowledge and best practice in this field are constantly changing. As new research and experience broaden our understanding, changes in research methods, professional practices, or medical treatment may become necessary.

Practitioners and researchers must always rely on their own experience and knowledge in evaluating and using any information, methods, compounds, or experiments described herein. In using such information or methods they should be mindful of their own safety and the safety of others, including parties for whom they have a professional responsibility.

To the fullest extent of the law, neither the Publisher nor the authors, contributors, or editors, assume any liability for any injury and/or damage to persons or property as a matter of products liability, negligence or otherwise, or from any use or operation of any methods, products, instructions, or ideas contained in the material herein.

Library of Congress Cataloging-in-Publication Data
A catalog record for this book is available from the Library of Congress

British Library Cataloguing-in-Publication Data
A catalogue record for this book is available from the British Library

ISBN: 978-0-08-101871-2 (print)
ISBN: 978-0-08-100993-2 (online)

Publisher: Matthew Deans
Acquisition Editor: Gwen Jones
Editorial Project Manager: Charlotte Cockle
Senior Production Project Manager: Priya Kumaraguruparan
Cover Designer: Vicky Pearson Esser

Typeset by SPi Global, India

Contents

List of contributors **ix**

1 Introduction **1**
M. Özgür Seydibeyoğlu, Amar K. Mohanty, Manjusri Misra

2 Mechanics of fiber composites **5**
Levent Aydin, Hatice Seçil Artem, Erkan Oterkus, Omer Gundogdu, Hamit Akbulut
2.1 Introduction **5**
2.2 Mechanics of continuous fiber-reinforced composites **5**
2.3 Mechanics of short fiber-reinforced composites **11**
2.4 Mechanics of woven fabric composites **22**
2.5 Interface mechanics in fiber-reinforced composites **26**
2.6 Mechanics of curved composites **27**
2.7 Strength failure theories **33**
2.8 Dynamic behavior of composites **40**
References **48**

3 Fiber reinforced composites **51**
Seçkin Erden, Kingsley Ho
3.1 Introduction **51**
3.2 Materials (reinforcements, matrices, fiber/matrix adhesion) **56**
3.3 Manufacturing **61**
3.4 Characterization and testing **72**
3.5 Fiber surface treatments **74**
3.6 Conclusion **75**
Acknowledgments **76**
References **76**
Further Reading **78**

4 Surface modification of fibers and sizing operations **81**
Esen Ozdogan, Tulay Gulumser, Asli Demir
4.1 Introduction and historical perspective **81**
4.2 Physical methods **82**
4.3 Chemical treatments **87**
4.4 Biochemical treatments **92**

4.5 Sizing **93**
4.6 Conclusion **94**
References **94**

5 Glass fibers **99**
Aref Cevahir
5.1 History of glass fiber **99**
5.2 Glass fiber manufacturing **99**
5.3 Types of glass fibers **103**
5.4 Glass fiber products **107**
5.5 Glass fiber sizing **109**
5.6 Composite interphase **116**
5.7 Conclusion **119**
References **120**

6 Carbon fibers **123**
Kazim Acatay
6.1 Introduction **123**
6.2 Different precursors for CF production **125**
6.3 Carbonization processes **133**
6.4 Recent developments and trends in CF technology **140**
6.5 CF in polymer-matrix composites **141**
6.6 Uses of CF in other matrices **148**
6.7 Conclusion **150**
References **150**

7 Aramid fibers **153**
Mustafa Ertekin
7.1 Introduction **153**
7.2 Fiber production **153**
7.3 Aramid fiber structure and properties **155**
7.4 Fiber and product forms **158**
7.5 Applications **158**
7.6 Conclusion **164**
7.7 Sources of further information **165**
References **166**

8 Basalt fibers **169**
Volkan Acar, Ferit Cakir, Elif Alyamaç, M. Özgür Seydibeyoğlu
8.1 Introduction to basalt fibers **169**
8.2 Preparation of basalt fibers **170**
8.3 Structural properties **171**
8.4 Basalt fiber-reinforced composites **173**
8.5 Surface treatments of basalt fibers **175**

8.6 Applications of basalt fiber **177**
8.7 Conclusion **181**
References **182**

9 Ceramic fibers **187**
Emre Yalamaç, Mucahit Sutcu, Suat Bahar Basturk
9.1 Introduction **187**
9.2 Oxide fibers **187**
9.3 Nonoxide fibers **192**
9.4 Production techniques of ceramic fibers **197**
9.5 Application of ceramic fibers **203**
References **204**

10 Natural fibers **209**
Ahmet Çağrı Kılınç, Cenk Durmuşkahya, M. Özgür Seydibeyoğlu
10.1 Introduction to natural fibers **209**
10.2 Plant fibers **212**
10.3 Conclusion and future outlook **229**
References **232**

11 The use of biotechnology for green composites **237**
Metehan Atagür, M. Özgür Seydibeyoğlu
11.1 Introduction to green composites **237**
11.2 Natural polymer sources **240**
11.3 Applications **244**
11.4 Conclusion and future outlook **245**
References **246**

12 Nanofibers for fiber-reinforced composites **251**
Nesrin Horzum, Nehir Arik, Yen Bach Truong
12.1 Introduction and historical perspective **251**
12.2 Electrospinning **252**
12.3 Carbon nanotubes/nanofibers **260**
12.4 Cellulose nanofibers **262**
12.5 Applications **264**
References **265**
Further Reading **274**

13 The use of nanotechnology for fibre-reinforced polymer composites **277**
Sibel Demiroglu, Vivekanandhan Singaravelu, M. Özgür Seydibeyoğlu, Manjusri Misra, Amar K. Mohanty
13.1 Introduction **277**
13.2 Nanotechnologies for matrix modification **279**
13.3 Nanotechnologies for fibre modification **283**

13.4 Future perspectives **291**
13.5 Conclusions **293**
Acknowledgments **293**
References **293**

14 Design and optimization of fiber composites **299**
Levent Aydin, Hatice Seçil Artem
14.1 Introduction **299**
14.2 Structural design **300**
14.3 Material selection **300**
14.4 Optimization **302**
References **312**
Further Reading **314**

15 Concluding remarks and future outlook **317**
M. Özgür Seydibeyoğlu, Amar K. Mohanty, Manjusri Misra

Index **319**

List of contributors

Volkan Acar Ataturk University, Erzurum, Turkey

Kazim Acatay Akdeniz Kimya San. ve Tic. A.S., Kemalpasa, Izmir, Turkey

Hamit Akbulut Ataturk University, Erzurum, Turkey

Elif Alyamaç Izmir Katip Çelebi University, Izmir, Turkey

Nehir Arik Izmir Katip Çelebi University, Izmir, Turkey

Hatice Seçil Artem Izmir Institute of Technology, Izmir, Turkey

Metehan Atagür Izmir Katip Çelebi University, Izmir, Turkey

Levent Aydin Izmir Katip Çelebi University, Izmir, Turkey

Suat Bahar Basturk Manisa Celal Bayar University, Manisa, Turkey

Ferit Cakir University of California, Berkeley, CA, United States

Aref Cevahir Sisecam Science and Technology Center, Kocaeli, Turkey

Asli Demir Ege University, Izmir, Turkey

Sibel Demiroglu Izmir Katip Çelebi University, Izmir, Turkey

Cenk Durmuşkahya Izmir Katip Çelebi University, Izmir, Turkey

Seçkin Erden Ege University, Izmir, Turkey

Mustafa Ertekin Ege University, Izmir, Turkey

Tulay Gulumser Ege University, Izmir, Turkey

Omer Gundogdu Ataturk University, Erzurum, Turkey

Kingsley Ho Cytec Engineered Materials, United Kingdom

Nesrin Horzum Izmir Katip Çelebi University, Izmir, Turkey

Ahmet Çağrı Kılınç Dokuz Eylul University, Izmir, Turkey

Manjusri Misra University of Guelph, Guelph, ON, Canada

Amar K. Mohanty University of Guelph, Guelph, ON, Canada

Erkan Oterkus University of Strathclyde, Glasgow, United Kingdom

Esen Ozdogan Ege University, Izmir, Turkey

M. Özgür Seydibeyoğlu Izmir Katip Çelebi University, Izmir, Turkey

Vivekanandhan Singaravelu VHNSN College, Virudhunagar, India

Mucahit Sutcu Izmir Katip Çelebi University, Izmir, Turkey

Yen Bach Truong Commonwealth Scientific and Industrial Research Organization (CSIRO), Clayton, VIC, Australia

Emre Yalamaç Manisa Celal Bayar University, Manisa, Turkey

Introduction

1

M. Özgür Seydibeyoğlu[*], *Amar K. Mohanty*[†], *Manjusri Misra*[†]
*Izmir Katip Çelebi University, Izmir, Turkey, †University of Guelph, Guelph, ON, Canada

The materials science and materials world are having a new paradigm, and many materials are now transforming to composite materials, replacing many metallic materials and ceramic materials. Metallic materials with well-known properties and well-known manufacturing techniques at an affordable price are still the first preference for the materials selection; however, in many applications, due to weight problems, corrosion, and fatigue issues, composites are becoming more and more important. The corrosion costs consume 3%–3.5% of the whole-world gross domestic product and contribute to many failures in the structural components [1]. Moreover, processing conditions for the composites and polymers are much more energy-efficient and more labor friendly compared to metallic materials. Ceramic materials with high-temperature performance and good strength are of great importance, but still, they lack the elasticity for many industrial applications.

In the materials' area, the composites especially fiber-reinforced composites are becoming more desired specifically in the transportation industry where fuel consumption is of great importance, and reduced CO_2 is another big issue. Composites are very critical for many automotive industries, aerospace, and marine applications. Carbon footprint and sustainability are the key factors in today's world, and composites are the key materials for these problems. Especially in the last decade, the composite aerostructures have grown more than 100% with compounded annual growth rate (CAGR) of 11.1% [2].

As the world's energy need is increasing, the composites are also very significant in the area of renewable energy sources like wind-turbine blades. Energy-storage tanks that can store natural gas, hydrogen, and many other critical gasses are of great importance for the composites. Restoring present pipelines with carbon composites has been also very critical for the gas-piping industry. A report in 2015 prepared by Global Wind Energy Council demonstrated the exponential growth of wind turbines [3]. It was reported that between the years of 2000 and 2015, there was 25-fold increase in the installed wind-turbine capacity [3].

Composites have been used in the construction industry since the foundation of steel reinforced concrete, but for certain areas, polymer composites with high flexibility of forming offer numerous advantages, especially in the area of reinforcing current buildings under the risk of earthquake attack.

Sporting goods such as golf, sailing boats, fishing roads, and new technology bikes are highly interesting engineering applications with very important new technological breakthroughs like the use of graphene in the bicycle frame being a superlight bicycle, which is very vital.

Fiber Technology for Fiber-Reinforced Composites. http://dx.doi.org/10.1016/B978-0-08-101871-2.00001-1

Another important application is the defense industry where the composites play key role in the battlefield due to weight saving and better ballistic performing materials. Aerospace structures in the military applications with engineered properties and nano-enhanced structures are very critical for the current defense industry. For military application, weight reduction, and structural features are not the only criteria; radio interference and radar absorption properties are also very critical.

As listed above, there are thousands of application areas for composites, but transportation, energy, and defense are top priority areas for the composites. This key technology triggers many companies' interests, and they invest significant funding for the composite-materials research. Recent technological improvements in the nanotechnology and biotechnology have strategic influence in the composite materials.

Another issue for many engineering applications is the cost of the raw materials, cost of the production line, and the final price of the products. There are many new approaches to lower the price of the carbon fiber, whereas new reinforcing fibers from natural resources are offering many new low-cost solutions, thereby providing socioeconomic wealth opportunities for the developing countries where they can have good materials.

As described, composite materials have utmost importance for the whole humanity and engineering field that can influence the whole community. Composite materials have been manufactured since very early times such as BC 3000 with natural fiber stone composites for housing in the time of Sumerians in Middle East. However, since the 1950s, with the discovery of glass fiber and other fibers, polymer-matrix composites and especially fiber-reinforced polymer composites have been of great importance. Various disciplines including chemistry, chemical engineering, materials science and engineering, textile engineering, and mechanical engineering have been predominantly working in the fiber-reinforced polymer composites to manufacture better materials for the humanity.

There have been numerous books on the composite materials, composite mechanics, composite interface, biocomposites, and nanocomposites. However, there is no single book on the fiber technology that is devoted to the composite materials. There are a significant number of textile books on man-made fibers that are used primarily in the area of textiles. For the composite-material world, this book will be the handbook for the fiber technology. The book covers many important reinforcing fibers such as glass, carbon, aramid, basalt, ceramic, and natural nanofibers. This book will be very helpful for the undergraduate and graduate students. The most important users will be the composite industry where fibers are used extensively with very limited fiber property information.

One of the most important aspects of this book is that some of the authors are from the industry especially glass fiber and carbon fiber chapters that are written by the industry experts with PhD degrees and whom they have really worked in the glass- and carbon-fiber manufacturing plants. Many books and scientific articles are written without industry information, lacking real-case applications, and moreover lacking trade secrets of the processes. Still, not all process details could be shared, but at least, a good overview of the production techniques for these fibers has been written in depth by these two industry experts with scientific background.

The book is enriched with faculty members from mechanical engineering department to exploit the mechanics of composites and to understand design criteria for the composite materials. One chapter is devoted to understand the surface properties of fibers and their influence on the composite properties. This part is written by faculty members from textile engineering department with textile chemicals and surface-coating expertise.

Moreover, new trends in the composite materials with biotechnology and natural fibers have been explained in detail. There are two chapters on biotechnology. One chapter is a kind of traditional review article on natural fiber composites, whereas the second chapter deals with the influences of the biotechnology on natural fiber composites such as the use of bioresins and biolubricants enhanced with life-cycle analysis.

As the technology is developing, nanotechnology is also very critical for the composites like in any engineering field, and two chapters are devoted to nanotechnology. One chapter is written by nanofiber experts, demonstrating the importance of nanofibers in the area of composites. The second chapter deals with new developments in the nanotechnology for the composites such as graphene, carbon nanotubes, and nanofibers on the interfacial properties. Furthermore, dendritic polymers and hyperbranched nanopolymers have influence the performance and processing of the resins on the composite structures.

With all these important developments in the composite area, this book will be very helpful for an engineer dealing with many important industrial applications. This book will also be very helpful for the scientists working in the area of material science and mechanical design to better understand fiber-polymer interaction and understand significant outcomes of this important area.

Last but not the least, this book will be very helpful for the students (graduate/undergraduate) in the universities that are studying textile engineering, mechanical engineering, material engineering, chemical engineering, chemistry, biotechnology, and nanotechnology.

References

[1] Schmidt G. World corrosion organization. World Corrosion Organization; 2009.
[2] Composites Forecasts and Consulting LLC; January 2014 Report.
[3] http://www.gwec.net/wp-content/uploads/2012/06/Global-Cumulative-Installed-Wind-Capacity-2000-2015.jpg.

This page intentionally left blank

Mechanics of fiber composites

2

Levent Aydin[*], *Hatice Seçil Artem*[†], *Erkan Oterkus*[‡], *Omer Gundogdu*[§], *Hamit Akbulut*[§]
[*]Izmir Katip Çelebi University, Izmir, Turkey, [†]Izmir Institute of Technology, Izmir, Turkey, [‡]University of Strathclyde, Glasgow, United Kingdom, [§]Ataturk University, Erzurum, Turkey

2.1 Introduction

The objective of this chapter is to emphasize the context in which the mechanics of fiber composites is examined. Constitutive equations describing the stress-strain relations, micromechanics and macromechanics approaches for mechanical analysis are reviewed. Since interfacial mechanics of composites is of primary importance in discussing the material behavior, this concept is also presented with its constitutive and governing equations. Finally, at the end of the chapter, strength failure theories for orthotropic materials and dynamic behavior of composites are discussed.

The mechanics of materials contended with stresses, strains, and deformations in engineering structures subjected to mechanical, thermal, and hygral loadings. A common assumption in the mechanics of conventional materials, such as steel and aluminum, is that they are homogeneous and isotropic [1]. However, fiber-reinforced composites are inhomogeneous and nonisotropic. As a result, the analysis of the mechanics of fiber-reinforced composites is much more complex than that of conventional materials. The mechanics of fiber-reinforced composite materials is mainly studied at two levels: (1) micromechanics level, in which the interaction of the constituent materials is examined on a microscopic scale. In micromechanical analysis, stiffness, strength, thermal, and moisture expansion coefficients of a lamina are found using the individual properties of constituents (fiber and matrix), (2) macromechanics level, in which the response of a fiber-reinforced composite material to mechanical and thermal loads is studied on a macroscopic scale. The material is assumed to be homogeneous. Stresses, strains, and deflections are determined using the equations of orthotropic elasticity.

2.2 Mechanics of continuous fiber-reinforced composites

Composites are materials in which a homogeneous matrix component is reinforced by a stronger and stiffer constituent that is usually continuous or short fibers. Continuous fiber-matrix composite materials include unidirectional or woven fiber laminae; laminae are stacked on top of each other at various angles to form a multidirectional laminate. The mechanical analysis of fiber-reinforced composites is performed in two levels: micromechanical and macromechanical analyzes.

In the following parts, micromechanical and macromechanical analyzes of continuous-fiber-reinforced composites have been introduced based on classical lamination theory.

Fiber Technology for Fiber-Reinforced Composites. http://dx.doi.org/10.1016/B978-0-08-101871-2.00002-3

2.2.1 Macromechanical analysis

2.2.1.1 Constitutive equations

The classical lamination theory based on Kirchoff's hypothesis is used to analyze the infinitesimal deformation of thin-laminated structures. In this theory, it is assumed that the laminate is thin and wide, layers are perfectly bonded, the material of each layer is linearly elastic and has a uniform thickness, and there exists a linear strain distribution through the thickness (small deformation). Thin-laminated structure subjected to mechanical in-plane loading is shown in Fig. 2.1. Cartesian coordinate system x, y, and z define global coordinates of the layered material. A layerwise principal material coordinate system is denoted by 1, 2, and 3, and fiber direction is oriented at angle θ to the x-axis [2,3].

Based on the theory, the resulting displacement field is then expressed as

$$\begin{aligned} u(x,y,z) &= u_0(x,y) - z\frac{\partial w_0}{\partial x} \\ v(x,y,z) &= v_0(x,y) - z\frac{\partial w_0}{\partial y}(x,y) \\ w(x,y,z) &= w_0(x,y) \end{aligned} \tag{2.1}$$

where u_0, v_0, w_0 are the displacement components along x, y, and z coordinate directions of a point on the midplane ($z=0$), respectively (Fig. 2.2).

Eq. (2.1) implies that straight lines normal to geometric midplane before deformation remain straight after deformation. In this regard, transverse normal strain (ε_{zz}) and shear components (γ_{xz} and γ_{yz}) become zero, and the strain field is then expressed as

$$\begin{aligned} \varepsilon_{xx} &= \frac{\partial u_0}{\partial x} - z\left(\frac{\partial^2 w_0}{\partial x^2}\right) \\ \varepsilon_{yy} &= \frac{\partial v_0}{\partial y} - z\left(\frac{\partial^2 w_0}{\partial y^2}\right) \\ \gamma_{xy} &= \left(\frac{\partial u_0}{\partial y} + \frac{\partial v_0}{\partial x}\right) - 2z\frac{\partial^2 w_0}{\partial x \partial y} \end{aligned} \tag{2.2}$$

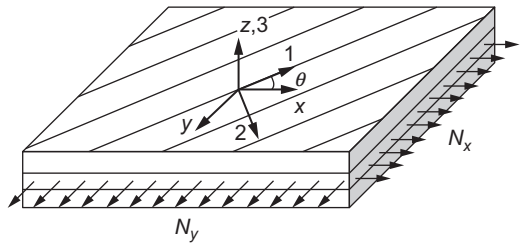

Fig. 2.1 A thin fiber-reinforced laminated composite subjected to in-plane loading [2].

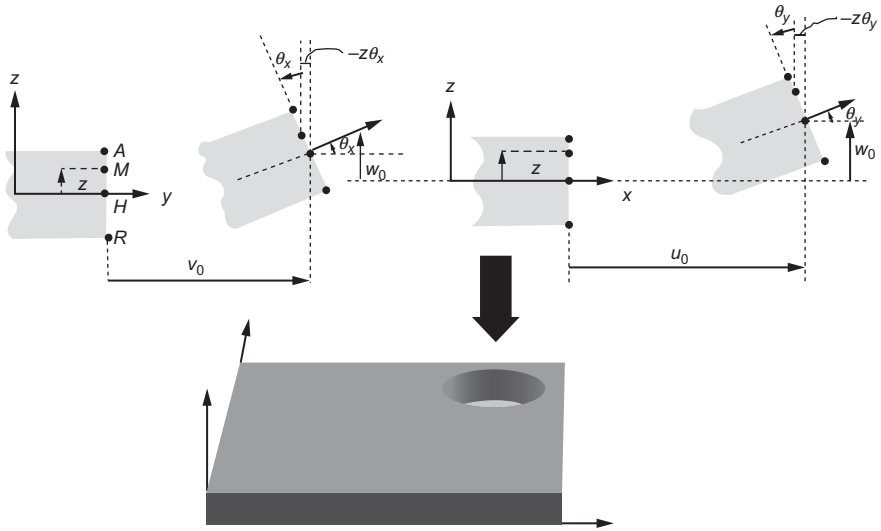

Fig. 2.2 Deformation in the case of classical theory of laminates [4].

Therefore, the nonzero three strains in generalized form including mechanical (M), thermal (T), and hygral (H) effects can be represented as in the following form [2]:

$$\begin{bmatrix} \varepsilon_{xx} \\ \varepsilon_{yy} \\ \gamma_{xy} \end{bmatrix} = \begin{bmatrix} \varepsilon_{xx}^{M} \\ \varepsilon_{yy}^{M} \\ \gamma_{xy}^{M} \end{bmatrix} + \begin{bmatrix} \varepsilon_{xx}^{T} \\ \varepsilon_{yy}^{T} \\ \gamma_{xy}^{T} \end{bmatrix} + \begin{bmatrix} \varepsilon_{xx}^{H} \\ \varepsilon_{yy}^{H} \\ \gamma_{xy}^{H} \end{bmatrix} \tag{2.3}$$

where

$$\begin{bmatrix} \varepsilon_{xx} \\ \varepsilon_{yy} \\ \gamma_{xy} \end{bmatrix} = \begin{bmatrix} \varepsilon_{xx}^{0} \\ \varepsilon_{yy}^{0} \\ \gamma_{xy}^{0} \end{bmatrix} + z \begin{bmatrix} \kappa_{xx} \\ \kappa_{yy} \\ \kappa_{xy} \end{bmatrix}$$

Here, the midplane strain matrix and the curvature matrix of the laminate subjected to loading are expressed as a function of the midplane displacements u_0 and v_0, respectively:

$$\begin{bmatrix} \varepsilon_{xx}^{0} \\ \varepsilon_{yy}^{0} \\ \gamma_{xy}^{0} \end{bmatrix} = \begin{bmatrix} \dfrac{\partial u_0}{\partial x} \\ \dfrac{\partial v_0}{\partial y} \\ \dfrac{\partial u_0}{\partial y} + \dfrac{\partial v_0}{\partial x} \end{bmatrix} \tag{2.4}$$

and

$$\begin{bmatrix} \kappa_{xx} \\ \kappa_{yy} \\ \kappa_{xy} \end{bmatrix} = \begin{bmatrix} \dfrac{\partial^2 w_0}{\partial x^2} \\ \dfrac{\partial^2 w_0}{\partial y^2} \\ 2\dfrac{\partial^2 w_0}{\partial x \partial y} \end{bmatrix} \tag{2.5}$$

And thermal and hygral strains are as follows:

$$\begin{bmatrix} \varepsilon_{xx}{}^{T} \\ \varepsilon_{yy}{}^{T} \\ \gamma_{xy}{}^{T} \end{bmatrix} = \begin{bmatrix} \alpha_{xx} \\ \alpha_{yy} \\ \alpha_{xy} \end{bmatrix} \Delta T \tag{2.6}$$

$$\begin{bmatrix} \varepsilon_{xx}{}^{H} \\ \varepsilon_{yy}{}^{H} \\ \gamma_{xy}{}^{H} \end{bmatrix} = \begin{bmatrix} \beta_{xx} \\ \beta_{yy} \\ \beta_{xy} \end{bmatrix} \Delta C \tag{2.7}$$

where

$$\begin{bmatrix} \alpha_{xx} \\ \alpha_{yy} \\ \alpha_{xy} \end{bmatrix} = \begin{bmatrix} \varepsilon_{xx}{}^{0} \\ \varepsilon_{yy}{}^{0} \\ \gamma_{xy}{}^{0} \end{bmatrix} \begin{matrix} \Delta C = 0 \\ \Delta T = 1 \end{matrix} \quad \text{and} \quad \begin{bmatrix} \beta_{xx} \\ \beta_{yy} \\ \beta_{xy} \end{bmatrix} = \begin{bmatrix} \varepsilon_{xx}{}^{0} \\ \varepsilon_{yy}{}^{0} \\ \gamma_{xy}{}^{0} \end{bmatrix} \begin{matrix} \Delta C = 1 \\ \Delta T = 0 \end{matrix}$$

After determining the strain field, the stress-strain relation for kth layer of composite plate (Fig. 2.3) based on the classical lamination theory can be written in the following form:

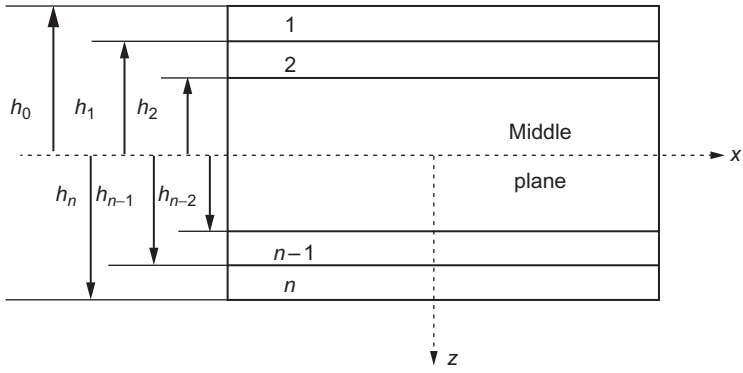

Fig. 2.3 Laminate convention [2].

$$\begin{bmatrix}\sigma_{xx}{}^{M}\\ \sigma_{yy}{}^{M}\\ \sigma_{xy}{}^{M}\end{bmatrix}_k = \begin{bmatrix}\bar{Q}_{11} & \bar{Q}_{12} & \bar{Q}_{16}\\ \bar{Q}_{12} & \bar{Q}_{22} & \bar{Q}_{26}\\ \bar{Q}_{16} & \bar{Q}_{26} & \bar{Q}_{66}\end{bmatrix}_k \begin{bmatrix}\varepsilon_{xx}\\ \varepsilon_{yy}\\ \gamma_{xy}\end{bmatrix} - \begin{bmatrix}\varepsilon_{xx}{}^{T}\\ \varepsilon_{yy}{}^{T}\\ \gamma_{xy}{}^{T}\end{bmatrix}_k - \begin{bmatrix}\varepsilon_{xx}{}^{H}\\ \varepsilon_{yy}{}^{H}\\ \gamma_{xy}{}^{H}\end{bmatrix}_k \tag{2.8}$$

where $\left[\bar{Q}_{ij}\right]_k$ are the elements of the transformed reduced stiffness matrix, determined as

$$\begin{aligned}
\bar{Q}_{11} &= Q_{11}cos^4\theta + 2(Q_{12}+2Q_{66})sin^2\theta cos^2\theta + Q_{22}sin^4\theta\\
\bar{Q}_{12} &= (Q_{11}+Q_{22}-4Q_{66})sin^2\theta cos^2\theta + Q_{12}\left(sin^4\theta + cos^2\theta\right)\\
\bar{Q}_{22} &= Q_{11}sin^4\theta + 2(Q_{12}+2Q_{66})sin^2\theta cos^2\theta + Q_{22}cos^4\theta\\
\bar{Q}_{16} &= (Q_{11}-Q_{12}-2Q_{66})sin\,\theta cos^3\theta + (Q_{12}-Q_{22}-2Q_{66})sin^3\theta cos\,\theta\\
\bar{Q}_{26} &= (Q_{11}-Q_{12}-2Q_{66})sin^3\theta cos\,\theta + (Q_{12}-Q_{22}+2Q_{66})sin\,\theta cos^3\theta\\
\bar{Q}_{66} &= (Q_{11}+Q_{22}-2Q_{12}-2Q_{66})sin^2\theta cos^2\theta + Q_{66}\left(sin^4\theta + cos^2\theta\right)
\end{aligned} \tag{2.9}$$

where the stiffness coefficients Q_{ij} that are related to the engineering constants are given as follows:

$$Q_{11} = \frac{E_1}{1-v_{21}v_{12}} \quad Q_{12} = \frac{v_{12}E_2}{1-v_{21}v_{12}} \quad Q_{22} = \frac{E_2}{1-v_{21}v_{12}} \quad Q_{66} = G_{12} \tag{2.10}$$

Here, E_1 and E_2, G_{12} are the longitudinal and transverse elastic modulus and in-plane shear modulus, respectively; v_{12} and v_{21} are major and minor Poisson's ratios.

For thin composite subjected to hygro-thermo-mechanical loading, in general, in-plane force resultants (force per unit width) and moment resultants (moment per unit width) have the following relations:

Force resultants:

$$\begin{bmatrix}N_x^M\\ N_y^M\\ N_x^M\end{bmatrix} = \begin{bmatrix}A_{11} & A_{12} & A_{16}\\ A_{12} & A_{22} & A_{26}\\ A_{16} & A_{26} & A_{66}\end{bmatrix} \begin{bmatrix}\varepsilon_{xx}{}^{0}\\ \varepsilon_{yy}{}^{0}\\ \gamma_{xy}{}^{0}\end{bmatrix} + \begin{bmatrix}B_{11} & B_{12} & B_{16}\\ B_{12} & B_{22} & B_{26}\\ B_{16} & B_{26} & B_{66}\end{bmatrix} \begin{bmatrix}k_{xx}\\ k_{yy}\\ k_{xy}\end{bmatrix} - \begin{bmatrix}N_x^T\\ N_y^T\\ N_{xy}^T\end{bmatrix} - \begin{bmatrix}N_x^C\\ N_y^C\\ N_{xy}^C\end{bmatrix} \tag{2.11}$$

The matrices [A] and [B] appearing in Eq. (2.11) can be defined as

$$A_{ij} = \sum_{k=1}^{N}\left[\bar{Q}_{ij}\right]_k(h_k - h_{k-1}) \quad (\text{Extensional stiffness}) \tag{2.12}$$

$$B_{ij} = \frac{1}{2}\sum_{k=1}^{N}\left[\bar{Q}_{ij}\right]_k\left(h_k^2 - h_{k-1}^2\right) \,(\text{Coupling stiffness})\,(i,j=1,2,6) \tag{2.13}$$

And $[N^T]$, and $[N^C]$ are the resultant thermal and hygral forces, respectively:

$$\begin{bmatrix} N_x^T \\ N_y^T \\ N_{xy}^T \end{bmatrix} = \Delta T \sum_{k=1}^{n} \begin{bmatrix} \bar{Q}_{11} & \bar{Q}_{12} & \bar{Q}_{16} \\ \bar{Q}_{12} & \bar{Q}_{22} & \bar{Q}_{26} \\ \bar{Q}_{16} & \bar{Q}_{26} & \bar{Q}_{66} \end{bmatrix}_k \begin{bmatrix} \alpha_x \\ \alpha_y \\ \alpha_{xy} \end{bmatrix}_k (h_k - h_{k-1}) \tag{2.14}$$

$$\begin{bmatrix} N_x^C \\ N_y^C \\ N_{xy}^C \end{bmatrix} = \Delta C \sum_{k=1}^{n} \begin{bmatrix} \bar{Q}_{11} & \bar{Q}_{12} & \bar{Q}_{16} \\ \bar{Q}_{12} & \bar{Q}_{22} & \bar{Q}_{26} \\ \bar{Q}_{16} & \bar{Q}_{26} & \bar{Q}_{66} \end{bmatrix}_k \begin{bmatrix} \beta_x \\ \beta_y \\ \beta_{xy} \end{bmatrix}_k (h_k - h_{k-1}) \tag{2.15}$$

Moment resultants:

$$\begin{bmatrix} M_x^M \\ M_y^M \\ M_{xy}^M \end{bmatrix} = \begin{bmatrix} \mathrm{B}_{11} & \mathrm{B}_{12} & \mathrm{B}_{16} \\ \mathrm{B}_{12} & \mathrm{B}_{22} & \mathrm{B}_{26} \\ \mathrm{B}_{16} & \mathrm{B}_{26} & \mathrm{B}_{66} \end{bmatrix} \begin{bmatrix} {\varepsilon_{xx}}^0 \\ {\varepsilon_{yy}}^0 \\ {\gamma_{xy}}^0 \end{bmatrix} + \begin{bmatrix} \mathrm{D}_{11} & \mathrm{D}_{12} & \mathrm{D}_{16} \\ \mathrm{D}_{12} & \mathrm{D}_{22} & \mathrm{D}_{26} \\ \mathrm{D}_{16} & \mathrm{D}_{26} & \mathrm{D}_{66} \end{bmatrix} \begin{bmatrix} k_{xx} \\ k_{yy} \\ k_{xy} \end{bmatrix} - \begin{bmatrix} M_x^T \\ M_y^T \\ M_{xy}^T \end{bmatrix} - \begin{bmatrix} M_x^C \\ M_y^C \\ M_{xy}^C \end{bmatrix} \tag{2.16}$$

where D_{ij} the bending stiffnesses, which are defined as in terms of lamina stiffness $\bar{Q}_{ij}$ as

$$D_{ij} = \frac{1}{3} \sum_{k=1}^{N} \left[\bar{Q}_{ij}\right]_k \left(h_k^3 - h_{k-1}^3\right) \tag{2.17}$$

In a more general representation, the constitutive equation of a laminated plate is obtained by grouping Eqs. (2.11) and (2.16) into a single-matrix equation of the form:

$$\begin{bmatrix} N_x \\ N_y \\ N_{xy} \\ M_x \\ M_y \\ M_{xy} \end{bmatrix} = \begin{bmatrix} A_{11} & A_{12} & A_{16} & \mathrm{B}_{11} & \mathrm{B}_{12} & \mathrm{B}_{16} \\ A_{12} & A_{22} & A_{26} & \mathrm{B}_{12} & \mathrm{B}_{22} & \mathrm{B}_{26} \\ A_{16} & A_{26} & A_{66} & \mathrm{B}_{16} & \mathrm{B}_{26} & \mathrm{B}_{66} \\ \mathrm{B}_{11} & \mathrm{B}_{12} & \mathrm{B}_{16} & \mathrm{D}_{11} & \mathrm{D}_{12} & \mathrm{D}_{16} \\ \mathrm{B}_{12} & \mathrm{B}_{22} & \mathrm{B}_{26} & \mathrm{D}_{12} & \mathrm{D}_{22} & \mathrm{D}_{26} \\ \mathrm{B}_{16} & \mathrm{B}_{26} & \mathrm{B}_{66} & \mathrm{D}_{16} & \mathrm{D}_{26} & \mathrm{D}_{66} \end{bmatrix} \begin{bmatrix} {\varepsilon_{xx}}^0 \\ {\varepsilon_{yy}}^0 \\ {\gamma_{xy}}^0 \\ k_{xx} \\ k_{yy} \\ k_{xy} \end{bmatrix} \tag{2.18}$$

The matrix given above is called as the stiffness matrix of the laminate. Here, the matrix B represents a coupling between stretching and bending of a laminate. In case the laminate is symmetrical, a stretching-bending coupling effect does not exist. Thus, the analyzing of the behavior of symmetrical matrices is much simpler than that of the laminates having a coupling effect.

2.2.2 Micromechanical analysis

In the macromechanical analysis discussed above, basic lamina constants E_1, E_2, G_{12}, and v_{12} are assumed to be known from direct experimental characterization of the unidirectional material. It is desirable to have reliable predictions of lamina constants as a function of constituent properties (matrix and fiber properties). A specialized area of composites involving a study of the interaction of constituent materials on the microscopic level is generally conducted by the use of a mathematical model describing the response of each constituent material. In this section, mechanics of material approach that the fibers and matrix are assumed to be under uniform stress is handled and the expressions are given for determination of the basic elastic properties of the lamina [5,6].

The longitudinal and transverse modulus, Poisson's ratio, and shear modulus are given, respectively, by the following relations:

$$E_1 = V_f E_{1f} + V_m E_m \tag{2.19}$$

$$E_2 = \frac{E_{2f} E_m}{V_f E_m + V_m E_{2f}} \tag{2.20}$$

$$v_{12} = V_f v_{12f} + V_m v_m \tag{2.21}$$

$$G_{12} = \frac{G_{12f} G_m}{V_f G_m + V_m G_{12f}} \tag{2.22}$$

where subscript 1 and 2 and f and m appearing in the above equations denote the longitudinal and transverse directions and fiber and matrix properties, respectively. V_f and V_m represent fiber and matrix volume fractions, respectively. In the above formulations, fibers are assumed to be transversely isotropic.

2.3 Mechanics of short fiber-reinforced composites

A number of models have been proposed to predict the physical properties of short-fiber and particulate-reinforced composites. These composite models can be grouped into five basic models: law of mixtures, shear lag, laminated plate, variational principle, and Eshelby's models. Law of mixtures and shear-lag models give poor estimation of stiffness of a composite where the aspect ratio of short fibers is small [7]. In addition, semiempirical models distinguish spherical and nonspherical particulate systems. These expressions are generally based on some physics arguments and determination of fitting parameters. Some semiempirical models that rely on the determination of adjustable parameters have been developed due to the complexity of the geometric features (filler aspect ratio, volume fraction, filler orientation, etc.) and inadequacies of the theoretical models.

2.3.1 Law of mixtures

It is considered that a composite with N different reinforcing elements is distributed in a matrix. Assume that each fiber has a shear modulus μ_i and volume fraction of fibers is V_i ($i = 1,2,3,\ldots,N$) and the shear modulus and volume fraction of matrix material are μ_0 and V_0, respectively. The shear modulus of composites μ_c is

$$\mu_c = \sum_{i=0}^{N} V_i \mu_i \tag{2.23}$$

where

$$\sum_{i=0}^{N} V_i = 1 \tag{2.24}$$

Assume that the externally applied shear strain γ_a is equal to shear strains in all phases including the matrix that can be explained as the average strain γ. Since the stress in the ith phase, σ_i, is given by $\mu_i \overline{\gamma}$, the average stress in the composite can be approached by

$$\overline{\sigma} = \sum_{i=0}^{N} V_i \sigma_i = \sum_{i=0}^{N} V_i \mu_i \overline{\gamma} \tag{2.25}$$

On the other hand, the average stress $\overline{\sigma}$ is related to the applied strain γ_a ($=\overline{\gamma}$) by

$$\overline{\sigma} = \mu_c \overline{\gamma} \tag{2.26}$$

If the shear moduli μ_c and μ_i are replaced by the strength of composite σ_c and reinforcing material σ_i, composite strength can be obtained as

$$\sigma_c = \sum_{i=0}^{N} V_i \sigma_i \tag{2.27}$$

In the case of two-phase system, matrix, and one kind of reinforced element, Eq. (2.27) can be written as

$$\sigma_c = V_0 \sigma_0 + V_1 \sigma_1 = V_m \sigma_m + V_f \sigma_f \tag{2.28}$$

where the indexes m and f define matrix and fiber, respectively. The value predicted by law of mixtures is an upper bound, because the strain in the fiber and the matrix are not equal [7,8].

2.3.2 Shear lag model

Shear-lag model was developed by Cox [9] and adequately predicts the stress transfer in fiber-reinforced composites, particularly for large differences in inclusion to matrix elastic modulus ratios [10]. It is assumed that short fibers having uniform length and

diameter are aligned in the loading direction and distributed uniformly throughout the material as seen in Fig. 2.4A. A unit cell shown in Fig. 2.4B represents the basic model, in which short fiber surrounded by matrix. The other boundary of the surrounding matrix is taken as midsurface between two short fibers. This short-fiber composite is subjected to the applied uniaxial strain e along the z direction. Let the axial displacements in the fiber and the matrix on the boundary of the unit cell ($r = D/2$) be denoted by u and v, respectively.

In addition, it is assumed that the difference in the axial displacements, *u and v*, is proportional to the shear stress τ_0 at the matrix-fiber interface. One can obtain

$$\frac{d\sigma_f}{dz} = -\frac{4\tau_0}{d} = h(u - v) \tag{2.29}$$

where σ_f is the axial stress in the fiber. The first equality in Eq. (2.29) was derived by considering the equilibrium of force along the z direction. It is noted that the positive direction of shear stress τ_0 is taken through the positive z axis. In this step, Hooke's law is also valid for the fiber as

$$\sigma_f = E_f \frac{du}{dz} \tag{2.30}$$

Micromechanics is concerned with the prediction of elastic, viscoelastic, and strength properties of composites form those of their individual constituents. The objective of any such analysis is to model a heterogeneous material by an anisotropic continuum. The stresses and strains obtained by continuum analyzes are to be considered as

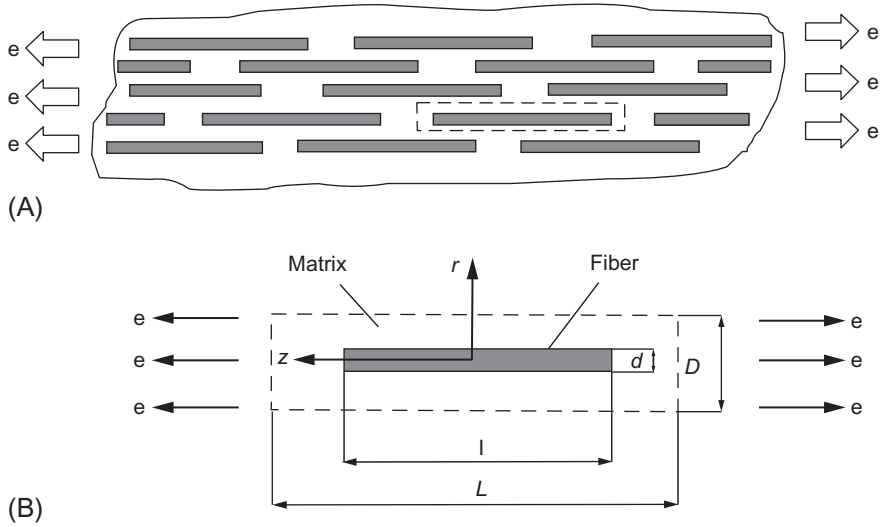

Fig. 2.4 Shear-lag model for aligned short-fiber composite: (A) representative short fiber and (B) unit cell model for shear-lag analysis [7].

averages over the smallest repetitive cell and are sufficiently accurate when changes in applied stresses are smaller distances of the size of the inclusions [8]. Micromechanics is still an area of active research in order to bring theoretical predictions into better agreement with experimental results. Reviews of earlier work pertaining to composites with continuous-fiber reinforcement can be found in textbooks [11,12] and review articles [13]. The various approaches proposed can be classified as follows: netting analysis, mechanics of materials, self-consistent model, variational, exact, statistical, discrete element, semiempirical methods, and microstructural theories. The usefulness of these theories lies in the fact that they provide some insight into the mechanics of fiber or particular application by the compounder and the stress analyst.

Most theories consider spherical, disk-shaped, or short-fiber isotropic inclusions in an isotropic matrix. Even though some fibers, such as Kevlar, are known to have a microfibrillar structure and are themselves anisotropic, the effective moduli predicted are in reasonable agreement with experimental results. The basic assumptions common to these analyzes are the following:

- The filler particles are of idealized shape (spherical, cubic, and rod-like).
- There is complete adhesion between matrix and filler.
- Elongations are small.
- Complete dispersion is achieved.
- Volume loadings are low enough to ignore interactions of order higher than two.
- The matrix can be considered to be continuous and homogeneous.

There are many examples of analytic and numerical modeling for microsized composites. However, in nanocomposite systems, several issues need to be developed. Some authors studying composite materials are generally interested in either prediction of elastic properties of the composite or volume-change problems.

Semiempirical models are most widely used expressions in the prediction of elastic modulus. These expressions are generally based on some physics arguments and determination of fitting parameters [14]. A better understanding of the mechanical behavior and predicted elastic modulus is essential in the development of the composites. This also assists the improvement of material processing. For this reason, the modulus of polymer composites has been extensively studied experimentally and predicted with a two-phase model by various researchers. Some semiempirical models that rely on the determination of adjustable parameters have been developed due to the complexity of the geometric features (filler aspect ratio, volume fraction, filler orientation, etc.) and inadequacies of the theoretical models as mentioned above. All of the theoretical modeling approaches based on the relations of the elastic constants are given in Eqs. (2.31a)–(2.31c). For an isotropic material, there are two elastic constants: Young's modulus (E) and Poisson's ratio (ν) to define the elastic response of the composites:

$$G = \frac{E}{2(1+\nu)} \tag{2.31a}$$

$$E = \frac{9KG}{3K+G} \tag{2.31b}$$

$$\nu = \frac{3K - 2G}{2(3K + G)} \tag{2.31c}$$

In the above equations, K refers to the bulk modulus, and G is shear modulus of the material. In the following section, semiempirical models for spherical and nonspherical particulate systems are investigated.

2.3.3 Semi empirical models for spherical particulate systems

Semiempirical models based on the physical parameters have the following general form [15]:

$$P_c = \frac{P_m\left(1 + \xi X V_f\right)}{1 - X\psi V_f} \tag{2.32a}$$

$$X = \frac{P_f - P_m}{P_f + xP_m} \tag{2.32b}$$

Here, P denotes the bulk modulus (K) or the shear modulus (G), and V_f is the volume fraction. The subscripts c, m, and f refer to the composite, matrix, and the filler, respectively. In this formulation, ξ and ψ can be treated as adjustable parameters that are specifically defined in each model. Based on the formulation given in Eqs. (2.32a), (2.32b), there are several formulations proposed in the literature in order to predict the elastic modulus of the composites reinforced by spherical fillers. In these systems, the reinforcing particles are considered to be spherical or near spherical; therefore, the effective aspect ratio is unity. The following four most commonly used models were developed by Guth and Gold, Halpin-Tsai (HT), Lewis-Nielsen (LN), and Chantler, Hu, and Boyd (Ch) that are related with the adjustable parameters ξ and ψ.

2.3.3.1 Halpin-Tsai model

Halpin and Tsai developed a widely used composite theory to predict the stiffness of continuous-fiber composites as a function of aspect ratio. This theory is based on the early micromechanical work of Hermans [16] and Hill [17]. Halpin and Tsai adapted Hermans' model for particulate systems. Based on Eq. (2.32), P represents the Young's modulus, ξ is a shape parameter that depends on matrix Poisson's ratio, filler geometry, orientation, and loading direction, and it was found to be 2 for particulate-filled composites. Moreover, for shear-modulus predictions, $\xi = 1$ can be used or the equality as follows:

$$\xi_G = \frac{7 - 5\nu_m}{8 - 10\nu_m} \tag{2.33a}$$

By including matrix Poisson's ratio (ν_m), the parameter can be calculated precisely. In the same manner for bulk modulus, the term is as follows:

$$\xi_K = \frac{2(1-2\nu_m)}{1+\nu_m} \tag{2.33b}$$

The last parameter, ψ, used in Eqs. (2.32a), (2.32b) is taken as 1 in Halpin-Tsai model. The Halpin-Tsai equations are known to fit some experimental data very well at low volume fractions, but it underestimates stiffness values at high volume fractions [18]. This has prompted some modifications to their model. By adapting this formulation to the short-fiber composites, Halpin and Tsai noted that the shape parameter, ξ, lies between 0 and ∞. For example, if ξ is taken as ∞, then Eqs. (2.32a), (2.32b) reduced to the rule of mixtures as in the following form [19]:

$$P = \nu_f P_f + \nu_m P_m \tag{2.34a}$$

However, for $\xi = 0$, Halphin-Tsai formulation becomes the inverse rule of mixture as follows:

$$\frac{1}{P} = \frac{\nu_f}{P_f} + \frac{\nu_m}{P_m} \tag{2.34b}$$

2.3.3.2 Lewis-Nielsen model

This model was developed by Nielsen [20] and Lewis and Nielsen [21] using the analogy between the stiffness of the composite and viscosity of a suspension of rigid particle in a Newtonian fluid. This model is also a modification of the Halpin-Tsai model. It was designed to compensate the Halpin-Tsai model's lack for the prediction of modulus at high-filler-loading composites. In their formulation, an equation in which the stiffness not only matches with dilute theory at low volume fractions but also displays rigid reinforcement as V_f approaches a packing limit ${V_f}^{\max}$. It is used to account for the limits imposed by the maximum packing for uniformly sized spherical particles. The following expressions are given for the model:

$$\xi_G = \frac{7-5\nu_m}{8-10\nu_m} \tag{2.35a}$$

$$\xi_K = \frac{2(1-2\nu_m)}{1+\nu_m} \tag{2.35b}$$

$$\psi = 1 + \left(\frac{1-{V_f}^{\max}}{\left({V_f}^{\max}\right)^2}\right) V_f \tag{2.35c}$$

Here, v_m is matrix Poisson's ratio and ${V_f}^{\max}$ is the maximum volume fraction of filler. For uniform sizes of spheres, ${V_f}^{\max}$ is 0.66 for random packing, and if the composite system does not have uniform size distribution of particles, then ${V_f}^{\max}$ is considered to

be between 0.66 and 1 [14]. The parameters, ξ_G and ξ_K, are used for the prediction of shear and bulk modulus, respectively. It is obvious that ξ_G and ξ_K are the same as in Halpin-Tsai model; however, the parameter ψ is a function of volume fraction and maximum volume fraction of the filler in the Lewis-Nielsen model.

2.3.3.3 S-combining rule

This approach considers a composite system with the stiff spherical inclusions in a more compliant matrix, such that for particulate-filled polymers with $P_f > P_m$. For rigid uniformly sizes of spheres, the adjustable parameters ξ_G, ξ_K, and ψ can be expressed as follows [18]:

$$\xi_G = \frac{7 - 5\nu_m}{8 - 10\nu_m} \tag{2.36a}$$

$$\xi_K = \frac{2(1 - 2\nu_m)}{1 + \nu_m} \tag{2.36b}$$

$$\psi = 1 + \left(\frac{1 - {V_f}^{\max}}{{V_f}^{\max}}\right)\left(V_f.{V_f}^{\max} + \left(1 + V_f\right)\left(1 - {V_f}^{\max}\right)\right) \tag{2.36c}$$

Here, ${V_f}^{\max}$ is the maximum volume fraction of the filler. Comparing the Halpin-Tsai, Lewis-Nilsen, and S-combining rule, it can be seen that the parameter ψ has different mathematical form in each model. Therefore, it can be useful to investigate the variation of ψ for appropriate maximum volume fraction of filler and V_f. Fig. 2.5 shows this effect for different values of ${V_f}^{\max}$. Another important difference among HT, LN, and S-combining rule models is that Young's modulus values may not be predicted directly by LN or S-combining models, while HT model allows prediction of Young's modulus of the composite without extra calculation. Young's modulus can be generated from the predicted values of bulk modulus K and shear modulus G through the auxiliary expression given in Eqs. (2.31a)–(2.31c) for LN or S-combining models.

2.3.3.4 Chantler, Hu, and Boyd (CHU) model

Chantler and coworkers presented a new phenomenological model based on the classic Hertzian elastic contact theory. The following expression can be used to predict the elastic modulus of composites (E_c) [22]:

$$E_c = E_m\left(E_f/E_m\right)^{1-\left(1-V_f\right)^{\beta}} \tag{2.37a}$$

where

$$\beta = \frac{2\left[\left(1 - \nu_f^2\right)/\left(1 - \nu_m^2\right)\right]^{1.7}}{ln\left(E_f/E_m\right)} \tag{2.37b}$$

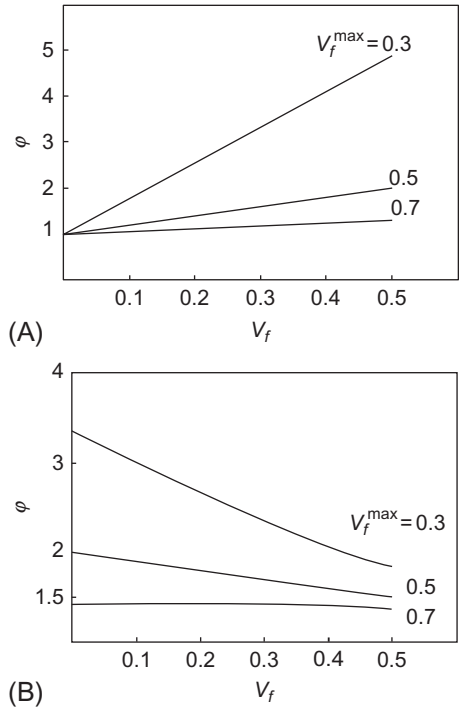

Fig. 2.5 Effect of adjustable parameter ψ for (A) Lewis-Nilsen model and (B) S-combining rule with different values of V_f^{max}.

where v_f and v_m are Poisson's ratio of the filler and matrix and E_m and E_f are the elastic modulus of matrix and filler, respectively. The results of this study demonstrate that the previous phenomenological model given in Braem et al. [23] is deficient if the modulus ratio E_f/E_m is higher than 10. A modified approach gives much improved predictions for composite modulus and also satisfies the boundary conditions for bulk filler and resin materials. In contrast to the previously mentioned models (HT, LN, and S), CHB model considers Poisson's ratio of the filler (v_f). However, the reported studies about the nanocomposite modeling indicate that the effective material parameter is only v_m. As in HT model, CHB model also allows calculation of Young's modulus directly.

2.3.3.5 Guth and Gold model

By adapting the Einstein coefficient, (K_E) is equal to 2.5 in the Einstein equation, which is valid only at very low concentrations (< %10) of the filler, Guth and Gold [24] obtained the following formulation that is only applicable to elastomers filled with a certain amount of spherical fillers, and the formulation can be used for concentrations up to 30%:

$$E_c = E_m\left[1 + 2.5V_f + 14.1V_f^2\right] \tag{2.38a}$$

Most of the models adequately predict the behavior for particulate-filled systems in the volume-fraction concentration in the range of $0 \leq V_f \leq 1/3$; however, only S-combining rule and Lewis-Nielsen models have the capability of prediction at higher volume-fraction concentrations of filler [18]. To increase the capability of prediction of Guth and Gold model at higher volume fraction, the equation is modified in the following form, which is valid at filler concentration of up to 45%:

$$E_c = E_m\left[1 + 2.5V_f + 16.2{V_f}^2\right] \tag{2.38b}$$

2.3.4 Semi empirical models for nonspherical particulate systems

The composite systems such as in layered clay/polymer nanocomposites contain platelet like nonspherical particles. Nonspherical particulate-reinforced composites have slightly higher elastic modulus (E) than those based on spherical particulate systems. There are several important models that have appropriate prediction capability of elastic modulus of the nonspherical filled composite systems. In this section, we consider four different models developed for the estimation of elastic modulus of inorganic clay-layer-incorporated thermoset polymer nanocomposites.

2.3.4.1 Halpin-Tsai model

Halpin-Tsai equations are widely used expressions in order to predict reinforcement effect of fillers in nanocomposite systems with both spherical (or near spherical) and nonspherical filled systems. Halpin-Tsai equations were modified by Halpin and Kardos [19] for the plate-like filler as expressed in the following form:

$$E_c = \frac{E_m\left(1 + \xi\eta V_f\right)}{1 - \eta V_f} \tag{2.39a}$$

where

$$\eta = \frac{E_f/E_m - 1}{E_f/E_m + \xi} \tag{2.39b}$$

Here, E_f denotes elastic modulus of the filler, and ξ is the shape factor depending on the filler orientation and loading direction. For the rectangular plate-like filler in a composite system, ξ is equal to $2w/t$ in which w is the width and t is the thickness of the dispersed phase. The effect of aspect ratio on Halpin-Tsai model is illustrated in Fig. 2.6. The aspect ratio α has very significant effect on elastic modulus of the composite even at low volume fraction of the filler.

2.3.4.2 Modified Halpin-Tsai model

Lewis and Nielsen [21] and Nielsen [20] considered the maximum volumetric packing fraction of the filler ψ as an additional parameter in order to improve the prediction ability of the classical HT model. Maximum volumetric packing fraction can be

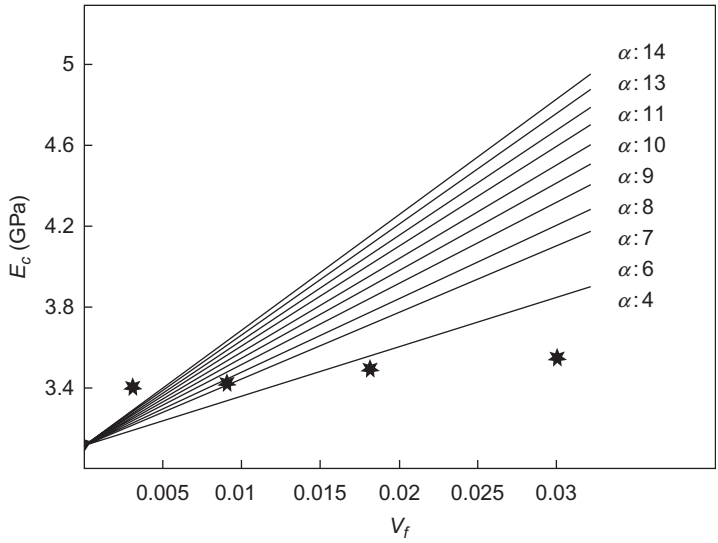

Fig. 2.6 Effect of the aspect ratio, α, on the elastic modulus of the composite reinforced by nonspherical particulate fillers based on Halpin-Tsai equation (experimental data for MMT/epoxy are presented with (✸)).

defined as the ratio of true volume of the filler to apparent volume occupied by the filler. Modified Halpin-Tsai model can be written in the following form:

$$E_c = \frac{E_m\left(1+\xi\eta V_f\right)}{1-\psi\eta V_f} \tag{2.40a}$$

where

$$\psi = 1+\left(\frac{1-{V_f}^{\max}}{\left({V_f}^{\max}\right)^2}\right)V_f \tag{2.40b}$$

$$\eta = \frac{E_f/E_m-1}{E_f/E_m+\xi} \tag{2.40c}$$

Based on Lewis and Nielsen [21] and Nielsen [20] modification, Fig. 2.7. shows the effect of the aspect ratio α on the elastic modulus of the composite reinforced by nonspherical particulate fillers based on modified Halpin-Tsai equation. Similar to Halpin-Tsai model for nonspherical systems, the modified Halpin-Tsai model predicts a significant effect of aspect ratios of filler on the modulus of the composite.

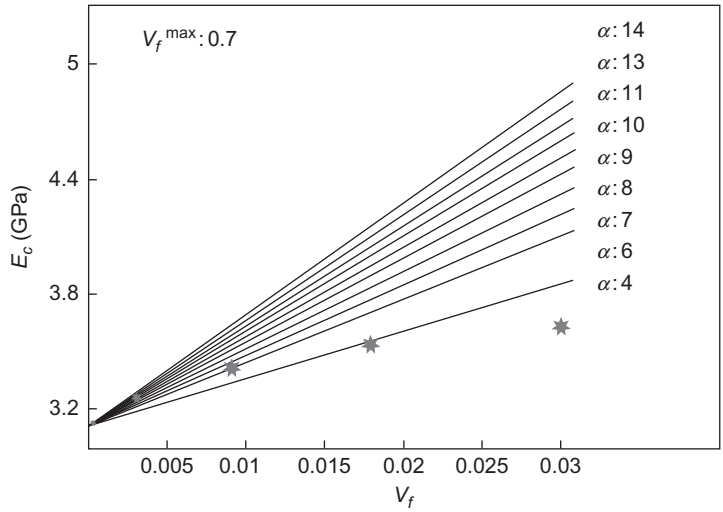

Fig. 2.7 Effect of the aspect ratio α on the elastic modulus of the composite reinforced by nonspherical particulate fillers based on modified Halpin-Tsai method for $V_f{}^{\max}=0.7$ (experimental data for OMMT/epoxy are presented with (✸)).

2.3.4.3 Guth model

The relations between Young's modulus and the concentration of filler given by Guth and Gold in Eqs. (2.38a), (2.38b) were modified by Guth [25] for nonspherical filled particulate composites. This modified model considers the chains composed of spherical fillers that are similar to rod-like filler particles embedded in a continuous matrix. By introducing a shape factor to original Guth and Gold equation, Guth developed a new expression as in the following form:

$$E_c = E_m\left[1+0.67\alpha V_f+1.62\left(\alpha V_f\right)^2\right] \tag{2.41}$$

where α is the shape factor (length/width of the filler), E_m is the elastic modulus of the matrix, and E_c is the elastic modulus of the composite [26].

2.3.4.4 Brodnyan model

Modifying the Mooney equation [27,28] expressed the following equation to predict the elastic modulus of the nonspherical particulate composites under the restriction of $1<\alpha<15$:

$$E_c = E_m\mathrm{Exp}\left(\frac{2.5V_f+0.407(\alpha-1)^{1.508}V_f}{1-V_f/V_f{}^{\max}}\right) \tag{2.42}$$

2.4 Mechanics of woven fabric composites

Orthogonal two-dimensional woven-fabric composites consist of threads such as strands, yarns, and woven rovings in warp direction L and weft (fill yarns) direction T that are principal directions. Woven have good stability in the warp and filling directions. Weaves repeat after a certain number of warp, weft strands, or yarns. Plain weave, 3×1 twill, cross ply weave, and unidirectional weave are some common weave styles. Weaves contain repetitive pattern in both directions as shown in Fig. 2.8. Some disadvantages of woven fabrics related to the design of certain composite products can be regarded as anisotropy, poor in-plane shear resistance, difficult handling of open constructions, and yarn-to-fabric tensile translation efficiency due to yarn crimp and crimp exchange [30].

Mechanical properties in plain-weave fabric become almost identical in two directions of warp and weft. However, the plain-weave fabric enables a high degree of crimp to the fibers, which decreases some mechanical performances of the composite. In twill-weave fabric, a regular diagonal pattern is produced on the cloth. The twill-weave cloth provides slippage that occurs between the fibers. In unidirectional-weave fabric, the threads are formed in the warp direction. The warp threads in the unidirectional weave are held together by fine weft threads. Maximum mechanical performance is obtained in the warp direction [4].

2.4.1 Constitutive equations

In mechanical analysis of the woven-fabric laminates, the elastic properties of warp and left unidirectional layers shown in Fig. 2.9 are used as in the following form:

$$\text{Warp layer}: \quad E_{Lwp}\ E_{Twp}\ v_{LTwp}\ G_{LTwp}$$

$$\text{Weft layer}: \quad E_{Lwf}\ E_{Twf}\ v_{LTwf}\ G_{LTwf}$$

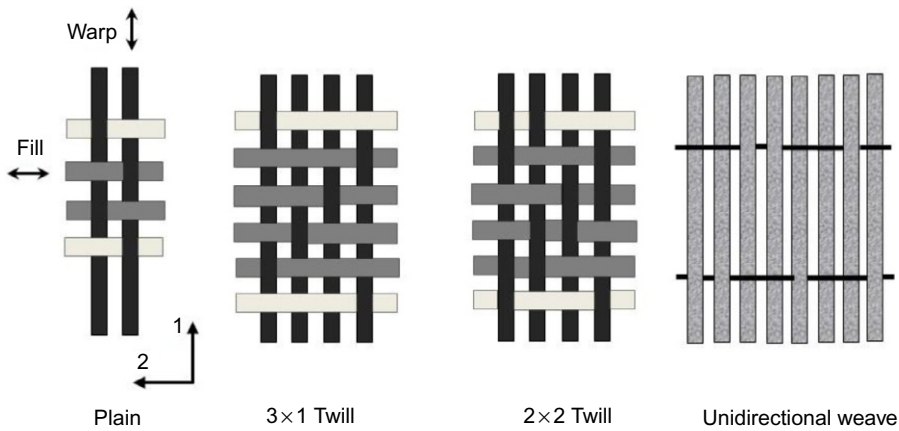

Fig. 2.8 Schematic representation of woven-fabric weave styles [29].

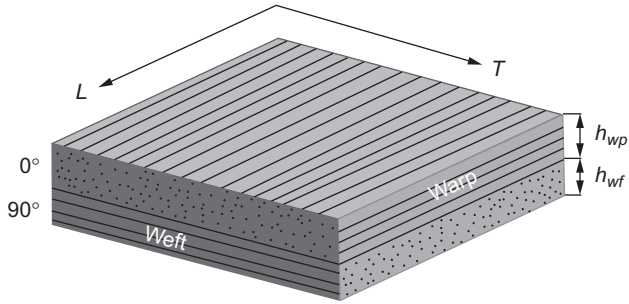

Fig. 2.9 Laminate analogy of a layer of reinforced cloth.

These elastic properties refer to the respective principal directions of each layer.

The reduced stiffness matrix coefficients of the warp layer with respect to the principal direction of the warp layer and thus reinforced cloth layer can be given from Eq. (2.10) as follows:

$$Q_{11}^{wp} = \alpha_{wp} E_{Lwp} \quad Q_{12}^{wp} = \alpha_{wp} \nu_{LTwp} E_{Lwp} \quad Q_{22}^{wp} = \alpha_{wp} E_{Twp} \tag{2.43}$$

$$Q_{16}^{wp} = Q_{26}^{wp} = 0 \quad Q_{66}^{wp} = G_{LTwp} \tag{2.44}$$

where

$$\alpha_{wp} = \frac{1}{1 - \dfrac{E_{Twp}}{E_{Lwp}} \nu_{LTwp}^2}$$

Similarly, the reduced stiffness matrix coefficients of the weft layer can be expressed in its principal directions as follows:

$$Q_{11}^{wf} = \alpha_{wf} E_{Lwf} \quad Q_{12}^{wf} = \alpha_{wf} \nu_{LTwf} E_{Twf} \quad Q_{22}^{wf} = \alpha_{wf} E_{Twf} \tag{2.45}$$

$$Q_{16}^{wf} = Q_{26}^{wf} = 0 \quad Q_{66}^{wf} = G_{LTwf} \tag{2.46}$$

where

$$\alpha_{wf} = \frac{1}{1 - \dfrac{E_{Twf}}{E_{Lwf}} \nu_{LTwf}^2}$$

The extension stiffness matrix coefficients A_{ij} $(i, j = 1, 2, 6)$ given by Eq. (2.12) that define the behavior of the cloth reinforcement layer can be expressed as

$$A_{ij} = h_{wp} Q_{ij}^{wp} + h_{wf} Q_{ij}^{wf} \tag{2.47}$$

where h_{wp} and h_{wf} are warp and weft layer thicknesses expressed as functions of the thickness e_c of the layer and of the balancing coefficient k along the warp in the following forms:

$$h_{wp} = ke_c \quad h_{wf} = (1-k)e_c \tag{2.48}$$

The cloth is specified as unidirectional in both warp and weft directions for $k=1$ and 0, respectively. The cloth is balanced for $k=1$.

The in-plane behavior of a cloth-reinforced layer is defined by the following constitutive equation:

$$\begin{bmatrix} N_x \\ N_y \\ N_{xy} \end{bmatrix} = \begin{bmatrix} A_{11} & A_{12} & 0 \\ A_{12} & A_{22} & 0 \\ 0 & 0 & A_{66} \end{bmatrix} \begin{bmatrix} \varepsilon_{xx}^0 \\ \varepsilon_{yy}^0 \\ \gamma_{xy}^0 \end{bmatrix} \tag{2.49}$$

For the case of tension in the warp direction, in-plane resultant forces are

$$N_x \neq 0, \quad N_y = 0, \quad N_{xy} = 0 \tag{2.50}$$

Then, $N_x = A_{11}\varepsilon_{xx}^0 + A_{12}\varepsilon_{yy}^0$, and hence

$$N_x = \left(A_{11} + \frac{A_{12}^2}{A_{22}}\right)\varepsilon_{xx}^0 \quad \text{can be obtained} \tag{2.51}$$

Elastic properties, the Young modulus, and Poisson's ratio in the weft direction are as following:

$$E_L = \frac{1}{e_c}\left(A_{11} - \frac{A_{12}^2}{A_{22}}\right) \tag{2.52}$$

$$v_{LT} = \frac{A_{12}}{A_{22}} \tag{2.53}$$

For the case of tension in the weft direction, Young's modulus E_T and the Poisson ratio v_{TL} are described, respectively as

$$E_T = \frac{1}{e_c}\left(A_{22} - \frac{A_{12}^2}{A_{11}}\right) \quad v_{TL} = \frac{A_{12}}{A_{11}} = v_{LT}\frac{E_T}{E_L} \tag{2.54}$$

For the case of in-plane shear in the weft direction, the shear modulus G_{LT} is defined as

$$G_{LT} = G_{TL} = \frac{1}{e_c}A_{66} \tag{2.55}$$

The elastic constants of a two-dimensional cloth-reinforced layer obtained by the equations given above can be written in the following form substituting the A_{ij} coefficients as

$$E_L = (1-\alpha)\left[k\alpha_{wp}E_{Lwp} + (1-k)\alpha_{wf}E_{Twf}\right] \tag{2.56}$$

$$E_T = (1-\alpha)\left[k\alpha_{wp}E_{Twp} + (1-k)\alpha_{wf}E_{Lwf}\right] \tag{2.57}$$

$$v_{LT} = \frac{k\alpha_{wp}v_{LTwp}E_{Twp} + (1-k)\alpha_{wf}v_{LTwf}E_{Twf}}{k\alpha_{wp}E_{Twp} + (1-k)\alpha_{wf}E_{Lwf}} \tag{2.58}$$

$$G_{LT} = kG_{LTwp} + (1-k)G_{LTwf} \tag{2.59}$$

where

$$\alpha = \frac{\left[k\alpha_{wp}v_{LTwp}E_{Twp} + (1-k)\alpha_{wf}v_{LTwf}E_{Twf}\right]^2}{\left[k\alpha_{wp}E_{Lwp} + (1-k)\alpha_{wf}E_{Twf}\right]\left[k\alpha_{wp}E_{Twp} + (1-k)\alpha_{wf}E_{Lwf}\right]} \tag{2.60}$$

The above expressions (Eqs. 2.56–2.59) can be simplified for various types of cloths by the value of the balancing coefficient k. For example, in the case where the fibers in the warp and weft directions are identical, the cloth is called balanced [29]. In fact, in this case, $k = 1/2$, and the moduli in warp and weft directions become identical:

$$E_{Lwp} = E_{Lwf} = E_{Lu} \tag{2.61}$$

$$E_{Twp} = E_{Twf} = E_{Tu} \tag{2.62}$$

$$v_{LTwp} = v_{LTwf} = v_{LTu} \tag{2.63}$$

$$G_{LTwp} = G_{LTwf} = G_{LTu} \tag{2.64}$$

where E_{Lu}, E_{Tu}, G_{LTu}, and v_{LTu} are the moduli of a unidirectional layer having a volume fraction equal to that of the reinforced cloth layer. In this regard, Eqs. (2.56)–(2.59) are expressed as follows:

$$E_L = E_T = (1-\alpha)\alpha_u(E_{Lu} + E_{Tu}) \tag{2.65}$$

$$v_{LT} = \frac{2v_{LT_u}}{1 + \dfrac{E_{Lu}}{E_{Tu}}} \tag{2.66}$$

$$G_{LT} = G_{LT_u} \tag{2.67}$$

where

$$\alpha_u = \frac{1}{1 - \dfrac{E_{Tu}}{E_{Lu}}v_{LT_u}^2}$$

2.5 Interface mechanics in fiber-reinforced composites

This section is mainly based on the study presented by Lei et al. [31]. Material's microstructure has an essential role in mechanical behavior of fiber-reinforced composites. As a microstructural entity, "interface" between fiber and matrix components has the responsibility to transfer load from matrix to fiber. However, there are various issues that may occur at the interface including interface debonding and damage. The quality of the interface has a significant effect on mechanical properties such as impact and fracture. Hence, it is important to investigate the behavior of the interface region and its effect on macrostructural properties.

The interface region may encounter several issues. These are interface intact bonding, interface debonding, interface completely debonding, and fiber pullout. During the debonding process, the interface properties continuously change. In order to analyze the interface, it is important to calculate the interfacial stresses. By using Cox's shear-lag model, it is possible to relate the fiber axial stress, σ, and the interfacial shear stress, τ, as

$$\tau = -\frac{r}{2}\left(\frac{d\sigma}{dx}\right) \tag{2.68}$$

Before interface debonding occurs, the fiber axial stress can be expressed by using Piggot's model as

$$\sigma = \sigma_{app}\frac{sinh\left[n(L-x)/r\right]}{sinh\left(ns\right)} \tag{2.69}$$

where x is the distance to the fiber entry, σ_{app} is the stress acting on the fiber out of the matrix, L is the effective length of the stress transfer, s is the fiber aspect ratio, and n is a constant, which depends on geometry and material properties of fiber and matrix.

By using Eqs. (2.68), (2.69), the interfacial shear stress along the fiber can be expressed as

$$\tau = \sigma_{app}\frac{ncosh\left[n(L-x)/r\right]}{sinh\left(ns\right)} \tag{2.70}$$

If a fiber pullout experiment is performed, the aspect ratio of the fiber is large. Therefore, fiber stress and shear stress at the fiber entry, that is, $x = 0$, can be calculated as

$$\sigma_m = \sigma \tag{2.71a}$$

$$\tau_m = \frac{n\sigma}{2} \tag{2.71b}$$

If the fiber stress exceeds the fiber strength σ_b, then fiber fracture can occur. On the other hand, if the interfacial shear stress exceeds the interfacial shear strength τ_b, then interface debonding can occur:

$$\sigma_m = \frac{2\tau_m}{n} \geq \sigma_b \quad \text{Fiber fracture} \tag{2.72a}$$

$$\tau_m = \frac{n\sigma}{2} \geq \tau_b \quad \text{Interface debonding} \tag{2.72b}$$

Moreover, if fiber strength is high and interfacial shear strength is low, then it is likely that interfacial debonding will occur as the damage mode.

2.6 Mechanics of curved composites

This section is mainly based on the study presented by Akbarov and Guz [32]. Curved composites are unidirectional fibrous and layered composites where fibers or layers are in the form of curvatures. These curvatures occur due to either design features or technological processes. If the curvatures are due to design features, then they can be modeled as periodical. However, if the curvatures are due to technological processes, then they are considered as local.

For simplicity, let us assume that curvatures only exist in Ox_1x_2 plane as shown in Fig. 2.10. The total thickness of N number of curved layers can be calculated as

$$\Delta H = h_1 + h_2 + \cdots + h_N \tag{2.73}$$

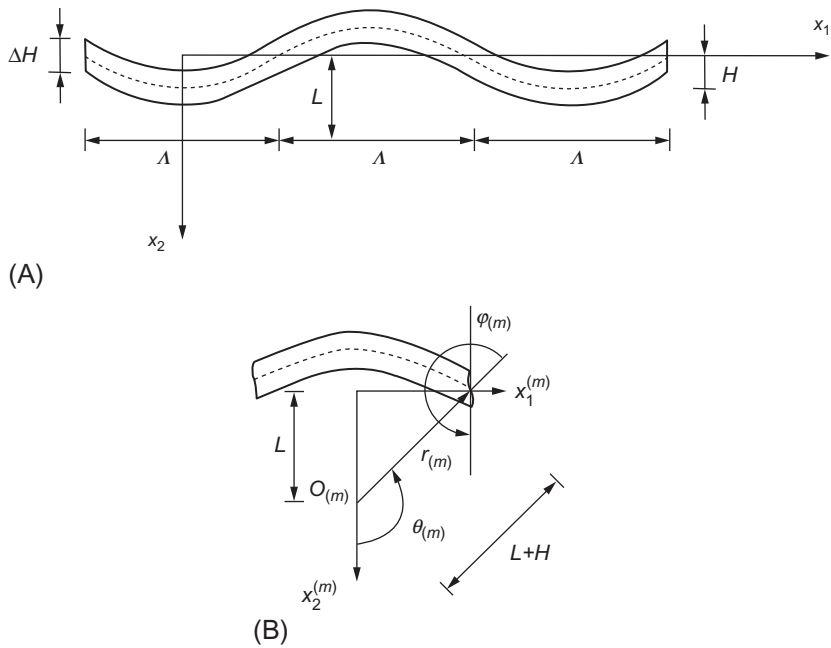

Fig. 2.10 (A) Representative layer and (B) approximation of the representative [32].

where h_i is the thickness of the ith layer. The maximum layer thickness is defined as

$$h' = \max\{h_1, h_2, \ldots, h_N\} \tag{2.74}$$

In Fig. 2.10, Λ is the half wavelength of the curvature, and H is the rise of the curve. It can be assumed that the composite material has a regular and periodic curvature with a period of 2Λ and following conditions should hold

$$h' \ll H, \quad \Delta H \ll \Lambda, \quad H \ll \Lambda, \quad \Lambda \ll L, \quad \Lambda \ll d \tag{2.75}$$

In order to obtain the constitutive relationships, Fig. 2.10A can be approximated as in Fig. 2.10B based on the inequalities given in Eq. (2.70). Note that a local coordinate system is introduced for each half period. For the mth half period, the local Cartesian coordinates are defined as

$$x_1^{(m)} = x_1 - (m-1)\Lambda, \quad x_2^{(m)} = x_2, \quad x_3^{(m)} = x_3 \quad -\infty \le m \le +\infty \tag{2.76}$$

The local Cartesian coordinate system can also be related to a local cylindrical coordinate system as

$$r_{(m)} cos\theta_{(m)} = x_2^{(m)} - (-1)^m L, \quad r_{(m)} sin\theta_{(m)} = x_1^{(m)}, \quad \varphi_{(m)} = 2\pi - \theta_{(m)} \tag{2.77}$$

For the mth half period, the stress-strain relationships in cylindrical coordinates can be written as

$$\sigma_{rr} = \overset{\circ}{A}_{11}\varepsilon_{rr} + \overset{\circ}{A}_{12}\varepsilon_{\theta\theta} + \overset{\circ}{A}_{13}\varepsilon_{33} \tag{2.78a}$$

$$\sigma_{\theta\theta} = \overset{\circ}{A}_{12}\varepsilon_{rr} + \overset{\circ}{A}_{22}\varepsilon_{\theta\theta} + \overset{\circ}{A}_{23}\varepsilon_{33} \tag{2.78b}$$

$$\sigma_{33} = \overset{\circ}{A}_{13}\varepsilon_{rr} + \overset{\circ}{A}_{23}\varepsilon_{\theta\theta} + \overset{\circ}{A}_{33}\varepsilon_{33} \tag{2.78c}$$

$$\sigma_{\theta 3} = 2\overset{\circ}{A}_{44}\varepsilon_{\theta 3} \tag{2.78d}$$

$$\sigma_{r3} = 2\overset{\circ}{A}_{55}\varepsilon_{r3} \tag{2.78e}$$

$$\sigma_{r\theta} = 2\overset{\circ}{A}_{66}\varepsilon_{r\theta} \tag{2.78f}$$

where $\overset{\circ}{A}_{ij}$ and $\overset{\circ}{G}_{ij}$ are effective (normalized) elastic constants and $\overset{\circ}{A}_{44} = \overset{\circ}{G}_{23}$, $\overset{\circ}{A}_{55} = \overset{\circ}{G}_{13}$, and $\overset{\circ}{A}_{66} = \overset{\circ}{G}_{12}$.

Based on the inequalities given in Eq. (2.75), a small parameter, ε, can be defined as

$$\varepsilon = \frac{\Lambda}{\pi L} \ll 1 \tag{2.79}$$

since

$$\Lambda^2 \approx 8LH \quad \text{and} \quad \varepsilon = \frac{\Lambda}{\pi L} \approx \frac{8H}{\pi \Lambda} \ll 1 \tag{2.80}$$

Hence, the stress-strain relationships given in Eqs. (2.78a)–(2.78f) can be written in Cartesian coordinates by using the parameter ε as

$$\sigma_{11} = A_{11}\varepsilon_{11} + A_{12}\varepsilon_{22} + A_{13}\varepsilon_{33} + 2A_{16}\varepsilon_{12} \tag{2.81a}$$

$$\sigma_{22} = A_{12}\varepsilon_{11} + A_{22}\varepsilon_{22} + A_{23}\varepsilon_{33} + 2A_{26}\varepsilon_{12} \tag{2.81b}$$

$$\sigma_{33} = A_{13}\varepsilon_{11} + A_{23}\varepsilon_{22} + A_{33}\varepsilon_{33} + 2A_{36}\varepsilon_{12} \tag{2.81c}$$

$$\sigma_{12} = A_{16}\varepsilon_{11} + A_{26}\varepsilon_{22} + A_{36}\varepsilon_{33} + 2A_{66}\varepsilon_{12} \tag{2.81d}$$

$$\sigma_{23} = 2A_{44}\varepsilon_{23} + 2A_{45}\varepsilon_{13} \tag{2.81e}$$

$$\sigma_{13} = 2A_{45}\varepsilon_{23} + 2A_{65}\varepsilon_{13} \tag{2.81f}$$

where

$$A_{11} = A_{11}^{\circ} + \varepsilon^2\left(-A_{11}^{\circ} + A_{12}^{\circ} + 2G_{12}^{\circ}\right)2sin^2\theta \tag{2.82a}$$

$$A_{12} = A_{12}^{\circ} + \varepsilon^2\left(A_{11}^{\circ} + A_{22}^{\circ} - 2A_{12}^{\circ} - 4G_{12}^{\circ}\right)sin^2\theta \tag{2.82b}$$

$$A_{23} = A_{23}^{\circ} + \varepsilon^2\left(A_{13}^{\circ} - A_{23}^{\circ}\right)sin^2\theta \tag{2.82c}$$

$$A_{16} = \varepsilon\left(-A_{11}^{\circ} + A_{12}^{\circ} + 2G_{12}^{\circ}\right)sin\theta \tag{2.82d}$$

$$A_{26} = \varepsilon\left(A_{11}^{\circ} - A_{12}^{\circ} - 2G_{12}^{\circ}\right)sin\theta \tag{2.82e}$$

$$A_{36} = \varepsilon\left(A_{23}^{\circ} - A_{13}^{\circ}\right)sin\theta \tag{2.82f}$$

$$A_{33} = A_{33}^{\circ} \tag{2.82g}$$

$$A_{22} = A_{22}^{\circ} + \varepsilon^2\left(-A_{22}^{\circ} + A_{12}^{\circ} + 2G_{12}^{\circ}\right)2sin^2\theta \tag{2.82h}$$

$$A_{13} = A_{13}^{\circ} + \varepsilon^2\left(A_{23}^{\circ} - A_{13}^{\circ}\right)sin^2\theta \tag{2.82i}$$

$$A_{44} = G_{23}^{\circ} + \varepsilon^2\left(G_{13}^{\circ} - G_{23}^{\circ}\right)sin^2\theta \tag{2.82j}$$

$$A_{66} = G_{12}^{\circ} + \varepsilon^2\left(A_{11}^{\circ} + A_{22}^{\circ} - 2A_{12}^{\circ} - 2G_{12}^{\circ}\right)sin^2\theta \tag{2.82k}$$

$$A_{45} = \varepsilon\left(G_{13}^{\circ} - G_{23}^{\circ}\right)sin\theta \tag{2.82l}$$

$$A_{55} = G_{13}^{\circ} + \varepsilon^2 \left(G_{23}^{\circ} - G_{13}^{\circ}\right) sin^2\theta \tag{2.82m}$$

and

$$\theta = \frac{\pi X_1}{\Lambda} \tag{2.83}$$

The formulation can be extended to 3D by considering the periodic curved structure. In this case, the half wavelengths are labeled as $\Lambda 1$ and $\Lambda 3$ along *Ox1* and *Ox3* directions, respectively. The equation of the median surface can be expressed as

$$x_2 = F(x_1, x_3) = \varepsilon f(x_1, x_3) \tag{2.84}$$

The stress-strain relationship for the midsurface can be defined by using the local coordinate system *Ox1*, *Ox2*, and *Ox3*:

$$\sigma_i = A_{ij}^{\circ} \varepsilon_j \tag{2.85a}$$

where

$$\sigma_i = \sigma_{ii} \ (i = 1,2,3) \tag{2.85b}$$

$$\varepsilon_i = \varepsilon_{ii} \ (i = 1,2,3) \tag{2.85c}$$

$$\sigma_4 = \sigma_{23} \tag{2.85d}$$

$$\sigma_5 = \sigma_{13} \tag{2.85e}$$

$$\sigma_6 = \sigma_{12} \tag{2.85f}$$

$$\varepsilon_4 = \varepsilon_{23} \tag{2.85g}$$

$$\varepsilon_5 = \varepsilon_{13} \tag{2.85h}$$

$$\varepsilon_6 = \varepsilon_{12} \tag{2.85i}$$

These relationships can also be expressed in global coordinates:

$$\sigma_i = A_{ij} \varepsilon_j \quad i, j = 1,2,3,4,5,6 \tag{2.86}$$

where the material constants in global coordinates are functions of the equation of the median surface:

$$A_{ij} = A_{ij}\left(A_{nm}^{\circ}, F(x_1, x_3)\right) \tag{2.87}$$

By satisfying the following condition

$$\varepsilon^2\left[\left(\frac{\partial f}{\partial x_1}\right)^2+\left(\frac{\partial f}{\partial x_3}\right)^2\right]<1 \quad 0\le\varepsilon<1 \tag{2.88}$$

The material constants can be expressed as

$$A_{ij}=\begin{cases} A_{ij}^{\circ}+\sum_{k=1}^{\infty}\varepsilon^{2k}A_{ijk} & \text{for combinations } ij=11,12,13,22,23,33,44,55,66 \\ \sum_{k=1}^{\infty}\varepsilon^{2k-1}A_{ijk} & \text{for combinations } ij=14,16,24,26,34,45,56 \\ \sum_{k=1}^{\infty}\varepsilon^{2k}A_{ijk} & \text{for combinations } ij=15,25,35,46 \end{cases} \tag{2.89}$$

Explicit forms of A_{ijk} are given in Ref. [33]. Moreover, by using Eq. (2.89), Eq. (2.86) can be rewritten as

$$\sigma_{ij}=\mu_{ij\alpha\beta}\frac{\partial u_\alpha}{\partial x_\beta} \quad i,j,\alpha,\beta=1,2,3 \tag{2.90}$$

where

$$\mu_{ij\alpha\beta}=\mu^0_{ij\alpha\beta}+\sum\nolimits_{k=1}^{\infty}\varepsilon^{2k-1}\mu^{(2k)}_{ij\alpha\beta}+\sum\nolimits_{k=1}^{\infty}\varepsilon^{2k}\mu^{(2k)}_{ij\alpha\beta} \tag{2.91}$$

Explicit forms of $\mu^{0}_{ij\alpha\beta}$, $\mu^{(2k-1)}_{ij\alpha\beta}$, and $\mu^{(2k)}_{ij\alpha\beta}$ are given in Ref. [32]. Finally, the equation of motion, that is,

$$\frac{\partial\sigma_{ij}}{\partial x_j}=\rho\frac{\partial^2 u_i}{\partial t^2} \tag{2.92}$$

can be written by utilizing the expressions given in Eqs. (2.90), (2.91), as

$$L_{i\alpha}u_\alpha+\sum\nolimits_{k=1}^{\infty}\varepsilon^{2k}K_{i\alpha k}u_\alpha+\sum\nolimits_{k=1}^{\infty}\varepsilon^{2k-1}R_{i\alpha k}u_\alpha=0 \tag{2.93}$$

where

$$L_{i\alpha}=\mu^{(0)}_{ij\alpha\beta}\frac{\partial^2}{\partial x_j\partial x_\beta}-\rho\delta_i^\alpha\frac{\partial^2}{\partial t^2} \tag{2.94a}$$

$$K_{i\alpha k}=\frac{\partial}{\partial x_j}\left(\mu^{(2k)}_{ij\alpha\beta}\frac{\partial}{\partial x_\beta}\right) \tag{2.94b}$$

$$R_{i\alpha k} = \frac{\partial}{\partial x_j}\left(\mu_{ij\alpha\beta}^{(2k-1)}\frac{\partial}{\partial x_\beta}\right) \tag{2.94c}$$

and δ is the Kronecker delta.

It is not possible to obtain closed-form solutions for Eq. (2.93). However, an approximate solution can be obtained by expressing physical quantities in the series of the small parameter, ε:

$$\sigma_{ij} = \sum_{q=0}^{\infty}\varepsilon^q\sigma_{ij}^{(q)} \tag{2.95a}$$

$$\varepsilon_{ij} = \sum_{q=0}^{\infty}\varepsilon^q\varepsilon_{ij}^{(q)} \tag{2.95b}$$

$$u_i = \sum_{q=0}^{\infty}\varepsilon^q u_i^{(q)} \tag{2.95c}$$

$$P_j = \sum_{q=0}^{\infty}\varepsilon^q P_j^{(q)} \tag{2.95d}$$

$$\varphi_i = \sum_{q=0}^{\infty}\varepsilon^q\varphi_i^{(q)} \tag{2.95e}$$

Hence, the equation of motion can be rewritten as (Fig. 2.11)

$$L_{i\alpha}u_\alpha^{(q)} + \sum_{k=1}^{q/2}K_{i\alpha k}u_\alpha^{(q-2k)} + \sum_{k=1}^{(q+1)/2}R_{i\alpha k}u_\alpha^{(q+1-2k)} = 0 \tag{2.96}$$

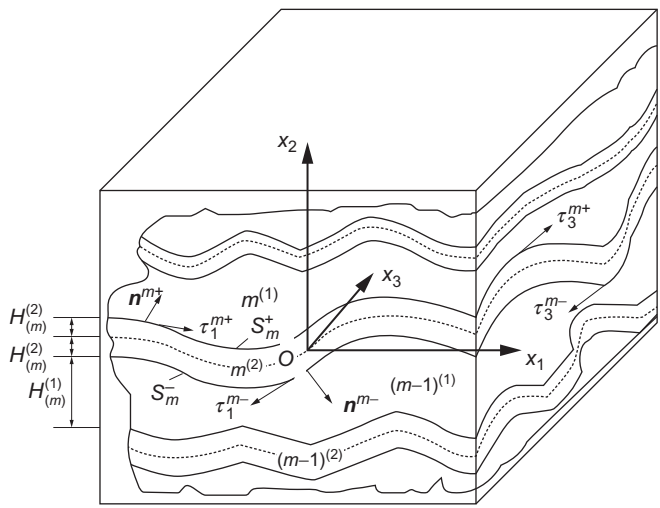

Fig. 2.11 Laminated composite [32].

The formulation can also be extended for laminated composites by imposing complete cohesion conditions between the layers:

$$\sigma_{ij}^{(1)m}|_{S_m^+} n_j^{m,+} = \sigma_{ij}^{(2)m}|_{S_m^+} n_j^{m,+}, \quad \sigma_{ij}^{(1)m_1}|_{S_m^-} n_j^{m,-} = \sigma_{ij}^{(2)m_1}|_{S_m^-} n_j^{m,-} \tag{2.97a}$$

$$u_i^{(1)m}|_{S_m^+} = u_i^{(2)m}|_{S_m^+}, \quad u_i^{(1)m_1}|_{S_m^-} = u_i^{(2)m_1}|_{S_m^-} \tag{2.97b}$$

where s_m^+ and s_m^- are upper and lower surfaces of the $m^{(2)}$ th filler layer $m_1 = m - 1$.

2.7 Strength failure theories

2.7.1 Introduction

Since a composite material is obviously heterogeneous at the constituent material level, material properties and stress-strain relations may change from point to point. However, the macromechanical stress-strain relations of a lamina can be expressed in terms of average values of stress and strain and effective properties of an equivalent homogenous material [34]. In this part, first, the constitutive equations for an orthotropic material will be introduced. Then, determination of strength and stiffness of an orthotropic lamina will be emphasized. Finally, biaxial strength criteria regarding an orthotropic lamina will be acquainted.

2.7.2 Constitutive equations for orthotropic materials

A unidirectionally reinforced lamina in the L-T plane is illustrated in Fig. 2.12. For this lamina, a state of plane stress can be defined by the settings

$$\sigma_Z = 0 \quad \tau_{TZ} = 0 \quad \tau_{ZL} = 0 \tag{2.98}$$

and

$$\sigma_L \neq 0 \quad \sigma_T \neq 0 \quad \tau_{LT} \neq 0 \tag{2.99}$$

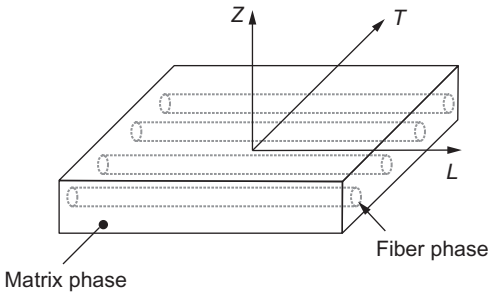

Fig. 2.12 Principal material axes for an orthotropic lamina.

The state of plane stress is an idealization for practical usage of a lamina having fibers in its plane. It is considered that a single lamina can withstand against only in-plane loadings since its capability of load carrying in-plane is natural. Some examples such as automobile panels, thin-pressure vessels, fuselages, and wings of aircraft may be given for the in-plane loaded structural elements [35].

For an orthotropic lamina imposed to the plane stress state, the following strains emerge in the out-of-plane

$$\varepsilon_Z = S_{13}\sigma_L + S_{23}\sigma_T \quad \gamma_{TZ} = 0 \quad \gamma_{ZL} = 0 \tag{2.100}$$

where

$$S_{13} = -\frac{\nu_{LZ}}{E_L} = -\frac{\nu_{ZL}}{E_Z} \quad S_{23} = -\frac{\nu_{TZ}}{E_T} = -\frac{\nu_{ZT}}{E_Z} \tag{2.101}$$

The strain-stress relations in the L-T plane is written in the matrix form as

$$\begin{Bmatrix} \varepsilon_L \\ \varepsilon_T \\ \gamma_{LT} \end{Bmatrix} = \begin{bmatrix} S_{11} & S_{12} & 0 \\ S_{12} & S_{22} & 0 \\ 0 & 0 & S_{66} \end{bmatrix} \begin{Bmatrix} \sigma_L \\ \sigma_T \\ \tau_{LT} \end{Bmatrix} \text{ or } \begin{Bmatrix} \varepsilon_L \\ \varepsilon_T \\ \gamma_{LT} \end{Bmatrix} = [S] \begin{Bmatrix} \sigma_L \\ \sigma_T \\ \tau_{LT} \end{Bmatrix} \tag{2.102}$$

where square matrix is the compliance matrix $[S_{ij}]$, members of which are given in terms of the engineering constants as

$$S_{11} = \frac{1}{E_L} \quad S_{22} = \frac{1}{E_T} \quad S_{12} = -\frac{\nu_{LT}}{E_L} = -\frac{\nu_{TL}}{E_T} \quad S_{66} = \frac{1}{G_{LT}} \tag{2.103}$$

When Eq. (2.102) is inverted, the stress-strain relations are written as

$$\begin{Bmatrix} \sigma_L \\ \sigma_T \\ \tau_{LT} \end{Bmatrix} = \begin{bmatrix} Q_{11} & Q_{12} & 0 \\ Q_{12} & Q_{22} & 0 \\ 0 & 0 & Q_{66} \end{bmatrix} \begin{Bmatrix} \varepsilon_L \\ \varepsilon_T \\ \gamma_{LT} \end{Bmatrix} \text{ or } \begin{Bmatrix} \sigma_L \\ \sigma_T \\ \tau_{LT} \end{Bmatrix} = [Q] \begin{Bmatrix} \varepsilon_L \\ \varepsilon_T \\ \gamma_{LT} \end{Bmatrix} \tag{2.104}$$

where the $[Q]$ is the so-called reduced stiffness matrix, members of which are written in terms of the engineering constants (see Eq. 2.10).

From the Q_{12} given by Eq. (2.10), the following reciprocal relation reveals

$$\nu_{TL}E_L = \nu_{LT}E_T \quad \text{or} \quad \frac{\nu_{LT}}{E_L} = \frac{\nu_{TL}}{E_T} \tag{2.105}$$

2.7.2.1 Stress-strain relations for a lamina of arbitrary orientation

Because the laminates have low stiffness and strength properties in the transverse direction, they are not often formed only as unidirectional laminae. For this purpose,

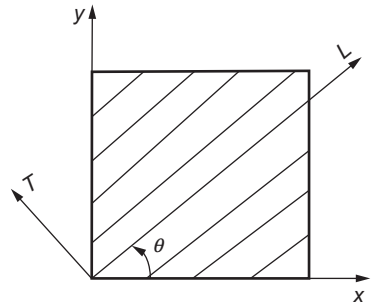

Fig. 2.13 Positive rotation of principal material axes from *x*-*y* axes.

some laminae in the laminates may be placed at different angles. It is thus necessary to develop the stress-strain or the strain-stress relations for an angle lamina. The coordinate systems used for an angle lamina are given in Fig. 2.13. The axes *L*-*T* are called the principal material or local axes, in which the direction *L* is parallel to the fibers and the direction *T* is perpendicular (transverse) to the fibers. The axes *x*-*y* are called the global axes or the off axes. The angle between the two axes is denoted by an angle θ. A relation is, now, needed between the stresses and strains and those in the structure axes. Then, stress-strain relations should be transformed from one coordinate system to another.

At this point, the global and local stresses in any angle lamina are related to each other through the reinforcement angle, θ:

$$\begin{Bmatrix} \sigma_L \\ \sigma_T \\ \tau_{LT} \end{Bmatrix} = [T] \begin{Bmatrix} \sigma_x \\ \sigma_y \\ \tau_{xy} \end{Bmatrix} \quad \text{and} \quad \begin{Bmatrix} \sigma_x \\ \sigma_y \\ \tau_{xy} \end{Bmatrix} = [T]^{-1} \begin{Bmatrix} \sigma_L \\ \sigma_T \\ \tau_{LT} \end{Bmatrix} \tag{2.106}$$

where $[T]$ and $[T]^{-1}$ are the transformation matrix and its inverse, which are defined taking as $s = sin\ \theta$ and $c = cos\ \theta$:

$$[T] = \begin{bmatrix} c^2 & s^2 & -2cs \\ s^2 & s^2 & 2cs \\ cs & -cs & c^2 - s^2 \end{bmatrix} \quad \text{and} \quad [T]^{-1} = \begin{bmatrix} c^2 & s^2 & 2cs \\ s^2 & s^2 & -2cs \\ -cs & cs & c^2 - s^2 \end{bmatrix} \tag{2.107}$$

Similarly, the strain-transformation equations are as

$$\begin{Bmatrix} \varepsilon_L \\ \varepsilon_T \\ \frac{1}{2}\gamma_{LT} \end{Bmatrix} = [T] \begin{Bmatrix} \varepsilon_x \\ \varepsilon_y \\ \frac{1}{2}\gamma_{xy} \end{Bmatrix} \quad \text{and} \quad \begin{Bmatrix} \varepsilon_x \\ \varepsilon_y \\ \frac{1}{2}\gamma_{xy} \end{Bmatrix} = [T]^{-1} \begin{Bmatrix} \varepsilon_L \\ \varepsilon_T \\ \frac{1}{2}\gamma_{LT} \end{Bmatrix} \tag{2.108}$$

However, with a matrix $[R]$ introduced by Reuter,

$$[R] = \begin{bmatrix} 1 & 0 & 0 \\ 0 & 1 & 0 \\ 0 & 0 & 2 \end{bmatrix} \tag{2.109}$$

the strain-transformation equations can be rewritten as

$$\begin{Bmatrix} \varepsilon_L \\ \varepsilon_T \\ \gamma_{LT} \end{Bmatrix} = [R] \begin{Bmatrix} \varepsilon_L \\ \varepsilon_T \\ \frac{1}{2}\gamma_{LT} \end{Bmatrix} \quad \text{and} \quad \begin{Bmatrix} \varepsilon_x \\ \varepsilon_y \\ \gamma_{xy} \end{Bmatrix} = [R] \begin{Bmatrix} \varepsilon_x \\ \varepsilon_y \\ \frac{1}{2}\gamma_{xy} \end{Bmatrix} \tag{2.110}$$

When Eqs. (2.102, 2.104, 2.106–2.110) obtained above are combined according to the rules of matrix, the stress-strain relations in x-y plane are found as [3,35]

$$\begin{Bmatrix} \sigma_x \\ \sigma_y \\ \tau_{xy} \end{Bmatrix} = [T]^{-1} \begin{Bmatrix} \sigma_L \\ \sigma_T \\ \tau_{LT} \end{Bmatrix} = [T]^{-1}[Q][R][T][R]^{-1} \begin{Bmatrix} \varepsilon_x \\ \varepsilon_y \\ \gamma_{xy} \end{Bmatrix} \tag{2.111}$$

in which $[R][T][R]^{-1}$ is shortly $[T]^{-T}$ where the superscript T denotes the matrix transpose. With the use of abbreviation in the form of $\left[\bar{Q}\right] = [T]^{-1}[Q][T]^{-T}$, the stress-strain relations in x-y coordinates becomes

$$\begin{Bmatrix} \sigma_x \\ \sigma_y \\ \tau_{xy} \end{Bmatrix} = \left[\bar{Q}\right] \begin{Bmatrix} \varepsilon_x \\ \varepsilon_y \\ \gamma_{xy} \end{Bmatrix} = \begin{bmatrix} \bar{Q}_{11} & \bar{Q}_{12} & \bar{Q}_{16} \\ \bar{Q}_{12} & \bar{Q}_{22} & \bar{Q}_{26} \\ \bar{Q}_{16} & \bar{Q}_{26} & \bar{Q}_{66} \end{bmatrix} \begin{Bmatrix} \varepsilon_x \\ \varepsilon_y \\ \gamma_{xy} \end{Bmatrix} \tag{2.112}$$

in which $\left[\bar{Q}\right]$ denotes the transformed reduced stiffness matrix (see Eq. 2.9).

Similarly, the strain-stress relations in x-y coordinates can be written as

$$\begin{Bmatrix} \varepsilon_x \\ \varepsilon_y \\ \gamma_{xy} \end{Bmatrix} = [\bar{S}] \begin{Bmatrix} \sigma_x \\ \sigma_y \\ \tau_{xy} \end{Bmatrix} = \begin{bmatrix} \bar{S}_{11} & \bar{S}_{12} & \bar{S}_{16} \\ \bar{S}_{12} & \bar{S}_{22} & \bar{S}_{26} \\ \bar{S}_{16} & \bar{S}_{26} & \bar{S}_{66} \end{bmatrix} \begin{Bmatrix} \sigma_x \\ \sigma_y \\ \tau_{xy} \end{Bmatrix} \tag{2.113}$$

in which the $[\bar{S}]$ denotes the transformed reduced compliance matrix, elements of which are written similar to the $\left[\bar{Q}\right]$

$$\begin{aligned}
\bar{S}_{11} &= S_{11}c^4 + (2S_{12} + S_{66})s^2c^2 + S_{22}s^4 \\
\bar{S}_{22} &= S_{11}s^4 + (2S_{12} + S_{66})s^2c^2 + S_{22}c^4 \\
\bar{S}_{12} &= (S_{11} + S_{22} - S_{66})s^2c^2 + S_{12}\left(s^4 + c^4\right) \\
\bar{S}_{16} &= 2(S_{11} - S_{12} - 0.5S_{66})sc^3 - 2(S_{22} - S_{12} - 0.5S_{66})s^3c \\
\bar{S}_{26} &= 2(S_{11} - S_{12} - 0.5S_{66})s^3c + 2(S_{22} - S_{12} - 0.5S_{66})sc^3 \\
\bar{S}_{66} &= 4(S_{11} + S_{22} - 2S_{12} - 0.5S_{66})s^2c^2 + S_{66}\left(s^4 + c^4\right)
\end{aligned} \tag{2.114}$$

2.7.3 Determination of strength and stiffness of an orthotropic lamina

Both strength and stiffness characteristics of an orthotropic lamina are reasonably necessary for the design of laminates. The axes of principal stress do not coincide with the axes of principal strain due to orthotropy. In a given lamina, the strength in one direction can be higher than another; the highest stress might not be the stress governing the design. Therefore, a rational comparison of the actual stress field with the allowable stress field can be required, irrespective of any principal values. The first step in such a procedure is the establishments of the allowable stresses or strengths in the principal material directions, which is the basic of the study of strength for an orthotropic lamina [35].

The three basic strengths in a lamina under in-plane loading can be mentioned, which are shown in Fig. 2.14 when the tensile strength is equal to the compressive strength in it:

X is the axial (longitudinal) strength (in the 1-direction)
Y is thetransverse strength (in the 2-direction)
S is the shear strength (in the 1–2 plane)

If a lamina has different mechanical properties in tension and compression, five strengths are needed as

X_t is the axial (longitudinal) strength in tension
X_c is the axial (longitudinal) strength in compression
Y_t is the transverse strength in tension
Y_c is the transverse strength in compression
S is the shear strength

2.7.3.1 Determination of stiffness and strength for a lamina

The properties (stiffness and strength) in the principal material axis can be determined with some experiments. If the experiments are performed properly, the strength and stiffness values of the material may be adequately revealed. The stiffness characteristics of a lamina are listed as follows:

E_L is the Young's modulus in the longitudinal (fiber) direction
E_T is the Young's modulus in the transverse direction
G_{LT} is the Shearing modulus
ν_{LT} is the Major Poisson's ratio
ν_{TL} is the Minor Poisson's ratio

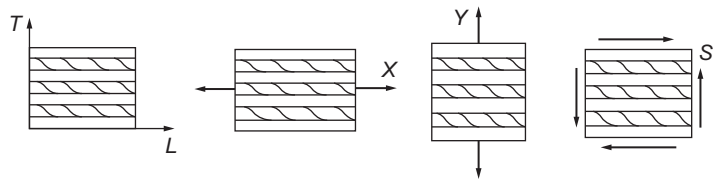

Fig. 2.14 Basic strengths for orthotropic lamina.

where only three of E_L, E_T, ν_{LT}, and ν_{TL} are independent. E_L and ν_{LT} may be measured by a tension-test fixture using a sample in the fiber direction. While the normal strain-strain (ε_L-σ_L) values in the fiber direction are sufficient for E_L, the transverse (ε_T) strain in addition to ε_L is necessary for determination of Poisson's ratio ν_{LT}. Similarly, E_T and ν_{TL} may be measured by a tension-test fixture using a sample in the transverse direction. While the normal strain-strain (ε_T-σ_T) values in the transverse direction are sufficient for E_T, the transverse (ε_L) strain in addition to ε_T is needed for Poisson's ratio ν_{TL}. Upon determination of these for the elastic properties, the satisfaction in terms of correctness of the conducted experiments may be done with Eq. (2.105) as follows:

$$\frac{\nu_{LT}}{E_L} = \frac{\nu_{TL}}{E_T} \tag{2.115}$$

For the determination of the remaining property G_{12}, there are several experimental techniques such as 45° off-axis test, torsion-tube test, sandwich crossbeam test, rail shear test, and Iosipescu test.Also, the strength characteristics for a lamina are listed as follows:

X (X_t or X_c) is the Longitudinal (tensile or compressive) strength (L-direction)
Y (Y_t or Y_c) is the Transverse (tensile or compressive) strength (T-direction)
S is the Shear strength (L-T plane)

where tensile or compressive strengths are of different values for some materials. The strengths X (X_t or X_c) and Y (Y_t or Y_c) can be determined by a tensile test machine. The shear strength S may be obtained by means of experiments such as torsion-tube test, rail shear test, and Iosipescu test [34,35].

2.7.4 Biaxial strength criteria for an orthotropic lamina

Although the strength of a material is determined by uniaxial tests, in fact, the structural elements may be exposed to biaxial or triaxial state of stress. Therefore, uniaxial strength values obtained for principal axis are classed with those of multiaxial loading conditions for the design of elements of machine and structure.

The strengths of principal material directions are X_t, X_c, Y_t, and Y_c, which are tensile and compressive strength in the fiber direction and transverse direction, respectively, and S is shearing strength. However, since tensile and compressive strengths of some materials are same, they are described as X in the fiber direction and Y in transverse direction.

Some criteria such as the maximum normal, the maximum shearing (Tresca), and the maximum distortional energy (von Mises) are fairly well for the conventional engineering materials, which are accepted as isotropic. Unfortunately, these theories are not adequate for composite materials. For this reason, the following biaxial strength criteria that are commonly exploited for the design of composites will be examined: (a) Tsai-Hill failure criterion, (b) Hoffman failure criterion, and (c) Tsai-Wu tensor failure criterion. In the implementations of these criteria, composite material is regarded as orthotropic and homogeneous, and the stress components

calculated from the loadings at the different angles are needed to be transformed into the biaxial stress components in the principal material axis.

2.7.4.1 Tsai-Hill failure criterion

Tsai-Hill failure criterion, which is related to the amount of distortion energy rather than dilatation for any isotropic body, is an adapted version of von Mises' yield criterion to orthotropic composite plates. It is, however, known that distortion is not independent from dilatation in orthotropic materials. Although detailed information given in the bibliography [35], Tsai-Hill failure criterion for an orthotropic plate can be expressed in the form:

$$\frac{\sigma_L^2}{X^2} - \frac{\sigma_L \sigma_T}{X^2} + \frac{\sigma_T^2}{Y^2} + \frac{\tau_{LT}^2}{S^2} = 1 \tag{2.116}$$

where σ_L, σ_T, and τ_{LT} are the transformed stresses into the principle axis and X, Y, and S are failure principle strengths for a single orthotropic lamina. Here, X_t or X_c and Y_t or Y_c should be employed depending on the signs of σ_L and σ_T. According to this theory, when Eq. (2.116) is greater than or equal to 1, the lamina is accepted to be damaged.

It is reported that the agreement is quite good between the Tsai-Hill failure criterion and experiment from the results obtained, for some materials, for example, the E-glass-epoxy at various orientations in biaxial stress states [35]. Hence, the Tsai-Hill failure criterion is applicable to failure prediction for composite materials. However, the applicability of a failure criterion depends on whether the material is brittle or ductile. Therefore, it would be advisable to browse other some criteria.

2.7.4.2 Hoffman failure criterion

Some materials, when subjected to tensile and compressive loadings, exhibit different behaviors. On this occasion, Hoffman had developed an equation for especially brittle materials inspired by the Tsai-Hill failure criterion. Hoffman failure criterion can be expressed in the following form:

$$-\frac{\sigma_L^2}{X_c X_t} + \frac{\sigma_L \sigma_T}{X_c X_t} - \frac{\sigma_T^2}{Y_c Y_t} + \frac{X_c + X_t}{X_c X_t}\sigma_1 + \frac{Y_L + Y_T}{Y_c Y_t}\sigma_2 + \frac{\tau_{LT}^2}{S^2} = 1 \tag{2.117}$$

The Hoffman failure criterion comes to the same point with the Tsai-Hill criterion for equal strength values in tension and compression. It is noted that the Hoffman failure criterion is in good agreement with some materials such as glass-epoxy, graphite-epoxy, and boron-epoxy [35].

2.7.4.3 Tsai-Wu tensor failure criterion

This failure theory is based on the total strain energy failure theory of Beltrami, which is widely used for composite materials with different strengths in tension and compression [3,36]. Even if the proceeding biaxial failure criteria give very good results

for some materials, they are inadequate in their representation of experimental data for some other materials. For this purpose, Tsai and Wu had improved the correlation between a criterion and experiment, which increased the number of terms in the prediction equation. In order to symbolize the interaction between stresses in two directions a new strength should be defined.

Tsai and Wu had postulated a new formula for the Tsai-Wu tensor failure criterion that considerably resembles the Tsai-Hill failure criterion as follows:

$$\frac{\sigma_L^2}{X^2} - 2F_{12}\sigma_L\sigma_T + \frac{\sigma_T^2}{Y^2} + \frac{\tau_{LT}^2}{S^2} = 1 \tag{2.118}$$

where F_{12}, a coefficient of the product of σ_1 and σ_2, is not $-X^{-2}$ and thus it differs from the Tsai-Hill failure criterion. F_{12} can be determined with only a biaxial tension test described by $\sigma_1 = \sigma_2 = \sigma$, and all other stresses are zero. For calculating the value of F_{12}, an empirical expression is suggested as [3]

$$F_{12} = -\frac{1}{2}\sqrt{\frac{1}{X_t X_c Y_t Y_c}} \tag{2.119}$$

Since the Tsai-Wu tensor failure criterion discriminates between the compressive and tensile strengths of a lamina, this failure theory has more general use than the Tsai-Hill failure theory.

2.8 Dynamic behavior of composites

This section presents dynamic behavior of composites by discussing longitudinal vibration of bars, transverse vibration of beams and laminated plates, and damping analysis of composites.

2.8.1 Longitudinal vibrations in composite bars

Linear longitudinal vibrations in a homogeneous isotropic bar (Fig. 2.15) are governed by the equation:

$$\frac{\partial}{\partial x}\left(AE\frac{\partial u}{\partial x}\right) = \rho A\frac{\partial^2 u}{\partial t^2} \tag{2.120}$$

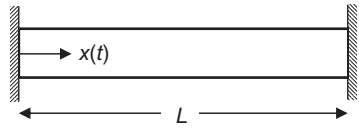

Fig. 2.15 Linear fixed-fixed bar of length L and cross-sectional area A.

where x is the distance from the left end of the bar, t is time, u is the longitudinal displacement of cross section $A(x)$ at a distance x from end of the bar and time t, ρ is mass density of the bar, and $E(x)$ is the modulus of elasticity of the bar.

As for a heterogeneous linear elastic composite bar, the density ρ and the elasticity modulus E in Eq. (2.120) can be replaced with the effective properties of an equivalent homogeneous material. The effective modulus E will specifically depend on the orientation of fibers relative to the axis of the bar, namely, $E = E_1$ and $E = E_2$ for longitudinal and transverse directions, respectively.

If the cross-sectional area and the elasticity modulus are constants, Eq. (2.120) will reduce to

$$c^2 \frac{\partial^2 u}{\partial x^2} = \frac{\partial^2 u}{\partial t^2} \tag{2.121}$$

where c is the wave speed and given as $c = \sqrt{E/\rho}$.

Separation of variables can be used to solve Eq. (2.121) by assuming a solution of the form:

$$u(x,t) = \chi(x)T(t) \tag{2.122}$$

where $\chi(x)$ is a function of x alone, but not on t, and $T(t)$ is a function of t alone, but not on x. When this assumed solution is substituted into Eq. (2.121), then variables are separated:

$$c^2 \frac{1}{\chi}\frac{d^2\chi}{dx^2} = \frac{1}{T}\frac{d^2T}{dt^2} \tag{2.123}$$

is obtained. The left-hand side of Eq. (2.123) is a function of x alone, but not on t, and the right-hand side of it is a function of t alone, but not on x, which can be possible only if both are equal to a constant, and let this constant be $-\omega^2$. Then, Eq.(2.123) can be written as two ordinary differential equations as follows:

$$\frac{d^2T}{dt^2} + \omega^2 T = 0 \tag{2.124a}$$

$$\frac{d^2\chi}{dx^2} + \left(\frac{\omega}{c}\right)^2 \chi = 0 \tag{2.124b}$$

Solutions to these equations are given in the form of

$$T(t) = c_1 \sin \omega t + c_2 \cos \omega t \tag{2.125a}$$

$$\chi(x) = c_3 \sin \frac{\omega}{c}x + c_4 \cos \frac{\omega}{c}x \tag{2.125b}$$

where constants c_1 and c_2 can be determined from initial conditions and constants c_3 and c_4 can be determined from boundary conditions. When boundary conditions of

$u(0,t)=0$ and $u(L,t)=0$ for a fixed-fixed bar is substituted into Eq. (2.125b), $c_4=0$ and

$$sin\frac{\omega}{c}L=0 \tag{2.126}$$

are found. Similarly, boundary conditions for other types of end supports can easily be found in any vibration books.

Eq. (2.126) is an eigenvalue equation, and hence, it has an infinite number of solutions as follows:

$$\frac{\omega_n L}{c}=n\pi \quad n=1,2,\ldots \tag{2.127}$$

where n is the mode number and ω_n natural frequencies in radians per seconds. Therefore, displacements for the nth mode of vibration is given as

$$u_n(x,t)=(A\,sin\,\omega_n t+B\,cos\,\omega_n t)sin\frac{n\pi x}{L} \tag{2.128}$$

where $A=c_1c_3$ and $B=c_2c_3$. The eigenfunction providing the mode shape for the nth mode is given by

$$\chi_n(x)=sin\frac{n\pi x}{L} \tag{2.129}$$

Finally, the general solution is obtained by summing up all modal responses as follows:

$$u(x,t)=\sum\nolimits_{n=1}^{\infty}(A\,sin\,\omega_n t+B\,cos\,\omega_n t)sin\frac{n\pi x}{L} \tag{2.130}$$

Mode shapes and natural frequencies for the first three modes are depicted in Fig. 2.16 for a fixed-fixed bar of length L, cross-sectional area A, and modulus of elasticity E.

One of the basic approaches for determining mechanical properties of composite materials is vibration experiments. Specifically, if the natural frequency of the nth mode is measured in an experiment, one can easily determine the effective modulus of the composite material.

2.8.2 Transverse vibration of composite beams

Linear transverse vibration of a homogeneous, isotropic, elastic beam (Fig. 2.17) can be governed by the Bernoulli-Euler-type equation without taking into consideration shear and rotary inertia effects during the formulation, which is given as

$$-\frac{\partial^2}{\partial x^2}\left(EI\frac{\partial^2 w}{\partial x^2}\right)=\rho A\frac{\partial^2 w}{\partial t^2} \tag{2.131}$$

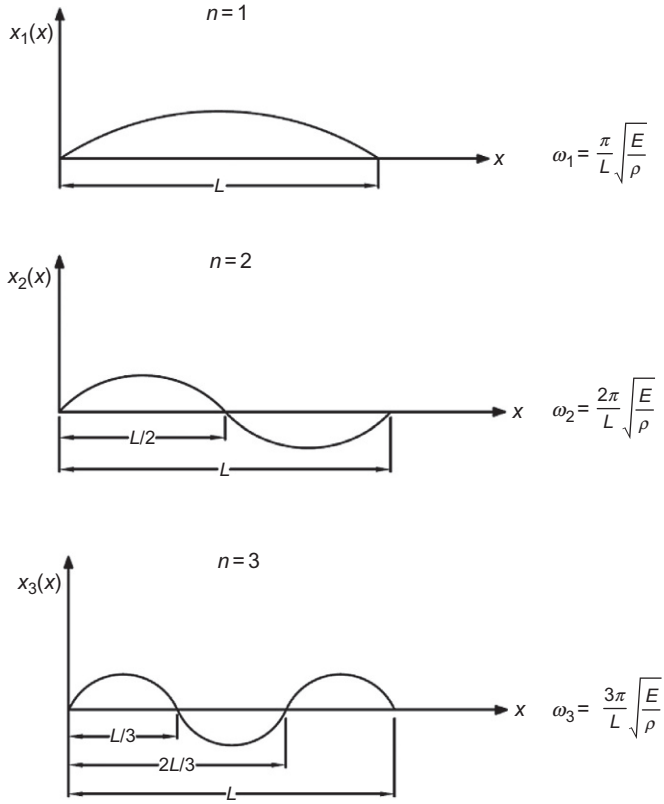

Fig. 2.16 Mode shapes and natural frequencies of a fixed-fixed bar for the first three modes of longitudinal vibration.

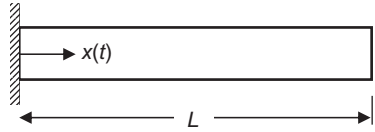

Fig. 2.17 Cantilever beam in transverse vibration.

where I is the moment of inertia of the cross section about the neutral axis of the beam while $w = w(x, t)$ is the transverse displacement of the same axis of the beam. Other constants, that is, x, t, ρ, A, and E, are as defined in previous section. If EI is constant across the beam, then the governing equation reduces to

$$EI\frac{\partial^4 w}{\partial x^4} + \rho A\frac{\partial^2 w}{\partial t^2} = 0 \tag{2.132}$$

This equation can be solved for orthotropic composite beams using separation variables again by assuming that modulus E can be replaced by the effective modulus E_f.

Assuming a solution in the form of

$$w(x,t) = W(x)e^{i\omega_n t} \tag{2.133}$$

yields an ordinary differential equation of the form:

$$\frac{d^4W(x)}{dx^4} - k^4W(x) = 0 \tag{2.134}$$

where ω is the frequency, $W(x)$ is the mode shape function, and the constant k is given as

$$k = \left(\frac{\omega^2\rho A}{EI}\right)^{1/4} \tag{2.135}$$

The solution for Eq. (2.134) is given as follows:

$$W(x) = C_1 sin\, kx + C_2 cos\, kx + C_3 sinh\, kx + C_4 cosh\, kx \tag{2.136}$$

where the constants C_1, C_2, C_3, and C_4 can be determined by applying boundary conditions. A detailed explanation of boundary conditions and their applications is beyond the scope of this book and can be found in a vibration book covering continuous vibrations.

The eigenvalue equation resulted by the application of boundary conditions is solved to determine natural frequencies and mode shapes of the vibrating system. As an illustration, for a cantilever beam, the natural frequency equation is given as

$$\omega_n = k_n^2\sqrt{\frac{EI}{\rho A}} \quad n = 1, 2, 3, \ldots \tag{2.137}$$

where n is the mode number, and for the first three modes, they are computed as $k_nL = 1.875, 4.694, 7855$. First three mode shapes for a cantilever beam are shown on Fig. 2.18.

2.8.3 Transverse vibration of orthotropic plates

In this section, a general equation of motion for a laminated composite plate in transverse vibration is simply presented. Summation of forces acting on an infinitesimal element can be written according to Newton's second law as

$$\frac{\partial N_x}{\partial x} + \frac{\partial N_{xy}}{\partial y} = \rho_0\frac{\partial^2 u^0}{\partial t^2} \tag{2.138}$$

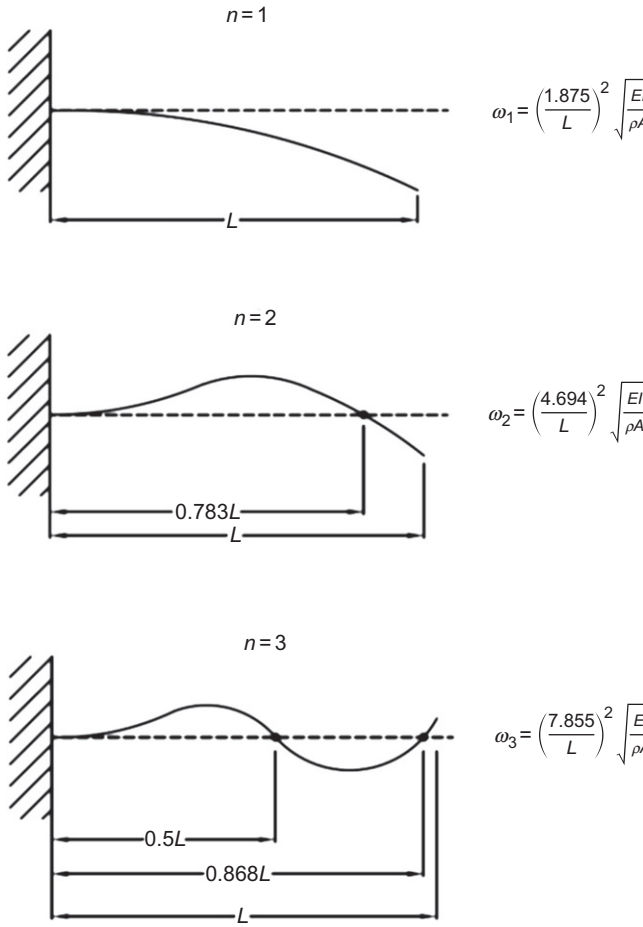

Fig. 2.18 Mode shapes and natural frequencies for the first three modes of transverse vibration of the cantilever beam.

$$\frac{\partial N_y}{\partial y} + \frac{\partial N_{xy}}{\partial x} = \rho_0 \frac{\partial^2 v^0}{\partial t^2} \tag{2.139}$$

$$\frac{\partial Q_x}{\partial x} + \frac{\partial Q_y}{\partial y} + q(x, y) = \rho_0 \frac{\partial^2 w}{\partial t^2} \tag{2.140}$$

where N's and Q's are respective in-plane stress resultants and ρ_0 is the mass per unit area of the laminate. The displacements u, v, and w are in the directions of x, y, and z, while the superscript zero shows middle-surface displacements in respective directions. $q(x,y)$ stands for the transverse distributed force.

On the other hand, by neglecting rotary inertia, moments can be summed about x and y axis and then simplified to get

$$\frac{\partial M_y}{\partial y}+\frac{\partial M_{xy}}{\partial x}=Q_y \tag{2.141}$$

$$\frac{\partial M_x}{\partial x}+\frac{\partial M_{xy}}{\partial y}=Q_x \tag{2.142}$$

respectively. Eqs. (2.141), (2.142) can be substituted in Eq. (2.140) to yield

$$\frac{\partial^2 M_x}{\partial x^2}+2\frac{\partial^2 M_{xy}}{\partial x\partial y}+\frac{\partial^2 M_y}{\partial y^2}+q(x,y)=\rho_0\frac{\partial^2 w}{\partial t^2} \tag{2.143}$$

Eqs. (2.138)–(2.140), (2.143) are the equations of motion of the plate in stress and moment resultants. These equations of motion can be rewritten in terms of displacements by substituting laminate force-deformation, strain-displacement, and curvature-displacement relations into above equations and then solved for the desired boundary conditions.

As an example, results for the free transverse vibration of a rectangular orthotropic plate of size $a\times b$ are given here without proof for simply supported case. Based on the discussion of Ashton and Whitney [37], one may obtain the equation of motion of an orthotropic plate as follows:

$$D_{11}\frac{\partial^4 w}{\partial x^4}+2(D_{12}+2D_{66})\frac{\partial^4 w}{\partial x^2\partial y^2}+D_{22}\frac{\partial^4 w}{\partial y^4}+\rho_0\frac{\partial^2 w}{\partial t^2}=0 \tag{2.144}$$

where $w=w(x,y,t)$ is the displacement in z direction and D's are constants arising from the integration of some stiffness terms. By using separation of variables and applying appropriate boundary continuous, one may obtain the frequency equation as

$$\omega_{mm}^2=\frac{\pi^4}{\rho_0 a^4}\left[D_{11}m^4+2(D_{12}+2D_{66})(mnR)^2+D_{22}(nR)^4\right] \tag{2.145}$$

and the mode shape function as

$$W(x,y)=A_{mn}sin\frac{m\pi x}{a}sin\frac{n\pi y}{b} \tag{2.146}$$

where m and n are mode indexes, a and b are plate dimensions in x and y directions, respectively, and $R = a/b$ is the plate aspect ratio.

Numerical results for frequencies and mode shapes of two square plates are included here as presented by Ashton and Whitney [37]. One of the plates is orthotropic with ratios $D_{11}/D_{22}=10$ and $(D_{12}+2D_{66})/D_{22}=1$, and the other one is isotropic with ratios $D_{11}/D_{22}=1$ and $(D_{12}+2D_{66})/D_{22}=1$. Table 2.1 presents

Table 2.1 First four natural frequencies for a simply supported orthotropic and isotropic plates [37]

	Orthotropic $\omega = k\pi^2/b^2\sqrt{D_{22}/\rho_0}$			Isotropic $\omega = k\pi^2/b^2\sqrt{D/\rho_0}$		
Mode	***m***	***n***	***k***	***m***	***n***	***k***
1st	1	1	3.62	1	1	2.0
2nd	1	2	5.68	1	2	5.0
3rd	1	3	10.45	2	1	5.0
4th	2	1	13	2	2	8.0

the lowest four natural frequencies for the two plates, while Fig. 2.19 compares the corresponding mode shapes for the plates. Nodal lines are denoted by dotted lines on the figure. It is noted that sequence of mode numbers for increasing frequency differs for orthotropic and isotropic plates.

2.8.4 Analysis of damping in composites

The aim of this section is to cover linear viscoelastic damping analysis of composites. Damping is defined as the dissipation of mechanical energy during dynamic deformation of structures. In metallic structures, much of the damping is accepted to be arising from structural joints rather than damping within the metal itself. Conversely, polymer

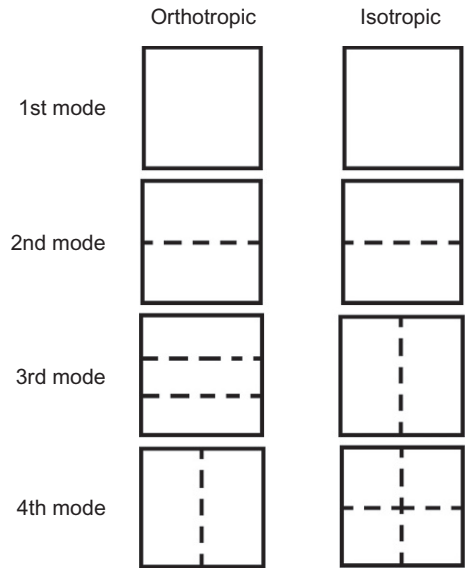

Fig. 2.19 First four mode shapes for a simply supported orthotropic and isotropic plates [37].

composites present a high damping and lightweight properties, which provides flexibility for designers pursuing a trade-off between damping and stiffness.

Damping is one of the most important aspects of structural materials under dynamic loads. Although the viscoelastic behavior of composite materials seems to be the main mechanism for damping, thermoelastic damping, coulomb friction, and cracks or delaminations are other sources of energy dissipations. Thermoelastic damping generally arises in metallic composites rather than polymer-based composites. Damping due to cracks or delaminations can be experimentally measured using some nondestructive testing methods but cannot be utilized as a criterion in the design of structures.

Some analytic damping prediction tools have been developed in the literature at either micromechanical or macromechanical level. For instance, thermoelastic and dislocation damping models are established to predict damping without the need of material-damping properties. For the viscoelastic type of damping, usually one of two approaches is tackled. The first approach comprises the utilization of elastic viscoelastic correspondence principle together with elasticity theory. The second one is related to the strain energy formulation in which the relation of total damping is established with the damping in each element.

In conclusion, since damping is an important issue in the design of dynamically loaded composite structures, its prediction has a growing interest among designers. Some analytic prediction methods have been developed in the literature and shortly pointed out here.

References

[1] Mallick PK. Fiber-reinforced composites: materials, manufacturing and design. New York, NY: CRC Press, Taylor and Francis Group; 2008.
[2] Aydin L, Artem HS. Comparison of stochastic search optimization algorithms for the laminated composites under mechanical and hygrothermal loadings. J Reinf Plast Compos 2011;30(14):1197–212.
[3] Kaw AK. Mechanics of composite materials. New York, NY: CRC Press, Taylor and Francis Group; 2006.
[4] Berthelot JM. Composite materials: mechanical behavior and structural analysis. Berlin: Springer Verlag; 1999.
[5] Daniel IM, Ishai O. Engineering mechanics of composite materials. New York: Oxford University Press; 1994.
[6] Aydin L. Design of dimensionally-stable laminated composites subjected to hygro-thermo-mechanical loading by stochastic optimization methods [Ph.D. thesis]. İzmir: İzmir Institute of Technology; 2011.
[7] Taya M, Arsenault RJ. Metal matrix composites : thermomechanical behavior. Oxford: Pergamon Press; 1989.
[8] Gültürk E. The effects of diatom frustule filling on the quasi-static and high strain rate mechanical behavior of polymer matrices [Ph.D. thesis]. İzmir: Izmir Institute of Technology; 2010.
[9] Cox HF. The elasticity and strength of paper and other fibrous materials. Br J Appl Phys 1952;3:29–72.

[10] Nairn JA. On the use of shear-lag methods for analysis of stress transferunidirectional composites. Mech Mater 1997;26(2):63–80.
[11] Garg SK, Svalbonas V, Gurtman GA. Analysis of structural composite materials. New York, NY: Marcel Dekker; 1973.
[12] Agarwal BD, Broutman LJ. Analysis and performance of fiber composites. New York, NY: J. Wiley & Sons; 1980.
[13] Chamis CC, Sendecyj GP. Critique on theories predicting thermoelastic properties of fibrous composites. J Compos Mater 1968;2:332.
[14] Lingois P, Berglund L. Modeling elastic properties and volume change in dental composites. J Mater Sci 2002;37:4573–9.
[15] Mcgee SH, Mccullough RL. Models for the permeability of filled polymer systems. Polym Compos 1981;2:149.
[16] Hermans JJ. The elastic properties of fiber reinforced materials when the fibers are aligned. Proc K Ned Akad Wet Ser B 1967;65:1–9.
[17] Hill RJ. Theory of mechanical properties of fibre-strengthened materials. I. Elastic behaviour. J Mech Phys Solids 1964;12:199.
[18] Whitney JM, McCullough RL. Delaware composites design encyclopedia: micromechanical materials modeling, vol 2. Pennsylvania: Technomic Publishing; 1990.
[19] Halpin JC, Kardos JL. The Halpin-Tsai equations: a review. Polym Eng Sci 1976;16:344–52.
[20] Nielsen LE. Generalized equation for the elastic moduli of composite materials. J Appl Phys 1970;41:4626–7.
[21] Lewis TB, Nielsen LE. Dynamic mechanical properties of particulate-filled composites. J Appl Polym Sci 1970;14:1449–71.
[22] Chantler PM, Hu X, Boyd NM. An extension of a phenomenological model for dental composites. Dent Mater 1999;15:144–9.
[23] Braem M, Van Doren VE, Lambreehts P, Vanherle G. Determination of young's modulus of dental composites. A phenomenological model. J Mater Sci 1987;22:2037–42.
[24] Guth E, Gold O. New foundation of general relativity. Phys Rev 1938;53:322.
[25] Guth E. Theory of filler reinforcement. J Appl Phys 1945;16:20.
[26] Wu YP, Jia QX, Yu DS, Zhang LQ. Modeling young's modulus of rubber-clay nanocomposites using composite theories. Polym Test 2004;23:903–9.
[27] Mooney M. The viscosity of a concentrated suspension of spherical particles. J Colloid Sci 1951;6:162–70.
[28] Brodnyan JG. The concentration dependence of the Newtonian viscosity of prolate ellipsoids. Trans Soc Rheol 1959;3:61.
[29] Akkerman R. Laminate mechanics for balanced woven fabrics. Compos Part B 2006;37:108–16.
[30] Chou TW, Ko FK. Textile structural composites. New York, NY: Elsevier Science Publishing Company; 1989.
[31] Lei Z, Li X, Qin F, Qiu W. Interfacial micromechanics in fibrous composites: design, evaluation, and models. Sci World J 2014;2014:1–9. Article ID 282436, http://dx.doi.org/10.1155/2014/282436.
[32] Akbarov SD, Guz AN. Mechanics of curved composites and some related problems for structural members. Mech Adv Mater Struct 2004;11(6):445–515.
[33] Akbarov SD, Guz AN. Mechanics of curved composites. Dordrecht/Boston, MA/London: Kluwer Academic; 2000.

[34] Gibson RF. Principles of composite material mechanics. New York, NY: McGraw Hil; 1994.
[35] Jones RM. Mechanics of composite materials. Philadelphia: Taylor and Francis; 1999.
[36] Tsai SW, Wu EM. A general theory of strength for anisotropic materials. J Compos Mater 1971;5:58–80.
[37] Ashton JE, Whitney JM. Theory of laminated plates. Lancaster, PA: Technomic Publishing Co.; 1987.

Fiber reinforced composites

3

Seçkin Erden[*], *Kingsley Ho*[†]
[*]Ege University, Izmir, Turkey, [†]Cytec Engineered Materials, United Kingdom

3.1 Introduction

3.1.1 Definitions

Composite materials can be generally defined as a heterogeneous mixture of at least two different materials in micro-scale, possessing new properties other than that of its constituents and usually an almost homogeneous structure in macro-scale. The opportunity to combine this mixture of properties brings about the most distinguishing feature of a composite material, which is the possibility to tailor its properties according to the requirements of the desired application. In the case of mechanical properties, it can be achieved by altering the type as well as the loading of reinforcement(s), which is the load-bearing constituent of a composite, or by modifying the matrix formulation, the binder constituent that holds the reinforcement together. Additionally, the interaction between these two fundamental constituents also has an important effect on the composite properties.

Reinforcement constituent of the composites is usually in the form of fibers/fabrics or particles/fillers. In the latter case, the final product is named as particulate composite, which includes usually micron-sized particles. In case the reinforcement is a type of nanoparticle such as carbon nanotube (CNT) or graphene as an outcome of the developments in nanotechnology, the end material is then named as nanocomposite.

The material in the first case mentioned above, i.e., the one having fibers/fabrics as the reinforcement constituent is named as fiber reinforced composite, which is the focus of this chapter and forms at the same time the basis of this book. Fig. 3.1 shows a typical fiber reinforced composite material where the reinforcement is in the form of fibers, which are in this example aligned in two directions, namely longitudinal and transverse, forming a crossply configuration. It should be noted that the end use applications for fiber reinforced composites are rarely in the form of a monolithic laminate panel, but more shaped in a complex geometry. The role of lay-up orientation designs utilizes the load-bearing capability of the material during its service life. However, from a materials design point of view, this fulfills the criteria of a standard test pyramid. Nevertheless, in this illustration, it can be seen that the fibers are surrounded well by the binding matrix laminate, which are stacked in through-the-thickness direction, at the end forming a laminated composite structure, i.e., a layered product consisting of plies of fibers embedded within the matrix.

Other ingredients of composites are fillers and additives. Fillers have been mostly used to replace some portions of the expensive constituents in order to reduce the cost of the material and also to improve some properties of the composite. Wood flour, saw

Fiber Technology for Fiber-Reinforced Composites. http://dx.doi.org/10.1016/B978-0-08-101871-2.00003-5

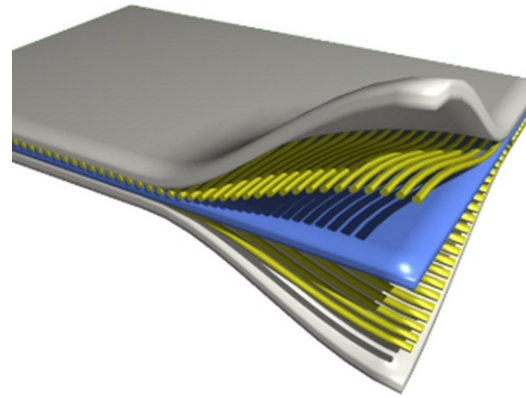

Fig. 3.1 Illustration of a typical fiber reinforced composite [1].

dust, and calcium carbonate are typical examples for fillers. In the meantime it can also be the most expensive constituent within a fiber reinforced composite system. In the case of composite fuselage of commercial aircrafts for example, particles that are of high toughness are added to brittle matrix formulation to enhance mechanical properties. Besides, brittle particles are also added to low cost thermoplastic resins in order to stiffen up the properties of the composite. Additives are used to add a desired function to the matrix such as color, fire retardance, UV radiation protection, electrical conductivity, ease of removability from mold, etc. Fillers and additives can also affect the mechanical properties of the composite, which made them to be also considered as reinforcement material [2–5].

The microstructure of fiber reinforced composite materials is composed of the fiber and the matrix, which are the fundamental constituents of the composite, and additionally the interphase region as illustrated in Fig. 3.2. The interphase is defined as the region where the physical, mechanical, and chemical properties differ from those of the original fiber and the matrix as a result of thermal, chemical, and mechanical influences. Factors occurring within the interphase region can be listed as variable crosslink density and molecular weight, transcrystallinity, impurities, sizings, voids, fiber surface chemistry, fiber topography, and morphology [6]. Interphase region has been reported to appear in between a point within the fiber and a point inside the matrix

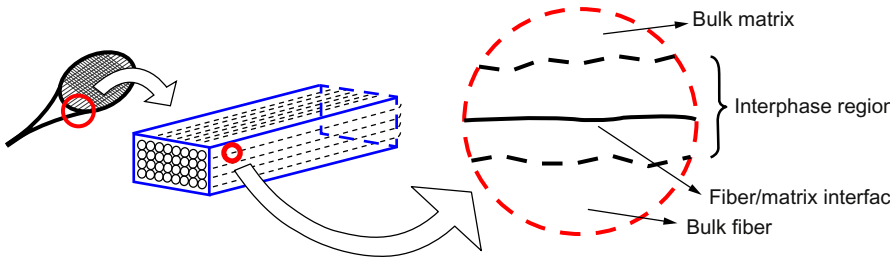

Fig. 3.2 Schematic illustration of a fiber reinforced composite product from macro-scale to micro-scale with a focus on the interphase region.

beyond the interface, which is the boundary surface between the fiber and the matrix. The interface is known to form the fiber/matrix bonding, which affects the load transfer within the composite and consequently influences its mechanical properties [7].

3.1.2 Applications

Composites occur in nature. Plant and bone structures can be shown as well-known examples. Wood is formed of cellulose fibers bound by lignin while the bone has hydroxyapatite and collagen as its constituents. On the other hand, man-made composites date back to early houses made of mud and straw. Concrete, a mixture of aggregate, cement, and sand, is another example, which today also has steel reinforcing bars as a constituent. Modern composites can be assumed to have originated in the 1950s with the usage of fiberglass, which has glass fibers and polyester matrix as its constituents. This composite material has been widely used in the production of boats, water tanks, early cars, etc. Today composites are used in numerous fields such as energy (Fig. 3.3), marine applications (Fig. 3.4), sports, automotive (Fig. 3.5), aerospace and aeronautics, biomedical applications (Fig. 3.6), civil engineering, military, and even music industry. Examples in aeronautical applications can be the Airbus A380, which has 25% by weight of its parts made of composites, and Boeing 787 Dreamliner, which has 50% composites by weight [12].

Fig. 3.3 A 157 m high wind turbine at the North Sea [8].

Fig. 3.4 The SeaGen tidal energy converter [9].

Fig. 3.5 A composite coil spring developed for Audi [10].

Fig. 3.6 A composite wheelchair [11].

3.1.3 Current and future market outlook

By 2016, composite materials industry is expected to reach $27.4 billion while the market for end products made with composite materials is expected to reach $78 billion. The breakdown of the industry value into sectors is as follows: $4 billion transportation, $0.8 billion marine, $3.7 billion wind energy, $4 billion aerospace, $2.8 billion pipe and tank, $4.4 billion construction, $5.2 billion electricals and electronics, $1.6 billion consumer goods, and $0.8 billion others [13].

The glass fiber reinforced plastics production is forecast to reach 1.1 million tons in Europe in 2016. Its breakdown into the sectors is: 35% transportation, 15% electricals and electronics, 34% construction, 15% sports and leisure, and 1% others [14].

An interesting result is obtained when the global demand for carbon fiber reinforced plastics (CFRP) for 2015 is examined. While the aerospace and defense industry covers 30% of the total demand in tons (Fig. 3.7), it has 61% share of market value in terms of US$ (Fig. 3.8). Other sectors lose their high shares in tons when it comes to market value except for marine industry, which just keeps its share as 1% in both cases. This outcome shows that the aerospace and defense industry manufactures the most value added carbon composite products [14].

China, being the world leader in terms of volume consumption, will continue its leadership with a market value of $11.5 billion in 2018. The United States, being the second largest composite market, is expected to reach a market value of $12 billion by 2020 [15].

Global demand for carbon fiber is forecasted as 100.5k tons for 2020, and 120k tons for 2022, which will result in a market value of $4.2 billion. On the other hand, demand for CFRP is estimated as 155k tons for 2020, and 191k tons for 2022 [14].

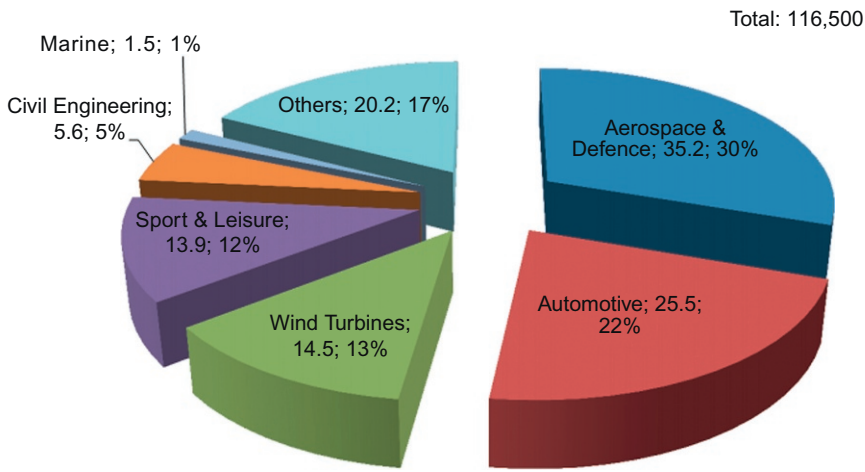

Fig. 3.7 Carbon composite demand breakdown in tons for 2015 [14].

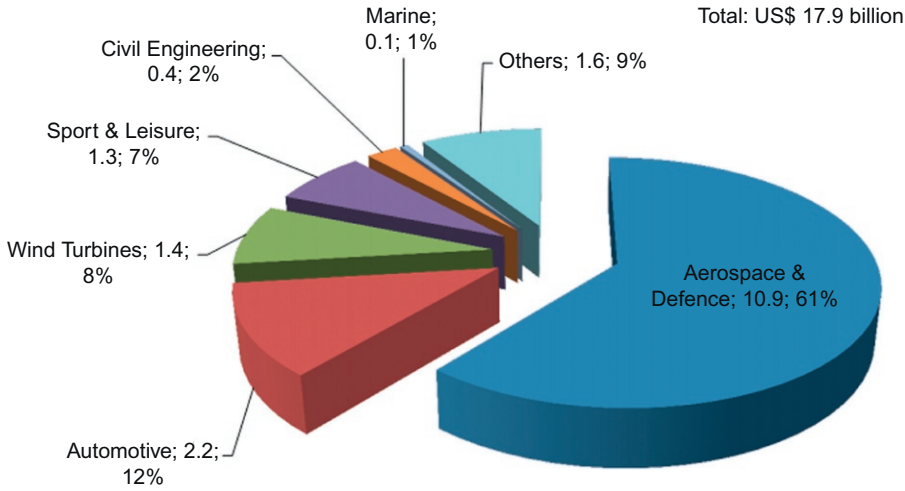

Fig. 3.8 Carbon composite demand breakdown in billion $US for 2015 [14].

The market for CFRP materials could reach US$20,284 million by 2022, according to a new report published by Allied Market Research. This represents a CAGR of 8.1% during the period 2016–22. North America is the major revenue-generating regional market and would continue to be the leader until 2022. While aerospace and defense projects such as Boeing and Airbus are the primary drivers for growth and development of the CFRP market, the high costs of CFRP and long production cycles is expected to restrain the market growth. The thermosetting segment accounted for more than two-thirds of the market revenue in 2015 and would continue to lead the market until 2022. This was attributed to its mechanical properties such as tensile strength, compressive strength, hardness, and temperature independence. The epoxy resin segment accounted for more than 60% share in world thermosetting CFRP market, in terms of both market volume and revenue, in 2015. Pultrusion and winding is the most commonly adopted manufacturing process as the process generates high production volumes in minimal time; approximately 23,565 tons CFRP was manufactured using this process in 2015. The aerospace and defense industry generates the highest revenue, which generated about US$5576 million in revenues in 2014 [16].

3.2 Materials (reinforcements, matrices, fiber/matrix adhesion)

3.2.1 Reinforcements

Fibers are generally classified as natural (plant, animal, or mineral based) and synthetic fibers (nylon, acrylic, aromatic polyester, polyethylene, aramid, glass, carbon, boron, silicon carbide, stainless steel, aluminum, etc.) as shown in Fig. 3.9 [17–19]. Synthetic fibers are comprised of tens to thousands of single fibers or filaments having

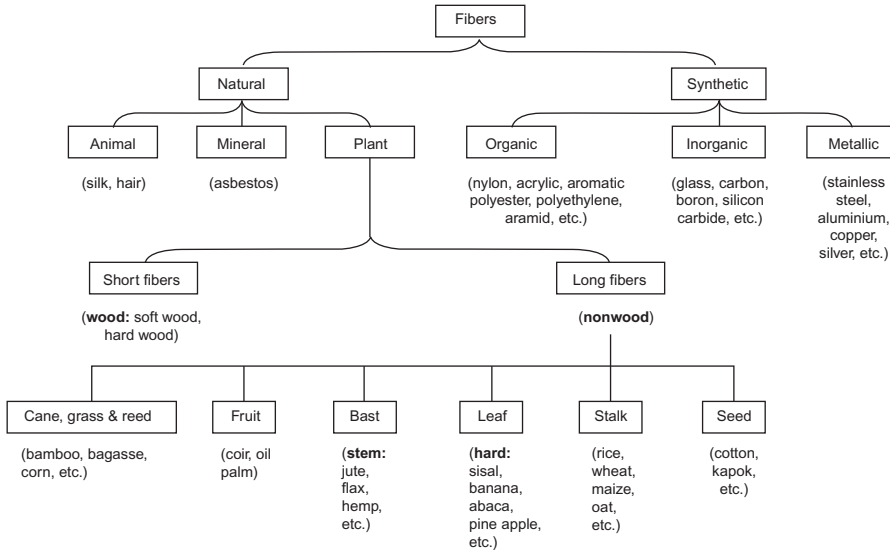

Fig. 3.9 Classification of fibers.

diameters in the range of about 5–20 μm (e.g., carbon fibers can have 1, 2, 3, 6, 9, 12, 24, 48k, or 50k filaments with diameters of 5–7 μm and ranges from standard strength, intermediate modulus, and ultra-high modulus). While fiber reinforcements are basically in continuous form or a chopped form of 5 mm average length, technological developments also introduced nanofiber reinforcements, which have submicron diameters and varying lengths for different materials (e.g., carbon nanofibers can be approximately a few to 200 μm long) [20,21].

In the case of particulate composites and chopped or nanofiber composites, dispersion within the matrix becomes an important phenomena as the rheological, mechanical, electrical, thermal, and morphological properties are affected. A sample study on nanocomposites revealed that poorly dispersed CNTs caused higher storage modulus, loss modulus, and complex viscosity when compared to the case of well dispersed CNTs, resulting in a more solid-like rheological behavior. Poor dispersion decreased the tensile strength and elongation at break value of the nanocomposites while tensile modulus remained unaffected. Both of the dispersion cases showed a similar percolation threshold of electrical conductivity, but the well dispersed nanocomposites had higher electrical and thermal conductivities. The morphological investigations pointed out to the presence of aggregates of pristine CNTs in the nanocomposites with poor dispersion [22].

Fiber reinforcements can also have a form of connected structures named as fabric or cloth, which can be woven, nonwoven, knitted, or braided. Woven fabrics are produced by interlacing of warp and weft yarns with types of weave styles such as plain, twill, satin, etc., which affect main fabric properties such as stability, drape, porosity, smoothness, balance, symmetry, and crimp [23]. Other fabric architectures like

triaxial, multiaxial, multiply, 3D, and 5D constructions are available and all these fabric architectures are well-known to influence composite processing and end material properties, which are obviously seen especially in studies focused on mechanical properties [24–27]. Knitted fabrics have high degree of deformability, which provides drapeability causing an exceptional formability, therefore allowing the creation of complex preforms (near net shape dry fabric structure of the desired product, which is processed to produce composite part). Although decrease of in-plane composite mechanical properties due to severe bending of fibers is an important concern, knitting is preferable for 3D fabric constructions with through-the-thickness reinforcement [28,29]. Similarly, braided fabrics have the disadvantage of fiber bending during the process, which again accounts for the reduced in-plane mechanical properties of the composite. Despite this, braiding allows the creation of multiaxial preforms and 3D constructions with through-the-thickness reinforcement having excellent damage tolerance [30]. Nonwoven fabrics are produced by bonding of chopped or continuous fibers by mechanical, chemical, or thermal means. Usually chemical bonding technique is used for producing mats, which is a nonwoven fabric composed of randomly oriented chopped or continuous fibers. Stitching, a way of mechanical bonding, which prevents stiffening of the texture and thereby protects the initial softness of the fibers, is also used to produce multilayer nonwoven fabrics by assembling unidirectional (UD) fabrics with different orientations such as longitudinal, transverse, ±45 degrees, etc. Stitched fabrics, which are also named as noncrimp fabrics, have reduced crimp resulting in increased strength when compared to woven fabrics. UD fabrics are the most basic ones having almost all their fibers laid in one direction only. They can be constructed by stitching, weaving, and bonding [23,31]. All the above mentioned fabric production methods also allow the creation of hybrid fabrics and their composites, which can be grouped as interply hybrids (stacked homogeneous layers of different materials), intraply hybrids (layer with different fiber materials), and intermingled hybrids (mixture of different fiber materials) [32]. It is also worth mentioning of z-pinning, another method of improving through-the-thickness composite properties, which can be defined as a means of nailing the laminate plies to fix them via friction and adhesion. The main difference of this technique from the similar ones such as 3D weaving, stitching, knitting, and braiding is that the latter ones are used in case of dry fabrics while z-pinning is applicable to prepregs, which are matrix impregnated fabrics [33].

Mats and chopped fibers are discontinuous type of reinforcements while continuous fiber and fabric (other than mat) are continuous reinforcements. Discontinuous reinforcements can be randomly oriented as in the case of mats, or aligned along desired axis as in the case of aligned chopped fibers by using techniques such as electric field, etc.

Mat, chopped fiber, or multidirectional continuous fiber reinforced composites and particulate composites behave like they have the same mechanical properties in all three directions. Therefore, they are called quasi-isotropic materials. UD, crossply, or aligned chopped fiber reinforced composites have the same properties in two directions and show a different property in the third direction. That is why they are called orthotropic or transversely isotropic materials.

3.2.2 Matrices

Fiber reinforced composites can be classified into four groups according to their matrices: metal matrix composites (MMCs), ceramic matrix composites (CMCs), carbon/carbon composites (C/C), and polymer matrix composites (PMCs) or polymeric composites (Fig. 3.10). Matrix, which has the primary role of holding the reinforcement together, is considered also as resin especially in the case of polymers. PMCs, which distinguish from other types especially because of their lightweightness, are further classified as thermoset, thermoplastic, and elastomeric composites. Thermosets have crosslinked polymer chains at the cure stage, which at the end leads to a rigid product that cannot be reshaped. Thermoplastics, unlike thermosets, can be further heated and remelted, which allows them to be reshaped as a new product and therefore recycled more broadly when compared to thermosets. What is most advantageous for thermosets is that they can be used at elevated temperatures as they do not loose structural rigidity when heated. Typical examples for thermosetting polymer matrices are polyester, vinyl ester, epoxy, phenolic, cyanate ester, polyurethane, polyimide, and bismaleimide. On the other hand, polyamide, polyetyhlene, polypropylene, PEEK, thermoplastic polyimide, thermoplastic polyurethane, polycarbonate, PLA, polysulfone, polyphenylene sulfide are common examples of thermoplastic polymer matrices [34]. Elastomers, like thermosets, achieve crosslinking as a result of the process called vulcanization. The well-known elastomeric material is rubber and therefore elastomeric composites are usually named as rubber composites. Elastomers differ from thermosets and thermoplastics with their highly elastic mechanical behavior. Some examples of elastomeric composites are polyester fiber reinforced hoses, aramid fiber-reinforced automobile tires, steel-wire, or mesh-reinforced heavy-duty truck tires [35]. Recent advances also led to studies involving CNT incorporation into rubbers with an attempt to replace the usual carbon black or mineral fillers [36].

MMCs contain a metal element or alloy as the matrix phase, e.g., aluminum, magnesium, lead, aluminum-lithium, titanium, copper, and their alloys. MMCs are usually in the form of particulate composites, which have aluminum oxide, zirconium oxide, thorium oxide, graphite, titanium carbide, silicon carbide, boron, tungsten, and molybdenum as example reinforcements [37]. CMCs have matrix materials such as Al_2O_3,

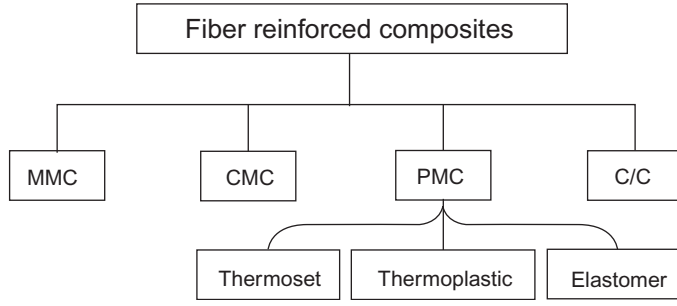

Fig. 3.10 Classification of composites according to matrix type.

Si_3N_4, SiC, ZrO_2, TiO_2, WC, Cr_2O_3, etc., which have melting points of over 1600°C. Reinforcements used are in the form of monofilaments, fibers, whiskers, particles, and recently nanoparticles such as CNTs. General reinforcement materials are SiC, Al_2O_3, Al_2O_3-SiO_2, Al_2O_3-ZrO_2, boron, etc. [38,39]. C/C composites are composed of carbon based reinforcements and a matrix material based on carbon. State of the constituents may be different such as graphite and carbon. These composites find applications in aerospace parts due to requirements such as high strength and oxidation resistance at elevated temperatures like 1650°C. Typical examples are gas turbine rotors, jet engine nozzles, crucibles for molten metals, disk brakes for cars, and pistons for internal combustion engines [40].

3.2.3 Fiber/matrix adhesion

Controlling the interface properly to provide the composite with improved mechanical performance and structural integrity, requires understanding of the mechanisms of adhesion which are specific to each fiber/matrix system, and the physicochemical characterization of the interface with regard to the origin of adhesion. Adhesion can be attributed to mechanisms including adsorption and wetting, interdiffusion, electrostatic attraction, chemical bonding, reaction bonding, exchange reaction bonding, and mechanical interlocking. In addition to the major mechanisms, hydrogen bonding, van der Waals forces, and other low energy forces may also be involved [7]. To briefly explain these main mechanisms:

Adsorption and wetting is useful in determining the wettability of the fibers by the matrix. By using the measured "contact angle" between the fiber and the matrix, and "surface free energy" of the matrix, the "thermodynamic work of adhesion," which is the theoretical energy value required to separate the fiber and the matrix, can be calculated. It is also called "theoretical adhesion" value. Contact angle between a solid surface and a liquid is also a measure of wettability itself. Incase of contact angles less than 90 degrees the liquid is called "wetting" while for the ones greater than 90 degrees the liquid is named "nonwetting." If the "test liquid" is water, than for the wetting case the solid surface is qualified as "hydrophilic" and for the nonwetting case as "hydrophobic." If there is a great amount of gas or vapor adsorption on the solid surface, then the term "spreading" is also taken into account. An example for a well developed technique to determine the direct wetting of the fiber by the matrix can be the drop-on-fiber contact angle measurement (Fig. 3.11). This is realized by wetting a single fiber or filament by the matrix, and then fitting curves to the drop profile images captured using an optical microscope.

Interdiffusion of atoms or molecules between both constituents may result in bonding of the fiber and the matrix. Coupling agents, which enhance fiber/matrix compatibility, have been found to be effective in the formation of such interactions. Electrostatic attraction is caused as a result of different surface charges occurring on the constituents of the composite material. Chemical bonding between the fiber and the matrix is a result of chemical reactions that take place at the interface. These can be triggered by surface treatments causing active surface functional groups at the interface. Examples of such treatments can be sizing, oxidation via plasma, chemical

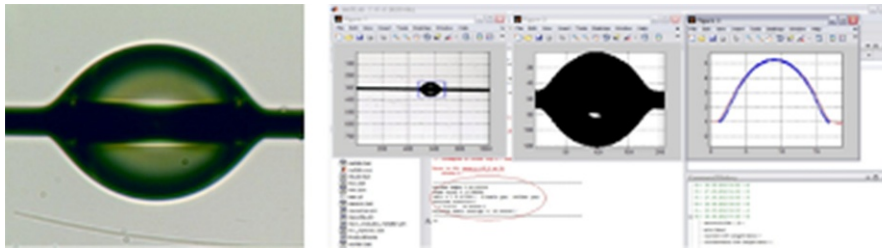

Fig. 3.11 Determination of the matrix contact angle via drop-on-fiber method.

or electrochemical methods, application of coupling agents, etc. Reaction bonding can be an adhesion mechanism in case of MMCs, which happens as a result of reactions occurring at the interface. Mechanical interlocking is caused as a result of etching of the fiber surface. Oxidation treatments are usually applied to increase fiber surface roughness, which is a measure of mechanical interaction between the fiber and the matrix. BET surface area is another magnitude used to determine the level of mechanical bonding between the two constituents of the composite material.

3.2.4 Estimation of composite properties

The opportunity to select from a variety of reinforcement and matrix types and materials mentioned above allows the possibility of tailoring the properties of produced composite materials yet in the design phase according to the requirements of the desired application. This is realized by estimation of the composite properties as described in the "rule of mixtures" concept where "fiber volume fraction" (v_f) definition, which is the ratio of the volume of fibers to the volume of matrix, is introduced. This is also named as "fiber loading level" and is also realized as weight fraction in practice. Density, coefficient of thermal expansion, modulus of elasticity, shear modulus, Poisson's ratio, and tensile strength are the composite material properties that can be estimated by knowing the fiber volume fraction and the same properties of each constituent. Properties of some composites and conventional materials are given in Table 3.1 to give an overview of comparison in between (Note: Composite properties are in longitudinal direction).

3.3 Manufacturing

The criteria for selecting a manufacturing process depend on the production rate, cost, strength, and size and shape requirements of the composite part [45]. Compression molding (SMC/BMC compression molding), hand lay-up, spray-up, vacuum infusion, vacuum bagging, resin transfer molding (RTM), vacuum assisted resin transfer molding (VARTM), autoclave molding, filament winding, centrifugal casting, automated fiber placement (AFP), pultrusion, injection molding, RIM (RRIM, SRIM), vacuum forming, and stamp forming are most of the manufacturing techniques used in

Table 3.1 Properties of some composites and conventional materials [35,41–46]

Material	Ultimate tensile strength [MPa]	Tensile modulus [GPa]	Coefficient of thermal expansion [10^{-6} K^{-1}]	Thermal conductivity [W/m K]	Density [g/cm^3]	Melting Point [°C]
Epoxy	27.5–90	2.4	35	0.34	1.15	–
Polyester	40–90	2–4.5	50–110	0.2	1.2–1.5	–
Nylon 6/6	75.9–91.5	1.58–3.79	50	0.17	1.1–1.15	255–265
Polypropylene	25–38	1–1.4	110	0.2	0.9	160
Polycarbonate	45–70	2.2–2.4	70	0.2	1.06–1.2	230–260
Wood	5	11	–	0.1–0.2	0.4–0.75	–
Steel	300–1800	210	–	–	7.8	1371–1482
Aluminum	75–700	75	20–25	237	2.8	660
E-glass fiber	3450	72.5	1.3	5	2.5	>1540
Carbon fiber	2760–5170	210–290	7–8.5	7–10	1.76–2.15	–
Graphite fiber	1725–2070	345–517	–	–	1.67–2.02	>3500
Aramid fiber (Kevlar)	3600–4100	131	–	60	1.44	–
E-glass/epoxy (v_f=0.55)	1080	39	7	–	2.1	–
Graphite/epoxy (v_f=0.62)	760–2139	145–220	(−0.079) to (−0.54)	–	1.6–1.7	–
Carbon/epoxy (v_f=0.63)	2280	142	(−0.9)	–	1.58	–
Kevlar/epoxy (v_f=0.6)	1280	87	(−2)	–	1.38	–
Carbon/carbon	>276	>69	1.1	11.5	<2.99	>4100
SiC fiber	2520–3920	182–406	–	–	2.55–3	–
Al_2O_3 matrix	200–310	380	8.5	–	3.95	2050
SiC matrix	–	414	4.8	–	3.17	2300–2500
ZrO_2 matrix	–	138	7.6	–	5.8	2500–2600
Al 2024/B fiber (v_f=0.46–0.64)	1460–1940	220–275	–	–	–	–
Cu/SiC fiber (v_f=0.23–0.37)	680–900	172–202	–	–	–	–
Mg/SiC fiber (v_f=0.34–0.5)	1000–1331	109.6–230.3	–	–	–	–

composite production. Prepregging is a method of manufacturing a semifinished product named prepreg, which helps producing composite parts with controlled fiber volume fraction. Also, sandwich structures are used for the production of light and stiff parts having high flexural strength. Machining and joining of composites is important to obtain the final form of the parts to be used especially in the assembly of products with multiparts. Repair of composites are required as a consequence of deformations during service and aging as a result of repetitive loading, environmental effects, etc. Recycling has gained importance especially in the last decade due to the environmental concerns as can be seen in EU directives, which recently became a concern of sustainability and nowadays the PLM (product lifecycle management).

3.3.1 Compression molding (SMC/BMC compression molding)

Compression molding is one of the widespread production methods, which utilizes fibers and matrices, prepregs, sheet molding compounds (SMC), and bulk molding compounds (BMC) as raw materials. The production is done by applying pressure and (if required) heat to molds in which the raw materials are placed. SMC is one of the most common closed compression molding techniques. SMC resin mats are produced from a high-viscosity fiber/resin compound (Fig. 3.12). The viscosity of the fiber/resin compound decreases during further processing in the closed mold under heat and pressure (approx. 70 bar). As a result, the thermosetting resin containing the isotropically dispersed reinforcing fibers flow into the closed mold, where it cures.

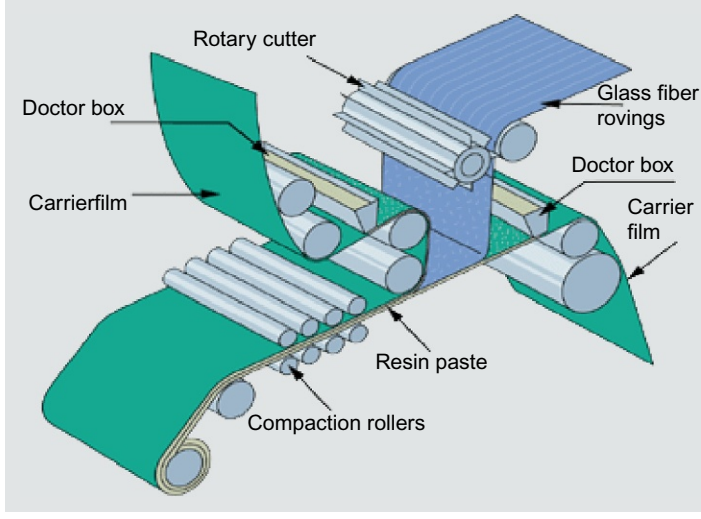

Fig. 3.12 Schematic of the SMC production.
With kind permission of Wacker Chemie AG, https://www.wacker.com/cms/en/industries/pl_composites/pl_comp_appl/sheetmoulding.jsp [accessed 16.12.16].

3.3.2 Hand lay-up

Hand lay-up is by far the most widely used process and is used in a wide range of industries. Following application of the liquid release agent (wax, silicone spray, etc.), a gel coat is applied preferably. This high resin containing coat, which usually contains pigments and fillers, forms the decorative exterior surface of the finished part. The gel coat is followed by a layer of resin and then the reinforcement. The resin is forced through the reinforcing material by rolling, thus removing air and completely impregnating the reinforcement. The procedure is continued by placing the next reinforcement layer on top and applying the resin similarly until the desired number of layers is reached (Fig. 3.13).

3.3.3 Spray-up

Chopped glass fibers and resins are supplied to an open mold. This involves feeding the rovings into a chopper and then blowing them into a precured resin (Fig. 3.14). The advantage is the high speed with which the material can be applied. After application, the material is usually consolidated with a hand roller in the same way as with hand lay-up.

3.3.4 Vacuum infusion

It is also called by its patented name SCRIMP, which is performed by flowing the resin through the reinforcement placed on an open mold with the help of a vacuum pressure that also creates a pressure on the layers by the pushing of the membrane called vacuum bag (Fig. 3.15).

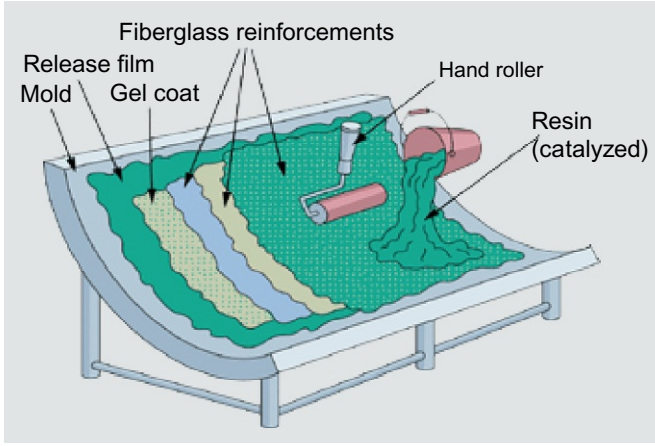

Fig. 3.13 Illustration of the hand lay-up process.
With kind permission of Wacker Chemie AG, https://www.wacker.com/cms/en/industries/pl_composites/pl_comp_appl/handlayup.jsp [accessed 16.12.16].

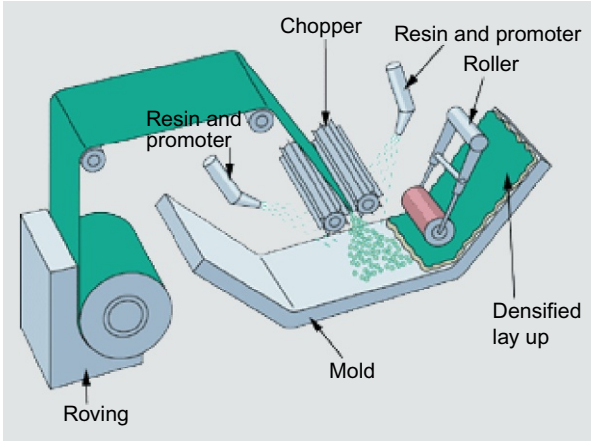

Fig. 3.14 Spray-up technique. With kind permission of Wacker Chemie AG, https://www.wacker.com/cms/en/industries/pl_composites/pl_comp_appl/sprayup.jsp [accessed 16.12.16].

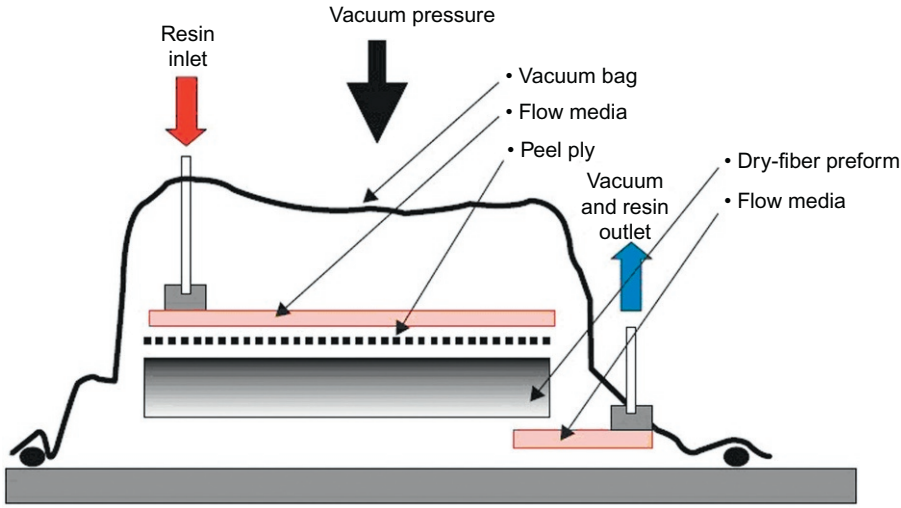

Fig. 3.15 A schematic view of vacuum infusion technique.

3.3.5 Resin transfer molding (RTM), vacuum assisted resin transfer molding (VARTM)

RTM involves the injection of a low-viscosity thermoset into the closed mold under moderate pressure (usually 3.5–7 bar) via one or more injection ports. The injected resin fills all the voids in the mold, impregnating and wetting the entire surface of

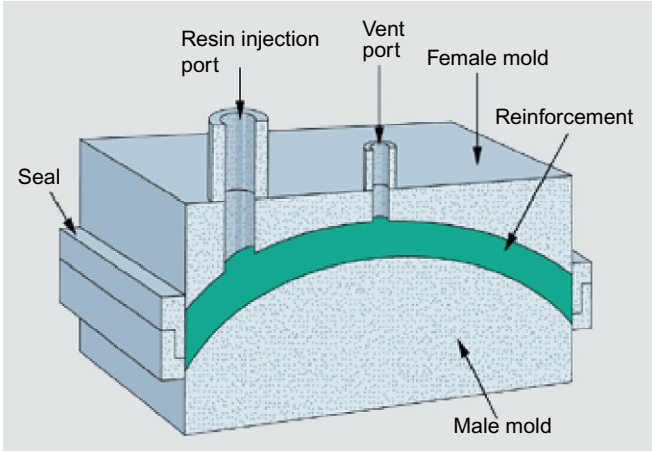

Fig. 3.16 RTM method.
With kind permission of Wacker Chemie AG, https://www.wacker.com/cms/en/industries/pl_composites/pl_comp_appl/resintransmould.jsp [accessed 16.12.16].

the reinforcing material (Fig. 3.16). The reinforcement comprises a variety of fiber types and forms, such as fiber tows, mats, or woven structures. RTM is used in the transportation, wind power, and construction sectors. It is particularly suitable for producing complex three-dimensional shapes. Differently in VARTM technique, a vacuum is applied to enhance resin flow and reduce void formation—the part is typically heat cured.

3.3.6 Vacuum bagging

Vacuum bagging utilizes the application of vacuum to the constituents enclosed by a membrane. Differently from vacuum infusion, there is no flow of resin through the bagging environment (Fig. 3.17). If heat is required for the cure, IR source, heating table, oven, or autoclave can be used.

3.3.7 Autoclave molding

Autoclave is one of the most traditional manufacturing methods used in fiber reinforced composite. Until today, it is the only method to cure thermoset materials in order to ensure low level of porosity. A good example is the carbon fiber reinforced composite fuselages that are made using autoclave process. Other nonstructural loading parts are also made using out-of-autoclave process but the porosity often exhibit 2% or more. It is the unique pressure that the autoclave generates that made the process so expensive. This production method uses the same setup as in vacuum bagging (Fig. 3.17), but additionally a pressure is applied onto the enclosing membrane inside a closed chamber called autoclave (Fig. 3.18), which can also provide controlled cooling of the part. High quality parts in terms of mechanical performance can be manufactured by this technique.

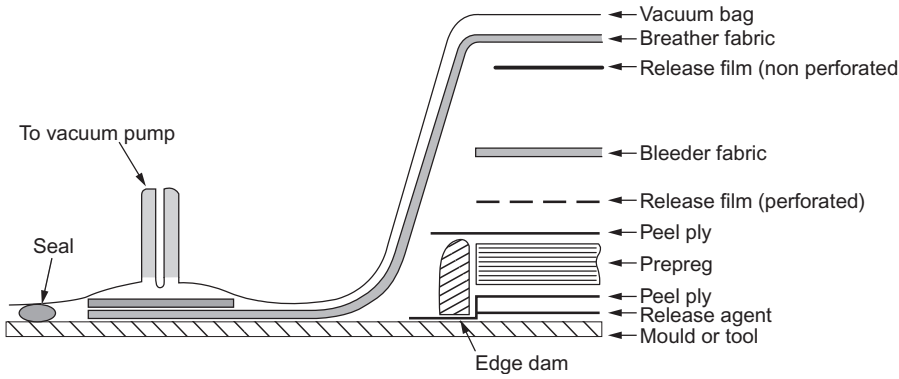

Fig. 3.17 Vacuum bagging setup.

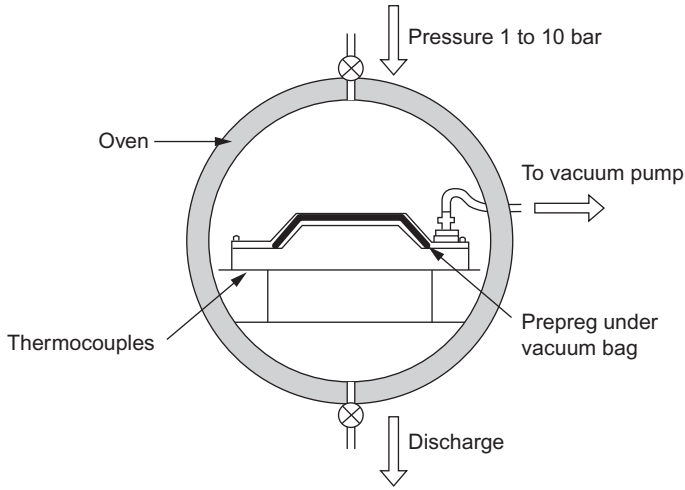

Fig. 3.18 Schematic of the autoclave process.

3.3.8 Filament winding

It is the most common method to produce parts with axial symmetry. The fibers are impregnated by passing through the resin bath and then wound on a mandrel having a diameter value appropriate to achieve the required part dimension (Fig. 3.19). The resin bath is attached to a transversely traveling head, whose speed arranges the winding angle of the fibers. Cylindrical tanks and large pipes are especially produced by this method.

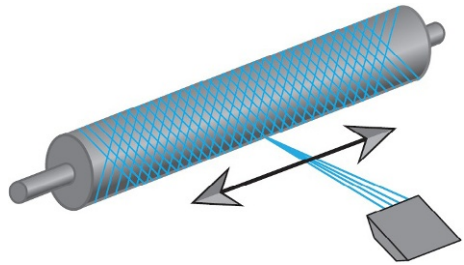

Fig. 3.19 Filament winding technique.

3.3.9 Centrifugal casting

It is another method of producing cylindrical parts. Contrary to filament winding, it can result in good outer surface quality because this time the composite is produced inside a hollow mandrel whose internal surface quality determines the outer surface quality of the composite product. The constituents are fed inside the rotating mandrel, so that the centrifugal force pushes the material onto the internal surface of the mandrel on which the composite is formed.

3.3.10 Automated fiber placement (AFP), automated tape laying (ATL)

ATL and AFP are rather new technologies in the composite industry because of the involvement of robots. There are a hand full of OEMs (original equipment manufacturers) who built these machines based on various heading mechanisms. The ultimate goal is to ensure that incoming tapes are heated and melted slightly to bond the plies together. The precision is critical and the quality of the incoming tape also place a key role. They are often UD fiber reinforced prepregs and their slit edges and alignment influences the speed, quality of the lay-up parts, and the scrap rate of the material.

3.3.11 Pultrusion

In the pultrusion of thermosets, the reinforcing fibers are impregnated by passing them through a resin bath. The resin-impregnated fiber strand is then brought to the near net shape at a number of preform stations and shaped and cured in a heated mold (Fig. 3.20). This method is used for consumer articles and in the electrical and construction sectors and therefore also known as wire coating.

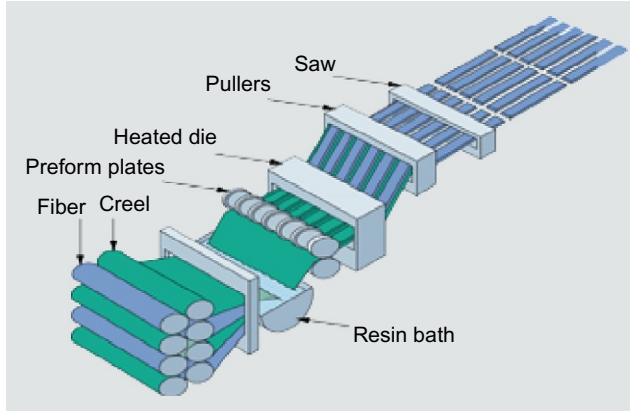

Fig. 3.20 Pultrusion method.
With kind permission of Wacker Chemie AG, https://www.wacker.com/cms/en/industries/pl_composites/pl_comp_appl/pultrusion.jsp [accessed 16.12.16].

3.3.12 Injection molding

Injection molding is one of the most common processes that is used in the plastics industry. It can be found in pure plastic products and when it comes to composite materials it remains a popular route of manufacturing due to its high production rate. In most cases, the plastic is combined with a filler such as chopped short fiber. The use of an extruder allows for the blending of the chopped fiber with the resin under controlled shear rate. Up to 30% fiber loading is found in injection molded short fiber composites and to achieve a good homogeneous mixing, materials are often passed through the barrel several times following chopping before the final shape is made with the aid of expensive tooling. Final product is shaped usually by hydraulic or pneumatic presses.

3.3.13 Reaction injection molding (RIM: RRIM, SRIM)

Reaction injection molding is modified to make fiber reinforced composites. Thermoset resins are widely used in this case because of their intrinsic low viscosity and ability to penetrate through the reinforcement phase. The process itself can accommodate short chopped fibers (RRIM: reinforced reaction injection molding). In the meantime, for higher performance parts and components, the reinforce phase is often in the form of a fabric such as woven fabrics or noncrimp fabrics. Once again just like injection molding, the tooling involved in this manufacturing processing is usually the expensive component and furthermore this is a much slower processes because the resin itself needs to go through a heat cure profile that involves heating up, holding, and cooling down. Release agents are often also required to remove the part from the mold once it is completed. Structural reaction injection molding (SRIM) is a combination of

RIM and RTM, resulting in shorter processing times than RRIM. Polyurethane resin is widely used in RRIM and SRIM methods especially to produce parts for the automotive industry such as bumper beams and body panels.

3.3.14 Thermoforming

This process allows shaping of thermoplastic sheets after being heated usually by IR sources. If shaping of the composite part is realized by vacuum, the process is called *vacuum (thermo)forming*. If a positive air pressure is applied on the sheet material to push it onto the mold cavity, then the process is named *pressure thermoforming or blow forming*. Both methods can utilize male or female molds. If the product is formed by pushing a male or female mold into the corresponding opposite one, the process is called *mechanical thermoforming (stamp forming)*. Stamp forming is also sometimes known as belt pressing and usually involves pressure being applied to thermoplastic composite blanks or sheets. The pressing rate of this manufacturing process is rather low in the form of meters per hour. The reason for this is because preheating is usually required prior to pressure being applied through the mold. Cooling also needs to take place once the temperature of the material that is being pressed is below their gel point. The cooling rate also determines the crystallinity depending on the polymer itself.

3.3.15 Prepregging

It is a method that makes use of a semifinished or mid-product named "prepreg," which originates from the preimpregnation process of the reinforcement by the resin (Fig. 3.21). This method allows the storage of this "film composite," which has controlled fiber volume ratio, to be used later in the composite part production process.

3.3.16 Sandwich construction

Sandwich constructions are manufactured by pressing thick core of honeycomb, foam, or balsa between thin high strength prepreg sheets (Fig. 3.22). They allow achievement of very low weight, high stiffness, durability, design freedom, reduced production costs. These structures are produced by autoclave processing, vacuum bagging, or pressing. They are preferred when light weight, stiffness, and strength are required. Typical applications are aircraft, ship, and train interiors.

3.3.17 Machining

Operations such as cutting [by saws, files, routers, etc. using a diamond coated tool, and recently waterjet (The possibility of water absorption has to be well considered) and laser cutting (Local matrix degradation occurs)], trimming, drilling, routing, sanding, grinding, milling are required in order to create holes and slots for the assembly of produced parts, to achieve the required tolerances, to prepare the surfaces for bonding, coating, and painting, and to produce prototypes from starting materials such as a composite rod, tube, plate, block, etc. [45].

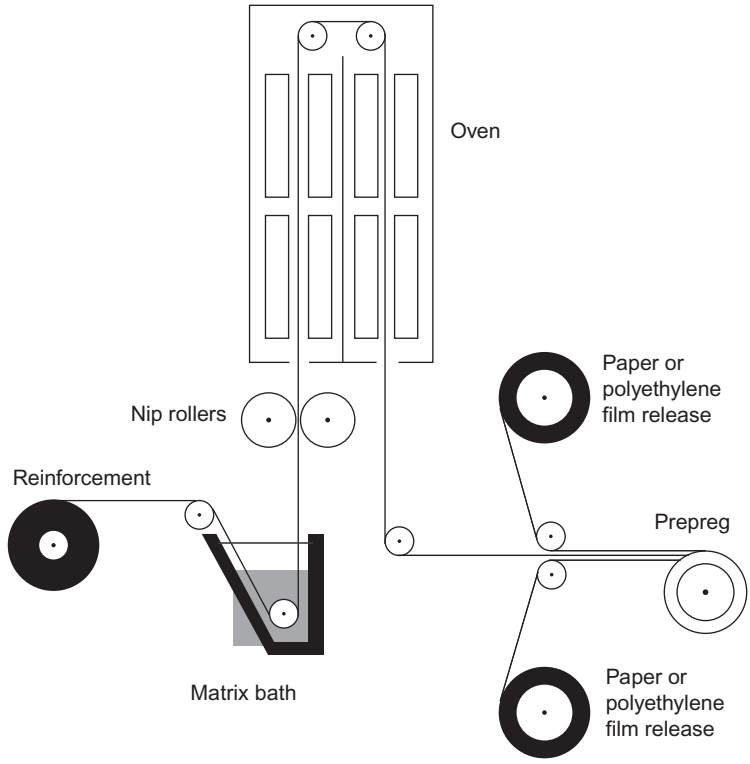

Fig. 3.21 Prepreg process.

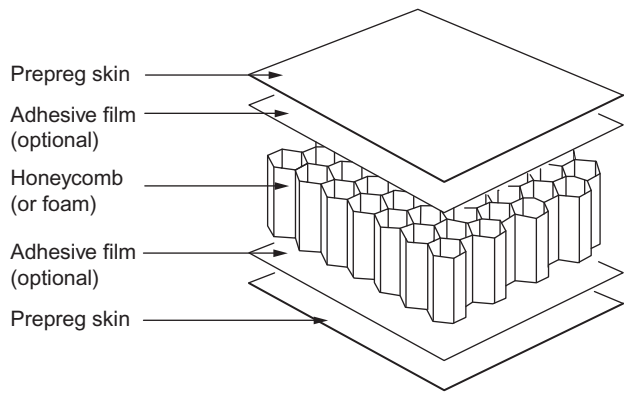

Fig. 3.22 A typical sandwich construction.

3.3.18 Joining

Assembly of a product, which is formed of several components, always requires the joining of a composite part to either another composite part or a metal part. Besides, repair of composite parts are sometimes required during service. Adhesive bonding and mechanical joints (bolted, threaded, riveted, screw and pin) are two methods of joining metals and composites. Joining methods for composites according to the material type can be listed as follows [35,47]:

PMCs: Adhesive, fusion, weld or rivet bonding, mechanical fastening, and integral mechanical attachment.
MMCs: Fusion or nonfusion welding, brazing, weld brazing, adhesive or weld bonding, and mechanical fastening.
CMCs: Adhesive or sinter bonding, fusion or nonfusion welding, brazing, and cementing.
C/C composites: Adhesive or cobonding, brazing, and mechanical fastening.

3.3.19 Recycling

Waste disposal and waste management is the key to the future. Private companies as well as governments are bringing in legislations in order to actively tackle this challenge. The overall aim is to reduce the quantity of material going into landfill and utilize any possible means of recycling composite materials. A lot of work has gone into looking at the various stages of manufacturing of composite materials in an attempt to recycle any constituents, semifinished products, product scraps, or parts. For example, in the case of thermoplastic matrices continuous fiber composites are disintegrated using heat and the resulting fibers are chopped into thermoset resin systems or reused directly as in the case of high quality glass fibers [48]. Alternatively semifinished products are chopped for compounding and this is a possibility on thermoplastic systems. As for thermoset composites, recycling is quite limited because of the crosslinking of the cured polymer. Reuse as filler material after chopping or grinding of the composite is an option. This also counts for the end-life cost of thermosets. Another possible reuse of polymeric composites is energy recovery by combustion [43]. End of service life materials is a more long term vision. If one is to take a look at the retired civil aircrafts parked out in the desserts around the globe after decommission, a lot of the valuable components had been taken out and what is left is either low cost value or heavily contaminated. The same applies to electronic waste that a large portion of the world's population is generating. It is not always bad examples we see around how the world reacts to recycling, for we can also see for instance that paper, plastic, and cans are making good progress in some of the more developed countries and cities. Various journal and magazine articles had already case studies covered and it is important that the effort of recycling does not stop [45].

3.4 Characterization and testing

Previously in Sections 3.2 and 3.3, the importance of materials selection and process of manufacturing have been discussed and it is not only afterwards that characterization and testing are to be done. In fact it is the reverse meaning that the testing of fiber

reinforced composites are best to be subdivided into various stages and examined in a flow chart form of:

(1) Raw materials—i.e., quality of batches
(2) During manufacturing—i.e., online and offline
(3) Postmanufacturing—i.e., quality of produced parts
(4) Testing the parts to the limit—i.e., until failure
(5) During and postservice—i.e., live monitoring and postmortem analyses

Some of the techniques are applicable at different stages of the composite materials and their constituents, and therefore, better off be subdivided into a more technique based family rather than a process stage category.

3.4.1 Analyses

To examine the general analyses of composite materials, the following categories are applicable with specific examples illustrated:

- IR, UV-vis, and Raman spectrometry are widely used for both resin and fiber to look for chemical functionalities and defects in fibers, etc., For instance changes in the bulk or near surface crystal structure of the fiber can be measured using XRD [49].
- Microscopy ranges from optical to SEM, TEM, and AFM. The morphology of fiber surfaces, fiber/matrix interface, fiber and composite cross sections, and also the fracture sites after mechanical testing can be viewed under optical and SEM. While TEM is not directly for composites, it is useful for nanoparticle studies to examine the levels as small as single atomic layers. Examples of recent work topics regarding the composites can be the growth of CNT, graphene, or other carbon nanostructures on carbon fiber surfaces, and the incorporation of such nanostructures into the resin for matrix modification purposes. AFM, however, is used for examining fiber surface topography and especially to determine fiber surface roughness. Also, it helps mapping of the elastic modulus variations around a composite interface. It has been used in the literature also to determine the elastic and shear moduli of CNTs.
- Chromatography related tools are used on both fibers and resin in order to determine molecular weight as well as surface energies. They are important in particular for tailoring the chemistry and for confirmation on process related variations.
- Surface analyses such as topography or composition and chemistry of constituents are widely used. For example XPS surface chemistry of the fiber in terms of surface atomic composition of the fiber and bonding energy of functional groups present on the fiber surface. Sample area of about 5 mm^2 may be required for analyses and aluminum foil wrapping may help to prevent spreading of fiber tow ends [49]. Furthermore, techniques such as zeta potential allows for the electrokinectic properties of fibers and resins to be measured while BET determines the corresponding surface area. Wettability is also an area that falls into the surface analyses category as this explores interactions between the fiber and the matrix.
- Thermal analyses including DSC and TGA are conventional yet highly important for measuring glass transition temperatures, crystallinity and cold crystallization, degree of cure, degradation onset, etc.

3.4.2 Testing

Testing can be subdivided into imaging, mechanical, rheological, and thermal. Imaging (DIC, contactless extensometry) and mechanical are frequently combined

together to provide extra information. Mechanical testing on individual constituents within a fiber reinforced composite system is more leaning toward the development phase of the material and quality control. Once the composite is made via specific processing routes—the list of mechanical tests can go on forever with traditional tests such as tensile and compression being the basics while open-hole, toughness, and shear are more applications driven. Thermal testing again is often combined with mechanical tests such as DMA (dynamic mechanical analysis), hot-wet properties to allow for predictions of in service as well as service life behaviors. Thermal testing may also be combined with fluid resistivity behavior of the material as well as thermal cycling. If one is to explore the number of test standards available in Europe and in the United States, it will be appreciated that the amount of information is so vast that it is beyond the scope of this chapter to try and have it summarized. The key is to be able to identify and specify the test that allows for the targeted mode of interest to be examined. For example, if it is surface functionality—XPS may be a good tool, or if influence of chemical modifications to the resin—molecular weight, toughness, fluid resistance, elongation at break, glass transition temperature etc. may well be looked at. If the material is to be subjected to continuous cyclic loading over the service life, then creep and fatigue properties are the ones that should not be missed.

3.5 Fiber surface treatments

The reinforcement phase of a composite system in general consists of 60% fiber, of which it is this 60% of the volume that bares the load in which the composite is subjected to during its surface life. The discussion on fiber surface treatments (FSTs) can be broadly subdivided into categories based on the fiber type. For example, sizing of glass fiber using a silane coupling agent can be classified as FST [50]. At the meantime, if the reinforcing fiber type is carbon, the surface treatment process tends to be an electrical process. This is not limited to continuous fiber reinforced composites, but also extends to short and long fiber composites. The authors in the review article gave a nice summary of the intended uses of FST techniques [51,52]:

- Increases the wettability of the fiber surface by the matrix resin.
- The removal of weak boundary layer, e.g., contaminant species or gas molecules physically adsorbed on the fiber surface. This would provide a more intimate contact between the fiber and the polymer to ensure a significant level of van der Waals force, which being a short-range force would otherwise be relatively weak.
- To allow for the matrix molecules to become physically entangled with, or diffuse into, the molecular network of polymer coating applied on the fibers.
- To promote mechanical interlocking between the fiber and the matrix. This can be achieved by creating surface porosity, into which resin molecules can penetrate.
- Increase the level of fiber bridging and in return to reduce crack propagation.
- To increase the number of active sites on the fiber surface for subsequent chemical bonding with the unreacted species in the matrix resin.
- By applying a thin layer of “coupling agent” that will chemically bond to both; fiber and matrix.

In all cases, surface treatments are designed to enhance and optimize mechanical performance by which it meets the end use requirements of the material. The way that interactions between fibers and the matrix is quantified in the form of interfacial adhesion and such phenomenon is measured in the form of wettability in most cases, which in turn leads to the surface free energy aspect as an important criterion. Consequently, this is followed by studies aiming at modification of the interface/interphase either by FSTs or matrix modification in order to achieve improved interfacial bonding between the fiber and the matrix [53]. The changing of surface properties of the reinforcing constituents of the composite, to enhance the fiber/matrix adhesion, will be only summarized in this part of the chapter as they are the focused subject of another chapter of this book. These treatments can be grouped generally as oxidative and nonoxidative treatments, which can be listed as follows [54]:

3.5.1 Oxidative

Liquid phase oxidation: Electrochemical oxidation (HNO_3, NaOH) and chemical oxidation (HNO_3, H_2O_2, $KMnO_4$, etc.).

Gaseous oxidation: Oxidation in air, oxidation in oxygen and oxygen containing gases, and catalytic oxidation. Plasma oxidation: O_2, N_2, NH_3, etc.

3.5.2 Nonoxidative

Whiskerization, plasma polymerization, polymer grafting, pyrolytic carbon deposition.

Based on the studies done by various researchers, it can be concluded that surface treatment of fibers is essential to improve their adhesion with various matrices. Treatment significantly influences the following characteristics:

- Treatment alters the morphology and increases the roughness of fiber surface.
- Increased roughness increases surface area on fiber surface to improve interactions between fiber and matrix.
- Surface treatment also influence chemical structure of fibers and enhance chemical bonding with matrix.
- Different treatments have different influence on fiber surface. Optimization is required to select appropriate treatment method according to application and desired properties.

Last but not the least, the type and the level of FST is one of the most guarded trade secrets of fiber manufacturers. It is not only the fact that it drives specific performances of the fiber end use parts or components, there is not a direct standardized measurement technique that relates to the level of FSTs.

3.6 Conclusion

This book chapter introduced composites and in particular the fiber reinforced composites as it is the focused topic of this book. Fundamental definitions such as reinforcement, matrix, interphase, interface, rule of mixtures, fiber volume fraction,

and fiber/matrix adhesion were given. Types of reinforcements and matrices were mentioned briefly although various types of fibers are topics of individual chapters of the book. Properties of some materials were tabulated and some example applications of composite materials were mentioned. Fiber reinforced composite material market was explained in terms of current situation and future outlook. Manufacturing processes of the composites were briefly explained with accompanying illustrations. Characterization and testing of composites, which are most important to know the materials' properties were given afterwards. The chapter was completed with the explanation of FSTs, which affect tailoring of fiber/matrix adhesion and are a detailed subject of another chapter of the book.

Acknowledgments

The authors are very much grateful to Hexcel Corporation and Wacker Chemie AG for their contribution in this book chapter by giving kind permissions to use their images within the required parts of the text.

References

[1] https://commons.wikimedia.org/wiki/File:Composite_3d.png [accessed 16.12.16].
[2] Sain MM, Kokta BV, Imbert C. Structure-property relationships of wood fiber-filled polypropylene composite. Polym-Plast Technol Eng 1994;33(1):89–104.
[3] Kokta BV, Raj RG, Daneault C. Use of wood flour as filler in polypropylene: studies on mechanical properties. Polym-Plast Technol Eng 1989;28(3):247–59.
[4] da Silva ALN, Rocha MCG, Moraes MAR, Valente CAR, Coutinho FMB. Mechanical and rheological properties of composites based on polyolefin and mineral additives. Polym Test 2002;21(1):57–60.
[5] Clingerman ML, Weber EH, King JA, Schulz KH. Development of an additive equation for predicting the electrical conductivity of carbon-filled composites. J Appl Polym Sci 2003;88:2280–99.
[6] Drzal LT, Herrera-Franco PJ. Measurement methods for fiber-matrix adhesion. In: Dillard DA, Pocius AV, editors. Composite materials in adhesion science and engineering—I: The mechanics of adhesion. Amsterdam: Elsevier; 2002.
[7] Kim J-K, Mai Y-W. Engineered interfaces in fiber reinforced composites. Amsterdam: Elsevier; 1998.
[8] https://commons.wikimedia.org/wiki/File:Windmill_D1_(Thornton_Bank).jpg [accessed 10.12.16].
[9] Summerscales J. Composite materials and structures for the marine environment, https://www.fose1.plymouth.ac.uk/sme/composites/marine.htm [accessed 10.12.16].
[10] http://www.hexion.com/epoxyphenoliccomposites/automotive/new_breakthroughs/ [accessed 10.12.16].
[11] http://inhabitat.com/carbon-black-is-a-sleek-minimalist-wheelchair-for-active-people/ [accessed 11.12.16].
[12] Composites Symposium 2011, http://www.euroaviasevilla.es/compositesymposium/why_composites.php [accessed 12.12.16].
[13] Lucintel Brief. Growth opportunities in global composites industry. Texas: Lucintel Brief; 2011.

[14] Witten E, Kraus T, Kühnel M. Composites market report; 2016.
[15] Claunch EC. Forecasting on composites—markets, products, and demands. J Textile Apparel Technol Manage 2015;9(2):1–6.
[16] Allied Market Research Report 2017.
[17] Saba N, Tahir PM, Jawaid M. A Review on potentiality of nano filler/natural fiber filled polymer hybrid composites. Polymers 2014;6(8):2247–73.
[18] Bismarck A, Mishra S, Lampke T. Plant fibers as reinforcement for green composites. In: Mohanty AK, Misra M, Drzal LT, editors. Natural fibers, biopolymers, and biocomposites. CRC Press; 2005.
[19] Fan M, Fu F. Advanced high strength natural fibre composites in construction. Cambridge: Woodhead Publishing; 2017.
[20] Poveda RL, Gupta N. Carbon nanofibers: structure and fabrication. Carbon nanofiber reinforced polymer composites. Berlin: SpringerBriefs in Materials; 2016. http://dx.doi.org/10.1007/978-3-319-23787-9_2.
[21] Beachley V, Wen X. Effect of electrospinning parameters on the nanofiber diameter and length. Mater Sci Eng C Mater Biol Appl 2009;29(3):663–8.
[22] Song YS, Youn JR. Influence of dispersion states of carbon nanotubes on physical properties of epoxy nanocomposites. Carbon 2005;43(7):1378–85.
[23] Kumar RS. Textiles for industrial applications. Boca Raton, FL: CRC Press; 2014.
[24] Juska T. Mechanical properties and impact damage resistance of composites fabricated by low cost, vacuum assisted, resin transfer molding. In: Survivability, structures and materials directorate research and development report; 1993.
[25] Pearce NRL, Guild FJ, Summerscales J. The use of automated image analysis for the investigation of fabric architecture on the processing and properties of fibre-reinforced composites produced by RTM. Compos A Appl Sci Manuf 1998;29(7):829–37.
[26] Alavudeen A, Rajini N, Karthikeyan S, Thiruchitrambalam M, Venkateshwaren N. Mechanical properties of banana/kenaf fiber-reinforced hybrid polyester composites: effect of woven fabric and random orientation. Mater Des 2015;66(A):246–57.
[27] Cavallaro PV. Effects of weave styles and crimp gradients in Woven Kevlar/epoxy composites. Exp Mech 2016;56(4):617–35.
[28] Hamada H, Ramakrishna S, Huang ZM. Knitted fabric composites in 3-D textile reinforcements in composite materials. In: Miravete A, editor. Boca Raton, FL/Cambridge: CRC and Woodhead; 1999.
[29] Leong KH, Ramakrishna S, Huang ZM, Bibo GA. The potential of knitting for engineering composites—a review. Compos Part A 2000;31:197–220.
[30] Dow MB, Dexter HB. Development of stitched, braided and woven composite structures in the ACT program. Hampton, VA: Langley Research Center; 1997.
[31] Wang Y. Effect of consolidation method on the mechanical properties of nonwoven fabric reinforced composites. Appl Compos Mater 1999;6(1):19–34.
[32] Pegoretti A, Fabbri E, Migliaresi C, Pilati F. Intraply and interply hybrid composites based on E-glass and poly(vinyl alcohol) woven fabrics: tensile and impact properties. Polym Int 2004;53:1290–7.
[33] Mouritz AP. Review of z-pinned composite laminates. Compos Part A 2007;38:2383–97.
[34] Vinson JR, Sierakowski RL. The behavior of structures composed of composite materials. Kluwer; 2004.
[35] Messler RWJ. Joining of materials and structures from pragmatic process to enabling technology. Amsterdam: Elsevier; 2004.
[36] Bokobza L. Multiwall carbon nanotube elastomeric composites: a review. Polymer 2007;48(17):4907–20.

[37] Sayuti M, Sulaiman S, Vijayaram TR, Baharudin BTHT, Arifin MKA. Manufacturing and properties of quartz (SiO_2) particulate reinforced Al-11.8%Si matrix composites. In: Hu N, editor. Composites and their properties. Croatia: InTech; 2012.
[38] Amateau MF. Ceramic composites. In: Peters ST, editor. Handbook of composites. Chapman & Hall; 1998.
[39] Yamamoto G, Hashida T. Carbon nanotube reinforced alumina composite materials. In: Hu N, editor. Composites and their properties. Croatia: InTech; 2012.
[40] Buckley JD. Carbon-carbon composites. In: Peters ST, editor. Handbook of composites. Chapman & Hall; 1998.
[41] Budinski KG. Engineering materials properties and selection. New Jersey: Prentice Hall; 1996. p. 119–45.
[42] Peters ST. Introduction, composite basics and road map. In: Peters ST, editor. Handbook of composites. Chapman & Hall; 1998.
[43] Biron M. Thermoplastics and thermoplastic composites. Technical information for plastics users.
[44] Daniel IM, Ishai O. Engineering mechanics of composite materials. Oxford University Press; 1994.
[45] Mazumdar SK. Composites manufacturing—materials, product, and process engineering. Boca Raton, FL: CRC Press; 2002.
[46] Mallick PK. Fiber-reinforced composites—materials, manufacturing, and design. CRC Press; 2008.
[47] Kedward KT, Kim H. Joining and repair of composite structures. ASTM International; 2004.
[48] Pebly HE. Reuse and disposal. In: Peters ST, editor. Handbook of composites. Chapman & Hall; 1998.
[49] Rivière JC, Myhra S. Handbook of surface and interface analysis—methods for problem solving. New York: Marcel Dekker Inc; 1998.
[50] Iglesias JG, González-Benito J, Aznar AJ, Bravo J, Baselga J. Effect of glass fiber surface treatments on mechanical strength of epoxy based composite materials. J Colloid Interface Sci 2002;250(1):251–60.
[51] Tiwaria S, Bijweb J. Proc Technol 2014;14:505–12.
[52] Jang BZ. Control of interfacial adhesion in continuous carbon and Kevlar fiber reinforced polymer composites. Compos Sci Technol 1992;44(4):333–49.
[53] Erden S, Yıldız H. Enhancement of interfacial strength in 'carbon fiber/thermoplastic matrix' composites. In: 3rd international technical textiles congress, Istanbul, December; 2007. p. 426–45.
[54] Tang L, Kardos JL. A review of methods for improving the interfacial adhesion between carbon fiber and polymer matrix. Polym Compos 1997;18(1):100–13.

Further Reading

[1] https://www.wacker.com/cms/en/industries/pl_composites/pl_comp_appl/sheetmoulding.jsp [accessed 16.12.16].
[2] https://www.wacker.com/cms/en/industries/pl_composites/pl_comp_appl/handlayup.jsp [accessed 16.12.16].
[3] https://www.wacker.com/cms/en/industries/pl_composites/pl_comp_appl/sprayup.jsp [accessed 16.12.16].

[4] Hexcel Direct Processes Technology: http://hexcel.com/user_area/content_media/raw/Direct_Processes_Technology.pdf [accessed 16.12.16].
[5] https://www.wacker.com/cms/en/industries/pl_composites/pl_comp_appl/resintransmould.jsp [accessed 16.12.16].
[6] hexcel prepreg_technology: http://www.hexcel.com:82/pdf/Technology%20Manuals/Prepreg_Technology/index.html [accessed 16.12.16].
[7] https://www.wacker.com/cms/en/industries/pl_composites/pl_comp_appl/pultrusion.jsp [accessed 16.12.16].

This page intentionally left blank

Surface modification of fibers and sizing operations

4

Esen Ozdogan, Tulay Gulumser, Asli Demir
Ege University, Izmir, Turkey

4.1 Introduction and historical perspective

Composite materials emerged very early as a brick where straw is mixed with clay or mud. Today, they have high modulus of elasticity and provide materials with stiffness, high strength, and low weight features as a highly structural engineered materials. The usage areas of composites are varied such as automotive, construction, biomedical, aerospace, and defense applications. Fiber-reinforced composites are used to a great extent in our daily lives. The performances of these composites mainly depend on the surface properties of fibers. The mechanical properties of a fiber-reinforced composite rely primarily on the degree of adhesion between the matrix and the fiber. Therefore, the need for surface modification of fibers arises for obtaining proper adhesion. Textile fiber surfaces are considered to be good examples of mechanical interlocking as they have a porous nature. The surface treatments that result in microroughness on the surface improve adhesion strength by proving mechanical interlocking. The roughening of the surface can also result in the formation of a larger surface. Surface roughness also affects and increases adhesion [1–3].

The role of the reinforcing filaments in the composite can be completed if there is a proper bonding between the fiber and the matrix. So the structure and properties of the fiber-matrix interface play a major role in the mechanical and physical properties of composite materials [4,5].

The fiber length, fiber orientation, fiber surface, fiber cross-section, and fiber linear density have significant effects on strength and modulus properties of the composites. Many recent researches have focused on developing surface treatments to change the chemical and physical properties of polymer surfaces without affecting bulk properties. Treatments that are used for modifying polymer surfaces enhance the chemical nature of the surface of the polymers. The aim of these methods is to produce special functional groups at the surface; increase surface energy, electrical conductivity, hydrophilicity, or hydrophobicity; improve chemical inertness, dyeability, and handling; or modify surface crystallinity or roughness [2,6,7].

Traditional fiber-reinforced composites use various types of glass, carbon, aluminum oxide, and many others as reinforcing components [8]. Among the fibers used in composites, natural fibers attract more attention because they are alternative solutions to the ever-depleting petroleum sources. Besides the environmental advantages, they have low density with high specific strength and stiffness and they are readily available worldwide. The

Fiber Technology for Fiber-Reinforced Composites. http://dx.doi.org/10.1016/B978-0-08-101871-2.00004-7

usage of natural fibers as reinforcement of polymer matrices will improve the mechanical properties of the matrices such as tensile, flexural, and impact properties [5,8–14].

The weak points of the natural fibers are their high water absorption characteristics and weak interfacial bonding with the matrix material of composites. Due to the large industrial potential of natural fibers, their surface modification is becoming an important field of research. The majority of research in the area of fiber improvement focuses on the fiber-matrix interfacial adhesion and decreasing water. In most of the natural fibers, it is necessary to reduce hydrophilicity of the fiber by reducing the number of hydroxyl in order to improve the adhesion between fiber and polymer matrix [4,13,15–19].

Natural fibers have cellulose in their chemical structure. It is of importance since it contains a variety of natural materials such as waxes and lignin. Cellulose microfibrils are bonded by lignin compose fibers. The physical properties of natural fibers primarily rely on their chemical structure including degree of polymerization, orientation, crystallinity, cellulose content as well as the extraction methods used. The properties of fibers show difference substantially depending on its location the plant quality, part of the plant from where they are taken. Several fibers have different cross-sectional area, length, and defects such as microcompressions, cracks, or pits [4].

The surface modification treatments are attracting more attention since the bonding area between resin and fiber is crucial for all types of composites. Therefore, it is necessary to develop applications, which are compatible with the eco-friendly, efficient, and respect to the environment behind the progress of composites [20].

To reinforce the fibers of composites can be modified chemically and physically. Physical methods such as ozone, UV, plasma, laser treatments, and electron beam irradiation can be applied. Chemical methods including alkaline, acetylation, silane, oxidative treatments, graft copolymerization, and some others such as permanganate, esterification, maleated coupling, and isocyanate treatments are used [9,12,16,21,22].

4.2 Physical methods

Physical treatments change the structure and surface properties of the fibers without the usage of chemicals. Since they do not require chemicals, physical methods are considered as environmental friendly processes. There are many methods for surface modification of fibers. The majority of research in this area concentrates on the fiber-matrix interfacial adhesion. In this section, plasma surface modification, as the most commonly applied physical surface modifications of composites, and other methods (heat, UV, ozon, etc.) are explained.

4.2.1 Plasma treatment

The composite structural properties can be improved by increasing fiber-matrix interfacial adhesion through fiber surface modifications, modifying matrix resins, and improving the compatibility of matrix by fiber surface finishing treatments. In composite production, the degree of adhesion between fibers is so significant.

The biggest potential market of natural fibers is in composite products. Thus, to enhance adhesion of natural fibers with and matrix and their synthetic similitudes, plasma treatments have appeared as an alternative method. During plasma

modification, the interface adhesion can be improved by increased mechanical bonding between the matrix and the fiber.

Plasma treatment is a physical method. Plasmas can be generated when a gas is exposed to an electromagnetic field at near ambient temperature and low pressure. They can be classified as atmospheric and low-pressure plasmas, which are used for surface modification of materials. Atmospheric plasmas can be produced under atmospheric conditions. They can be applied to industrial scale applications more easily. Plasma surface modifications can be distinguished depending on the nature and type of the gases used. The better fiber-matrix interfacial bonding can be achieved at the end of plasma treatments [23].

To obtain the strong adhesion by plasma treatment, the surface properties and characteristics of the material should be known. There are mainly four mechanisms that provide to adhesion for polymers:

(a) chemical bondings such as ionic, covalent, and hydrogen bonds;
(b) interdiffusion of chains (polymer diffusion-driven linking);
(c) other weak interatomic forces; and
(d) mechanical interlocking (surface topography) [24].

Natural fibers are encouraging substitute for other technological reinforcing fibers because of their disposable properties, low density, availability possibilities, and mechanical properties. In addition natural fibers have great value when processed due to their low abrasive features in comparison to harder inorganic fillers. The usage of natural fibers for the purpose of reinforcement material in composites requires a considerable adhesion between the synthetic matrix and the fiber. Also, the surface treatments of thermoplastic materials were found to be effective in obtaining composite structures. Generally, plasma exposure enhances the relative surface oxygen content and improves adhesion property. The properties of composites from cellulosic fibers and thermoplastic polymers have been investigated by several authors. Most studies indicated that mainly argon and air plasma treatments enhanced the compatibility between thermoplastic matrix and fibers [25].

In the study made by Bozaci et al. (2010), jute fibers were subjected to atmospheric plasma treatment and air was used as a process gas. The results showed that the effects of atmospheric plasma treatment on jute fiber properties improved the surface and mechanical properties to be used for composite materials. From pull out tests, it was obtained that greater plasma power and treatment time resulted in greater IFSS values due to mechanical interlocking. It was probable that plasma treatment improved jute fiber-polyester matrix adhesion by changing the surface properties of jute fibers [26].

High-temperature mechanical pulp and high alpha hardwood fibers treated by plasma to improve their adhesion to thermoplastics in another study. Air and argon plasma treatments improved the tensile strengths and moduli of wood fiber-polypropylene composites. It was shown that the best result was obtained when both the wood fiber and the plasma-treated polypropylene surfaces [27].

In a study of flax fiber-reinforced polyester composites were treated by helium cold plasma treatment. The authors were examined the treated composites in terms of their mechanical properties and water permeabilities. The analysis of the water permeability

and mechanical results showed that plasma treatment improved the fiber-matrix adhesion and enhanced the mechanical properties [28].

The sisal-high density polyethylene composites were prepared by Martin et al. (2000). The outcomes showed that some improvements in mechanical properties of the composites are obtained by means of the plasma treatments [29].

Jute fibers were treated in radio frequency and low-frequency plasma reactors. In the treatments, O_2 gas was used at for different plasma powers to increase the interfacial adhesion between the jute fiber and polyester matrix. The interlaminar shear strength (ILSS), tensile, and flexural strengths were increased with both types of plasmas. Treatment made by radio frequency plasma system showed greater improvement on the mechanical properties of jute/polyester composites compared with low-frequency plasma system. The effect of plasma treatment on the mechanical structures of jute fibers was investigated by Sinha et al. Also, the changes on interfacial adhesion of jute fibers/unsaturated polyester were researched. The rougher surface and degradation of fiber due to an etching mechanism caused by plasma process resulted in the development of hydrophilicity of the fibers. However, the flexural strength of composites treated for 10 min with plasma showed an improved mechanical strength up to 14% in comparison to raw fiber composites [30,31].

The influence of argon plasma on the interfacial adhesion of poly-*p*-phenylenebenzobisoxazole fiber-bismaleimide composites and aging behaviors were examined by Liu et al. The ILSS was greatly increased to 62.3 MPa with an increase of 39.7% at 200 W plasma power. The surface roughness and wettability values of fiber were increased. The SEM images showed that the fracture shifted from the interface to the matrix. The ILSS decreased to approximately 54.0 MPa after 10–30 days. The composite had a high retention of 90% in the ILSS at moisture conditions [32].

Interfacial properties of carbon fiber-reinforced nonpolar structure polyarylacetylene resin composites were modified by cold oxygen plasma treatment in a study. ESCA results showed that plasma treatment increased the amount of elemental oxygen on fiber surface markedly. AFM images indicated that weak surface regions of fibers had been etched and removed, and the roughness of fiber surface was increased. Also, ILSS values of composites were improved significantly [33].

Corona treatment is the most widely used atmospheric pressure plasma process. This treatment on cellulosic fibers and hydrophobic matrix was found to be effective for the improvement of the compatibilization between hydrophilic fibers and a hydrophobic matrix.

The mechanical characteristics of jute fiber/epoxy composites can be enhanced by corona discharge treatment. The yarn tenacity decreased with an increasing corona energy value. Moreover, corona-treated fibers had higher free surface energy with increasing treatment time [34].

Biename et al. were investigated the mechanical properties of corona-treated hemp fiber/polypropylene composites. The treatment of matrix or fibers gave rise to a significant increase in tensile strength values. The modification of fiber caused improvement on the properties of the composites up to 30% of Young modulus [35].

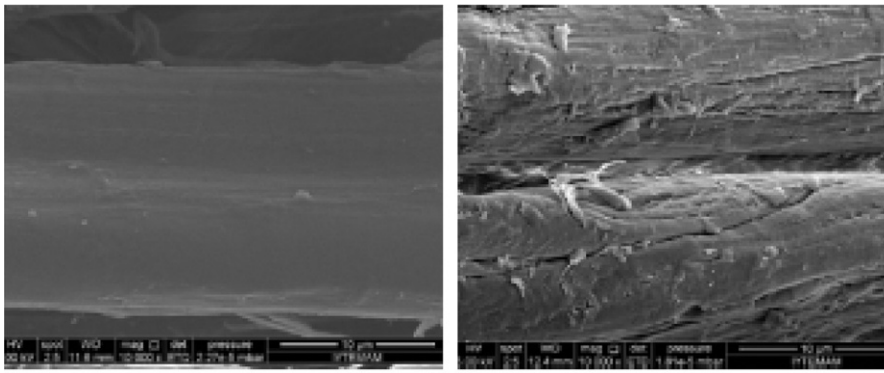

Fig. 4.1 SEM images of (A) argon-treated flax fiber untreated flax and (B) argon plasma-treated flax fiber [21].

In another study of hemp fiber mats and flax, they were treated by corona to improve tensile modulus and strength of the composites. The surface images of the fibers confirmed that relatively short treatment periods of corona treatment were found enough to enhance adhesion between fibers. It was also showed that no further improvement achieved by applying longer corona treatment times [19] (Fig. 4.1).

The trend of increasing popularity of the plasma treatment studies and majority of various plasma treatments indicate that plasma treatment is a very profound method to modify the interfacial properties between fibers and polar/nonpolar resins.

4.2.2 Other physical treatments

4.2.2.1 UV treatment

Surface treatments which are based on UV are carried out in ambient atmosphere. The substrate and UV bulb distances have significant influences over the effectiveness of the fiber surface's oxidation. In this method, UV radiation emitted by high-energy lamp resulted in the formation of the atomic oxygen. In the situation without vacuum, before reaching the polymer surface, the atomic oxygen can react with other gas molecules. The increment of surface density of oxygenated species was detected as smaller with the increasing distance between substrate and UV source. The UV treatment causes higher polarities of the fiber surface. By this way, the hydrophilicity of fibers and the composite strength were enhanced. The study about properly treated jute fibers made by Mathieson and Bradley showed that it is possible to get an increase of 30% in composite strength, after a 10-min treatment at a distance of 150 mm away from the UV lamp. When substrate-UV bulb distance was increased for constant treatment time, some improvements in composite flexural strength were seen. At the end, the excessive treatment conditions, such as short distances or long treatment times, caused the degradation of fiber tenacity. It can be concluded that to improve the

composite strength, it is necessary to get an increase in polarity of the fiber surface and a decrease of the fiber strength. Moreover, the UV treatment of the jute yarn gave results of higher polarity along with increased treatment time and constant bulb-substrate distance. It is possible to achieve an increase of the composite flexural strength of about 30%, under optimum treatment conditions [34].

4.2.2.2 Gamma radiation

Gamma radiation treatment is made by depositing energy on the plant fiber in the composite and radicals were produced on the cellulose chain by hydrogen and hydroxyl abstraction, ruptures of some carbon-carbon bonds and chain scission. Peroxide radicals are generated when matrix polymers are irradiated in the presence of oxygen. By the help of the active sites which gamma radiation produced in fiber and matrix, better bonding between the filler and polymer matrix was obtained. The mechanical strength of the composite was improved consequently [36].

4.2.2.3 Heat treatment

In surface modification of composites, fibers are heated or composites are processed at temperatures at which the components of natural fibers begin to decompose. As the result of heat treatment, polymers change physically and chemically. Physical changes have some effects over enthalpy, weight, strength, color, and crystallinity. On the other hand, chemical changes reduce the degree of polymerization by bond scission, creation of free radicals, and formation of different functional groups and these effects increase in the presence of air. Cellulosic fibers have a special importance among the fibers used in composites. Factors affecting the thermal degradation of cellulose-based fibers are the ambient atmosphere and pressure. The degradation process is speeded up with the occurrence of reaction products. While the cellulose-containing composites are processed, the degradation products can be found in the interface or in the polymer melt. Oxidation of the polymer matrix may be resulted because of the degradation products. The treatment factors which control the heating are time, temperature, and composition of the gaseous atmosphere in the oven. It can be said that heat treatment may be accepted as an interesting alternative and has many advantages, such as application easiness, simplicity, low cost, and no chemicals. The disadvantages are necessity of control for every factor and requirement of high precision [37].

4.2.2.4 Ozone treatment

Ozone treatment is a method that can be used to modify the surface activity of fibers to improve the mechanical characteristics of them to be used for composites. In the study made by Fu et al., it was tried to modify carbon fiber-reinforced polyarylacetylene resin composites in manner of mechanical interfacial properties by means of ozone surface oxidation treatment. The results showed that on the carbon fiber surface, elemental oxygen was increased significantly. Besides the elemental oxygen, some other oxygen groups such as carbonyl and carboxyl were seen on the fiber surface. There are some positive changes such as the improvement of surface chemical activity,

modification of the wettability, and increase of fiber surface roughness degree. As the result, better interfacial binding between the carbon fibers and resin were obtained. Khanchaitit and Aht-Ong investigated some combined effects of UV and different gas species such as exposures of nitrogen, air, oxygen, air/ozone, and oxygen/ozone. Polyethylene teraphtalate (PET) fiber surfaces were examined with the methods above also for the effects of exposure time on the morphology and chemistry of them. Applied test results showed that the PET fibers treated with UV/O_2-O_3 increased the tensile strength of the composite when compared with the untreated one [38,39].

4.2.2.5 Excimer UV laser

Excimer UV laser-induced etching is a type of ablative photodecomposition process. It can be applied to polymers mainly to increase their hydrophilicity and adhesion. Most of the excimer laser frequencies used are in the wavelength range of 193–351 nm. One of the main surface features of excimer laser-treated polymers is the presence of threshold fluence dependent on the UV. By changing the intensity and time of the photoetching process, surface roughness can be controlled [40].

4.3 Chemical treatments

For the surface modification of fibers to be introduced in composites, some chemical treatments such as alkali, silane, acetylation, benzoylation, acrylation, maleated coupling agents, isocyanates, permanganate can be used [8,12].

The aim of the chemical treatments is to improve the adhesion between the fiber surface and the polymer matrix, and some additional benefits are obtained such as improving mechanical properties and decreasing water absorption. It is expected from chemical treatments for the optimization of the interface of fibers. Chemicals that are used in chemical treatments may activate hydroxyl groups or introduce new moieties that can effectively make bonds with the matrix.

The bond between fibers and polymer matrix is very important because they affect directly the performance of the composites. Chemical treatments improve the separation of individual fibers and the adhesion with the composite matrix. As the result of chemical treatments, negative or positive effects may occur. Depending upon the components of the composite, choice of the treatment is the key point [41].

Besides interfacial adherence performances, mechanical properties were also studied particularly on composites made with natural fiber. This issue is very important because generally such kinds of composites are composed of hydrophilic natural fibers and hydrophobic polymer matrices. The properties of the adhesion are depended on humidity adsorption capacity and the presence of noncellulosic components. These studies are focused on different treatment methods of natural fibers' surfaces to improve interfacial bonding and resistance to humidity [9,42].

Many studies have been made about natural fiber composites because they have some advantages over inorganic reinforcing fibers. These advantages are low density and cost, bio-degradability, less abrasiveness, and renewable. Because natural fibers have some disadvantages such as thermal and mechanical degradation during

processing, low wettability, incompatibility with some hydrophobic polymeric matrices, and high moisture absorption, these weak points are tried to be overcome by chemical surface modifications [43].

Chemical methods depend upon the application method of chemicals to the surface of fibers forming composites. Some methods such as dissolution, coating and impregnation with a dilute resin, or different combination of these treatments may be applied [44].

4.3.1 Alkaline treatment

Alkaline treatment of cellulosic fibers in polymer matrices is a common method to modify the fibers in order to remove the lignin, waxes, and, more importantly, the hemicelluloses [8,12,16,45,46].

By this treatment, the adhesion between the fibers and the polymer matrix is enhanced. It is also a simple and a cheap technique. The advantageous points of alkalization are the positive effects over cellulosic and the noncellulosic components. Fiber fibrillation of bast fibers is also important. As the result of the fibrillation, fiber diameter reduces. At the end, the effective area in contact with the matrix does not only increase, but also an increase in the aspect ratio can be seen. Together with the enhanced fiber-matrix adhesion and rougher fiber topography, composite properties improve after treatment with alkali.

In some studies of plant-based fiber and polymer systems, it was seen that is the alkali-treated fibers treated with alkali method give a better reinforcement property than their unmodified ones. When fiber and matrix adhesion was improved, some properties of the composite such as the tensile and flexural characteristics will improve, too. Alkali treatment reduced the fatigue properties for some composites due to a better fiber-packing density and caused a high-fiber content in the composite [13,43,44].

As the result of alkali treatment, it can be said that the hydrophylic OH groups are reduced and surface roughness of the fiber is increased. In conventional processes alkaline treatment is normally used for the cleaning of plant-based natural fibers. In composites surface roughness changes, reactive sites increase, at the result a better mechanical interlocking and adhesion with the matrix will be obtained and then the increase in the interfacial strength of the composite will be obtained [5,8,9,36,47–49].

4.3.2 Silane treatment

Silane treatment is made by using a silane, inorganic chemical compound with chemical formula SiH_4. It is used as a coupling agent to modify the surface of the plant fiber in composites. At the two ends of silane agent, there are reactive groups; one of them can react with hydroxyl-rich surface and the other one can interact with the polymer matrix [8,13,36,50,52].

The chemical link between the fiber surface and the matrix is formed through a siloxane bridge. During the silane treatment of the fiber, several stages of hydrolysis, condensation, and bond formation are occurred. During condensation process, two reactive groups do their tasks as mentioned earlier. The reactions occurred at both

sides lead to the improvement in fiber matrix adhesion and stabilization of the composite properties. Silane coupling chemicals also make a surface coating over the micropores on the surface of natural fibers. Penetration of silane coupling develops interlocked coatings of fiber surface mechanically. It is defined that tensile flexural and ILSSs are also developed [46,50].

The theory of chemical bonding explains the mechanisms of interfacial bonding made by silane coupling agents. The bifunctional silane molecules form a link between the resin and the cellulosic fiber through the siloxane bridge. The factors affecting the microstructure of the silane coupling agent also affect and control the composites' mechanical and physical properties. Except then the silane's chemical structure, dispersion aids and initiator contribute to the chemical and physical changes at the interface and they affect the composites' mechanical properties. As a result it can be said that silane treatment of fibers interfacial adhesion and the mechanical properties of the composites are significantly improved. There are also some studies with silane treatment about surface modification of glass fiber composites. Silane treatment improves the adhesion of glass fiber to the polymer matrix and also stabilizes the composite material [5,8,9].

4.3.3 Oxidative treatment

4.3.3.1 Permanganate treatment

Permanganate, containing permanganate group, is a good source of cellulose radical former by the help of MnO_3^- ion formation. Highly reactive Mn^{3+} ions initiate a graft copolymerization. When the water adsorption of fiber-reinforced composite is needed to be decreased, permanganate treatment is useful. This treatment is performed by soaking fibers in a permanganate solution; concentration of this solution is very important and needs to be controlled with a great care. Mostly potassium permanganate is chosen. Permanganate method is the best one to improve the bonding properties of fiber-polymer interfaces [8,13,53] (Fig. 4.2).

4.3.3.2 Peroxide treatment

Organic peroxides are capable of decomposing to form free radicals. These radicals have the ability to react with hydrogen groups which are found on both of the matrix and cellulose fibers. The free radicals of the form RO_ have bonding capabilities. Generally benzoyl peroxide and dicumyl peroxide are used in order to make the surface modifications of natural fibers. Peroxide treatment gives results of the decrease

Fig. 4.2 The reaction between fiber and potassium permanganate.

in the hydrophilicity and increase in the tensile properties. A study was made to treat the carbon fibers with peroxide, it was defined that surface roughness was increased and this improved interface adhesion which is between carbon fibers and resin to form the composite. In this study functional groups containing oxygen were found to be increased and they caused the chemical reaction between carbon fiber and resin [8,54].

4.3.4 Graft copolymerization

Several methods have been tried during last decade for the graft copolymerization, which is defined as one of the most effective methods of surface modification. For the synthesis of graft copolymers, an active site, which may be a free radical or another chemical group, on the preexisting polymeric backbone should be created firstly. And then a polymerization of a chosen monomer on the active sites starts the formation of the graft copolymer. Graft copolymerization may be grouped as different methods. Physical, chemical, physicomechanical, and radiation techniques can be applied for this aim [13].

Acrylation and acrylonitrile grafting are important methods of graft copolymerization. Acrylic acid (CH_2═CHCOOH) is used to improve interfacial bonding. CH_2═CHCOOH reacts with the cellulosic hydroxyl groups found at the fiber. The reaction between fiber and acrylic acid and acrylonitrile is shown in Figs. 4.3 and 4.4, respectively.

In order to enhance properties of moisture resistance, hydrophilic hydroxyl groups of the fiber are reduced with reactions mentioned earlier. Peroxide radicals are used as initiators in graft copolymerization of acrylic acid. Peroxide forms oxygen-oxygen bonds and as the result of this coupling mechanism between the fiber and matrix by acrylic acid, properties of the interface and the composite are improved. Grafting on the fiber by acrylonitrile with the formula of AN (CH_2═CH—C═N) is also a useful surface modification treatment. For the reaction with cellulose molecules, acrylonitrile initiates free radicals by dehydrogenation and oxidation. Interaction between activated free radical sites and monomer of the matrix is provided. Some mechanical properties of the composite and the interface's interlocking efficiency are increased by the copolymerization process between the fiber and matrix. Acrylic acid can be used also for the graft polymerization to modify glass fibers, too [8,50].

Fig. 4.3 The reaction between fiber and acrylic acid.

Fig. 4.4 The reaction between fiber and acrylonitrile.

4.3.5 Other chemical treatments

4.3.5.1 Esterification-based methods

Esterification treatment methods are used to form ester bonds with the fiber surface. There is a variety of chemicals that are capable of forming these bonds. Four chemical processes are mostly applied in this group. Acetylation, benzylation, propionylation, and treatment with stearates are employed for esterification. Among these four methods, acetylation is the most famous one [55].

By this way cellulosic fibers are plasticized. In the acetylation method, acetic anhydride is used and hydroxyl groups of the outer part of the cellulose are replaced with acetyl groups. As the result of this modification, cellulose polymers become hydrophobic. By the help of acetylation, low moisture absorption leads to this hydrophobic structure and enables advantages in composite materials. The dimensional stability of the composites improves, surface roughness increases, and better interlocking with the matrix occurs as the result of this treatment. Also removal of hemicellulose ingredient and lignin constituents of the treated fiber also can be seen [8,9,13,36,48,50].

In the acetylation reaction, acid catalyst may or may not be used on fiber. In general acetylation is made with acetic acid and acetic anhydride; acetic anhydride is more preferable because acetic acid's reaction capacity with the cellulose is weak. The cellulosic materials are first put in acetic acid and then reacted by acetic anhydride [50,51].

More importantly, when compared with the composites including untreated cellulosic fibers, this esterification treatment improves the interface properties and better mechanical properties such as tensile, flexural, and impact properties of the composites are obtained. The increased hydrophobicity reduces the dielectric constant of the composite and increases the volume resistivity [36].

Acetylation treatment increases also thermal stability of composites including treated fibers. An interesting report was about acetylation of polyester composites that was reinforced with cellulosic parts. At the result, bio-resistance was higher, tensile strength loss was less than the composites treated with silane. Acetylation increased the interface properties of some flax/polypropylene composites, too [8,9].

4.3.5.2 Maleated coupling

Maleated coupling is one of the methods for improving the properties of adhesion among fiber surface and the polymer matrix. Maleated coupling treatment reduces water absorption and improves mechanical properties such as fiber strength. An example of the treatment of natural fibers with maleated polypropylene copolymer providing covalent bonds across the interface and high interfacial adhesion can be given [8,13,56].

Besides improving the mechanical properties and water absorption resistance, maleic acid grafting increases composites' dimensional stability. This method is also cost efficient. Generally maleated coupling methods can be used directly. It is easy to apply this method because there is no need to add a new process step. A study with a hydrophobic fiber, carbon, gave advantageous results with this method by introducing some

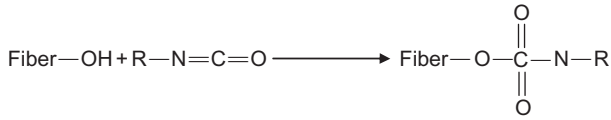

Fig. 4.5 The reaction between fiber and isocyanate coupling agent.

functional groups over the surface, proving the strength of these agents for surface modification [12,57].

4.3.5.3 *Isocyanate treatment*

Isocyanate treatment is an effective coupling method. Hydroxyl groups of the fibers are in target for this treatment. In this treatment functional group of isocyanate, —N=C=O, is capable of working as a coupling agent. By this way, strong covalent bonds are formed and better compatibility of cellulosic fibers with binder resin is obtained. An interesting study was performed with this treatment over carbon fibers, positive effects were obtained, especially the mechanical properties and interfacial bonding between fibers and polymer matrix were improved [8,13,53,58]. Coupling agent, isocyanate, reacts with the fiber as shown in Fig. 4.5.

4.4 Biochemical treatments

In the scope of biochemical treatments, the application possibilities of enzymes are widely searched. Enzyme treatment is an environmental friendly method and also cost, energy, and water are saved with providing a high fiber quality. Enzyme modifications mostly used to improve surface properties of fibers in composites by removing unwanted components. During these modifications, fiber surface is not damaged. The surface modification of fibers by enzymes improves adhesion and as well as some mechanical properties such as increment of modulus, failure strains, and strength properties of the resulting composites. When enzymatic treatment is compared with other chemical surface treatments, it is advantageous because the reaction only occurs on the polymer surface and so it is a milder treatment with less damage of the fibers. Oxidative and/or hydrolytic enzymes can be applied for surface modifications [1,7,40,59].

Enzyme-treated fibers can successfully be used as reinforcing materials for the development of polymer composites. The mechanical properties of composites were also improved [19,60].

Targeted enzymatic treatment of unwanted materials from the fibers improves the coherence among fibers and matrix, and thus resulting positive effects for some randomly orientated composites [61].

It can be concluded that enzymes proving their superiorities in surface treatment bring many advantages in composite structures.

4.5 Sizing

4.5.1 Carbon fibers

Sizing applications have important effects on fiber-matrix adhesion and resulting composites' properties. These treatments are mostly applied to the glass and carbon fibers. In order to improve fiber-polymer matrix compatibility without giving damage to the fibers, these fibers are coated with a sizing resin immediately after manufacture [62,63].

Carbon fibers have smooth surface and chemical inertness so they have a weak adhesion to the matrix. Surface treatment methods applied to the carbon fibers aim to improve some surface characteristics and to increase surface's quantity. These methods add great to the interfacial properties among carbon fibers and the matrix. The expectation from the sizing agent is to act as a lubricant and so facilitate fiber handling during composite manufacture without damaging the fiber. Here type and structure of the sizing agent determines the capabilities for these duties. The improvement of fiber surface both physically and chemically is very important in order to get sufficient reactivity between the carbon fiber and the matrix. These agents can increase the wettability of the carbon fiber surface to the matrix resin. Some weak boundary layers may originate after surface treatment and existing coating has the ability to remove them. Besides these improvements, there are some more advantages of sized carbon fibers such as higher surface energy and polarity components. Carbon atoms are hydrophobic but sizing increases water adsorption quantity and adsorption rate. Sizing is necessary for the composites including carbon fibers [64–67].

In fact commercially available carbon fibers are normally coated by a sizing layer on the surface. To get satisfactory results in manner of improving interfacial adhesion between fibers and matrix, type of the sizing agent is important; some tests should be applied in order to evaluate the efficiency of sizing at the end [68].

In the manufacture of carbon fibers, the step of sizing is not applied immediately after carbonizing. Firstly surface of carbon fibers is oxidized to some extent for the addition of oxygen atoms to give the fibers better bonding properties. This treatment also makes some differences over the surface of carbon fibers for better mechanical bonding properties. Controlling of oxidation is very important in order to avoid any damages that can cause fiber failure. After the surface treatment, the fibers are taken into sizing treatment [69].

As a result, two main roles are aimed for the sizing of carbon fibers: One main goal is to protect the fiber and to prevent individual filaments from breaking. The second role is to provide compatibility in a composite material by increasing adhering property to the matrix resin [69,70,73].

4.5.2 Glass fibers

In the manufacture of glass fiber, sizing is applied to increase fiber-matrix adhesion and affect the final properties of the composites positively [62].

In fact sizing treatment is made for the glass fibers for the same tasks as with the carbon fibers, described above; protection of the fiber with sizing process provides compatibility with the molding process of composite structures [63,71].

In the processes of glass fiber production, as glass fibers come down from the hot bushings, they are cooled and immediately after cooling, the fibers are coated with sizing agent. In order to have continuous, smooth, and consistent production, the quality of sizing must remain constant during the process [72].

As a result it can be said that sizing enables glass fibers, a better performance in the composite matrix.

4.6 Conclusion

In order to obtain better characteristics and performance of the composites, surface modifications and some sizing operations are needed. The fiber modification methods discussed in this chapter have different levels of success, but they have some common obvious effects such as enhancement of the fiber-matrix adhesion [8,19,50,63,70]. There are additional benefits that result improving mechanical properties and decreasing water absorption. Although surface modifications affect the costs negatively, they can solve the problem of incompatibility between fiber and polymer matrix.

Recently more polymer composites with natural fibers are met in polymer composites. Usage of natural fibers in composites is advantageous and beneficial in environmental point of view, but there are some disadvantages because of hydrophilic character of the natural fibers. Hydrophilicity lowers the compatibility with the natural fiber and matrix and as the result mechanical properties of the composites will be poorer. By the help of surface modifications, hydrophobic character is increased and adhesion with the matrix is improved.

In latest years, some high-performance fibers such as aramid, high strength polyethylene, are also used in composite structures. The usage of these fibers seems to increase in near future. With the similar purposes mentioned earlier, surface treatment of these fibers is also applied. Chemical etching and grafting, plasma treatment, and application of coupling agents are the most applied surface treatment methods of these high-performance fibers. As the result, mechanical properties of the composites and interface adhesion between the fiber and the matrix are enhanced [74]. With the proper polymer matrixes, these fibers promise interesting composite structures very soon. When manmade fibers are taken into account in manner of sizing operations, sizing is applied in the manufacture of glass and carbon fibers in order to get positive impacts on fiber-matrix adhesion and the resulting properties of the composites, consequently.

In future, it can be defined that studies on surface modifications of natural fibers will increase and some natural products such as lignin, zein, chitin, and chitosan will also be used because they have been found to increase fiber/matrix adhesion. Sizing operations will keep their importance for some chemical fibers, too [9].

References

[1] Kenealy W, Diller GB, Ren X. Enzymatic modification of fibers for textile and forest products industries. In: Edwards V, Buschle- Diller G, Goheen S, editors. Modified fibers with medical and specialty applications. Netherlands: Springer; 2006. p. 191–208.

[2] Hockenberger AS. Surface modification of textiles for composite and filtration applications. In: Wei Q, editor. Surface modification of textiles, UK; 2009. p. 238–40.

[3] Graupner N, Rößler J, Müssig J. Fiber/matrix adhesion of cellulose fibers in PLA, PP and MAPP: a critical review of pull-out test, microbond test and single fiber fragmentation test results. Compos A: Appl Sci Manuf 2014;63:133–48.
[4] Guterl V, Ehrburger P. Role of chemistry in advanced carbon-based composites. In: Delhaès P, editor. Fibers and composites. London: Taylor & Francis; 2003.
[5] Mohanty AK, Misra M, Drzal LT, editors. Natural fibers, biopolymers, and biocomposites. USA: Taylor & Francis; 2005.
[6] Jayamania E, Hamdanb S, Rahmanb MR, Bin Bakria MK. Dielectric properties of lignocellulosic fibers reinforced polymer composites: effect of fiber loading and alkaline treatment. Mater Today: Proc 2015;2:2757–66.
[7] Mamun AA, Bledzki AK. Micro fiber reinforced PLA and PP composites: enzyme modification, mechanical and thermal properties. Compos Sci Technol 2013;78:10–7.
[8] Li X, Tabil LG, Panigrahi S. Chemical treatments of natural fiber for use in natural fiber-reinforced composites: a review. J Polym Environ 2007;15(1):25–33.
[9] John MJ, Anandjiwala RD. Recent developments in chemical modification and characterization of natural fiber-reinforced composites. Polym Compos 2008;29 (2):187–207.
[10] Yan L, Chouw N, Huang L, Kasal B. Effect of alkali treatment on microstructure and mechanical properties of coir fibers, coir fiber reinforced-polymer composites and reinforced-cementitious composites. Constr Build Mater 2016;112:168–82.
[11] Shanmugam D, Thiruchitrambalam M. Static and dynamic mechanical properties of alkali treated unidirectional continuous Palmyra Palm Leaf Stalk Fiber/jute fiber reinforced hybrid polyester composites. Mater Des 2013;50:533–42.
[12] El-Sabbagh A. Effect of coupling agent on natural fiber in natural fiber/polypropylene composites on mechanical and thermal behaviour. Compos Part B 2014;57:126–35.
[13] Kalia S, Kaith BS, Kaur I. Pretreatments of natural fibers and their application as reinforcing material in polymer composites—a review. Polym Eng Sci 2009;49 (7):1253–72.
[14] Orue A, Jauregi A, Unsuain U, Labidi J, Eceiza A, Arbelaiz A. The effect of alkaline and silane treatments on mechanical properties and breakage of sisal fibers and poly(lactic acid)/sisal fiber composites. Compos A: Appl Sci Manuf 2016;84:186–95.
[15] Cai M, Takagic H, Nakagaito AN, Katoh M, Uekic T, Geoffrey IN, et al. Influence of alkali treatment on internal microstructure and tensile properties of abaca fibers. Ind Crop Prod 2015;65:27–35.
[16] Huo S, Thapa A, Ulven CA. Effect of surface treatments on interfacial properties of flax fiber-reinforced composites. Adv Compos Mater 2013;22(960):109–21.
[17] Fiore V, Di Bella G, Valenza A. The effect of alkaline treatment on mechanical properties of kenaf fibers and their epoxy composites. Compos Part B 2015;68:14–21.
[18] Omrani E, Menezes PL, Rohatgi PK. State of the art on tribological behavior of polymer matrix composites reinforced with natural fibers in the green materials world. Eng Sci Technol Int J 2015;19(2):717–36.
[19] Faruk O, Bledzki AK, Fink HP, Sain M. Biocomposites reinforced with natural fibers: 2000–2010. Prog Polym Sci 2012;37(11):1552–96.
[20] Le Duigou A, Bourmauda A, Balnoisa E, Daviesb P, Baley C. Improving the interfacial properties between flax fibers and PLLA by a water fiber treatment and drying cycle. Ind Crop Prod 2012;39(1):31–9.
[21] Bozaci E, Sever K, Sarikanat M, Seki Y, Demir A, Ozdogan E. Effects of the atmospheric plasma treatments on surface and mechanical properties of flax fiber and adhesion between fiber-matrix for composite materials. Compos Part B Eng 2013;45 (1):565–72.

[22] Haameem JAM, Abdul Majid MS, Afendi M, Marzuki HFA, Fahmi I, Gibson AG. Mechanical properties of Napier grass fiber/polyester composites. Compos Struct 2016;136:1–10.
[23] Karahan HA, Ozdogan E. Improvements of surface functionality of cotton fibers by atmospheric plasma treatment. Fibers Polym 2008;9(1):21–6.
[24] Shenton MJ, Lovell-Hoare MC, Stevens GC. Adhesion enhancement of polymer surfaces by atmospheric plasma treatment. J Phys D Appl Phys 2001;34:2754–60.
[25] Shishoo R, editor. Plasma technologies for textiles. Cambridge, England: Woodhead publishing Limited; 2007.
[26] Bozaci E, Sever K, Demir A, Seki Y, Sarikanat M, Ozdogan E. Effect of the atmospheric plasma treatment parameters on surface and mechanical properties of jute fabric. Fibers Polym 2010;10(6):781–6.
[27] Yuan X, Jayaraman K, Bhattacharyya D. Effects of plasma treatment in enhancing the performance of woodfiber-polypropylene composites. Compos A: Appl Sci Manuf 2004;35(12):363–1374.
[28] Marais S, Gouanve F, Bonnesoeur A, Grenet J, Poncin-Epaillard F, Morvan C, et al. Unsaturated polyester composites reinforced with flax fibers: effect of cold plasma and autoclave treatments on mechanical and permeation properties. Compos A: Appl Sci Manuf 2005;36(7):975–86.
[29] Martin AR, Manolache S, Mattoso LHC, Rowell RM, Dense F. Plasma modification of sisal on high density polyethylene composites: effect on mechanical properties. In: Proceedings from the third international symposium on natural polymers and composites; 2000. p. 431–6.
[30] Seki Y, Sarikanat M, Sever K, Erden S, Gulec HA. Effect of the low and radio frequency oxygen plasma treatment of jute fiber on mechanical properties of jute fiber/polyester composite. Fibers Polym 2010;11(8):1159–64.
[31] Sinha E, Panigrahi S. Effect of plasma treatment on structure, wettability of jute fiber and flexural strength of its composite. J Compos Mater 2009;43(17):1791–802.
[32] Liu D, Chen P, Chen M, Yu Q, Lu C. Effects of argon plasma treatment on the interfacial adhesion of PBO fiber/bismaleimide composite and aging behaviors. Appl Surf Sci 2011;257(23):10239–45.
[33] Zhang X, Huang Y, Wang T. Plasma activation of carbon fibers for polyarylacetylene composites. Surf Coat Technol 2007;201:4965–8.
[34] Gassan J, Gutowski VS. Effects of corona discharge and UV treatment on the properties of jute-fiber expoxy composites. Compos Sci Technol 2000;60(15):2857–63.
[35] Ragoubi M, Bienaime D, Molina S, George B, Merlin A. Impact of corona treated hemp fibers onto mechanical properties of polypropylene composites made thereof. Ind Crop Prod 2010;31(2):344–9.
[36] Zhou Y, Fan M, Chen L. Interface and bonding mechanisms of plant fiber composites: an overview. Compos Part B 2016;101:31–45.
[37] Pickering K, editor. Properties and performance of natural-fiber composites. In: Cambridge, England: Woodhead Publishing Limited; 2008.
[38] Fu HJ, Huang YD, Liu L. Influence of fiber surface oxidation treatment on mechanical interfacial properties of carbon fiber/polyarylacetylene composites. Mater Sci Technol 2004;20(12):1655–60.
[39] Khanchaitit P, Aht-Ong D. Continuous surface modification process with ultraviolet/ozone for improving interfacial adhesion of poly(ethylene terephthalate)/epoxy composites. Polym Compos 2006;484–90.
[40] Pastore C, Kiekens P. Surface characteristics of fibers and textiles. NY: CRC Press; 2000.

[41] Baley C, Busnel F, Grohens Y, Sire O. Influence of chemical treatments on surface properties and adhesion of flax fiber-polyester resin. Compos Part A 2006;37:1626–37.
[42] Mechakra H, Nour A, Lecheb S, Chellil A. Mechanical characterizations of composite material with short Alfa fibers reinforcement. Compos Struct 2015;124:152–62.
[43] Bachtiar D, Sapuan SM, Hamdan MM. The effect of alkaline treatment on tensile properties of sugar palm fiber reinforced epoxy composites. Mater Des 2008;29 (7):1285–90.
[44] Weyenberga IV, Ivensa J, Costerb AD, Kinob B, Baetensb E, Verpoesta I. Influence of processing and chemical treatment of flax fibers on their composites. Compos Sci Technol 2003;63:1241–6.
[45] Merlini C, Soldi V, Guilherme MOB. Influence of fiber surface treatment and length on physico-chemical properties of short random banana fiber-reinforced castor oil polyurethane composites. Polym Test 2011;30:833–40.
[46] Zahari WZW, Badri RNRL, Ardyananta H, Kurniawan D, Nor FM. Mechanical properties and water absorption behavior of polypropylene/Ijuk fiber composite by using silane treatment. Prod Manag 2015;2:573–8.
[47] Yu T, Wu C, Wang C, Rwei S. Effects of surface modifications on the interfacial bonding of flax/β-polypropylene composites. Compos Interfaces 2013;20(7):483–96.
[48] Anbukarasi K, Kalaiselvam S. Study of effect of fiber volume and dimension on mechanical, thermal, and water absorption behaviour of luffa reinforced epoxy composites. Mater Des 2015;66:321–30.
[49] El-Abbassi FE, Assarar M, Rezak A, Lamdouar N. Effect of alkali treatment on Alfa fiber as reinforcement for polypropylene based eco-composites: mechanical behavior and water ageing. Compos Struct 2015;133:451–7.
[50] Kabir MM, Wang H, Lau KT, Cardona F. Chemical treatments on plant-based natural fiber reinforced polymer composites: an overview. Compos Part B 2012;43:2883–92.
[51] Mohanty AK, Misra M, Drzal LT. Surface modifications of natural fibers and performance of the resulting biocomposites: an overview. Compos Interfaces 2001;8(5):313–43.
[52] Xie Y, Hill CAS, Xiao Z, Militz H, Mai C. Silane coupling agents used for natural fiber/polymer composites: a review. Compos Part A 2010;41:806–19.
[53] Kumar V, Amar T, Singha S. Surface modification of biopolymers. NJ: John Wiley & Sons; 2015.
[54] Guo H, Huang YD, Meng LH, Liu L, Fan DP, Liu DX. Interface property of carbon fibers/epoxy resin composite improved by hydrogen peroxide in supercritical water. Mater Lett 2009;63:1531–4.
[55] Pickering K, editor. Properties and performances of natural-fiber composites. England: Woodhead Publishing Ltd.; 2008.
[56] Kazayawoko M, Balatineczj J, Matuanal. M. Surface modification and adhesion mechanisms in woodfiber-polypropylene composites. J Mater Sci 1999;34:6189–99.
[57] Xu B, Wang X, Lu Y. Surface modification of polyacrylonitrile-based carbon fiber and its interaction with imide. Appl Surf Sci 2006;253:2695–701.
[58] Zhang Y, Zhang Y, Liu Y, Wang X, Yang Ling Bin. A novel surface modification of carbon fiber for high-performance thermoplastic polyurethane composites. Appl Surf Sci 2016;382:144–54.
[59] Hauser P. Pretreatments of textiles prior to dyeing: plasma processing. USA: InTech; 2011.
[60] Kaith BS, Pathania D, Kumara A, Thakur P, Knittel CE, Schauer CL, et al. The development of antibacterial and hydrophobic functionalities in natural fibers for fiber-reinforced composite materials. J Environ Chem Eng 2016;4:1743–52.

[61] Liu M, Silva DAS, Fernando D, Meyer AS, Madsen B, Daniel G, et al. Controlled retting of hemp fibers: effect of hydrothermal pre-treatment and enzymatic retting on the mechanical properties of unidirectional hemp/epoxy composites. Compos Part A 2016;88:253–62.
[62] Rudzinski S, Häussler L, Harnisch Ch, Mäder E, Heinrich G. Glass fiber reinforced polyamide composites: thermal behaviour of sizings. Compos Part A 2011;42:157–64.
[63] Berg J, Jones FR. The role of sizing resins, coupling agents and their blends on the formation of the interphase in glass fiber composites. Compos Part A 1998;29:1261–72.
[64] Zhang RL, Zhang JS, Zhao LH, Sun YL. Sizing agent on the carbon fibers surface and interface properties of its composites. Fibers Polym 2015;16:657–63.
[65] The making of carbon fiber; 2008. http://www.compositesworld.com/blog/post/the-making-of-carbon-fiber [accessed 22.06.16].
[66] Gndinger F, Middendorf P, Fox B. Interfacial shear strength studies of experimental carbon fibers, novel thermosetting polyurethane and epoxy matrices and bespoke sizing agents. Compos Sci Technol 2016;133:104–10.
[67] Yuan H, Zhang S, Lu C, He S, An F. Improved interfacial adhesion in carbon fiber/polyether sulfone composites through an organic solvent-free polyamic acid sizing. Appl Surf Sci 2013;279:279–84.
[68] Dai Z, Shi F, Zhang B, Li M, Zhang Z. Effect of sizing on carbon fiber surface properties and fibers/epoxy interfacial adhesion. Appl Surf Sci 2011;257:6980–5.
[69] How is it made; 2016. http://zoltek.com/carbonfiber/how-is-it-made [accessed 27.08.16].
[70] Sizing for carbon-fiber; 2016. http://www.compositesworld.com/articles/sizing-for-carbon-fiber [accessed 01.09.16].
[71] Sizing Treatment, http://www.compositesworld.com/articles/sizing-for-carbon-fiber) [accessed 11.07.16].
[72] http://www.materialstoday.com/carbon-fiber/features/sizing-stability-is-a-key-element-for-glass-fiber/) [accessed 18.08.16].
[73] http://www.materialstoday.com/carbon-fiber/features/sizing-stability-is-a-key-element-for-glass-fiber/) [accessed 18.08.16].
[74] Kim JK, Ma YW. Engineered interfaces in fiber reinforced composites. UK: Elsevier; 1998.

Glass fibers

5

Aref Cevahir
Sisecam Science and Technolgy Center, Kocaeli, Turkey

5.1 History of glass fiber

Glass makers experimented glass fiber production from the ancient time but mass manufacture of glass fiber started in 1893 by Edward Drummond Libbey who exhibited a dress made from fabric combining silk and glass fiber [1]. Russell Games Slayter in 1938 was issued first patent considering glass wool production [2]. The produced fiber showed good electrical insulation properties and for this reason glass fiber products are named as electrical glass or E-glass. Starting from 1939 glass fibers were used as insulators in the warships of US navy. Furthermore, during World War II glass fiber manufacturing and development in the production of unsaturated polyester resin was the driving force to produce radar domes (Radom's) and structural parts of the aircrafts using hand layup technique. For the first time in 1953 General Motors started mass production of the entire body of Chevrolet Corvette sport cars using glass fiber and utilizing sheet molding compound (SMC) technique

Improvements in the technology, consumer awareness, and government regulations resulted in glass fiber manufacturers spending millions of dollars to minimize waste. Reducing furnace emission is the major challenge for glass fiber manufacturers in which dust, sulfur dioxide, and nitrogen oxides plays the important role. The use of oxygen combustion makes advantage of decreasing the emission of nitrogen oxide to the environment. Glass makers produce fluorine- and boron-free glasses to eliminate fluorine pollution and minimize air pollutants in manufacturing. Industrial demands are always a driving force to produce new fibers with high mechanical strength and corrosion resistance. In this regard, S glass, ECR glass, boron-free, and many other type of glasses are produced.

5.2 Glass fiber manufacturing

In the modern glass fiber manufacturing plant direct manufacturing process is preferred. In this process raw materials are stored separately in the silos and metered to the mixing tank by accurate weighing, followed by transfer to the batch silo to charge to the furnace. This system is computer controlled and air tight in a way to prevent spreading of dust to the atmosphere.

The raw materials that are used in the manufacturing of E-glass are sand for silica, clay for alumina, colemanite or boric acid for boron oxide, and limestone or calcite for

Fiber Technology for Fiber-Reinforced Composites. http://dx.doi.org/10.1016/B978-0-08-101871-2.00005-9

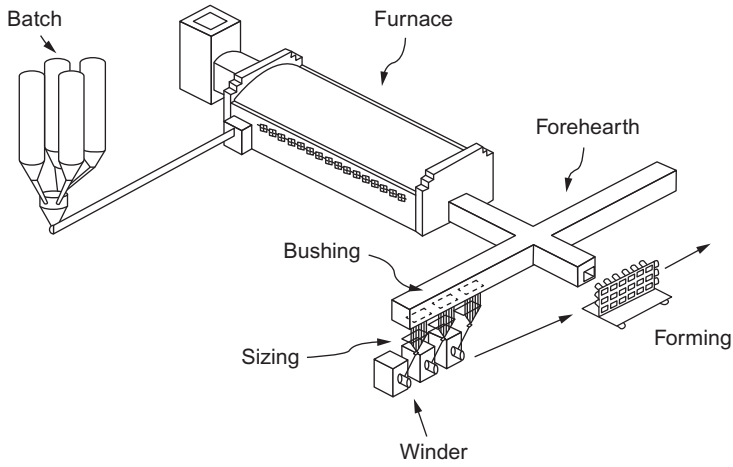

Fig. 5.1 Continuous glass fiber manufacturing process.
AGY (Advanced Fiber Glass Yarn Co. Inc.). High strength glass fibers. Technical paper. Continuous glass fiber manufacturing process; March 2004.

calcium oxide. E-glass furnace is generally rectangular with a short channel at the exit that is connected to the narrow forehearth channel along which fiber forming is done (Fig. 5.1).

The best refractory material that is used to build the wall of furnace is dense chromium oxide which is resistant to the corrosive molten E-glass. The refractory is baked by zircon blocks and another layer of clay blocks. As a source of energy natural gas is usually used to build up heat with a temperature of around 1600°C and to melt the raw materials as they are fed to the furnace. During formation of the E-glass and as it moves to the furnace exit the electrodes and bubblers in the bottom of furnace produce convection of the glass on the top of melt and accordingly evolved gasses are removed and the chemical reactions are finalized.

As the molten E-glass leaves the furnace it enters into the forehearth channel and conveys into bushing where fiber is formed. The bushing is like spinneret of the synthetic fiber industry, however, it is rectangular in shape and made of platinum and rhodium alloy to withstand high temperature and corrosivity of molten E-glass (Fig. 5.2). Presence of rhodium in the bushing alloy increases the hardness and stiffness that extends the lifetime of bushing. The bushing is heated electrically to enhance better temperature control and the uniformity of the fibers that flow through thousands of tips, nozzles. The diameter of the nozzles range from 0.75 to 2.0 mm and as winder or chopper pulls the fibers its linear speed may rise up to 60 m/s [4].

By variation in the winder or chopper speed or output capacity of the bushing the fiber diameters can be changed and therefore fibers with various diameters are produced. Fibers with different diameters are named as seen in Table 5.1 [5].

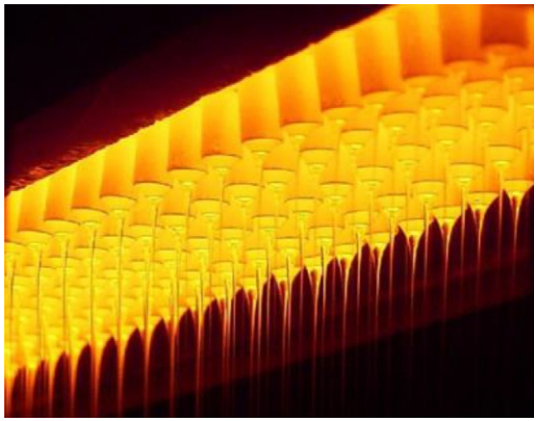

Fig. 5.2 Flow of the glass fiber from bushing.
From Woltz GmbH.

Table 5.1 Letter designation of glass fiber diameter

Filament design	Average diameter (μ)
D	5.33
E	7.32
G	9.50
H	10.67
J	11.75
K	14.19
M	15.86
N	17.38
T	23.52

E-glass melt should have a narrow viscosity range between 600 and 1000 P. The rate of fiber production at the nozzle is the function of the rate of flow of glass and can be described by the Poiseuille's equation:

$$F \propto \frac{r^4 h}{l\eta}$$

where F is the rate of flow, r is the radius of the nozzle at its narrowest cylindrical section, h is the height of the glass above the nozzle, and η is the viscosity of the glass [5].

As the liquid glass leaves the tip of the nozzle, it is quenched rapidly by circulating cold air and spraying water. The glass will be fully solidified when it reaches the size applicator that is few meters under bushing (Fig. 5.3). In this stage the aqueous size is applied to the glass surface by either roller or belt applicator [1]

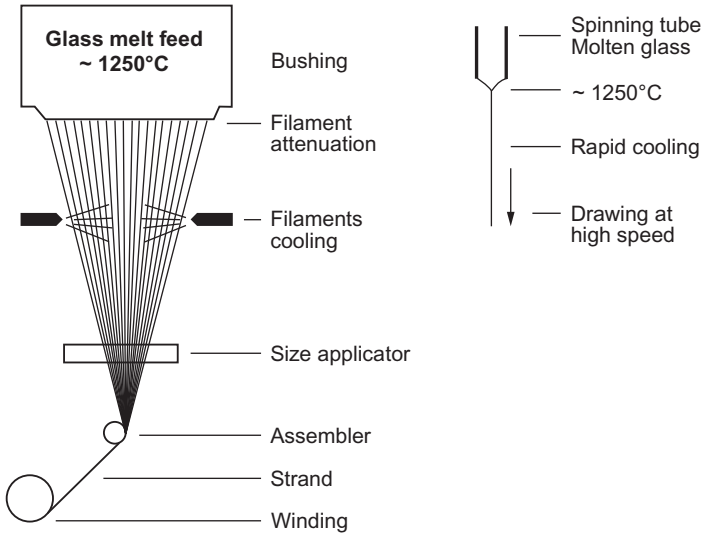

Fig. 5.3 Continuous filament forming process [6].

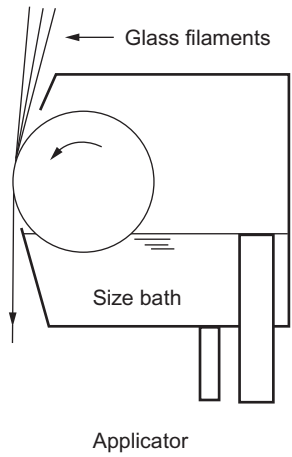

Since the glass filaments is wetted by water and size, it can be gathered through split shoes which are usually rotatable grooved disks.

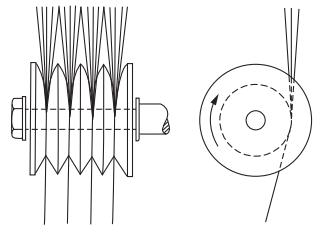

The attenuated glass fibers are traditionally wound on collet which is cylinder powered by winder. The fibers are usually wound on the paper or plastic tube that is slid onto the collet. The function of the tube is to facilitate handling of the forming cakes. The rotation speed of the collet is the key parameter to determine the fiber diameter in the final form. Also, the temperature adjustment of the bushings affect the filaments diameter as well. The other important part of the winder is the traverse that places individual strands to the collet in such fashion that the cake has even build up and the strands can be easily wound after drying [1,7,8].

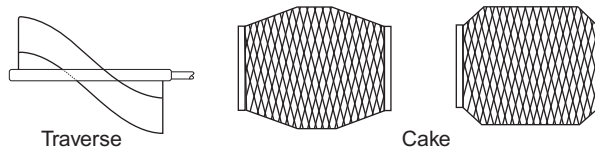

5.3 Types of glass fibers

In general, E-glass named as calcium alumino-borosilicate glass with less than 1% alkali oxide, Na_2O. Most glasses contain small amount of fluoride which assist the melting of raw materials and lower the liquidus temperature of the glass. The E-glass, occasionally, has density of 2.62 g/cm^3 and refractive index of 1.562.

The composition of E-glass after long producing time is varying as a result of some factors that encourage or force manufacturers to revise the formulation. The need to reduce the atmospheric pollution due to gasses and dust discharged from E-glass furnaces causes production problems and cost of raw materials. Also, the need to improve some properties like corrosion resistance and higher mechanical performance of composite end products lead to production of new types of glass fibers (Tables 5.2–5.4) [1,6].

As seen in Tables 5.2 and 5.3 different types of glass fibers with various mechanical properties were made to fulfill the industrial demands.

In some specific applications like cement and concrete reinforcements AR glasses (alkali resistant) are used which contain ZrO_2. Presence of ZrO_2 (1%–18%) in addition to high content of alkali oxides (Na_2O+K_2O, 11%–21%) and TiO_2 (0%–12%) enhance alkali resistance properties [3].

In Table 5.3 trend in the evolution of commercial E-glass is shown. At the beginning E-glass manufacturing began with boron-free glass composition and then in 1943 by addition of boron processing temperature reduced from 1288°C to 1200°C. In 1951 the batch cost was decreased by reducing the amount of B_2O_3 from 10% to 5%–7%. Also, the amount of MgO was reduced significantly and the standard formulation for E-glass was established [6]. By the 1960s, emission of boron and fluorine from melt in a commercial furnace into the atmosphere became an important issue from environment and health aspects. Costly pollution control devices resulted in the design of new fluorine-free and essentially boron-free E-glass compositions that commercialized in 1996 [6]. From the beginning of 2000s more challenges were undertaken to consume lower amount of energy and produce environmentally friendly E-glass for general-purpose applications. As it can be seen from Table 5.3 addition of TiO_2, flux, in combination with boron reduces processing cost and viscosity of melt.

Table 5.2 Different types of glass fibers [9]

Fiber	Composition (wt%)												
	SiO_2	B_2O_3	Al_2O_3	CaO	MgO	ZnO	TiO_2	Zr_2O_3	Na_2O	K_2O	Li_2O	Fe_2O_3	F_2
General-purpose fibers													
Boron-containing E-glass	52–56	4–6	12–15	21–23	0.4–4	…	0.2–0.5	…	0–1	Trace	…	0.2–0.4	0.2–0.7
Boron-free E-glass	59.0	…	12.1	22.6	3.4	…	1.5	…	0.9	…	…	0.2	…
	60.1	…	13.2	22.1	3.1	…	0.5	…	0.6	0.2	…	0.2	0.1
Special-purpose fibers													
ECR-glass	58.2	…	11.6	21.7	2.0	2.9	2.5	…	1.0	0.2	…	0.1	Trace
D-glass	74.5	22.0	0.3	0.5	…	…	…	…	1.0	<1.3	…	…	…
	55.7	26.5	13.7	2.8	1.0	…	…	…	0.1	0.1	0.1	…	…
S-, R-, and Te-glass	60–65.5	…	23–25	0–9	6–11	…	…	0–1	0–0.1	…	…	0–0.1	…
Silica/quartz	99.9999	…	…	…	…	…	…	…	…	…	…	…	…

Table 5.3 **Physical and mechanical properties of commercial glass fibers [9]**

Fiber	Coefficient of linear expansion, 10^{-6}/°C	Specific heat cal/g/°C	Dielectric constant at room temperature and 1 MHz	Dielectric strength, kV/cm	Volume resistivity at room temperature $\log_{10}(\Omega\ cm)$	Refractive index (bulk)	Weight loss in 24 h in 10% H_2SO_4, %	Tensile strength at 23°C (73°F) MPa	Tensile strength at 23°C (73°F) ksi	Young's modulus GPa	Young's modulus 10^6 psi	Filament elongation at break, %
General-purpose fibers												
Boron-containing E-glass	4.9–6.0	0.192	5.86–6.6	103	22.7–28.6	1.547	~41	3100–3800	450–551	76–78	11.0–11.3	4.5–1.9
Boron-free E-glass	6.0	…	7.0	102	28.1	1.560	~6	3100–3800	450–551	80–81	11.6–11.7	4.6
Special-purpose fibers												
ECR-glass	5.9	…	…	…	…	1.576	5	3100–3800	450–551	80–81	11.6–11.7	4.5–4.9
D-glass	3.1	0.175	3.56–3.62	…	…	1.47	…	2410	349	…	…	…
S-glass	2.9	0.176	4.53–4.6	130	…	1.523	…	4380–4590	635–666	88–91	12.8–13.2	5.4–5.8
Silica quartz	0.54	…	3.78	…	…	1.4585	…	3400	493	69	10.0	5

Table 5.4 Evolution of commercial purpose E-glass fibers [6]

Year	1940	1943	1951	1996	2000
Composition, wt%					
SiO_2	60.0	54.0	54.5	60.01	56.50
B_2O_3	–	10.0	6.6	–	1.30
Al_2O_3	15.0	14.0	14.0	12.99	13.45
CaO	20.0	17.5	22.1	22.13	24.50
MgO	5.0	4.5	0.6	3.11	2.55
TiO_2	–	–	0.5	0.55	0.55
Na_2O	–	–	0.8	0.63	0.90
K_2O	–	–	0.2	0.14	–
Fe_2O_3	–	–	0.2	0.25	0.25
F_2	–	–	0.5	0.04	–

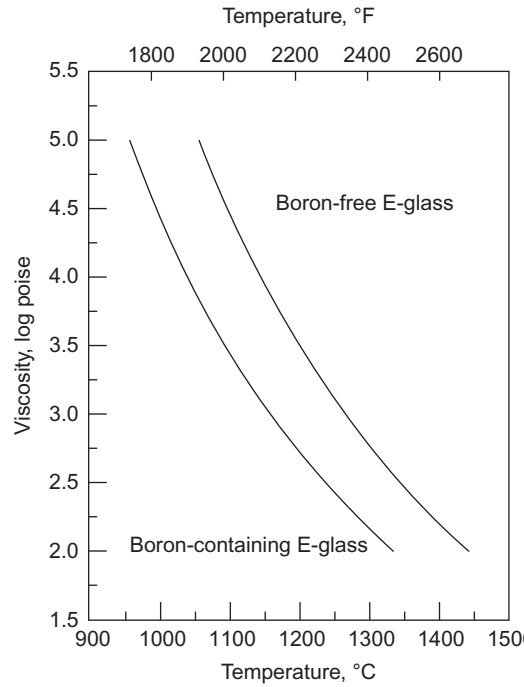

Fig. 5.4 Viscosity of boron-free and boron-containing E-glass [6,9].

Viscosity of glass melt is another important parameter by which production variables like energy and fiber forming temperature is affected. As it is seen in Fig. 5.4 decreasing the amount of boron in the glass formulation results in higher viscosity and consequently rising the processing temperature by about 90°C in the glass fiber manufacturing [9].

5.4 Glass fiber products

Glass fiber products are categorized into four major groups; chopped strands, direct draw rovings, assembled rovings, and mat products [6].

5.4.1 Chopped strands

Chopped strands are manufactured according to the three processes; dry chopping, semiwet, and direct chopping.

Dry chopping process: In this process glass fibers are attenuated from bushing and after applying size fibers are split into strands and wound in the form of cake or roving onto cardboard tube. Subsequently, wound fibers are dried in the air drying or radio frequency drying ovens. Dried cakes or rovings strands are unwinding, wetting with water and chopping (rotating glass cutter) followed by drying in the vibrational or fluidized bed driers. Finally, dried chopped strands are packaged.

Semiwet chopping process: In this process glass fibers are attenuated from bushing and after applying size fiber splits are winding in the form roving onto cardboard tubes. Wet rovings are covered with envelope to minimize evaporation of moisture. Semiwet rovings strands are unwinding and chopping followed by drying in the vibrational or fluidized bed driers. Then, dried chopped strands are packaged.

Direct chopping process: In this process glass fibers are attenuated from bushing and after applying sizing fiber strands are conducted to the chopper. Chopped fibers are dried in the vibrational or fluidized bed driers and finally dried chopped strands are packaged. Direct chopping process minimize the labor cost and because of continuous flow of glass without interruption, this process is the most cost effective one.

Chopped strands products are used in:

−injection molding process to reinforce wide range of thermoplastic polymers

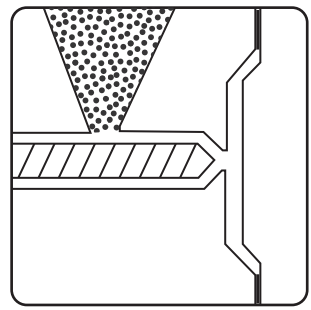

−dough molding compound or bulk molding compound (BMC) in which thermoset resins are pressed or injected to the molds to produce objects with complex shapes

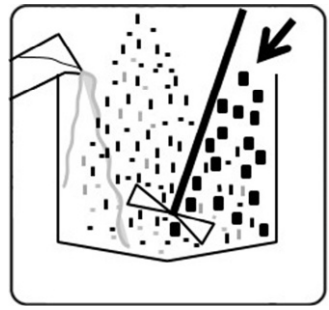

– water dispersing systems to manufacture glass felt or tissue to reinforce plaster and gypsum

5.4.2 Direct draw rovings

Direct draw roving glass fiber products are rovings at which glass fiber filaments are gathered into one single strand and the bundle of filaments is wound onto cardboard tubes. Wet rovings are dried using radio frequency driers and are commonly used in weaving, filament winding, and pultrusion applications in which either unsaturated polyester, vinyl ester, or epoxy resins are used.

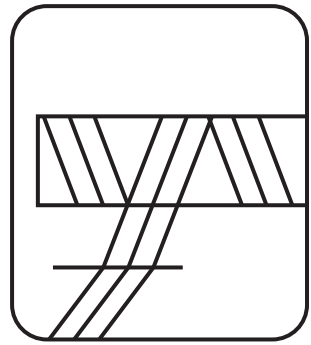

5.4.3 Assembled rovings

In this process first multistrand rovings are wound on collet in the form of cake and dried by conventional drying techniques. Then, several strands from cakes are brought together and wound to produce a cylindrical package containing bundles of individual strands.

A major application of assembled rovings are spray deposition (spray roving or gun roving) in which rovings are chopped or cut into separate strands and sprayed in combination with the resin to the mold. Assembled rovings are also used in SMC process in which fiber strands chopped over paste and mixed with thermoset dough and after certain period of time (maturation) pressed in the hot mold without loosing strand integrity too much.

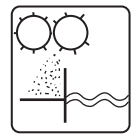

Translucent panel manufacturing

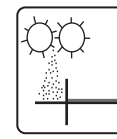

SMC paste manufacturing

5.4.4 Chopped and continuous strand mats

In this process first, glass strands are chopped into uniform length of 50 mm or continuous glass strands are distributed randomly over the conveyor belt [6]. As conveyor belt moves adhesive powders (polyester) or adhesive emulsions (poly(vinyl acetate)) are applied to the fiber strands to make adhesion in the contact points of strands in order to keep uniformity of glass strands mat. Adhesive powders or emulsion are dried and melt while conveyor belt goes through the drying oven. At the end of mat production line adhered fiber strands pass between cooling press rollers and form blanket shaped products (Fig. 5.5). Produced mats are usually named as powder bonded and emulsion bonded mats.

Chopped strand mat products are widely used in hand layup application. Continuous strand mat products are used either in hand lay up or resin transfer molding applications to manufacture composites (Fig. 5.6).

5.5 Glass fiber sizing

When one thinks about manufacturing of glass fiber products with diameter from 10.5 to 24.0 μm, we should think about protection of these thin filaments from damage either during manufacturing or during custom service. Therefore, the functionality of the size components during all process stages is considered.

In general, size of the glass fiber products contains:

– film forming agents,
– coupling agents,

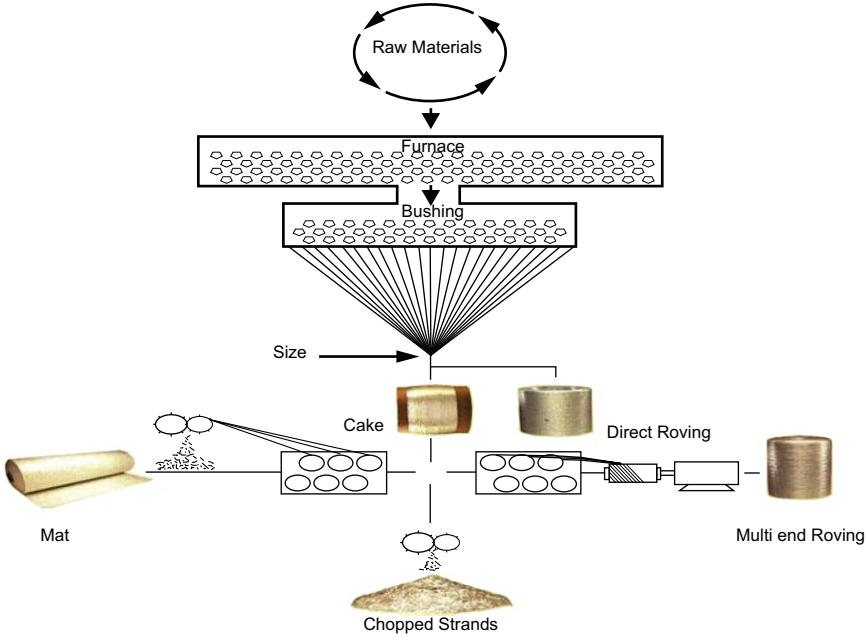

Fig. 5.5 Schematic illustration of glass fiber manufacturing and products. Courtesy of Camelyaf.

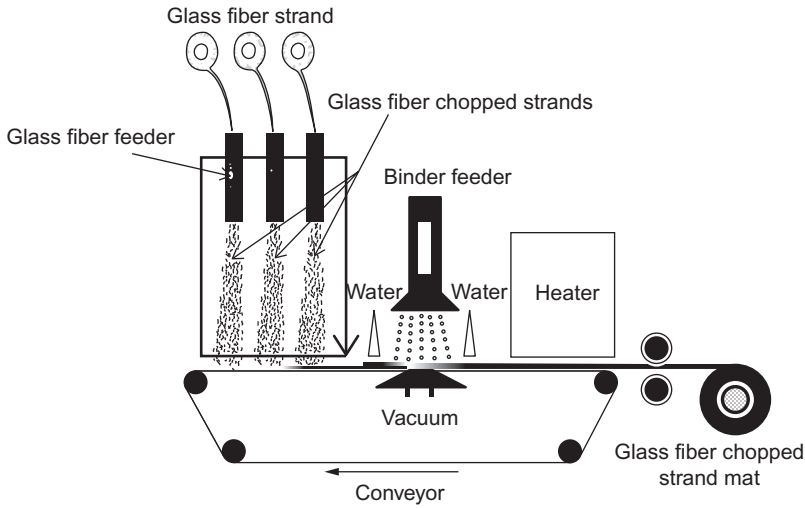

Fig. 5.6 Schematic diagram of chopped strand mat production line. Courtesy of Camelyaf.

- lubricating agents,
- surface active and emulsifying agents,
- antistatic agents,
- antioxidizing agents,
- plastifying agents and biocides [1,5].

5.5.1 Film forming agents

Film forming agents are water based polymeric materials that protect fibers from damage during processing and also keeps filaments together. Film formers are mostly emulsions in which emulsifying agents are adsorbed to the surface of polymer micelles and enhance dispersing in water. The presence of the film former emulsions in the size prevent loss of the chemicals during winding of glass fibers. As glass fibers are wound resultant centrifugal force and vibration from pulling fiber strands cause throwing out and loss of size.

The compatibility between matrix polymer and film formers can affect reinforcing properties of the produced composite [4]. On the other hand, reactivity of the film formers cause possible chemical reaction between film former-coupling agents, film former-polymer matrix, and film former-film formers. Blocked polyurethanes are reactive film formers that upon heating at certain temperature, deblocking will occur and isocyanates formed. Newly formed isocyanates are reactive towards coupling agents, chain end groups of the matrix polymers, and polyols of the other film formers. Table 5.5 shows the possible compatibility between film former polymers and composite matrices. It can be deduced from Table 5.5 to use hybrid (combination) of film formers to achieve a synergy or to obtain films with new properties. In the case of size compatible with polypropylene one should choose modified polypropylene which is maleic unhydride grafted polypropylene, PPgMAH (Fig. 5.7).

In contrast to polypropylene homopolymer grafted one can be dispersed in water in combination with emulsifying agents and maleic acid neutralizing agents, alkyl

Table 5.5 Compatibility between film formers and polymer matrices

Film former polymer	Matrix polymer
Poly(vinyl acetate), PVAc	Unsaturated polyester, vinyl ester, epoxy
Polyurethane	Polyamides, polyester (PET), polycarbonate
Polyester	Unsaturated polyester, vinyl ester, epoxy
Epoxy	Unsaturated polyester, vinyl ester, epoxy, polyester (PET)
Modified polypropylene	Polypropylene

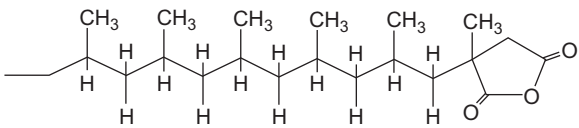

Fig. 5.7 Chemical structure of maleic anhydride grafted PP (PPgMAH) [9].

amines, which somehow facilitate dispersing of PPgMAH in water. Dispersion of polypropylene is done at high pressure (~9.0 bar) and high temperature (~175°C) with vigorous agitation [10]. According to the required properties grafted amorphous, atactic, crystalline, or isotactic polypropylene is selected to be dispersed in water and used in the size formulation.

5.5.2 Coupling agents (adhesion promoters)

Coupling agents are chemicals which enhance adhesion or bonding between fiber surface and polymer matrix. These types of chemicals are mostly organofunctional silane compounds that:

(i) displace adsorbed water on the glass surface,
(ii) create hydrophobic surface of the correct thermodynamic characteristics for complete wetting by the matrix and
(iii) Develop strong interfacial bonds between the fiber and resin. These may involve covalent bonding, hydrogen bonding, or in the case of thermoplastics, long compatible molecular chains that are completely solubilized into the polymer matrix, in analogy to graft and block copolymers employed in polymer blends.

The compatibility between coupling agent and matrix polymer directly affects the reinforcement properties of the composite. Table 5.6 presents the compatibility between coupling agents and composite matrices [5].

In general, the silanes given in Table 5.6 all have the following structure:

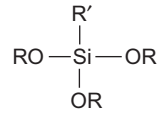

where R′ is a polymer-compatible or reactable organic group, R is either ethyl or methyl.

Table 5.6 Compatibility between coupling agents and polymer matrices

Coupling agent	Formulation	Matrix polymer
Amino silane	3-Aminopropyltriethoxysilane (APS)	Polyamides, polypropylene, polycarbonate, epoxy and polyester (PET)
Methacryl silane	3-Methacryloxypropyltrimethoxysilane (MPS)	Unsaturated polyester and vinyl ester
Vinyl silane	Vinyl triethoxysilane (VTS)	Unsaturated polyester and vinyl ester
Epoxy silane	3-Glycidyloxypropyltrimethoxysilane (GPS)	Epoxy, polyester (PET) and polycarbonate

In aqueous solution and usually in the presence of acetic acid which is used to adjust pH (of the size) to approximately 4, the alkoxy (RO) groups are hydrolyzed and can polymerize (oligomer) to give linear and branched poly (hydroxy siloxane) [11].

This equilibrium polymerization is strongly dependent on the nature of R′ so that the concentration at which only the silane triol exists in aqueous solution (in the absence of other auxiliaries) varies.

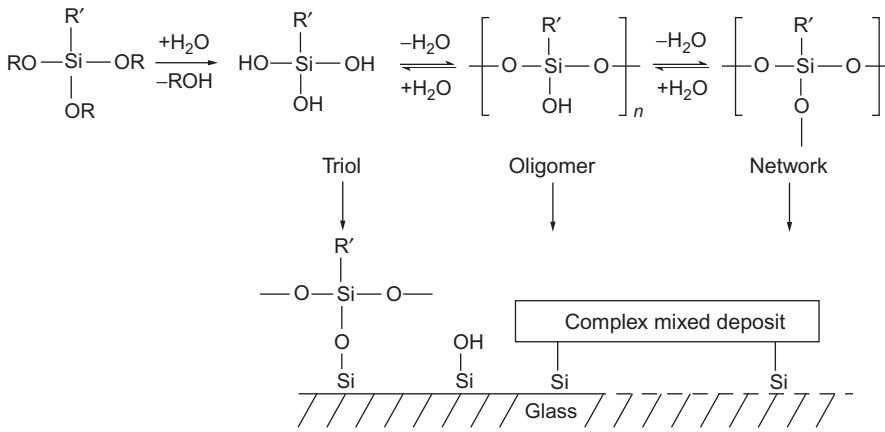

Considering glass surface one can say that the silicone atoms at the surface of glass will have hydroxy groups attached to them and therefore the hydrolyzed silane will be in competition for condensation with silanols of glass surface or through self-condensation. Moreover, coating the fiber with aminosilane solution followed by hot water extraction leaves a deposit that is highly hydrolytically resistant and have been referred as; physiosorbed layers, the loosely chemisorbed layer and strongly chemisorbed layer (Fig. 5.8) [5,12–14].

5.5.3 Lubricating agents

During glass fiber manufacturing or in the composite production lines fiber filaments should pass through metal or ceramic guides, metal bars and pipes without any breakage or damage. In order to fulfill this condition water based lubricating agents are added to the size. Lubricating agents are generally in the form of wax dispersions of long alkyl groups or modified polyethylene glycol (PEG) type chemicals. PEG 400, 600, or longer chains are modified with fatty acids and are widely used as lubricating agents.

5.5.4 Surface active and emulsifying agents

When size is coming into contact with the fiber filaments, it should wet the glass fiber surface and therefore film formers and other auxiliaries of the size cover the fiber surface. Surface active agents are the chemicals that reduce surface tension of the solution to some extent and enhance wetting of the fiber surface. Surface active agents and emulsifying agents are classified according to the polarity of their functionl

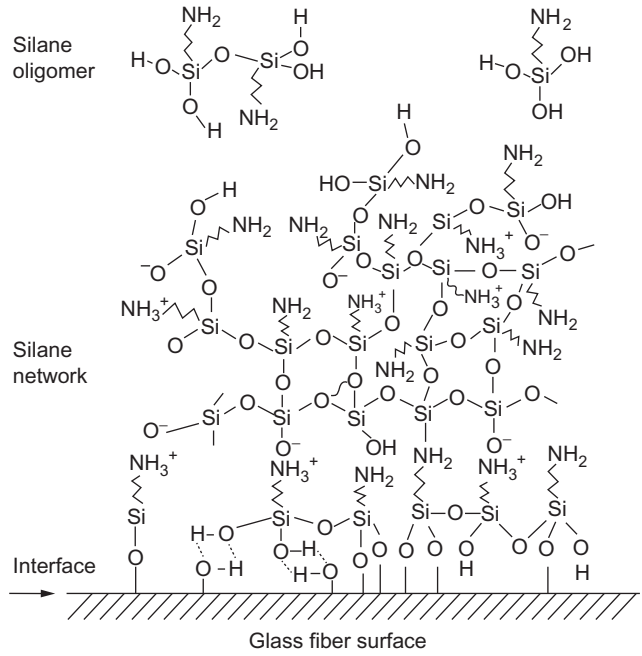

Fig. 5.8 Schematic presentation of the structure of hydrolyzed APS on E-glass showing the presence of the denuded glass surface and quaternary ammonium ions [12].

groups. In general, salts of fatty acids (anionic), quaternary amine salts (cationic), and modified PEG or sorbitan derivatives (nonionic) are the chemicals which are utilized in size. People who are expert in size preferred nonionic chemicals since most of the film formers are nonionic or weakly anionic dispersions.

5.5.5 Antistatic agents

Glass fibers are naturally charged by accumulating static electricity. Therefore, during processing or manufacturing of glass fibers electrically charged fiber strands may cause unwanted gathering of fiber strands and filaments, sparks, and even electrical shock. To overcome these problems water soluble antistatic agents are added to the size or applied to the glass strands during manufacturing of assembled rovings. Derivatives of quaternized ammonium salts, imidazolium ion salts, and modified PEG (polyethylene glycol or polyoxyethylene) are mostly preferred as antistatic agents. Antistatic agents are chosen according to the compatibility with other size ingredients and the polymer matrix of composite since migration of the antistatic agents to the surface of the composite is not desired.

5.5.6 Antioxidizing agents

Size materials which are mostly organic compounds are susceptible to oxidation during processing in which high temperature (>100°C) is utilized to dry the wet fiber strands. Oxidation of the organic chemicals in the size may cause discoloration,

degradation of polymeric film formers, lubricants, and auxiliaries. Therefore, to inhibit oxidation of the size some (chemicals) antioxidizing agents are added to the size. Hindered phenols, hindered amines, or sodium phosphinate type compounds are mostly used [15]. Antioxidizing agents are chosen considering solubility in the size and not interfering with curing of the composite (thermosets). Also, antioxidizing agents should not affect the color of the composite products.

5.5.7 Plastifying agents

Modification of film formers is a method to maintain new properties to size and consequently to the glass fiber products. For instance softening or increasing flexibility of the film formers may cause either softer or flexible glass fiber strands with better drapability and also increasing the wetting of the fiber strands by resin. Alkyl benzoate and phthalate derivatives are mostly used chemicals to plastify polymeric film formers.

5.5.8 Biocides

Size formulations contain polymeric and organic compounds which are susceptible to bacterial and fungi growth. Existence of such microbials in the size causes sedimentation or agglomeration of the chemicals which means damaging of size. Moreover, to inhibit the activity of microbials some chemicals, biocides, are added to size, ppm, to stop the growth of microbials. The chemicals which are used for this purpose should not disturb the stability of the size or interfere with the size components. Therefore, the best choices in this regard are salt of some organic acids (e.g., sodium citrate) or quaternized amines.

Coating the glass fiber filaments bring this idea into the mind that size covers the fiber surface completely. However, AFM picture (Fig. 5.9) shows that size covers the

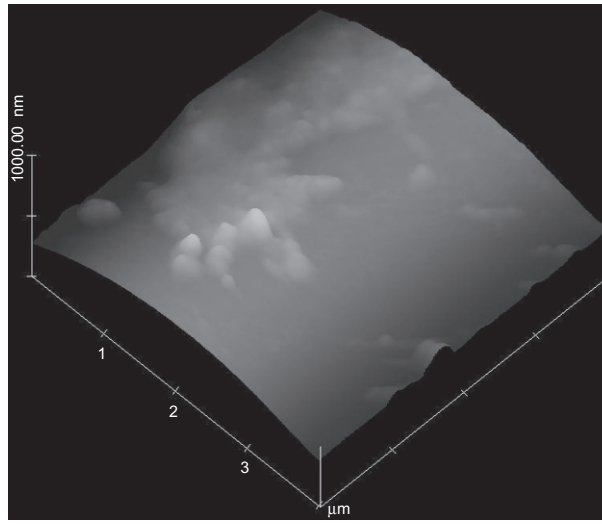

Fig. 5.9 AFM picture of glass fiber product of WR6 from Cam Elyaf San. A.S. Courtesy of Sisecam.

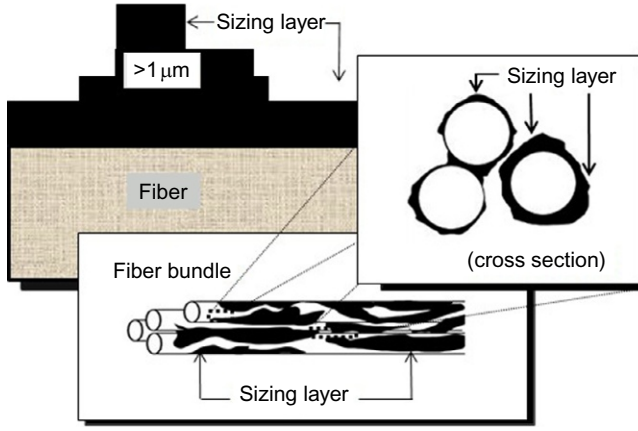

Fig. 5.10 Schematic picture of distribution of size layer in the glass fiber strands. Adapted from Wu HF, Dwight DW, Huff NT. Effects of silane coupling agents on the interphase and performance of glass-fiber-reinforced polymer composites. Compos Sci Technol 1997;57:975–83.

glass surface inhomogeneously since size adheres to the fibers and brings filaments together. Fig. 5.10 illustrates the schematic picture of size spreading over the filaments and in the strand bundles.

5.6 Composite interphase

Since 1990 the concept of fiber-matrix interface has expanded from two dimensional boundary into that of a fiber-matrix interphase exists in three dimensions (Fig. 5.11).

In a composite, the interphase exists from some point in the fiber where the local properties begin to change from the fiber bulk properties, through the actual fiber-matrix interface, into the matrix where the local properties again equal the bulk properties. During composite formation fiber surface and matrix come into contact and therefore chemical and physical bonds can form at the interface. Surface chemical groups can react with chemical groups in the matrix to form chemical bonds. Van der Waals attractive forces, hydrogen bonds, and electrostatic bonds can also be formed [16].

5.6.1 Thermosets

In the manufacturing process of thermoset resins wetting of the fibers are expressed by two means, wet through and wet out. Wet through terminology means wetting of fiber with resin. However, wetting out of the fiber means absorbing or impregnation of the resin by fiber followed by swelling and dissolution of size. In the processes

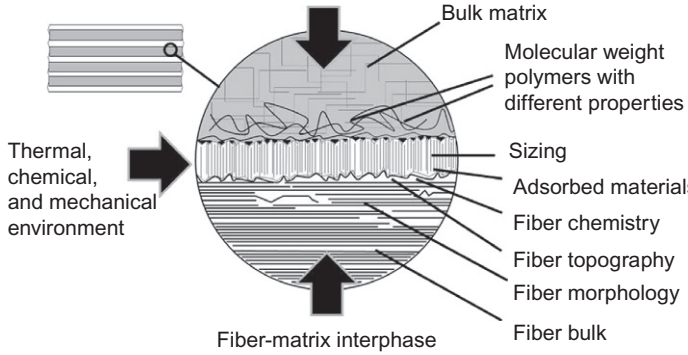

Fig. 5.11 Schematic diagram of the fiber-matrix interphase and some of the factors that contribute to its formation.
Adapted from DuŠek K, editor. Epoxy resins and composites II. Advances in polymer sciences, vol. 75. Berlin: Springer-Verlag; 1986.

like translucent panel or pipe manufacturing size of the glass fiber is easily wet out and therefore one can say that film formers are compatible with resin due to the matching of surface energies of resin and glass fiber surface. On the contrary, in the composite manufacturing processes like SMC or BMC size is not wet out by the matrix resin easily (size does not absorb or swell by resin because of high viscosity of paste) and just after a long period of time (maturation) size will absorb the resin. This phenomenon indicates low solubility of the film formers in the matrix resin. Degree of solubility or dissolution of size in matrix resin in some cases directly affects the surface properties or roughness in addition to the bulk properties of the obtained composites. A-class surfaces of the composites manufactured by BMC or SMC processes are the examples that show how size governs the surface appearance of articles made by those methods.

5.6.2 Thermoplastics

During manufacturing of thermoplastic composites reinforcing agents, glass fiber, and auxiliaries like fillers are kneaded in the extruder and converted to the granules or directly injected to the mold. In the course of kneading and even molding thermoplastics are getting into contact with glass fiber surface under high temperature (150°C–350°C), high pressure, and high shear force and therefore, interactions (reactions) between matrix polymers, film formers, coupling agents, and additives of the size may happen. Fig. 5.12 illustrates the schematic composite interphase where an IPN (interpenetrating polymer network) between network silane, film former, and resin matrix (R) forms.

Existence of the interphase in the composites is illustrated by Bergeret and shown in Fig. 5.13 by Gao [18]. Gao shows the boundary between interphase and both glass surface and matrix polymer [19].

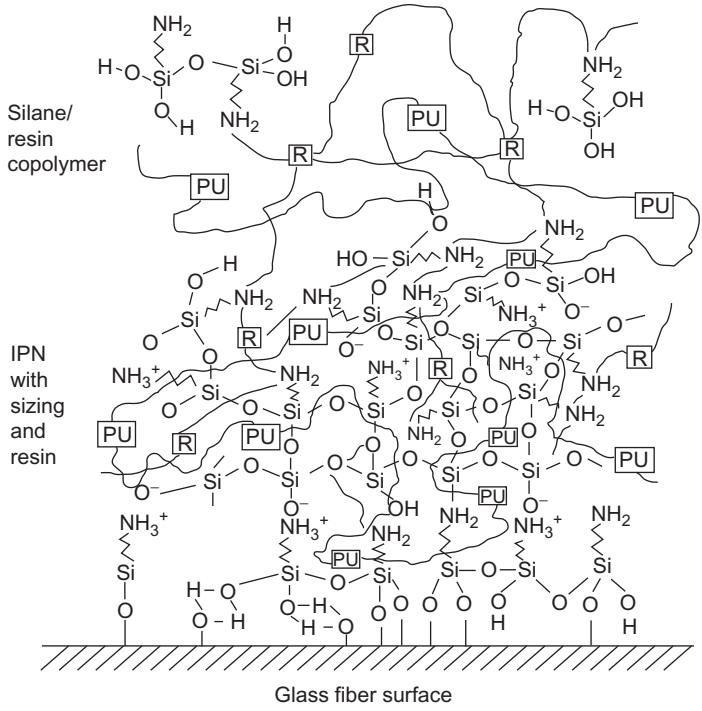

Fig. 5.12 Schematic picture of the composite interphase [17].

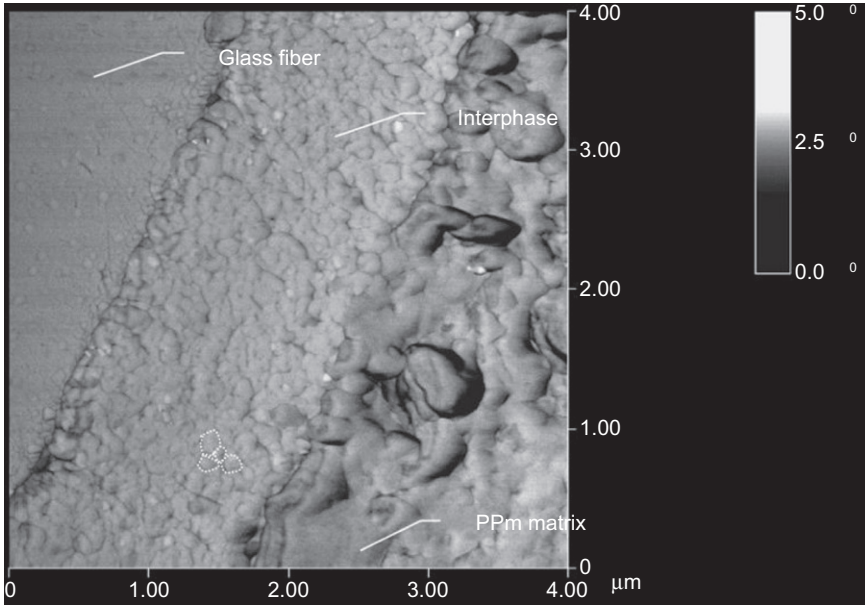

Fig. 5.13 AFM phase images of glass fiber reinforced polypropylene (PP) interphase (glass fiber/aminosilane-PP size/PPmatrix) [19].

Mäder claims that measuring the moduli of the bulk polymer, interphase and fiber can show the extent of reinforcement and the quality of the interphase and of course performance of the glass fiber size [4,19,20]. Therefore, it can be concluded that choosing appropriate film formers, coupling agents, and auxiliaries results better interphase [21,22].

5.7 Conclusion

Using glass fiber as a reinforcing agent in the composite industry shows a big trend since the price of the glass fiber is low in comparison to carbon fiber or Kevlar. For general-purpose application E-glass is seen to be a best choice and also for high technology applications various types of glass fiber like S glass or ECR glasses were introduced to the market. Glass fiber products have the advantages that it can be used either in the traditional composite manufacturing processes (hand layup) or it can be used in high technology composite manufacturing techniques like RTM.

As it was explained, existing compatibility between matrix and the size is the main issue that should be considered during composite design. Also, in designing of a size formulation compatibility and harmony among components and with matrix is a must.

Nano science and nanotechnology are also the tools that would affect the performance of the composites. For instance, addition of Nano clay, carbon nanotube, or grapheme to the size increased the mechanical strength of the glass fiber reinforced epoxy composite. Moreover, addition of Nano clay also increases corrosion resistance of the epoxy composite [23].

From the beginning of 21st century shortage of the energy is the main problem in the industry and to solve this problem two solutions are proposed; either create new energy sources or reduce energy consumption. Solar energy, wind turbine, and hydroelectric energy are the most common solutions in this respect. On the other hand, saving weight in transportation and in automotive industries is another solution to decrease energy consumption and therefore glass fiber reinforced composites look as a logical solution.

In the transportation and automotive industries the idea of lightweight vehicles is the driving force for composite manufacturers and according to the demand of customers glass fiber is widely used since it fulfills the composite market needs by considering low cost and availability in the glass fiber market. By looking at the growth of light vehicle sales to about 50% from 2010 to 2015, increasing the glass fiber production can also be considered [24].

As a new energy source wind turbine is widely used and to assemble wind blade, glass fiber reinforced composites are preferred due to low price and its availability in the market. In the recent years trend in the composite manufacturing increases in Europe and consequently the production of glass fiber increases as well. On the other hand manufacturing of LFT (long fiber thermoplastic) and GMT (glass mat thermoplastic) composites increases sharply in comparison to thermoset manufacturing processes [25].

References

[1] Lowenstein KL. The manufacturing technology of continuous glass fibers. Amsterdam: Elsevier; 1983.
[2] Slayter G. U.S. Patent 2133 235; 1938.
[3] AGY (Advanced Fiber Glass Yarn Co. Inc.). High strength glass fibers. Technical paper. Continuous glass fiber manufacturing process; March 2004.
[4] Thomason JL. Interfaces and interfacial effects in glass reinforced thermoplastics, In: Proceeding of 28th RisØ international symposium on materials science: interface design of polymer matrix composites-mechanics, chemistry, modelling and manufacturing, Roskilde, Denmark; 2007.
[5] Hearle JWS, editor. High-performance fibers. 1st ed. Cambridge: Woodhead Publishing Ltd.; 2001.
[6] Wallenberger FT, Bingham PA, editors. Fiberglass and glass technology. New York: Springer; 2010.
[7] Karian HG, editor. Handbook of polypropylene and polypropylene composites. New York: Marcel Dekker; 1999.
[8] Barch HW, Blair R. US Patent 4239 162; 1980.
[9] ASM Handbook. In: Miracle DB, Donaldson SL, editors. Composites, vol. 21; 2001.
[10] Temple CS. US Patent 5130 197; 1992.
[11] Materne T, de Buyl F, Witucki GL. Organosilane technology in coating applications: review and perspectives. Dow Corning, Form No. 26-1402A-01; 2012.
[12] Liu XM, Thomason JL, Jones FR. XPS and AFM study of interaction of organosilane and sizing with E-glass fibre surface. J Adhesion 2008;84(4):322–38.
[13] Jones FR. The chemical aspects of fiber surfaces and composite interfaces and interphases, and their influence on the mechanical behaviour of interfaces. In: Proceeding of 28th RisØ international symposium on materials science: interface design of polymer matrix composites-mechanics, chemistry, modelling and manufacturing, Roskilde, Denmark; 2007.
[14] Akovalı G, editor. The interfacial interactions in polymeric composites. Netherlands: Kluwer Academic Publishers; 1993.
[15] Schell PL, Meesters LA, Subramanian R. US Patent 6207 737; 2001.
[16] Wu HF, Dwight DW, Huff NT. Effects of silane coupling agents on the interphase and performance of glass-fiber-reinforced polymer composites. Compos Sci Technol 1997;57:975–83.
[17] DuŠek K, editor. Epoxy resins and composites II. Advances in polymer sciences, vol. 75. Berlin: Springer-Verlag; 1986.
[18] Bergeret A, Bozec MP, Quantin J-C, Crespy A, Gasca J-P, Arpin M. Study of interphase in glass fiber-reinforced poly(butylene terephthalate) composites. Polym Compos 2004;25 (1):12–25.
[19] Gao SL, Mäder E. Characterisation of interphase nanoscale property variations in glass fibre reinforced polypropylene and epoxy resin composites. Compos Part A 2002;33:559–76.
[20] Mäder E, Moos E, Karger-Kocsis J. Role of film formers in glass fibre reinforced polypropylene—new insights and relation to mechanical properties. Compos Part A 2001;32:633–9.

[21] Zinck P, Mäder E, Gerard JF. Role of silane coupling agent and polymeric film former for tailoring glass fiber sizings from tensile strength measurements. J Mater Sci 2001;36:5245–52.
[22] Mäder E, Gao S-L, Plonka R. Enhancing the properties of composites by controlling their interphase parameters. Adv Eng Mater 2004;6(3):147–50.
[23] Reddy B, editor. Advances in nanocomposites—synthesis, characterization and industrial applications. In: Nano reinforcements in surface coatings and composite interphases. INTECH; 2011. ISBN 978-953-307-165-7.
[24] Lucintel LLC. Growth opportunities in the global glass fiber market, April 2015.
[25] AVK Composites Market Report. Market developments, trends, outlook and challenges. Frankfurt, Germany: Federation of Reinforced Plastics; 2015.

This page intentionally left blank

Carbon fibers

6

Kazim Acatay
Akdeniz Kimya San. ve Tic. A.S., Kemalpasa, Izmir, Turkey

6.1 Introduction

Carbon is one of the most abundant elements in the universe with its sixth position in the periodic table. It is the most important actor in the organic chemistry with its capability to create four covalent bonds. Carbon atom has a unique property named catenation, which is used to define the tendency of linkage between the same elements to form longer chains. These covalent bonds create stable compounds like long chains, rings, and branches. The basic of carbon fiber (CF) manufacturing lies on this nature.

CFs are fibers consisting of at least 92 wt%, mostly more than 95 wt%, carbon, usually in the nongraphitic state. They are manufactured by the controlled pyrolysis of appropriate organic-based precursor fibers [1].

First CF was produced by Edison to use for the incandescent electric lamb and patented in 1880. However, the modern history of CF that had much better mechanical properties was started in 1950s. In the United States, the development has progressed due to space program and backed by strong support from US government agencies. The National Carbon Company, a division of Union Carbide, introduced a carbon cloth made by carbonizing rayon cloth in 1959. Meanwhile in Japan, a team led by Dr. Akio Shindo of the Industrial Research Institute in Osaka was the first to make CFs from polyacrylonitrile (PAN) fibers, filing for patents in 1959 [1]. After these initial inventions and studies, today, the CF sales became 53,000 tons in 2014 and forecasted to reach around 100,000 tons demand by 2020 with an average annual growth rate of 12% [2].

CFs are in between 5 and 10 μm in diameter fibers as shown in Fig. 6.1. They are manufactured in bundle form, and commercial CFs are described with ktex definition, which defines the number of fibers in the bundle in thousands (3 ktex means 3000 fibers in the bundle). Typically, 3k, 6k, 12k, 24k, and 48k (large tow) are available in the market. They are sold in continuous form wounded around bobbins in several kilometers length or in chopped form (staple fiber) at several millimeters in length.

The atomic structure of CF is similar to that of graphite, consisting of sheets of carbon atoms arranged in a regular hexagonal pattern (graphene sheets). The difference is being in the way these sheets interlock. Graphite is a crystalline material in which the sheets are stacked parallel to one another in a regular manner. The intermolecular forces between the sheets are relatively weak van der Waals forces, giving graphite its soft and brittle characteristics. Depending upon the precursor to make the fiber, CF may be turbostratic or graphitic or has a hybrid structure with both graphitic and turbostratic parts present. In turbostratic CF, the sheets of carbon atoms are

Fiber Technology for Fiber-Reinforced Composites. http://dx.doi.org/10.1016/B978-0-08-101871-2.00006-0

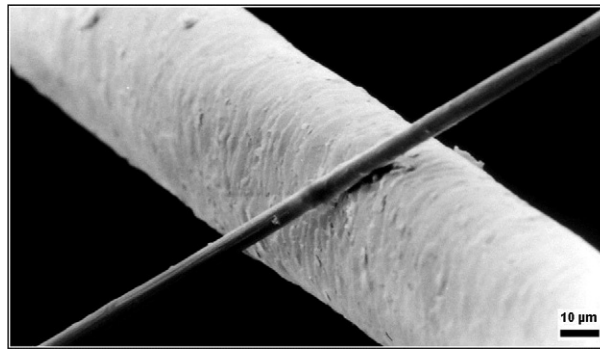

Fig. 6.1 An image to compare a human hair with a carbon fiber (6 µm dia.) [3].

haphazardly folded or crumpled together. CFs derived from PAN are turbostratic, whereas CFs derived from mesophase pitch are graphitic after heat treatment at temperatures exceeding 2200°C. Turbostratic CFs tend to have high-tensile strength, whereas heat-treated mesophase pitch-derived CFs have high Young's modulus (i.e., high stiffness or resistance to extension under load) and high thermal conductivity [3]. This is derived from the structure of their crystallites.

CFs are an important and promising raw material for fiber-reinforced composites, especially in high-performance (HP) applications because they offer the highest specific modulus and highest specific strength of all reinforcing materials [4]. CFs are ideal for applications where strength, stiffness, lower weight, and outstanding fatigue characteristics are critical requirements. Also, they are very applicable for high-temperature resistance, chemical inertness, and high-damping demanding applications. In addition to these, they have good electric conductivity and low linear coefficient of thermal expansion [5]. They have found application in a wide range of industry such as aerospace (aircraft and space systems), military, turbine blades, construction, lightweight cylinders and pressure vessels, medical, automobile, and sporting goods [6]. The global demand for CF was counted as 53,000 tons for year 2014, and its distribution relative to the application is shown in Fig. 6.2.

Several types of CFs with different mechanical and chemical properties are manufactured to serve those applications. According to their tensile modulus and strength, they are named as general purpose (GP), high strength (HS), intermediate modulus (IM), or high modulus (HM). Contrary to glass fiber, the mechanical values of fibers in CF business are not well defined and vary manufacturer to manufacturer.

As it has been mentioned at the beginning of the chapter, CFs are produced by controlled pyrolysis of precursor fibers. In this respect, as the first stage, a precursor fiber should be manufactured. Precursor fibers can be manufactured from different sources, and details will be given at the Section 6.2. After the precursor fiber production, the second stage is controlled pyrolysis of precursor fibers at controlled atmosphere and removes all of the atoms except carbon from the structure. This is called the carbonization to manufacture CFs and will be reviewed in the Section 6.3. In addition to

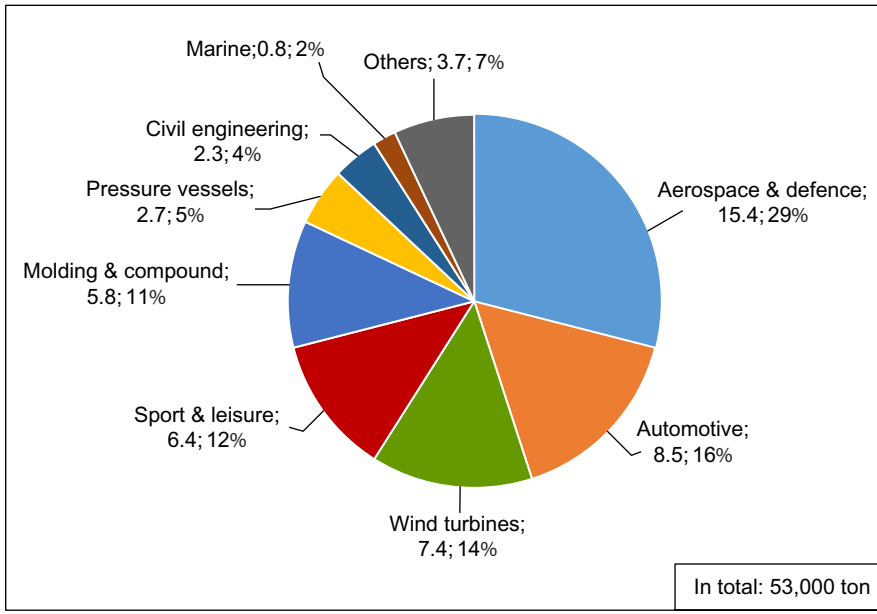

Fig. 6.2 Global CF demand in 1000 tons by application (2014) [2].

these, recent developments and trends in CF technology will be reviewed in Section 6.4 to give an understanding to the reader for the future in CF industry. In Sections 6.5 and 6.6, composite usage and composite production with CFs will be reviewed.

6.2 Different precursors for CF production

Precursor material is critical for ultimate properties of the resultant CF. Main precursor raw materials for CF production are PAN and pitch- and cellulose-based (such as rayon and lignin) materials. Their precursor production techniques vary, and each requires a different conversion process to be used in CF manufacturing.

An ideal precursor material should be easily converted to CF, give a high carbon yield after carbonization and allow to be processed economically. PAN-based precursor has 68% carbon content and has a carbon yield of 50%–55% after carbonization, whereas a cellulosic precursor has a carbon content of 44.4% but has a carbon yield of only 25%–30% in practice. Pitch-based precursors have higher carbon content and higher yield of 85% but with poorer compression and transverse properties as compared with PAN-based CFs [7]. So, for the selection of production technology and machinery, it is not an easy and straightforward choice. Nowadays, PAN is the main precursor material used for commercial CF manufacturing (∼96% of global production). The choice of the precursor material deeply affects the final properties. This can be clearly seen when commercially available CFs' tensile strength and modulus properties are combined on a graph like in Fig. 6.3 [8]. The tensile strength and modulus of

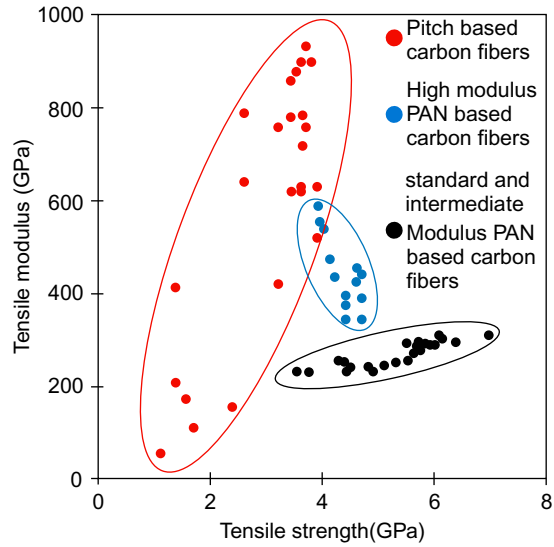

Fig. 6.3 A comparative graph showing tensile modulus versus tensile strength of commercially available pitch- and PAN-based CFs [8].

CF are directly related with the internal and external flaws and the crystal size, structure, and orientation within the fiber.

In addition to tensile strength and modulus values, some other distinctive differences are available between the resultant CFs. For example, mesophase pitch-based CFs have the highest density of 1.9–2.2 g/cm^3, meanwhile cellulosic-based CFs have the lowest density of 1.66. And, cellulosic-based CFs have the highest breaking elongation of 1.67%–1.82%, meanwhile pitch-based CFs have the lowest electric resistivity of 1.8×10^{-4} Ω cm.

6.2.1 PAN based precursors

PAN is mainly used for the production of acrylic fiber, which is a major synthetic fiber used in textile industry. However, the acrylic fiber for textile business is manufactured in copolymer form with at least 85% acrylonitrile monomer content. Acrylic fibers are soft and warm, with a woollike feel. Thus, they are mostly used for sweaters, tracksuits, carpets, furnishing fabrics, socks, gloves, etc. If less acrylonitrile is available, the fiber is called modacrylic (between 35% and 85% acrylonitrile monomer) fiber, and its properties and areas of use differ to mostly flame-retardant applications.

One specific property of PAN delayed its commercial availability even as acrylic fiber: it could not melt under heat without decomposition, thus not suitable for melt-spun processing. The PAN polymer precursors contain polar nitrile groups in their structure and have a high melting point, resulting from strong intermolecular interactions. Therefore, the PAN polymer precursors tend to degrade before the temperature reaches their melting point. To be converted to fiber, the proper solvent was not available until DuPont discovered dimethylformamide (DMF) in 1942. In 1950,

DuPont introduced Orlon as the first commercial acrylic fiber. Acrylic fibers passed through many development steps, and several other processes depending on different solvents and comonomers were emerged by other companies, like Bayer, Monsanto, and Courtaulds [9].

PAN-based precursors for the CF industry were developed by the companies established for the production of textile-grade acrylic fiber. Even the requirements from the final acrylic fiber are different in textile, and in CF application, the machineries and the processes to manufacture the white fiber are similar.

PAN-based fibers are ideal candidate for CF manufacturing because after carbonization their weight loss is relatively low. Thus, they have high carbon yield and do not melt during pyrolysis in an inert atmosphere. In addition to these, PAN polymer has a continuous carbon backbone and nitrile groups that are very suitable for cyclization to produce ladderlike chemical structure required for good mechanical properties in CF.

Contrary to copolymer PAN, homopolymer PAN is not easy to process into CF because it exhibits high initiation temperature for conversion during carbonization. The evolution of heat at this stage is sudden and rapid. Thus, the reaction is hard to control, and this rapid heat evolution can cause chain scission resulting to poor CF properties [1]. To control exothermicity, copolymers of PAN have been synthesized with appropriate comonomers. The comonomer content is lower when compared with the textile acrylic fiber. It is between 5 and 10 mol%, mostly around or less than 5 mol% [10]. However, their names and percentage in use are kept secret by the manufacturers and could not be understood after carbonization step. These are trade secrets because this knowledge greatly controls the final properties of CF. Inclusion of comonomers especially methacrylic acid, itaconic acid, and acrylamide into the PAN polymer main chain enhances the rate of degradation during stabilization step. These comonomers also serve to lower the temperature required for stabilization, thus ease the stabilization.

Typically, the weight-average molecular weight of a PAN precursor is between 90,000 and 140,000 g/mol with a polydispersity index of 1.5–3.0 [1].

Polymerization of acrylonitrile and comonomers to convert precursor is carried by free radical initiation. Several industrial methods are available, which are solution polymerization, bulk polymerization, emulsion polymerization, and suspension (aqueous dispersion) polymerization. In terms of CF industry, solution and aqueous dispersion polymerization have importance.

In solution polymerization, the radical polymerization is carried in a solvent media such as dimethylacetamide (DMAc), DMF, dimethyl sulfoxide (DMSO), and aqueous sodium thiocyanate solutions. At the end of the polymerization, the viscous polymeric solution called dope is ready for fiber drawing. However, this method has several drawbacks. Most important one is the relatively low conversion of monomers to polymer (50%–70%), which requires additional process steps to remove the unreacted acrylonitrile from the dope solution. In contrast, the suspension polymerization results higher conversions. In addition to this, because the product polymer is in solid suspension form, it can be easily filtered, and all unused reactants can be removed. In addition, the particle size can be controlled to speed up the filtration and drying steps. Polymer yield up to 90% is possible [7]. The product polymer can be stored in solid

powder form until it is needed. However, dissolution of the polymer before spinning is an additional step for this route.

Today, most acrylic polymers are produced by suspension polymerization method and continuously. In the suspension polymerization, deionized water is used as the continuous phase to remove the heat generated during reaction. For the initiation of the reaction, a redox system is used to generate free radicals in a water-based system at temperatures around 75°C and at about pH 3. An oxidizer like ammonium, potassium, or sodium persulfate; a reducing agent like sodium bisulfite, sodium metabisulfite, or sulfur dioxide; and a catalyst such as 1 ppm on the monomer mix of Fe^{2+} ion as $FeSO_4$ are used as the initiator system [1]. The resultant polymer molecules are formed and aggregate in the form of solid particles about 20–40 μm.

Before the spinning process, the filtered and dried particles are dissolved in a suitable solvent to manufacture the dope. The solid content of the dope varies according to the solvent used, molecular weight of the polymer used, and the spinning technique used. Usually, it is around 15–25 wt% ($10 \leq \left| \eta_o \right| \leq 200$ Pa/s) [7]. Although high solid content is good due to less amount of recycled solvent, the viscosity of the dope is the limiting factor. Too viscous dope generates pressure built-up at the spinneret and results low fiber production rate. Before the spinneret, very fine filtering of the dope is suitable to remove gels and impurities before reaching to the spinneret. The cleanness and precision of the spinneret holes play an important role on the quality of the filaments. The target is to generate an even surface and even diameter filaments. Spinnerets may be manufactured from stainless steel, tantalum, and gold-platinum alloy. Usually, they are in the form of round cup. The holes on the spinneret are drilled by laser drilling with a larger diametric conical inlet at the gear pump side and cylindrical capillary outlet at the coagulation bath side [1].

Several methods are available as the spinning method for PAN-based precursor production. However, wet spinning and air-gap spinning (dry-jet wet spinning) are the commonly used processes in industry.

In wet spinning, after passing the spinneret, dope is directly entered into coagulation bath, which is a mixture of water and the solvent used to dissolve the polymer. The spinneret is immersed into the bath. When the dope is born into a kind of nonsolvent and solvent mixture, the solvent in the dope diffuses to the coagulation bath, and the filaments start to solidify. The dope temperature is between 25°C and 120°C, and pressure before the spinneret is at 5–20 bar. The line speed in the coagulation bath is 3–16 m/min, and the tension applied to the fiber bundles is gradually increased through the spinning machine. The spinning bath can be designed in horizontally or vertically. The liquid in the coagulation is not stationary but circulates with a velocity. Circulation velocity, temperature, and solvent concentration in the bath are all important, and they are precisely controlled during the process. Usually, a directed flow pattern is generated in the bath to equalize the conditions experienced and to promote homogenous penetration of the nonsolvent into the bundle of filaments [7].

In air-gap spinning, the spinneret is not immersed into the coagulation bath but in the air and just 10–200 mm above the liquid level. The filaments undergo a jet stretch, and this produces a high degree of orientation prior to entering coagulation bath. The solid viscosity of the dope is higher (300–20,000 Pa s) than wet spinning; also the

polymer content is up to 30 wt% to achieve this high viscosity. Otherwise, the filaments combine with each other while traveling through the air gap.

Other process steps in the spinning machine are basically similar in both processes. They are washing, stretching, finish oil application, drying, collapsing, and relaxing. Washing is usually carried in countercurrent flow manner and aims to remove maximum solvent with hot water while stretching the fiber bundle. Initially, the temperature is kept around wet Tg of the filaments (about 65°C). As the solvent content decreased by washing processes, the temperature is increased and more stretch applied. Stretching is performed by passing the filament bundles over hot rollers with adjustable speed and applying the stretch by adjusting the speed of rollers. Total stretch of 12 times is typical. By this stretching action, the crystalline and amorphous regions are aligned in the fiber direction. The molecules within the chain slide past one another and aligned parallel [9]. Usually, finish oil is applied before the collapse stage to make it diffuse into the fiber. Finish oil has several critical services, like acting as a lubricant between fiber-metal interface, giving antistatic property to the fiber, and protecting the fiber against high-temperature contacts. Typical finishes are emulsions of sorbitan esters of long-chain fatty acids, polyoxyethylene, and silicones. Drying is carried to remove the water from the surface and within the fiber. As the fiber dries, it collapses, and a radial contraction of the fiber is observed. A decrease in porosity accompanies collapse, and as the fiber network oriented by drawing, the pores becomes smaller and elongated in the fiber direction [1]. If a slight relaxation process is applied after this stage, it improves and balances the stress/strain properties of the filaments in the bundle. A hot-wet environment under a slight pressure fuses the internal cracks and fissures, thus making the filaments more resistant to the environment at oxidation and carbonization process. At the end of the spinning machine, the precursors are collected in a cardboard or winded over a bobbin. Usually, large tows are placed into cardboards and delivered for carbonization process. The typical PAN-based precursor fiber diameter is in the range of 10–15 μm [8].

In principle, throughout all the processing stages, the fiber should be handled in great care to achieve good CF properties. Otherwise, consistency in the quality of mechanical properties is not possible to achieve. During precursor production and handling, the golden rule is to have least number of contact points in order to minimize damage.

6.2.2 Pitch based precursors

Pitch is the general name for the tarry substance that is highly viscous at room temperature and has very high carbon content. It is a complex mixture of many hundreds of aromatic hydrocarbons and heterocyclic compounds with an average molecular weight of 300–400. It can be produced from natural sources by destructive distillation of petroleum and coal or from synthetic sources by pyrolysis of polyaromatic compounds and polymers. The composition of a pitch varies widely according to the source of tar and the processing conditions. Pitch can contain more than 80% carbon, and as the aromaticity increases, the quality of the product CF increases.

Petroleum pitch can be obtained from the bottoms of catalytic crackers, steam cracking of naphtha and gas oils, and residues from various refinery processes. Crude product is usually passed through some refining processes before using for CF industry [1].

Coal tar is a by-product of the coking of bituminous coals to produce cokes. Coal-tar pitch is obtained from the coal tar using distillation and heat treatment processes. The pitch is the residue, which follows the removal of the heavy oil fractions [6]. Coal-tar pitch is generally more aromatic than petroleum pitch. However, it also contains high solid content that causes filament breakage during extrusion and thermal treatment. Because of this, petroleum pitch is preferred for CF production [11].

In the pitch-based precursor industry, two main types of pitch are in use, isotropic and mesophase pitch. Isotropic pitches are used to make GP grade of pitch CF. They are not graphitic and have poorer properties than the HP grade. To manufacture HP grade, a special treatment process is needed to convert the pitch to mesophase grade. Mesophase grade is optically anisotropic and graphitic in nature.

The isotropic pitch has to be treated to generate a product suitable for melt spinning, with a low volatility and filtered to remove solid particles. A wiped film evaporator is used to remove the low volatility components from the pitch, and the molten pitch is filtered to remove the solid impurities. This refining process raises the softening point by avoiding the formation of mesophase. At the end, the aromaticity of the pitch has been increased and became suitable for melt spinning.

To produce HP-grade pitch-based CF, usage of mesophase pitch is critical. Both isotropic and mesophase pitch CF are made from the same feedstock. An isotropic pitch, when pyrolyzed at about 425°C, generates a liquid-/crystal-type structure containing domains of highly oriented molecules named mesophase [1]. During the mesophase formation, domains of highly parallel, platelike molecules form and coalesce until 100% anisotropic material may be obtained [6]. Over the years, several methods have been investigated for the synthesis of mesophase pitch: (a) pyrolysis of pitch, (b) solvent extraction, (c) hydrogenation, and (d) catalytic modification. The catalytic method is preferred in the pretreatment of pitch for the best control of the processing parameters and the quality of the pitch [7]. It is claimed that a pitch suitable for spinning should preferably contain 40%–90% mesophase, with domain sizes greater than 200 μm, which will then produce a fiber with a highly oriented structure. Domain sizes smaller than 100 μm are observed unsuitable for spinning [1].

The pitch-based precursors are generated by melt spinning in an extruder. Melt spinning of pitch is difficult because of the rheological properties of molten pitch, and very narrow processing conditions are required. Especially, the viscosity of the mesophase is extremely temperature-dependent and the jet temperature should be accurately controlled, as a change of ±3.5°C at jet face will produce ±15% variation in the diameter. Also, too high temperature results thermal degradation of the pitch or dripping owing to low viscosity. The melt-spinning process involves three steps: melting the precursor, extrusion through a spinneret capillary, and drawing the fibers as they cool. Solid chips of pitch are fed through the hopper of a screw extruder fitted with off-gassing ports and evenly heated to give a uniform feed of molten pitch to the filter and then spinneret at the exit of the extruder. Pitch spinnerets have a

multiplicity of holes, which must be spaced about 1.1 mm apart of each other to avoid interfilament fusing [1]. Some initial orientation occurs as the molten pitch passes through the capillaries. After emerging from the capillaries, it is cooled by quench air. When it is still hot, the solid fiber is drawn before windup to give a highly oriented precursor fiber. This precursor fiber will not need further drawing at any subsequent carbonizing process. Fiber handling in the windup is difficult due to the low strength of the as-spun mesophase pitch (tensile strength around 0.04 GPa). Mesophase CFs usually have a larger diameter of 10–15 μm compared with 5–7 μm diameter for PAN carbon fibers. This is because larger diameter mesophase precursor fibers are preferred for easy handling and higher carbon yield; thus, size reduction in carbonization process is smaller [11]. Processing speeds up to 1000 m/min are quoted.

Spun mesophase pitch precursor fibers have a microstructure consisting of well-oriented polyaromatic molecules in microdomains. These microstructures are described as discotic nematic liquid crystals [7].

6.2.3 Cellulose-based precursors

Cellulose as a precursor material for making CFs was first used by Thomas Alva Edison during his studies to find suitable filament material for the incandescent electric lamp. At a later date, Edison developed a method by dissolving cellulosic materials like natural cellulose or cotton in a solvent, such as zinc chloride, to give a dope which could be extruded to a spin bath and then carbonized in inert atmosphere. Of course, the mechanical properties were very poor, and some treatments to improve it were studied by him as well [1]. Interest in CFs was renewed in the late 1950s when synthetic rayon in textile forms were carbonized to produce CFs for high-temperature missile applications [4]. After the introduction of PAN process in the late 1960s with the advantages of high carbon yield, higher mechanical properties, and less environmental problems, cellulose-based precursors lost their importance. However, nowadays, with increasing demand for lower thermal conductivity, high purity, low raw material cost, and high-flexibility CF for aerospace and medical applications, the interest to cellulose-based CF has been freshen up [12]. However, it has major drawbacks as well, such as comparatively lower mechanical properties, lower yield, and high processing cost to generate the precursor material [6].

Natural cellulose fibers cannot be used as precursors for high-performance CFs because of their discontinuous character. Also, they have a low degree of orientation, porous structure, and impurities [7]. Thus, possible materials are the regenerated cellulose fiber precursors like viscose, cuprammonium rayon, and textile-grade rayon. Nowadays, the viscose process has the highest technical significance in the production of rayon.

Process of manufacturing viscose rayon from cellulose pulp to fiber is carried out with the following steps, starting with pulp sheets: (1) steeping in aqueous NaOH, (2) shredding to crumbs, (3) aging of crumbs, (4) xanthating, (5) dissolving with NaOH, (6) filtering, (7) ripening for about 4 days, (8) deaeration, (9) wet spinning (typical bath contains H_2SO_4, Na_2SO_4, $ZnSO_4$, and H_2O) to coagulate, (10) drawing, (11) washing, and (12) winding or cutting. In principle, insoluble cellulose is reacted

first with sodium hydroxide then with carbon disulfide, and soluble sodium cellulose xanthate (viscose) is generated. Then, it is filtered and wet spin into a spin bath. The spin bath mixture is circulated at about 50°C. The size of the jet hole is about 0.05–0.10 mm in diameter. Once the cellulose xanthate is neutralized and acidified, a rapid coagulation of the rayon filaments occurs. The viscose coagulates in the spin bath, initially by forming a skin; as the bath liquid penetrates through into the center, all the viscose is converted to cellulose. This is followed by simultaneous stretching and decomposition of cellulose xanthate to regenerated cellulose. Sodium sulfate acts as a dehydrating agent for the gelled fiber. Zinc sulfate acts as a coagulant. The environment around the bath is extremely corrosive; hence, the use of precious metals for construction of the spinneret and spin bath is needed. A typical machine running speed is 75 m/min. As final treatment stage, acid on the fiber is removed by washing with water, and sulfur is removed by treatment with about 0.3% NaOH. A finish oil is applied before the fiber wound onto bobbins and dried [1,6].

Precursors made from regenerated cellulose contain defects like internal voids and interfilament bonding. Certainly, these defects lead to weak and brittle CF after carbonization. Lyocell fibers, a new kind of man-made cellulose fiber, may be a new solution at this stage and have the potential to leverage the mechanical properties of cellulose-based CFs. Lyocell fibers have an environmental-friendly production process and better fiber properties. They have higher tenacity, higher modulus, lower shrinkage in dry state, and lower tenacity and modulus reduction in the wet state. Their surface is round and smooth, and the molecular chains are highly oriented along the fiber axis [13]. Lyocell production process is an air-gap spinning process. 10–14 wt% cellulose has been dissolved in nontoxic *N*-methylmorpholine *N*-oxide (NMMO) solvent. The spinning dope has to be stabilized by additives such as isopropyl gallate to avoid side reactions [7].

6.2.4 Other precursor materials

In addition to above-mentioned three major precursor materials, researchers are continuously working on other potential alternatives. However, most of them are suitable to be used for general purpose CF because of their relatively poor mechanical properties. These researches are mostly aiming possible future low mechanical property requiring cheap CF applications, rather than available GP or HP applications. The details of each can be found elsewhere [1,7,11]; however, briefly mentioning on alternatives will be helpful for those interested.

Lignin is an important alternative to the main precursor materials because it is bio-renewable and the raw material is very cheap. It is produced as the by-product of the pulping process and cellulosic ethanol fuel production. It has different blends mostly depending on its source like kraft lignin, organosolv lignin, hardwood lignin, and alkaline lignin. For example, Uraki et al. melt-spun organosolv lignin obtained from birch wood. The mechanical properties of CF obtained are fiber diameter 14 ± 1 μm, elongation $0.98 \pm 0.25\%$, tensile strength 355 ± 53 MPa, and modulus 39.1 ± 13.3 GPa [14]. Also, ORNL researchers have conducted a lot of research on the application of alkaline lignin as a carbon precursor. The main obstacle is on

the cost of purification processes. Some researchers are also reacting or blending lignin with other polymers to discover new potentials [15,16].

Another potential precursor material is polyethylene (PE)-based raw materials. Because its carbon yield is very high, early investigations started in 1972. During the PE-based CF production to reach high carbon yields, the PE must be treated chemically to substitute hydrogen with heteroatoms so as to stabilize the carbon main chain of the polymer for carbonization. Sulfur is the best suitable heteroatom when the literature is checked. In this respect, PE is treated with concentrated sulfuric acid to obtain high carbon yields. The best carbon yields are around 65%, but the tensile strength (up to 1.54 GPa) and Young's modulus (134 GPa) are lower than PAN-based CF [7].

Nonheterocyclic aromatic polymers such as phenolic polymers, phenol formaldehyde resin, polyacrylether, polyamides (PAs), and polyphenylene have been investigated. Their easy cyclization, easy elimination of noncarbon atoms, and high carbon yield are advantages, but no breakthrough in mechanical properties is observed. Some heterocyclics studied are polyimides, polybenzimidazole, polytriadiazoles and are converted to CF with HM and as high as 90% carbon yield. However, their raw material costs are high [4].

6.3 Carbonization processes

After the production of precursors, the second step is the carbonization of the precursors and removing all of the atoms except carbon from the structure. This is not a one-step heat application but involves gradually increasing heat treatment. CF production is started with a step called oxidation or stabilization, where the dehydrogenation, oxidation, and nitrile cyclization reactions occur, and a condensed pyridine ring "ladder" structure is formed at 200–300°C. This is a time-consuming process and at least takes several hours. Generation of ladderlike structure is crucial for the resistance of material for further heat treatment. After the stabilization step, the ladderlike structure containing fibers are subjected to around 1000–1600°C high-temperature treatment for carbonization. If high-modulus fiber is aimed, this carbonization step is followed by at least 2000°C heat treatment to manufacture the resultant CF with more than 95% carbon containing. The details may vary according to the precursor used for CF production; however, the general scheme is similar.

6.3.1 Manufacturing of CF from PAN based precursor

CF from PAN precursor is produced by the oxidative stabilization of precursor followed by a two-stage carbonization process, with an extra heat treatment stage to manufacture a high-modulus fiber. The ultimate goal is to remove all elements other than carbon in the precursor with the minimum loss of carbons to increase the yield. CFs contain more than 95% carbon atom; the rest is mostly nitrogen.

A flow diagram of PAN precursor conversion to several CF types is drawn in Fig. 6.4. Just to visualize, the length of such a line is at least a hundred meter and increasing according to the machine capacity.

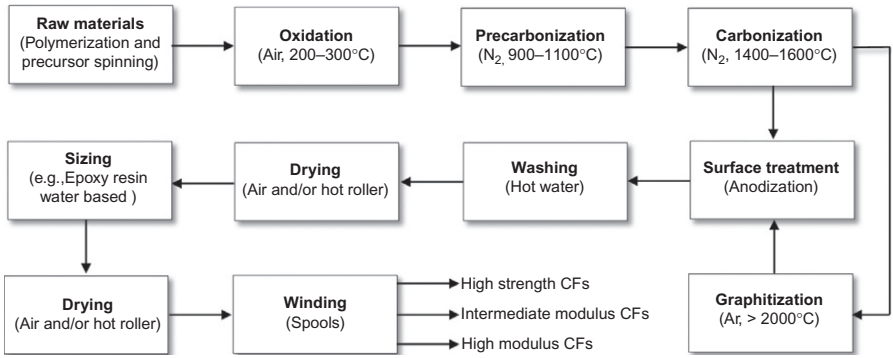

Fig. 6.4 Diagram of CF manufacturing process from PAN-based precursors [6].

As it is mentioned before, after the spinning of PAN precursor, the white fibers are usually winded over large bobbins or laid into cardboards. The fiber storage equipment is then connected to carbonization line.

Thermal stabilization (oxidation) process is the first step, and it is the most critical stage to create high-quality fibers. The PAN-based polymer precursor is stabilized by controlled low-temperature heating over the range of 200–300°C in air atmosphere. The precursor is converted to a form that could be further heat-treated without the occurrence of melting or fusion of the fibers. For the best practice of stabilization, the fiber should be converted at a slow heating rate to avoid possible runaway exotherms, hence for the best mechanical properties and process safety. Due to this fact, proper oxidation of the fiber generally takes hours, and a stepwise increase of temperature in the oven is applied. Significant increases in line speeds are achieved by using series of ovens to provide additional zones and where in each oven series of pass is applied [1]. During the stabilization, gasses, such as HCN, H_2O, CO_2, CO, NH_3, H_2, and CH_4; nitriles and miscellaneous tars; and finish are evolved. About 6–8 wt% take-up of O_2 in oxidation is also experienced. Since the reaction is strongly exothermic, a uniform temperature (±2°C) distribution should be provided, and noxious gasses must be removed in order to avoid the buildup of them and cause explosions. The amount of heat released and initiation temperature of stabilization is highly dependent on the amount and types of comonomers used. Incorporation of acidic groups reduces the exotherm and the onset cyclization temperature [11]. An optimum tension during stabilization leads to improvement in mechanical properties of the final fiber.

During stabilization, the linear PAN molecules are converted to an N-containing cyclic (ladderlike) structure. However, cyclization is a very complicated process, and there are several models proposed. Those are schematically reviewed in Fig. 6.5 [11]. The kinetics can be changed by many factors like precursor compositions, fiber structures, fiber diameters, temperature, and the environment. However, mainly, the stabilization rate is controlled by the diffusion of oxygen into the precursor fibers. Finer fibers are considered more suitable for stabilization. During oxidation,

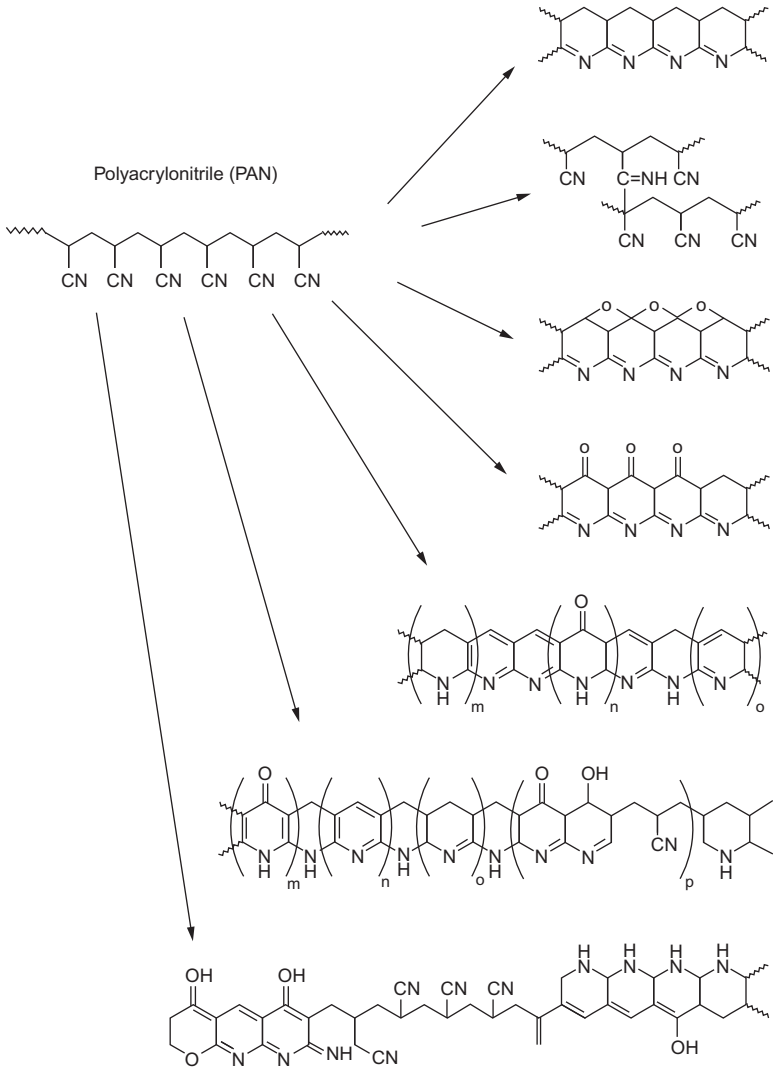

Fig. 6.5 Models on reactions during oxidation of PAN-based precursor [11].

the density of the PAN fiber is increased from 1.18 g/cm^3 to about 1.36–1.38 g/cm^3 of oxidized PAN fiber [1]. At the end, the oxidized fiber becomes suitable for further processing at higher temperatures. They contain 62–70 wt% carbon, 20–24 wt% nitrogen, 5–10 wt% oxygen, and 2–4 wt% hydrogen [7].

In the next step of the process, the stabilized precursor fiber tows, which are resistant to high temperatures, are exposed to thermal pyrolysis in an inert atmosphere and ultimately carbonized. Fiber is exposed to higher temperatures usually in two steps: low-temperature (LT) furnace up to 900–1000°C and high-temperature (HT) furnace

up to 1500–1600°C. In these furnaces, the temperature is gradually increased. At the early stages of carbonization, cross-linking reactions within the oxidized fiber takes place (Fig. 6.6). The cyclized structure starts to link up in the lateral direction with dehydrogenation and denitrogenation reactions. Dehydrogenation combined ladder molecules forming graphite-like ribbons, and denitrogenation was responsible for joining of ribbons to form sheetlike structures. A planar structure is obtained where the basal planes are oriented along the fiber axis. However, this structure is a

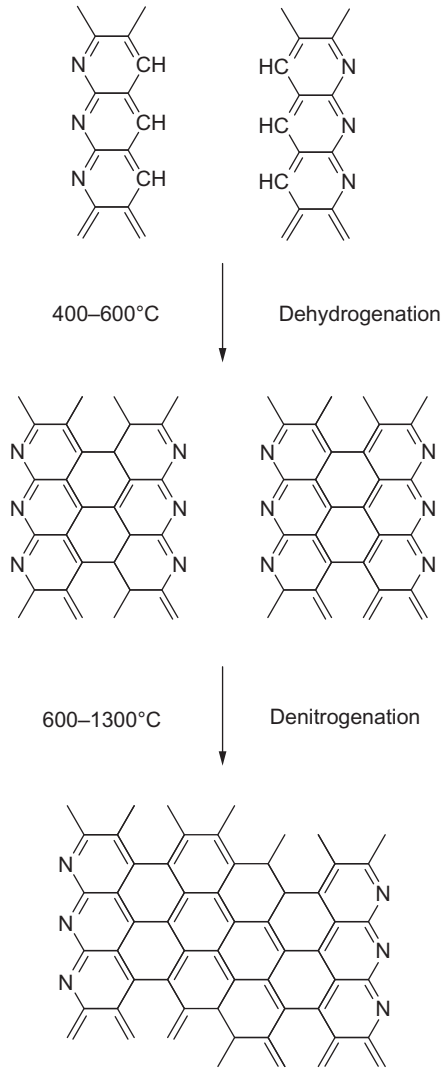

Fig. 6.6 Schematic formation of graphite structure [17].

turbostratic carbon phase and differs from graphite structure with its imperfections and discontinuity in the order.

The nitrogen in aromatic rings makes bonds between layer planes with the release of nitrogen; hence, compatibility is increased. This results an increase in tensile strength. For high-strength CFs, the ultimate carbonization temperature is selected between 1500°C and 1600°C, because a temperature, above ≈1600°C, decrease in tensile strength occurs [6]. The decrease in tensile strength is explained by the increased local defects [11]. The produced CFs can be heated more than 2000°C, even 3000°C to achieve higher modulus fibers. In this respect, graphitization furnaces are used. Especially, above 2000°C applications, argon is a must to use as inert medium because after 2000°C, nitrogen reacts with carbon to form cyanogen.

At the end, the volatile compounds are removed to give CFs with a carbon yield of about 50 wt% with respect to precursor. The resultant fiber contains >98 wt% carbon, 1–2 wt% nitrogen, and 0.5 wt% hydrogen [7]. And the surface of the CF is mostly dead to generate bonds needed at composite applications. So, it should be regenerated and conditioned for good adhesion at its final application point. This is performed by surface treatment and sizing applications.

When CFs are used without surface treatment, composites show low interlaminar shear strength (ILSS). This is originated from weak adhesion and poor bonding between the fiber and matrix [5]. Like precursor formulations, oxidation and carbonization conditions, surface treatment, and sizing application details are also trade secrets and kept confidential by the companies. But in principle, surface treatments increase the surface area and surface acidic functional groups and thus improve bonding between the fiber and resin matrix. This increases the wettability of the CF and enhances the ILSS [4]. Surface treatments may be classified into oxidative and nonoxidative treatments. The most often used method is liquid-type anodic oxidation treatment, and it could double the composite shear strengths with slight reductions (4%–6%) in fiber tensile strengths. In this method, Faraday's law applies, and 96,500 C liberates 1 g equivalent of O_2. Usually, to define and control the treatment level, current density is used and expressed in C/m. In the unit, a graphite cathode plate is available, and CF bundle forms the anode during the electrolysis of an acid or a salt solution. As electrolyte, ammonium sulfate is usually used in commercial scale. This electrolyte results carbonyl groups (—COOH) on the surface of the fiber. Then, the CF is washed to remove excess electrolyte. In this stage, CF requires some protection or lubrication for the ease of handling because it is brittle. A chemical called sizing is applied on the surface. This may be water soluble, but mostly, it is insoluble and applied to fiber bundle by passing through a sizing emulsion bath. Usually, they are epoxy resins and epoxy formulation emulsified in water. The fiber sizing, process to apply sizing, and sizing content are considered to be critical factors in the CF specification because they are crucial to control the composite properties [4]. The final CF having around 1.80 g/cm^3 density is ready for the usage in composite industry.

After sizing treatment, the dried CFs are collected using online winders over cartoon/plastic bobbins. Winding machines are with automatic doff. Consistent length of CF over a bobbin is important for CF downstream consumers like weavers, prepreggers, and filament winders. The weight of a finished spool varies in terms

of ktex of the CF, but it is up to 12 kg in weight and several kilometers in length. After winding, the spools are individually shrunk and packed into the cardboards.

6.3.2 Manufacturing of CF from pitch based precursor

The pitch-based precursor fibers, when spun, are very weak and thermoplastic in nature. They need to be chemically converted to resist higher temperature treatment during carbonization. This stabilization process is a kind of thermosetting. This is best accomplished by some kind of oxidation treatment in the gas phase mostly air. The temperature and heating rate are dependent on the type of precursor (isotropic or mesophase) and its molecular weight distribution. The higher the mesophase content and molecular weight of the pitch, the higher will be the softening temperature, and the higher oxidation temperature can be applied to make the fibers infusible. Otherwise, lower temperature processing results longer thermosetting time. Normal processing temperatures are between 275°C and 350°C. Temperature more than 400°C can result melting or excessive loss of carbon by burning. At normal processing temperatures, for mesophase fibers 60 min and for isotropic fibers 3 h of treatment are needed [1].

In industry, mainly two methods for air oxidation are employed during processing, and both are batch processes. First one is based on spinning the precursor on a heat-resistant spool and placing those spools into an oxidation oven with sufficient circulation. Second is to collect the spun fiber by piddling into a suitable container to facilitate subsequent removal, with the container preferably on a plating table and the fragile fiber drawn from the container, spread onto a conveyor belt and carried through the oxidation oven.

The control of oxidation process is critical; otherwise, underoxidized fiber will remain partly thermoplastic. This results to fusing of fibers to each other during the carbonization and poor CF properties, especially tensile strength. Overoxidation will produce a brittle product with very low tensile strength and will reduce the graphitizability of the pitch.

After stabilization, carbonization process is applied like in the PAN-based CF production. The greatest weight loss occurs in the early stages of carbonization. Therefore, it is better to apply an initial low-temperature carbonization stage to avoid disruption of the fiber structure. This is usually 0.5 min at 700°C followed by 0.5 min 900°C in inert nitrogen atmosphere [1].

After the initial carbonization stage, the temperature is increased to about 2000°C. Carbonization is achieved in a series of furnaces with separate temperature settings or one or more furnaces with different temperature zones. Throughout this stage, heteroatoms like H, N, O, and S is removed in H_2O, CO_2, CO, N_2, CH_4, H_2, and tar form. The principal gas involved is H_2.

After carbonization, a mesophase pitch-based fiber can be additionally heat-treated for graphitization in a similar type of furnace, using highly controlled inert atmosphere, in the range of 2800–3000°C. A residence time of 10 s may be employed. At the end, a high degree of orientation, where the carbon crystallites are parallel to the fiber axis, is achieved. These fibers are truly graphitic and have a structure characteristic of polycrystalline graphite with three-dimensional order [1].

6.3.3 Manufacturing of CF from cellulosic precursors

Rayon has a chemical formula of $(C_6H_{10}O_5)_n$, and the theoretical carbon yield is found as 44.4%. However, the actual yield is around 10%–30% due to the release of CO, CO_2, alcohols, ketones, and other carbons containing low-molecular-weight substances [11].

Similar to PAN- and mesophase pitch-based CF production, the conversion of cellulose-based precursors to CF includes thermal decomposition/oxidation, carbonization, and an optional graphitization. Even it is the first material used in CF production, little information is available in literature about the production process [1]. The rest of the process such as surface treatment, sizing, and winding are identical to the processing of the PAN-based CF.

The pyrolysis of cellulose is basically controlled by two reactions, dehydration and depolymerization (cleavage). This depolymerized structure is converted into graphite-like layers through repolymerization during high-temperature treatment.

The main reaction at low temperature is the dehydration reaction that results in the stabilization of cellulose for further heat treatment. During the dehydration, the elimination of the hydroxyl groups leads to conjugated double bonds, and as a result, the dehydrate cellulose ring becomes less accessible for cleavage than the original cellulose. In the first stage, H_2O dehydration is followed by physical desorption of water and dehydration of the cellulosic unit between 150°C and 240°C. Polymeric structure is retained, and the major mass loss is because of the evaporation of water. If dehydration in the early stages does not carried properly, this causes major mass loss during the carbonization process. Therefore, a slow heating rate of a few °C/h and use of flame retardants to catalyze the removal of the hydroxyl groups of cellulose or pyrolysis in a reactive atmosphere are common methods to promote dehydration reactions [6,7].

Over the range of 240–400°C, the thermal cleavage of the glycoside linkages and the scission of ether bonds occur. Depolymerization to monosaccharide derivatives occurs at this stage of carbonization. At temperature around 400°C, pyrolysis ceases, and the major chemical reactions are completed. At this temperature, the residue already has a carbon content of about 60%–70%. Carbonization is performed under an inert gas atmosphere at 900–1500°C. The release of noncarbon atoms results a residue with at least 95% carbon [7].

The reactions taking place during carbonization are rather complex and hard to monitor. However, in principle, the amorphous depolymerized char, formed during pyrolysis, is rearranged and condensed to form polycyclic rings, aromatic structures, and, at the end, graphite-like layers. A structure consisting of sp^3- and sp^2-hybridized carbon is formed. During this rearrangement shrinkage in fiber, increase in density and increase in tenacity are observed [7].

Graphitization of carbon is carried at temperatures between 1500°C and 3000°C. In this treatment, carbon content is increased to a level of more than 99%, and the graphite-like structure is grown, and density of the fiber is increased. The duration of graphitization is in the order of seconds and can be less than one second depending on the treatment temperature. If the graphitization is carried under stress, this leads to excellent mechanical properties of final CF by improving the orientation.

Although rayon fabrics are still being used to convert into CF cloth, the production of CF from rayon has limited commercial values due to its low carbon yield, high processing cost, and limited physical properties [11]. At present, CF based on cellulose amounts only around 1% of the total CF production [18]. After several acquisitions, today, the main producers of cellulose-based CFs are RUE SPA Khimvolokno (Belarus) and SGL Carbon (Germany) [19].

6.4 Recent developments and trends in CF technology

Many varieties of CFs have been developed for general and specific applications demanding very high requirements. During the development stages, the CF manufacturers enlarged their solution database, improved understanding, and gained experience. However, after more than 50 years of development studies on PAN-based CFs, still, the mechanical properties of resultant fibers are far from the theoretical limits. They are still at 10% of the theoretical strength of the carbon-carbon bond, and the modulus is about 30% of the theoretical modulus for PAN-based CF. In the pitch-based CF side, about 90% theoretical modulus is reached, however, with the expense of low tensile strength [20]. Therefore, basic research and understanding are still needed to achieve both properties to be superior at the same time.

Recently, another promising topic is reducing the cost of CF because new applications (which will generate more consumption) can only be generated by the reduction of the production cost per kg CF. Especially, high-volume applications like automobile industry are continuously demanding cheaper CF. Therefore, development studies in CF manufacturing are mostly focused on reduction in all related cost items. These may be precursor material, raw materials, and machinery used during precursor/CF production and even the composite manufacturing machinery. General scheme for the process steps and their costs in the PAN-based process is shown in Table 6.1 [21].

As shown in Table 6.1, 51% of the cost ($5.04 in $9.88) is generated from the precursor production; this brings the precursor stage cost-cut under the spotlight of many studies. Also, investigations on reducing the processing cost by implementing melt spinning of PAN have yielded promising results. The melt-assisted spinning process

Table 6.1 Cost of CF production today versus high volume in each processing step [21]

USD/kg	Precursor production	Thermal stabilization	Carbonization/ graphitization	Surface treatment	Spooling and packaging	Total cost
Baseline today	5.04	1.54	2.32	0.37	0.61	9.88
High-volume production	4.64	0.99	1.48	0.33	0.41	7.85

has produced CFs with a tensile strength of about 3.6 GPa and a modulus of about 233 GPa [11]. Using textile-grade PAN for low mechanical property demanding applications is also an issue for research. In pitch-based studies, focus is mainly on the production of mesophase pitch with lower cost, for example, application of new technologies for higher conversion. Recently, maybe the most popular topic is the precursor from renewable resources, especially from lignin. Because of very cheap starting material, all aspects of CF production by using lignin are focal point of many academic studies and industrial patents. In this class, due to relatively cheap raw material and high yield, polyolefins are another popular candidate for future progress.

Other important cost items are stabilization and carbonization processes. On these steps, new technologies are under research like microwave-assisted plasma technology [22]. By this technology, savings of 40% in direct production costs in carbonization stage and a reduction in the cost of finished CF of about 18% are stated. Also, by applying new stabilization and oxidation technology of nonthermal atmospheric pressure plasma based on close proximity indirect exposure (CPIE), researchers from ORNL reported an oxidation time of 35–40 min, instead of 80–120 min in conventional production [23]. It is clear that when these systems are applied into commercial manufacturing line, significant cost reduction will be gained.

Although the surface treatments and adaptations for the end use have very little impact on costs, they do have a significant impact on composite properties and their ultimate performance [24]. Especially, CF producers and sizing producers are continuously studying on this topic to improve the CF composite properties.

In addition to all, composite machinery producers are performing development studies on their equipment to increase the speed per cycle and consistency for future high-volume applications.

6.5 CF in polymer-matrix composites

Composite materials refer to materials containing more than one phase such that the different phases are artificially blended together. The constituent materials are significantly different with each other in terms of physical or chemical properties, and when combined, the resultant material exhibits characteristics different from the individual components.

A composite material consists of one or more fillers in a certain matrix. A CF composite refers to a composite in which at least one of the fillers is CF. CF may be in the form of either short or continuous, unidirectional or multidirectional, or woven or nonwoven. The matrix is usually polymer, metal, carbon, ceramic, or a combination of them. The mechanisms of the fiber-matrix bonding include chemical bonding, van der Waals bonding, and mechanical interlocking. Chemical bonding and van der Waals bonding require good and sufficient contact surface area between the fiber and matrix. The wetting between matrix and fiber should be adequate; thus, an appropriate contact area is generated for sufficient bonding. Due to this fact, surface treatment and sizing application are important to achieve wetting and bonding and result in high composite part physical properties. Another method to advance the contact is high-pressure application during the infiltration of the matrix through the fiber or

adding a wetting agent to the matrix before infiltration. The processing temperature is also affecting the wettability; thus, the infiltration temperature should be chosen to enhance the wetting [10].

Excessive reaction between matrix and fibers is also undesirable because it degrades the fibers, and reaction product(s) may be undesirable for the mechanical, thermal, or moisture resistance properties of the composite. Therefore, an optimum amount of reaction is preferred.

CF composites are mostly fabricated by the impregnation (or infiltration) of the matrix in the liquid state into the fiber preform, which is mostly in the form of a woven fabric. In the case of tubular shape composite part, the fibers may be impregnated in the form of a continuous bundle from a spool, followed by wounding of bundles on a mandrel. Instead of impregnation, the fibers and the matrix material may be intermixed in the solid state by mixing CFs and matrix material, by coating the CFs with the matrix material or by sandwiching CFs with foils of the matrix material. After impregnation or intermixing, fixing or curing is carried out usually under heat and pressure.

Nowadays, the decrease of the CF prices is enhancing their application areas in composite industry. Still, the main consumption is at aerospace and defense application, whereas the volume of automobile industry is increasing each year [2]. Hence, the research and development on the composite applications of CF is hyping in both industry and academia. In addition, developing or improving the production techniques for higher throughput to decrease the per part labor cost is under the spotlight as well.

In this section, main focus will be on CFs in polymer-matrix applications. CFs may be produced from any type of precursor raw material.

6.5.1 Types of reinforcements in CF composites

A tow of CFs is a bundle of nontwisted continuous carbon filaments, about 5–10 μm in diameter, with tow sizes of 3k, 6k, and 12k, normally surface-treated and sized. Higher k value tows are available, up to 410k, as well [1]. These fibers are used in discontinuous or continuous form in the composite applications.

In the discontinuous usage, CFs are used in needled mat, chopped, or milled form. In needled mat, the CF is dry laid, without any binder, but some of the fibers are also oriented in the thickness direction. Generally, these nonwovens are produced by repeated penetration of a set of barbed needles on the fibrous web for converting it into coherent and self-locking materials. In chopped form, CF bundle is generally cut 3 or 6 mm long with a reciprocating knife or a rotary blade. They are sized with suitable material according to matrices before chopping. In the milled CF production, sized fibers are cut into short staple form and milled to give a CF powder. Milled CFs are typically 30–3000 μm long, averaging about 300 μm with a mean L/D ratio of 30. They are used with appropriate resin to confer EMI/RFI shielding and in automobile air bags for rapid ignition [1].

In the continuous form usage, fabric architecture is mainly defined under four major forms as (1) nonwoven, (2) unidirectional, (3) planar (2-D) and (4) three-dimensional.

In this part of the chapter, several of these will be briefed, and the others including much more detail can be found at the following Refs. [1,6,10,25].

A fabric is defined as an integrated fibrous structure produced by fiber entanglement of yarn interlacing, interlooping, intertwining, or multiaxial placement [25]. Reinforcement materials can be designed with unique fiber architectures and can be preformed (shaped) depending on the product requirements and manufacturing process.

A unidirectional fabric is normally taken as a fabric with at least 90% of the fiber weight in one direction, which can be in warp or weft direction. The primary fiber can be held together by bonding with a meltable thermoplastic, hot melt or thermosetting adhesive, and weaving or stitching. Fibers are straight and uncrimped, and mechanical properties are enhanced by prepreg application [1].

Woven fabrics can be created by positioning the yarns at 0 and 90 degrees to one another and interlacing to form a series of regular geometric patterns. In a woven fabric, the yarns running parallel to the direction of weaving are named as warp (or ends), and the yarns running transverse to the direction of weaving are termed as weft (picks, fill, or woof). Plain, twill and satin weaves are the basic types. The plain weave is the simplest and most commonly used woven fabric. Each warp is passing alternately under and over each weft. The fabric is symmetrical and has good structural integrity. However, the weave has poor drape due to its tightness, and the high level of crimp in its nature reduces the mechanical property by about 15%. A twill weave is generated by passing the weft yarn over two or more warp yarns and then repeating that pattern one warp thread over so that a diagonal line is created. Twill weave has high density with good drapability and gives highest retention of fiber strength and modulus. The satin weave is characterized by each weft or warp passes over N yarns and under one crossing yarn. They are named as $N+1$ harness satin (e.g., four shaft passing over three and under one). Crimp is minimum so good translation of strength and modulus are achieved. This weave showed the highest bidirectional strength, is very pliable with high density and high-fiber-volume fraction. It has extremely good drapability but may be less stable than twill. Most common satin weaves are 4HS, 5HS, and 8HS [1].

Another type is the knitted fabric that is produced by interloping flexible yarns of one yarn set. The yarn is formed into loops, and the newly formed loops are intermeshed with previous knitted loops. Each loop in a knitted fabric is called a stitch. It is an expensive process but important for the manufacture of 3-D fabrics. There are two main types of knitting, weft knitting and warp knitting.

Braiding is another important reinforcement type for composites. It is a process of interlacing three or more threads diagonally to the product axis (parallel to the longest dimension of the resulting product) in order to obtain a thicker, wider, or stronger product [26]. In braiding, no two yarns are twisted around one another. There are two main forms of braid architecture, biaxial 2-D braid and triaxial 3-D braid.

In addition to these fabrics, many 3-D reinforcements are available. Some are multiaxial noncrimp reinforcements, woven 3-D fabrics, weaved 3-D fabrics, knitted 3-D fabrics, and braided 3-D multiaxial reinforcements.

In carbon reinforcement, it is possible to incorporate two or more different yarns (such as aramid or glass in addition to carbon) to form a hybrid carbon reinforcement,

enabling to incorporate the properties of the other material into the composite part or creating a new material between the performance levels of the two.

6.5.2 Types of polymeric matrices for CF composites

Polymer-matrix applications take 64% of 16.6 billion USD CF-based composite industry. In the polymer-matrix composite applications, there are two groups of resins in use, thermosetting resins and thermoplastic resins. Thermosetting resins get about 76% of the market; the rest is thermoplastic resins [2].

Thermosetting resins are generally found in liquid form, and they cure irreversibly. The curing is performed via heating, chemical reaction, or irradiation. Once they are cured, the material cannot be reheated and melted back to its original liquid form. Thermosetting resins are easy to process and laminate, stronger than thermoplastics and better suited to higher temperatures than thermoplastics. However, they are relatively more brittle. Within the thermosetting type, most widely used resins are cyanate ester, epoxy, phenolic, polyimide, and vinyl esters.

Cyanate esters (CE) belong to a class of HP thermosetting resins and contain at least two cyanate functional group. They can be cured by heating in the presence of a catalyst. The most common catalysts are transition metal complexes such as cobalt, copper, manganese, and zinc complexes. Its curing reaction involves trimerization of three CN groups to form triazine ring. From thermal performance point of view, they are in between the performance of epoxy resins and high-temperature polyimides. CEs possess a unique balance of properties and are particularly notable for their low dielectric constant and dielectric loss, low moisture absorption, low shrinkage, and low outgassing characteristics [6].

Epoxy resins are thermosetting resins that contain more than one epoxide group. Their curing reaction is carried by using a wide range of curing agents. There are several types of epoxy resins. One is bisphenol-A/F epoxy resins. They are synthesized by the reaction of epichlorohydrin with either bisphenol-A or bisphenol-F in the presence of a basic catalyst. Other types of epoxy resin are trifunctional epoxy resins and tetrafunctional epoxy resins. Trifunctional epoxy resin, trimethylolpropane-*N*-triglycidyl ether, is prepared by the reaction of trimethylol propane with epichlorohydrin. This epoxy resin has low viscosity, low temperature curing, noncrystallinity, and plasticity. Tetrafunctional epoxy resins are synthesized through the reaction of 1,3-diaminobenzene or 4,4′-aminodiphenyl methane with epichlorohydrin. Tetrafunctional epoxy resins have high cross-linking densities due to their large number of epoxy functionalities and are used in applications involving high-temperature resistance. The cured tetrafunctional epoxy resins show excellent chemical resistance, HM, UV-blocking effect, and thermal stability. Novolac epoxy resins synthesized by the reaction of phenolic novolac resin with the epichlorohydrin are another important to mention epoxy resin. Their multiple epoxide groups give them the opportunity to make multiple bonds, which results excellent resistance against temperature, chemicals, and solvents. During the cure of epoxy resins, a wide variety of curing agents such as amines, PAs, phenolic resins, anhydrides, isocyanates, polymercaptans, and catalytic curing agents are used. The cure kinetics and Tg of cured epoxy resins

are dependent on the molecular structures of the curing agents. The stoichiometric amount of curing agent directly affects the network structure, thus affects the final properties of the composite part. Epoxy curing agents can be divided into amine-type curing agents (triethylenetetramine and DDM), alkali-curing agents (imidazole and tertiary amine), anhydrides (phthalic anhydride (PA) and nadic methyl anhydride), and catalytic curing agents (*N*-benzylpyrazinium hexafluoroantimonate (BPH) and *N*-benzylquinoxalinium hexafluoroantimonate (BQH)) [6].

Phenolic resins are synthesized by the reaction of phenol and formaldehyde. According to the synthesis route, they are divided into resol and novolac resins. Resol resins are synthesized by the reaction of a molar excess of formaldehyde with phenol in the presence of a basic catalyst, while novolac resins are synthesized by the reaction of a molar excess of phenol with formaldehyde in the presence of an acidic catalyst.

Polyimide resins are synthesized by the polymerization of imide polymers. They are divided into two groups: aliphatic polyimides and aromatic polyimides. They possess a greater resistance to heat compared with any other unfilled organic material. Polyimides possess low dielectric constant, flexibility, polishability to angstrom-level surface finishes, excellent dimensional stability, low water absorption, high-temperature stability, excellent machinability, low outgassing and noncontaminating quality, exceptional mechanical strength, and low coefficient of thermal expansion. As a result, they are used in place of metals and glass in many HP applications in the electronics, automotive, and even the aerospace industries.

Vinyl ester is a resin produced by the esterification of an epoxy resin with an unsaturated monocarboxylic acid, so it combines the advantages of epoxy and polyester resins. These resins have higher flexibility like the epoxy resins and ease of processing, like the polyesters. Vinyl ester resins are stronger than the polyester resins and cheaper than the epoxy resins. Vinyl ester has lower viscosity compared with the polyester and epoxy resins. They offer better resistance to moisture absorption compared with the polyester resins [6].

Another major class of resin is the thermoplastic resins. They consist of long polymer molecules, which are not cross-linked. Thermoplastic resins can be repeatedly melted and reused. They are often supplied as granules and heated to permit fabrication using conventional molding methods like injection molding, rotational molding, extrusion, vacuum forming, and compression molding. Thermoplastic resins have high-impact strength, recyclability, and zero emissions. They can bond to other thermoplastics and be molded or shaped with reheat. Several major thermoplastic resins that can be used as polymer matrices for CF-reinforced polymer composites are acrylonitrile-butadiene-styrene (ABS), PA, polycarbonate (PC), polyetheretherketone (PEEK), polyethersulfone (PES), PE, and polypropylene (PP) resins [6].

ABS is a thermoplastic terpolymer, synthesized by the polymerization of acrylonitrile, butadiene, and styrene monomers. Industrial polymerization may be carried out by bulk, suspension, or emulsion polymerization methods. Usually, 50% of the polymer is styrene, and the remaining is butadiene and acrylonitrile. ABS resin is tough, economic, light, and heat- and stain-resistant. ABS resin can be processed by any of the standard processing methods.

PA are polymers with repeating units linked by amide, —CO—NH—, linkages. PAs can occur both natural (proteins) and artificial. They are commonly used in textiles, automobiles, and carpets due to their durability and strength. On the basis of the chemical structure of the main chain, PAs are classified as aliphatic PAs, polyphthalamides, and aromatic PAs. On the basis of the number of repeating units, PAs can be divided into homopolymers (nylon 66, made from hexamethylenediamine and adipic acid) and copolymers (nylon 6/66, made from caprolactam, hexamethylenediamine, and adipic acid). Nylon 66 is best known and used in the industry. It has relatively high melting point of 265°C [6].

PCs are synthesized by the reaction of bisphenol-A and phosgene, $COCl_2$. PC is a novel, highly flexible, durable and nonbreakable, and cost-effective thermoplastic resin and therefore finds many application in both domestic and industrial usage. In addition to these, PC has excellent impact resistance and optical clarity. A balance of useful properties, such as temperature resistance, impact resistance, and optical properties, positions PCs between commodity plastics and engineering plastics. PCs are easily molded and thermoformed.

PEEK resins are synthesized using step-growth polymerization by the dialkylation of bisphenolate salts. PEEK is a semicrystalline thermoplastic resin with excellent mechanical and chemical resistance properties even at high-temperature exposure. It has a Tg of 143°C and melting point of 343°C, which is relatively high temperature than the other alternatives. In addition to this, PEEK resins have very low flammability (rated as V-0), low moisture absorption, inherently good wear, abrasion resistance, and long-term hot-water/steam-exposure resistance. Due to its mentioned properties, PEEK resin is used as engineering material.

PES is an amorphous resin containing ether and sulfone on its backbone. PES resins exhibit high-temperature performance with a high Tg, good dimensional stability due to their noncrystalline structure, outstanding rigidity even at high temperatures, excellent insulation properties, biocompatibility, and inherent flame retardation. PES resins can be molded by conventional plastic processes, such as injection molding, extrusion, compression molding, sintering, and solution casting. PES composites bring distinct advantages over thermoset resins, such as shorter processing times, better toughness, reduced scrap, and reparability [6].

PE is the highest production volume plastic of the world. PE is a light and versatile polyolefin resin, manufactured by the polymerization of ethylene monomer. It has many application areas ranging from synthetic shopping bags to detergent bottles. PE can be shaped by using wide range of processes, and it has a flexibility, moisture resistance, and low-cost properties. Different types of PE are available, such as low-density PE (LDPE), linear low-density PE (LLDPE), and high-density PE (HDPE).

PP is a linear thermoplastic polymer made from the propylene monomer using Ziegler-Natta polymerization and metallocene catalysis polymerization. PP resins are cheap, low density, high-tensile and compressive strength, and excellent dielectric properties with an excellent resistance to several solvents, bases, and acids.

6.5.3 Manufacturing methods of CF composites

Matrix and the reinforcement are processed together to manufacture the composite parts with many different processes. According to the resin being thermoset or thermoplastic, the structuring process changes. They can be divided into two subgroups, open-molding processes and closed-molding processes [6].

Some of the open-molding processes, also known as open laminating, have been used for the longest time in the polymer-matrix composite industry to make thermoset composite products. It is a simple process with many advantages and uses basic material technology and investment. This molding method involves placing reinforcements and liquid resin onto an open mold (sometimes preimpregnated reinforcement is used) or onto other substrates to manufacture a sandwich construction and on-site repair. During open-mold process, molds are prepared by using the same resins used in the parts produced and fiberglass reinforcements. The mold is created applying a gel coat over the model; after that, sheets of fiberglass wetted with the catalyzed resin are applied in individual layers until the required thickness achieved. The open-mold process needs curing of the parts at room temperature, and the actual process will require 4–6 h from start to finish for each molding. For high-quality parts, well-trained operators and dedicated facilities are required. The methods of open-mold fabrication include wet layup, hand layup, spray layup, tape layup, filament winding, and autoclave molding.

Closed molding comprises a broad category of fabrication processes where the composite part is produced in a mold cavity formed by joining of two or more tool pieces. There are many variations of the closed molding process, each with its unique aspects. Several of them are as follows:

Resin transfer molding (RTM)—Uses liquid resin injection into the mold to impregnate the stationary preforms placed within the mold. Many thermoset resin parts are manufactured by this method. Process is cleaner and healthier with clean surface finish and close-dimensional tolerances.

Light RTM (LRTM)—In LRTM, resin flow rates cannot be accelerated above an optimum level while maintaining inner cavity mold pressures below the clamping forces of the external atmospheric pressures. Normally, injection pressure is less than 1 bar, and cavity vacuum level is −0.5 bar. Recently, LRTM is replacing traditional RTM in low-to-medium-volume applications due to its minimal tooling structure in marine, automobile, industrial, and medical composite molding applications. The products are having two finished sides and close dimensional tolerances.

Vacuum-assisted RTM (VARTM)—It is a single-sided molding process in which the dry reinforcement is placed into the mold and a cover (or a vacuum bag) is placed over it to form a vacuum-sealed environment. This process is applicable to larger, less complex-shaped composite parts and needs simple and low-cost tooling. Another advantage is by applying this process, high-fiber-volume panels are achievable.

Pultrusion—This process is used to manufacture in continuous lengths of fiber-reinforced plastics. The reinforcement fiber from the spool is used, and the liquid resin mixture (containing resin, fillers, and other additives) is in a bath. The fiber from

the spool is pulled, passed through the bath, thus impregnated with the resin and entered to a heated steel-forming die using a continuous pulling device where curing performed. On exiting the die, the cured profile is pulled to the saw for cutting into preferred length. Its initial investment is generally high; however, the process cost in high volume is low.

Thermoforming—It is a molding process to form sheets of plastic to a mold surface by using heat and vacuum and/or pressure force. This process is used for thermoplastics. Thermoforming is generally used for thin sheets, and thicker sheets cannot be formed.

Vacuum bagging—In this process, the wet laid-up laminate is sealed with a plastic film. The air under the bag is extracted by a vacuum pump. So, a pressure up to 1 bar is applied to the wet laid-up. By applying this technique, large products with a clean production method are possible. Top quality products can be generated by the use of prepregs. Typical applications are large one-off cruising boats, race car components, and core bonding in production boats.

Compression molding—The resin and reinforcement are shaped by hydraulic pressing between two halves of a steel mold. Sheet molding compound (SMC) is the well-known type of compression molding. In SMC process, the required resin, catalyst, mineral fillers, and reinforcement are premixed and poured to the mold then squeezed with more than 130 bar pressure and 175°C temperature for 1–3 min. After squeezing, the mold is opened and the part is taken out and ready for the next cycle. The automobile industry mostly uses this process because of their high-volume per part, and this situation justifies the capital cost associated with the tooling and the high-tonnage presses required.

Extrusion—This process is containing a machine called extruder, which contains a heated barrel with a screw in it. The resin is filled into this heated barrel, melted, and transferred by the aid of the screw. At the exit, a shaping unit, which is called die, is available. According to the shape of this die, pipes, ingots, guttering, and window sills can be manufactured. The process is continuous with low tool cost.

Injection molding—It is one of the the most extensively used process for composite part production of thermoplastics containing short fibers. The fiber/resin mixture is fed through the hopper of the injection molding equipment. This equipment is a kind of extruder machine with a mold at the exit. When the mixture is introduced to the machine, it enters to the heated screw section (barrel). While the mixture is melting, it is transferred through the screw. The molten material is collected in front of the screw by the rotation of the screw and then injected into the mold at high pressure. After injection is completed, the mold is cooled below the solidification temperature of the resin. After solidification, the mold is opened, and the part is ejected. Injection molds are very well automated, so the process is carried within a few seconds.

6.6 Uses of CF in other matrices

Besides polymeric composites of CF, other types of composites like carbon-carbon (C/C) composites, carbon-ceramic composites, and carbon-metal composites are available, and they are manufactured industrially.

C/C composite is a composite material consisting of CF reinforcement in a matrix of graphite. It is developed for the nose cones and exit cones of intercontinental ballistic missiles and also used at the brake disks and pads of Formula-1 race cars and several aircrafts. C/C composites find usage in structural application at high temperatures or where thermal shock resistance and a low coefficient of thermal expansion is needed. Even the details of the production process are not disclosed due to secrecy; the major steps of the production are as follows: In the first stage, the shape of the material is generated by using CF and organic binder such as plastic or pitch. Usually, coke or fine carbon aggregates are also added into the binder mixture. In the second stage, the layup is heated and pyrolyzed. The binder is turned to pure carbon, lost volume, and voids formed within the structure. In the final stage, the voids are repeatedly filled by forcing a carbon-forming gas like acetylene through the material at a high temperature for several days. Thus, the voids are filled with carbonization of acetylene within them. C/C materials have low density (1.6–1.98 g/cm^3), high-thermal conductivity, and excellent mechanical properties at elevated temperatures. They retain their properties above 2000°C without major deformation. C/C composites readily oxidize in air above 370°C, and cracks that later generate failure is generated. This may be prevented by using inhibitors to provide oxidation protection (like boron and phosphorus) or with the use of a barrier coating (noble metals or silicon) [1].

Carbon-ceramic composites are gaining attention because of their good oxidation resistance (compared with C/C composites) at high-temperature applications, and decreasing price of CFs makes the use of CF-reinforced concrete economical. The fibers in the matrix increase the toughness and strength of the composite due to their tendency to be partially pulled out during the deformation. This pullout absorbs energy, thus toughening the composite. Secondly, they decrease the electric resistivity of the composite. This is important for generating conductive concrete for nondestructive flaw detection. Another function to improve is to increase the thermal conductivity of the composite, as the ceramic is insulating. Finally, CFs decrease the drying shrinkage in ceramic matrices prepared by using slurries or slips. The categories of carbon-ceramic composites are (1) CF-reinforced concretes and gypsums, (2) CF-reinforced glasses, and (3) other CF-reinforced ceramics (MgO, Al_2O_3, SiC, and mullite). The CFs used in concretes and gypsums are usually short, isotropic, and pitch-based, least expensive CFs. CFs are attractive for concretes and gypsums because of their superior chemical stability compared with glass fibers (which tend to dissolve in the alkaline environment of concrete and gypsum). When CFs are used, they increase the flexural strength, flexural toughness, and durability under cyclic loads and decrease the compressive strength, drying shrinkage, and electric resistivity. CFs at 0.5% of the weight of the cement are suitable in concrete. CF-reinforced glasses are useful for space structural applications, like mirror back and supports, and booms and antenna structures. The glass matrices used include borosilicate glasses (Pyrex), aluminosilicate glasses, soda-lime glasses, and fused quartz [10].

Carbon-metal composites have higher modulus-to-density ratio, higher strength-to-density ratio (specific strength), better fatigue resistance, and better high-temperature mechanical properties (higher strength and lower creep rate), a lower thermal expansion coefficient and better wear when compared with the metal itself. Their good thermal properties, especially their low density, make them desirable for

aerospace electronics and orbiting space structures. On the other hand, they have higher fabrication cost and limited service experience disadvantages. The most popular fabrication method of CF-metal matrix composites is the infiltration of a preform by a liquid metal under pressure. Pressure is needed due to the difficulty of the liquid metal to wet the CFs. Another fabrication method is diffusion bonding. In this method, a group of alternating layers of CFs and metal foils are hot-pressed (such as at 24 MPa for 20 min). Hot pressing above the solidus of the matrix metal and the plasma spraying of the metal onto continuous fibers are other production methods. CFs used for metal-matrix composites are mostly in continuous fiber form, but short fibers are used as well. The matrices used are aluminum (most widely used), magnesium, copper, nickel, tin alloys, silver-copper, and lead alloys. Several application fields are structures (aluminum and magnesium), electronic heat sinks and substrates (aluminum and copper), soldering and bearings (tin alloys), brazing (silver-copper), and high-temperature applications (nickel) [10].

6.7 Conclusion

A considerable progress has been achieved in the past in understanding the fundamental material-process interactions in the field of CFs. However, challenges in cost reduction, tensile and compressive strength improvement, and alternative precursor development still remain.

Today, the CF market is dominated by PAN-based CFs with available tensile strengths up to 7 GPa, followed by pitch-based CFs with extremely HMs up to ~90% of the theoretical limit of 1060 GPa. However, other cheaper precursor systems should be studied deeper. Lignin, PE, and even the textile PAN may bring new opportunities especially to the low-end market.

The CF production technology at all parts of the process is still open for innovation. The production should be reviewed for higher machine capacity with implementation of new technologies.

Optimizing the CF microstructure can improve CF strength through decreasing its flaw sensitivity. So, the precursor morphology and processing conditions for each precursor system should be reevaluated repeatedly.

At the CF composite industry, as the CF price decreases, new developments are at the edge. Machine producers are continually studying to automate the manufacturing processes. Designers are becoming more familiar on using CF at new application requiring material challenges.

Therefore, the field of CF and CF composites is still holding many new opportunities for the research- and development-focused and innovation-driven companies and entrepreneurs.

References

[1] Morgan P. Carbon fibers and their composites. Boca Raton, FL: CRC Press; 2005.
[2] Kraus T, Kühnel M, Witten E. Composites market report 2015. Carbon Composites; 2015.

[3] Anon. Wikipedia; 2016. Available at: https://en.wikipedia.org/wiki/Carbon_fibers [accessed 05.12.16].
[4] Chand S. Carbon fibers for composites. J Mater Sci 2000;35:1303–13.
[5] Donnet JB, Bansal RC. Carbon fibers. New York: Marcel Dekker Inc.; 1990.
[6] Park S. Carbon fibers. Dordrecht: Springer Science; 2015.
[7] Frank E, et al. Carbon fibers: precursor systems, processing, structure, and properties. Angew Chem Int Ed 2014;53:5262–98.
[8] Newcomb BA. Processing, structure and properties of carbon fibers. Compos Part A 2016;91:262–82.
[9] Masson J. Acrylic fiber technology and applications. New York, NY: Marcel Dekker; 1995.
[10] Chung DL. Carbon fiber composites. Boston, MA: Butterworth-Heinemann; 1994.
[11] Huang X. Fabrication and properties of carbon fibers. Materials 2009;2:2369–403.
[12] Wu Q, Pan D. A new cellulose based carbon fiber from a Lyocell precursor. Text Res J 2002;72(5):405–10.
[13] Peng S, Shao H, Hu X. Lyocell fibers as the precursor of carbon fibers. J Appl Polym Sci 2003;90:1941–7.
[14] Uraki Y, et al. Preparation of carbon fibers from organosolv lignin obtained by aqueous acetic acid pulping. Holzforschung 1995;49(4):343–50.
[15] Maradur SP, et al. Preparation of carbon fibers from a lignin copolymer with polyacrylonitrile. Synth Met 2012;162(5–6):453–9.
[16] Seydibeyoglu MO. A novel partially biobased PAN-lignin blend as a potential carbon fiber precursor. J Biomed Biotechnol 2012;2012. Article ID 598324.
[17] Goodhew PJ, Clarke AJ, Bailey JE. Review of fabrication and properties of carbon-fibers. Mater Sci Eng 1975;17(1):3–30.
[18] Zhang H, Guo L, Shao H, Hu X. Nano-carbon black filled lyocell fiber as a precursor for carbon fiber. J Appl Polym Sci 2006;99:65–74.
[19] Dumanli AG, Windle AH. Carbon fibers from cellulosic precursors: a review. J Mater Sci 2012;47:4236–50.
[20] Chae HG, et al. High strength and high modulus carbon fibers. Carbon 2015;93:81–7.
[21] Warren CD. Low cost carbon fiber overview. Tennessee: ORNL; 2011.
[22] Paulauskas FL, Bigelow TS, Yarborough KD, Meek MM. Manufacturing of carbon fibers using microwave-assisted plasma technology. Society of Automotive Engineers, Inc.; 2000.
[23] Paulauskas FL. Advanced oxidation & stabilization of PAN carbon precursor fibers. ORNL; 2014.
[24] Monfort-Windels F. Part 4: Carbon fibre reinforced composites; 2014. Available at: http://www.pluscomposites.eu/sites/default/files/Technical%20series%20-%20Part%204%20-%20Carbon%20fibre%20reinforced%20composites_0.pdf [accessed 05.12.16].
[25] Ko F. Textile preforms for carbon-carbon composites. In: Buckley JD, Edie DD, editors. Carbon-carbon materials and composites. Saddle River, NJ: Noyes Publications; 1993. p. 71–104.
[26] Kyosev Y. Braiding technology for textiles. Cambridge: Woodhead Publishing; 2015.

This page intentionally left blank

Aramid fibers

7

Mustafa Ertekin
Ege University, Izmir, Turkey

7.1 Introduction

Aramid fiber was the first organic fiber used as reinforcement in advanced composites with high enough tensile modulus and strength. They have much better mechanical properties than steel and glass fibers on an equal weight basis. Aramid fibers are inherently heat- and flame-resistant, which maintain these properties at high temperatures.

The term "aramid" is designated for the fibers of the aromatic polyamide type in which at least 85% of the amide bonds (—CO—NH—) are attached directly to two aromatic rings, as defined by the US Federal Trade Commission. The configuration of these bonds as either para or meta is often used to classify the polymer.

The substitution of the aliphatic carbon backbone by aromatic groups brings about considerable changes in the properties of the resultant fibers. The first fiber of this class to be developed was Nomex from DuPont that appeared in the 1960s. This yarn is of only medium tenacity but is nonflammable and widely used for the production of fireproof clothing, electric insulation, etc. However, only a few years later, aramid fibers (Kevlar by DuPont also) with chains containing p-disubstituted benzene rings appeared. In addition to good thermal stability, these fibers also possess outstanding mechanical properties. Their outstanding potential is derived mostly from the anisotropy of their superimposed substructures presenting fibrillar, pleated, crystalline, and skin-core characteristics [1–5].

7.2 Fiber production

Commercially available compounds corresponding to the definition of aramid are poly-(*m*-phenylene isophthalamide) (MPDI), poly(*p*-phenylene terephthalamide) (PPTA), and copoly(*p*-phenylene-3,4-diphenyl ether terephthalamide) (ODA-PPTA) (Fig. 7.1). The most popular brand for MPDI fiber products is Nomex (DuPont); other meta-aramids are Teijinconex (Teijin), Apyeil (Unitika), New Star (Yantai), and X-Fiper (SRO Aramid Co., Ltd.). The first and largest manufacturer of PPTA fibers is DuPont under the trademark Kevlar. The other producer of para-aramid fiber is Teijin, which produces Twaron based on PPTA, and Technora based on the ODA-PPTA copolymer.

7.2.1 Synthesis of aramids

The chemical composition of Kevlar and Twaron para-aramid fibers is poly (*p*-phenylene terephthalamide) (PPTA). The usual synthetic method for aliphatic

Fiber Technology for Fiber-Reinforced Composites. http://dx.doi.org/10.1016/B978-0-08-101871-2.00007-2

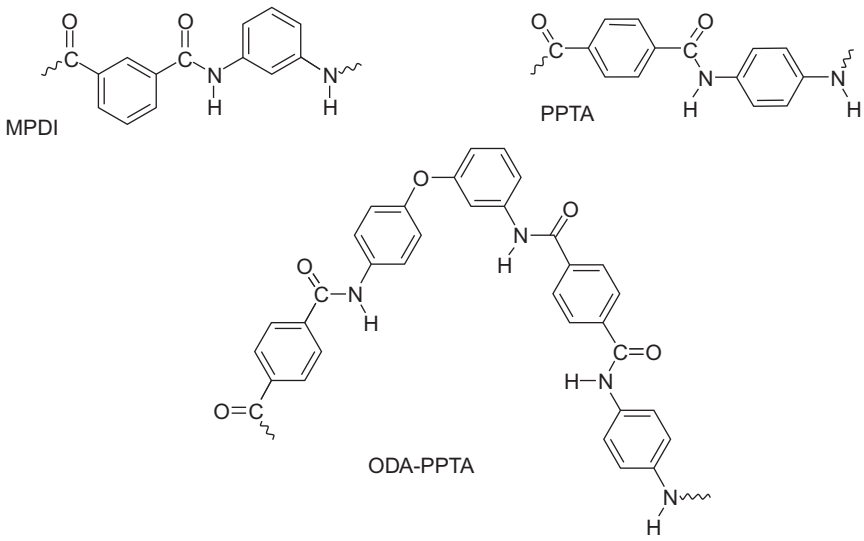

Fig. 7.1 Aramid polymers [6].

polyamides by melt polycondensation is not suitable for preparing high-molecular-weight aramids because of their very high melting point [7]. Therefore, PPTA molecule is synthesized from two monomers, 1,4-phenylenediamine (PPD) and terephthaloyl dichloride (TDC), using a complex solvent consisting of *N*-methyl-pyrrolidone (NMP) and $CaC1_2$ [8]. Production is made from monomers in three stages: polymerization, filament yarn spinning, and converting to staple and shortcut fiber or pulp.

MPDI aramid polymer is prepared most readily from the low-temperature polycondensation of *m*-phenylenediamine and isophthaloyl chloride in an amide solvent. Either dry- or wet-spinning method can be used to prepare MPDI fibers. According to the wet-spinning method, polymer solution is extruded through capillary holes into a coagulation bath, followed by staged washing, drawing, and drying [9].

In the production of aramid copolymer, Technora (by Teijin), three monomers, terephthalic acid, *p*-phenylenediamine (PDA), and 3,4-diaminodiphenyl ether, are used. The ether monomer provides more flexibility to the backbone chain, which results in a fiber that has slightly better compressive properties than PPTA aramid fiber made via the liquid crystal route. An amide solvent with a small amount of salt (calcium chloride or lithium chloride) is used as a solvent [10].

7.2.2 Fiber formation and spinning

In spinning of aramid fibers, a dry-jet wet-spinning system is employed. The dry-jet wet-spinning process is quite different from the conventional wet-spinning process. In the wet-spinning process, the nozzle is immersed in the coagulant bath. In the dry-jet wet-spinning process, solution is extruded through the spinneret just above the coagulant bath (of water or dilute sulfuric acid) [11]; this allows further orientation of the

polymer in the solution before the polymer starts to coagulate, due to the streamlined flow induced by the spinneret. The spinneret capillary and air gap cause rotation and alignment of domains, resulting in highly crystalline and oriented as-spun fibers [12]. The anisotropy of the solutions of aramid and the existence of liquid crystals are indicative of the very high orientation and association of the polymer molecules, which accounts for the very high strength and modulus of the yarns [4].

7.3 Aramid fiber structure and properties

In poly(*p*-phenylene terephthalamide), there are very stiff polymer chains, and this is due to the bonding of rigid phenylene rings in the para position. The other advantage of PPTA is the presence of amide groups at regular intervals along the linear macromolecular backbone, and due to this, extensive hydrogen bonding in a lateral direction between adjacent chains is achieved [13]. The structure is anisotropic and gives higher strength and modulus in the fiber longitudinal direction than in the radial direction [14]. Weak hydrogen bonds in the transverse direction result in low shear moduli, poor transverse properties, and low compressive strength.

Table 7.1 gives the typical properties of commercial aramid fibers. Kevlar 49 is the dominant form used today in structural composites because of its higher modulus. Kevlar 29 is used in composites when higher toughness, damage tolerance, or ballistic stopping performance is desired [15]. There are also other newly developed products available to meet other engineering needs such as an ultrahigh-modulus fiber, Kevlar 149 by DuPont.

The tensile properties of meta-aramids are not as high as for para-aramid because of the metaoriented chain configuration of meta-aramid. The chain configuration of meta-aramid provides more textile-like physical properties and excellent thermal stability [16]. The extreme order of the polymer chains in para-aramid fibers confers even greater structural rigidity. The glass transition temperature, T_g, is raised to 340°C, and the polymer only begins to degrade at 550°C. Aramid fibers are inherently flame-resistant with a limiting oxygen index (LOI) value of 29 [3]. Meta-aramids have been found to be self-extinguishing when removed from the flame. On exposure to a flame, a meta-aramid fabric hardens, starts to melt, discolors, and chars thereby forming a protective coating. An outstanding characteristic is also low smoke generation on burning. They have moderate tenacity and low elasticity modulus but excellent resistance to heat; thermal degradation starts at 375°C [17].

Fiber creep (long-term failure of fibers at loads below their breaking strength) under tension is undesirable for some high-performance applications such as composites and advanced materials. Aramid fibers are prone to significant short-term creep even at modest temperatures; however, long-term creep is negligible. The fibers are also prone to stress rupture under prolonged loading but are much less sensitive to this mode of failure than are glass fibers. Finally, aramid fibers are degraded in strength by prolonged exposure to UV light, and this can be a serious concern with cables having exposed fibers, but it is not a significant problem for aramid polymer matrix composites because the fibers are protected by the resin matrix [18].

Table 7.1 Properties of aramid fibers [6]

Commercial name	Kevlar		Twaron		Technora	Teijinconex		Nomex
Polymer	PPTA		PPTA		ODA/PPTA	MPDI		MPDI
Fiber type	K-29	K-49	Std	HM	Std	Std	HT	430
Density (g/cm^3)	1.44	1.44	1.44	1.45	1.39	1.38	1.38	1.38
Strength (GPa)	2.9	3	2.9	2.9	3.4	0.61–0.68	0.73–0.86	0.59
Elongation (%)	3.6	2.4	3.6	2.5	4.6	35–45	20–30	31
Modulus (GPa)	71	112	70	110	72	7.9–9.8	11.6–12.1	11.5

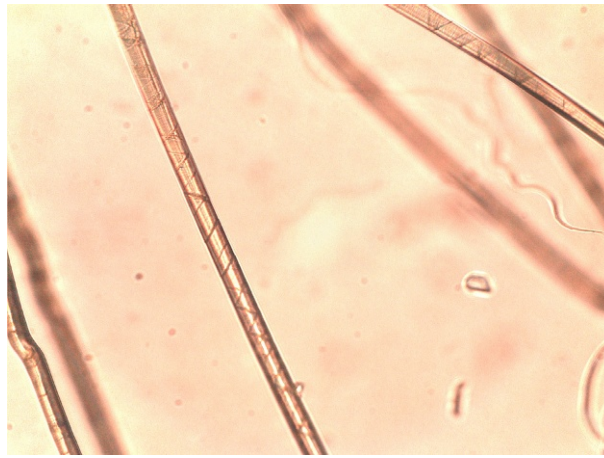

Fig. 7.2 Microscopic view of short staple para-aramid fiber.

Aramid fibers (Fig. 7.2) are characterized with low thermal conductivity resulting in high heat insulation and negative thermal expansion coefficient allowing to construct hybrid composite elements that do not change their dimensions under heating. Unlike inorganic fibers, aramid fibers have a high tendency to absorb moisture. For Kevlar 49, moisture absorption is around 4% at 60% relative humidity, while for Kevlar 149, it is around 1.5% [18,19]. They are chemically stable to nearly all treatments. Most organic liquid have little effect on them. However, strong acids, bases, and hypochlorite can cause degradation at elevated temperatures [2].

All high-strength organic fibers yield under compressive stress. This corresponds to the formation of structural defects known as kink bands (which appear to represent a shear failure across the fiber but in fact are caused by buckling of the individual elements of the fiber) [14]. However, this significant dislocation does not lead to major tensile strength loss. At a strain of 3%, the loss is only ~10%. This high degree of anisotropy of the para-aramids is reflected in fatigue properties. Tension-tension fatigue is very good. Compressive fatigue is not as good, especially at higher strains [20].

The aromatic nature of para-aramid is responsible for a substantial absorption of UV light, which, in turn, leads to a change of color due to oxidative reactions and drop in fiber properties [12]. Upon exposure, the yellow or gold fibers turn first orange and then brown, due to degradation. The degradation occurs only in the presence of oxygen and is not enhanced by either moisture or atmospheric contaminants [21].

Para-aramid fibers are self-screening, so light stability is dependent on the thickness of the exposed item. Very thin Kevlar 49 fabric, if exposed directly to very high intensity sunlight for an extended period, will lose about half its tensile strength within a few days. If the fabric is thicker, the majority is protected, and strength loss is minimized [22].

UV protection may also be effected simply by dense packing of the fiber itself, with or without a matrix.

Finishes—lubricants that aid in subsequent processing steps—are applied to aramid fibers for some applications. Available finishes are designed for such purposes as lubrication during weaving operations, improving abrasion resistance for cable applications, or better performance in rubber goods. If the fiber is to be used in a high-performance composite, however, the user will usually wish to avoid or remove any finish before impregnating the fiber with a matrix [21].

7.4 Fiber and product forms

The major fiber forms are continuous filament yarns, rovings, woven fabrics, short staple and spun yarns, fabrics, and pulp. Continuous filament yarns are preferred where very high mechanical properties are required, and staple fiber is used for textile applications. Aramid is also available as textured yam, needle-punched felts, spunlaced sheets, and wet-laid papers.

Para-aramid pulp is a highly fibrillated chopped fiber that can be used to reduce product brittleness, deliver product reinforcement and efficiency for applications such as friction products, sealing materials, and specialty paper products. Such products can be used to provide control in addition to the general reinforcement of resins such as epoxy [10]. Powder is used especially for applications such as rubber compounds, specialty coatings, and engineering plastics. Para-aramid fibers in paper form maintain strength, thermal and chemical stability, dimensional stability, resistance to abrasion, and excellent electric insulation for the paper market.

Continuous filament form of para-aramid fibers is generally woven into plain, twill, and satin weave fabric constructions. But they can also be knitted [23]. Para-aramid spun yarns (Fig. 7.3) that are the main source for protective clothing industry can be knitted or woven in various product forms [17,24].

As the aramid yarns and rovings are relatively flexible and nonbrittle, they can be processed in most conventional textile operations, such as twisting, braiding, weaving, knitting, carding, and felting. Yarns and rovings can be used in the filament winding, prepreg tape, and pultrusion processes. Fig. 7.4 shows some of these forms of aramid fiber.

Aramids are very tough fibers; they are somewhat difficult to cut, and their composites can be difficult to utilize. Special shears and other tools (Fig. 7.5) are available for cutting aramids [25].

Meta-aramid fibers can be found in chopped fiber, staple fiber, spun yarn, and fabric. They are especially used in heat- and flame-resistant solutions. While the meta-aramid fibers are not usually used as fiber reinforcements in composites, they are used extensively as reinforcements for honeycomb sandwich core materials. The use of such materials along with composite face sheet panels has greatly extended the overall usage of composite materials, particularly in the aerospace industry [26].

7.5 Applications

The properties of the aramid fibers make them suitable for many technical applications from ballistic protection and reinforced optical fiber cables to civil engineering products and applications in automotive.

Fig. 7.3 Ring spinning and weaving of para-aramid fibers.

7.5.1 Applications of meta-aramid fibers

Meta-aramid fibers have excellent thermal resistance, good textile-like properties and characteristics, but rather poor mechanical properties for high-performance fiber. The fibers from which these fabrics are made are inherently flame-resistant and do not melt or drip. A measure of the fiber's flammability is its LOI, which is the concentration of oxygen in air that is required to support combustion once the material is ignited. Materials with an LOI > 21 are considered nonflammable. The inherent flame resistance of meta- and para-aramids is essentially the same with LOI values of $\sim$28–29 [20]. For apparel applications, meta-aramids are generally preferred over para-aramids because the fabrics have a more comfortable, textile-like hand because of lower fiber modulus and higher elongation.

Fig. 7.4 Some product forms of aramids.

Fig. 7.5 Special shears and cutter for para-aramids.

Fabrics made up of meta-aramid fibers, are used in protective clothing of firemen, for gas and electric utility operatives, for worker of petroleum fuel, etc. They can also be used in transports, in seats and mattresses in public and private sectors and heat-exposed workplaces to protect people and products against fire risks. Fireproof doors in hotels and theaters can be made from them. Other applications include rubber reinforcement, filtration fabrics, sewing thread, paper makers, laundry, business machine felts, aircraft and other transportation upholstery, floor coverings, and contract furnishings for hospitals, day care centers, and nursing homes.

7.5.2 Applications of para-aramid fibers

Para-aramid fibers provide unique combinations of toughness, extra high tenacity, and modulus and exceptional thermal stability. Therefore, the end uses of para-aramid cover a broad range of technical applications. A summary of applications for aramids is given next.

7.5.2.1 Composites

Composites reinforced with para-aramid fibers have low density, high strength and specific modulus, good tensile fatigue properties, but low compressive strength and interlaminar shear strength and difficulty in cutting process [27,28]. It is generally difficult to obtain both good diametric tolerance and shredding-free surfaces for the composites reinforced with aramid fibers. To prevent shredding and surface delaminations for a clean hole, this type of composite structure is preloaded by tensile stress and cut by shear force [15].

The choice of resin system for use with aramid fibers is an important one. Epoxy resins give better translation of fiber properties than do polyesters, producing better shear strength and flexural properties but lower impact resistance. Vinyl ester resins give both good shear strength and impact resistance. Thermoplastic matrices are also

Fig. 7.6 Composite toe cap [30].

used, particularly in chopped fiber composites, because of their improved impact resistance over thermosets. However, for thermoplastics, the penetration of the resin into the fiber bundle and the quality of the fiber-matrix bond are almost always of concern [21].

There has been a focus on modifying aramid fibers for composite applications by altering the material's surface to achieve higher interfacial shear strength with the surrounding matrix when constructed into a composite. The most widely used methods being investigated are chemical and plasma surface treatments. The idea is if the interfacial shear strength increases between matrix and reinforcing material, the overall interfacial shear strength will increase. These modification techniques can achieve significantly higher interfacial shear strength and achieve higher mechanical strength properties [29].

The use of aramid composites can reduce the weight by 30% comparing with glass fiber composite materials. To reduce weight and improve economic efficiency, generally, aramid composites have been widely used in commercial aircraft and helicopters [5,25]. They also have found application in production of a composite toe cap (Fig. 7.6).

7.5.2.2 Protective clothing

Bulletproof vests, vehicle protection, flak jackets, helmets, nuclear shelters, cut protection, ballistics, heat-resistant workwear, flame-retardant textiles, protection panels, vehicle protection, strategic equipment shielding, gloves and sleeves for automotive, glass, steel and metal workers, chainsaw chaps and trousers for lumberjacks, and other apparel such as aprons and jackets.

Gloves of para-aramids offer exceptional cut resistance and can substantially reduce the risk of hand and finger injuries in glass- and metal-handling operations. Gloves (Fig. 7.7) are made primarily from spun yarns, although some are made from

Fig. 7.7 Knitted and woven para-aramid gloves.

textured filament yarns for applications where the tendency to form lint must be minimized. Gloves are made from 100% para-aramid yarns or from blends with other fibers, such as nylon or polyester, to reduce cost or to improve comfort or abrasion resistance. Some para-aramid gloves are coated or "dotted" with elastomers to enhance grip; others have leather sewn over the palms and fingers to provide puncture resistance or to increase abrasion resistance [31].

7.5.2.3 Ballistic protection

Aramids (Kevlar and Twaron) along with ultrahigh-molecular-weight polyethylenes (UHMWPE) (Dyneema and Spectra) and polyphenylene-2,6-benzobisoxazole (PBO and Zylon) are the most common fibers used for ballistic protection [32]. To meet the protection requirements for typical ballistic threats, approximately 20–50 layers of fabric are required [7]. The number of layers dictates the degree of protection. The ballistic performance of a woven fabric is dependent on the dynamic mechanical properties of constituent fibers and the fabric geometry (i.e., yarn linear density, type of weave, weave density, etc.). Usually, the ballistic fabric is densely woven square plain weave and basket weave. It has been observed that loosely woven fabrics and fabrics with unbalanced weaves result in inferior ballistic performance. The packing density of the weave, indexed by the "cover factor," is determined from the width and pitch of the warp and weft yarns and gives an indication of the percentage of area covered by the fabric. It is recognized that fabrics should possess cover factors from 0.6 to 0.95 to be effective when utilized in ballistic applications [33]. Knitting process could offer considerable advantages in terms of cost and production of the final design of a contoured armor, but it has not become successful probably because of the high degree of interlocking yarns and resultant fabric with too low an initial modulus [34].

Some other application areas are given in Table 7.2

Table 7.2 Other applications of aramid fibers [5, 21, 25, 35–37]

Applications	
Aircraft/aerospace	Panels, flooring, escape slides, pressure vessels, rocket motor cases, propeller and helicopter blades, parachutes, fairing, front wings, flap, rudder, stabilizer tip, tail cone, emergency export system, window frame, ceiling, bulkhead, door, luggage rack, seating, container of oxygen, nitrogen and helium, spacecraft cockpit, ventilation duct, etc.
Ropes and cables	Mooring lines, guy ropes, balloon tethers, oil rig risers, tensioner lines, pendant lines, optical fiber cables, ignition cables, electromechanical cables and fine gauge cables for electronic device applications such as mobile phone cables, computer power cords, USB cords, and MP3 earphone cables
Structural engineering	Pultruded beams, reinforcement for concrete, prestressing tendons, stay cables for bridges, curtain wall
Automotive	Car body panels, truck chassis beams, (hybrid with carbon fiber), brake linings, clutch facings, hoses and belts, belts in tires
Industrial	Conveyor belts, tarpaulins, chemical hoses, ventilation ducts, rotor vanes, high-grade printed circuit board (nonwoven aramid fabric impregnated with heat resistant epoxy resin)
Marine	Boat hulls, rigging, canoes, coated fabrics, sails
Sporting goods	Hockey sticks, tennis racquets, golf clubs, fishing rods, skis, sail clothes
Friction materials and gaskets	Brake linings, clutch facings, thixotropic additive
Medical applications	Prosthetics, fibrous bone cement
Tires	Truck and aircraft tires, high-speed tires, motorcycle tires, bicycle tires
Mechanical rubber goods	Conveyor belts, transmission belts, hydraulic hoses, hoses in off-shore, umbilicals

7.6 Conclusion

When Kwolek, the inventor of Kevlar at DuPont, was tasked with developing a synthetic material that might offer a lighter, more fuel-efficient alternative to metal reinforcements in automobile tires, she did not know that it would save thousands of lives [38]. Today, aramid fibers proved a range of technical applications by possessing a unique combination of high strength and modulus with low density where the strength-to-weight and stiffness-to-weight ratio is especially important. For the foreseeable future, the global demand for aramid fibers is expected to rise by about 7% annually [39], and aramid fiber manufacturers continue to expand their current production lines and create new product forms.

7.7 Sources of further information

7.7.1 Books

Research and commercial interest in application of aramid fibers in textiles and composites have increased. Many books are available, and a selection of journals can be viewed in the references for this chapter.

7.7.2 Journals

There are many journals with emphasis on fiber-reinforced polymer composites. A selection of journals can be viewed below; however, the list is not conclusive:

- Advanced Composite Materials
- Applied Composite Materials
- Composite Interfaces
- Composite Structures
- Composites Part A Applied Science and Manufacturing
- Composites Part B Engineering
- Composites Science and Technology
- International Journal of Polymer Science
- Journal of Applied Polymer Science
- Journal of Composites
- Journal of Composites for Construction
- Journal of Composite Materials
- Journal of Reinforced Plastics and Composites
- Plastics, Rubber and Composites
- Polymer Composites
- Polymers and Polymer Composites
- Progress in Polymer Science

7.7.3 Web sites

In the following, some addresses are compiled that will hopefully provide the reader with some additional interesting information and news:

http://www.dupont.com
http://www.teijin.com
http://www.compositesworld.com/
http://composite.about.com/
http://ipscience.thomsonreuters.com/
http://netcomposites.com/
http://www.mse.gatech.edu/
http://www.cmh17.org/
http://www.acmanet.org/
http://www.asc-composites.org/links.htm
https://compositesuk.co.uk/

http://www.nccuk.com/
http://www.jeccomposites.com/
http://www.jpscm.com/
http://www.acmanet.org/
http://www.materialstoday.com/reinforced-plastics/
http://www.wwcomposites.com/
http://compositesmanufacturingmagazine.com/
http://www.imperial.ac.uk/polymer-and-composite-engineering/
http://www.metyx.com/

References

[1] Pohl G, editor. Textiles, polymers and composites for buildings. Cornwall: Elsevier; 2010. p. 75.
[2] Maher RR, Wardman RH. The chemistry of textile fibres. Cambridge: Royal Society of Chemistry; 2015. p. 206, 228.
[3] Mouritz AP, Gibson AG. Fire properties of polymer composite materials, vol. 143. Dordrecht: Springer Science & Business Media; 2007. p. 45.
[4] Wootton DB. Rapra Technology Ltd. Staff. The application of textiles in rubber. Shawbury, Shrewsbury: Rapra Technology; 2001. p. 28.
[5] Hearle JW, editor. High-performance fibres. Cambridge: Elsevier; 2001. p. 25, 50, 55.
[6] Ertekin M. An investigation on the performance properties of woven fabrics produced with technical rigid-core spun yarns [Unpublished PhD thesis]. Ege University Engineering Faculty, Department of Textile Engineering; 2013.
[7] Bhattacharyya D, Fakirov S, editors. Synthetic polymer-polymer composites. Germany: Carl Hanser Verlag GmbH Co KG; 2012. p. 253, 274.
[8] Eichhorn SJ, Hearle JWS, Jaffe M, Kikutani T. Handbook of textile fibre structure, Volume 1: Fundamentals and manufactured polymer fibres. Cambridge: Elsevier; 2009. p. 395.
[9] Kelly A, Zweben CH. Comprehensive composite materials. Cambridge: Elsevier; 2000. p. 11.
[10] Chawla K. Fibrous materials. Cambridge: Cambridge University Press; 2016. p. 87, 88.
[11] Blades H, Du Pont. Dry jet wet spinning process. U.S. Patent 3,767,756; 1973.
[12] Jassal M, Ghosh S. Aramid fibres—an overview. Indian J Fibre Text Res 2002; 27(3):290–306.
[13] Afshari M, Sikkema DJ, Lee K, Bogle M. High performance fibers based on rigid and flexible polymers. Polym Rev 2008;48(2):230–74.
[14] Chang KK. Aramid fibers; 2016. Available from: https://polycomp.mse.iastate.edu/files/2012/01/3-Aramid-Fibers.pdf [accessed 29.09.16].
[15] Akovalı G, editor. Handbook of composite fabrication. iSmithers Rapra Publishing; 2001. p. 40, 71.
[16] Gunnarsson M, Nyman J. Short fibre reinforced elastomers [Unpublished Master thesis]. Lund Institute of Technology, Department of Production and Materials Engineering; 1998.
[17] Ertekin M, Kırtay E. Burning behaviour and mechanical properties of fabrics woven with ring spun aramid and flame retardant polyester yarns. J Text Apparel/Tekstil ve Konfeksiyon 2014;24(3):259–65.

[18] Baker A, Dutton S, Kelly D. Composite materials for aircraft structures. Reston, VA: American Institute of Aeronautics and Astronautics (AIAA), Inc.; 2004. p. 71.
[19] Vasiliev VV, Morozov E. Mechanics and analysis of composite materials. Oxford: Elsevier; 2001. p. 12.
[20] Lewin M, editor. Handbook of fiber chemistry. USA: CRC Press; 2007. p. 984, 1013.
[21] Clements LL. Organic fibers. In: Handbook of composites. California: Springer; 1998. p. 202–241, 215, 222.
[22] Annis PA, editor. Understanding and improving the durability of textiles. Cambridge: Elsevier; 2012. p. 110.
[23] Ertekin G, Oğlakcıoğlu N, Marmaralı A. High tenacity weft knitted fabrics for protective garments. In: 46th IFKT Congress, Romania; 2012.
[24] Ertekin M, Kırtay HE. Tensile properties of some technical core spun yarns developed for protective textiles. J Text Apparel/Tekstil ve Konfeksiyon 2015;25(2):104–10.
[25] Wang RM, Zheng SR, Zheng YG. Polymer matrix composites and technology. Cambridge: Elsevier; 2011. p. 83–84.
[26] Lightweight, Flame and Corrosion Resistant Solutions for Global Aerospace Industry; 2016. Available from: http://www.dupont.com/products-and-services/fabrics-fibers-nonwovens/fibers/brands/nomex-for-aerospace.html [accessed 26.09.16].
[27] Biron M. Thermosets and composites. Oxford: Elsevier; 2003. p. 90.
[28] Coffey A. Understanding the effect of stress on fibres. Res Matters (Issue) 2007;5.
[29] Langston TB. The mechanical behavior of air textured aramid yarns in thermoset composites [Published M.Sc. Thesis]. North Carolina State University; 2004. p. 7.
[30] Erden S, Ertekin M, Karavana HA, Seydibeyoğlu MÖ. Development of a composite overshoe protector for occupational safety, 114 M469 TÜBİTAK-1005 Project; 2016.
[31] Ertekin M, Kirtay HE. Cut resistance of hybrid para-aramid fabrics for protective gloves. J Text Inst 2015;1–8.
[32] Mahoney PF, Ryan J, Brooks AJ, Schwab CW, editors. Ballistic trauma: a practical guide. USA: Springer Science & Business Media; 2005. p. 73.
[33] Scott RA, editor. Textiles for protection. Cambridge: Elsevier; 2005. p. 536.
[34] Horrocks AR, Anand SC, editors. Handbook of technical textiles. Cambridge: Elsevier; 2000. p. 465.
[35] Alagirusamy R, Das A, editors. Technical textile yarns. Cambridge: Elsevier; 2010. p. 378.
[36] Rebouillat S, Steffenino B, Miret-Casas A. Aramid, steel, and glass: characterization via cut performance testing, of composite knitted fabrics and their constituent yarns, with a review of the art. J Mater Sci 2010;45(19):5378–92.
[37] Callister WD, Rethwisch DG. Materials science and engineering: an introduction, vol. 7. New York: Wiley; 2007. pp. 665–715, 649.
[38] Langer E. Stephanie Kwolek dies at 90; chemist created Kevlar fiber used in bullet-resistant gear. Available from: https://www.washingtonpost.com/national/stephanie-kwolek-dies-at-90-chemist-created-kevlar-fiber-used-in-bullet-resistant-gear/2014/06/20/9b5b4634-f883-11e3-a606-946fd632f9f1_story.html [accessed 29.09.16].
[39] Aramid fibers, 2016. Available from: http://www.teijin.com/ir/library/annual_report/pdf/ar_10_06.pdf [accessed 29.09.16].

This page intentionally left blank

Basalt fibers

8

Volkan Acar[*], *Ferit Cakir*[†], *Elif Alyamaç*[‡], *M.Özgür Seydibeyoğlu*[‡]
*Ataturk University, Erzurum, Turkey, [†]University of California, Berkeley, CA, United States, [‡]Izmir Katip Çelebi University, Izmir, Turkey

8.1 Introduction to basalt fibers

Among many other reinforcing fibers, basalt fiber has been the least studied fiber, especially in the area of polymer composites. The history of basalt fiber dates back to 1923 [1] (US Patent 1,462,446), and it was further improved during World War II. The United States and the Soviet Union investigated basalt fiber, especially for aerospace and military purposes, during the cold war. Investigations were conducted on the insulating and raw material properties of basalt fibers for the textile industry [2]. Unfortunately, basalt fibers could not be widely used for civilian applications due to the political issues in the world during that period. However, after 1995, basalt fibers were produced and used on a commercial scale due to declassification. After 2000, basalt fiber applications and scientific research have been gradually increased. Today, the basalt fiber industry is improving day by day, developing technology in composite research and applications. Basalt fiber is considered as a viable alternative to traditional glass fiber by the composite industry. Therefore, many manufacturers and suppliers around the world are interested in basalt fiber, but with unlimited basalt reserves, Russia plays a key role in basalt technology.

Basalt fibers are obtained from basalt rocks and can be considered as bio-based fibers because they are produced from natural resources, which is very critical for new-generation materials. Having better physicomechanical properties than glass fiber but being significantly cheaper than carbon fiber, basalt fiber has been used for many different composite applications. Besides effective individual use in composites, basalt fiber is also a good choice for hybrid composites due to its structural properties. Currently, hybrid composites can be seen as an interesting example of basalt fiber use in new composite structures. Traditional fibers have been commonly used together as reinforcing components in interply and intraply hybrid composites. Recently, basalt fibers have begun to be used in hybrid composites with other fibers. In a traditional carbon/glass hybrid composite, carbon fiber is the dominant load-bearing component of the structure. However, glass fiber is cheaper than carbon fiber. This composite is an optimized structure with multiple advantages in terms of costs and mechanical properties when considered as an individual composite part. When basalt fiber is evaluated for use in a hybrid composite, the strength of basalt fiber can be seen as a disadvantage compared with carbon fiber, but it generally has better strength than glass fiber. Otherwise, basalt fiber is cheaper than carbon fiber but at nearly the same price as glass fiber. Thus, it can be used as a reinforcement material instead of glass

Fiber Technology for Fiber-Reinforced Composites. http://dx.doi.org/10.1016/B978-0-08-101871-2.00008-4

fiber in hybrid composites because of its superior structural properties and similar costs. For all those reasons, basalt fiber is a promising material and a good alternative for composite manufacturers.

8.2 Preparation of basalt fibers

Basalt rocks are obtained from volcanic magma that is solidified in the open air after flowing as a hot fluid. Basalt fibers, which consist of plagioclase, pyroxene, and olivine minerals, are obtained by spinning basalt rocks under certain conditions. The general composition of basalt rocks is given in Fig. 8.1. As seen in this figure, the dominant chemical compounds are SiO_2 at 52.8%, Al_2O_3 at 17.5%, Fe_2O_3 at 10.3%, and CaO at 8.59% [3,4].

Basalt fiber manufacturing technology is remarkably simple. The basic method for production of basalt fiber is a melt-blowing technique such as the Junkers method. In this technique, basalt rocks are melted and poured into a rotating cylinder mechanism, and air jets are used to blow fiber off. In this way, fibers are shaped by means of blowing air and then being rapidly solidified. Basalt fibers produced by the Junkers method are low cost and have poor mechanical properties. Short basalt fibers can be easily manufactured at a low cost using this method. The production of continuous basalt fibers shows some similarities to glass fibers. Such fibers are produced by spinning melted basalt stones from a spinneret from 1350°C to 1420°C. Spun filament bundles of between 1.0 and 1.2 m are taken downward below the spinneret at between 2000 and 5000 m/min and then spooled. The general procedure for continuous basalt fiber production is shown in Fig. 8.2 [4].

After spinning, the fibers are generally woven to form composite structures. The woven fabrics of basalt (a) and carbon (b) fibers and also strands of carbon (c) and

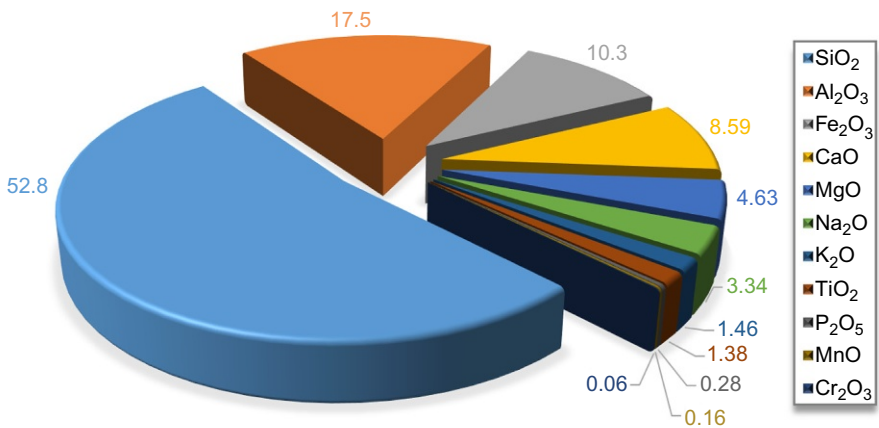

Fig. 8.1 Chemical compositions of basalt.
Reproduced from Dhand V, Mittal G, Rhee KY, Park S, Hui D. A short review on basalt fiber reinforced polymer composites. Compos Part B: Eng 2015;73:166–180. http://dx.doi.org/10.1016/j.compositesb.2014.12.011.

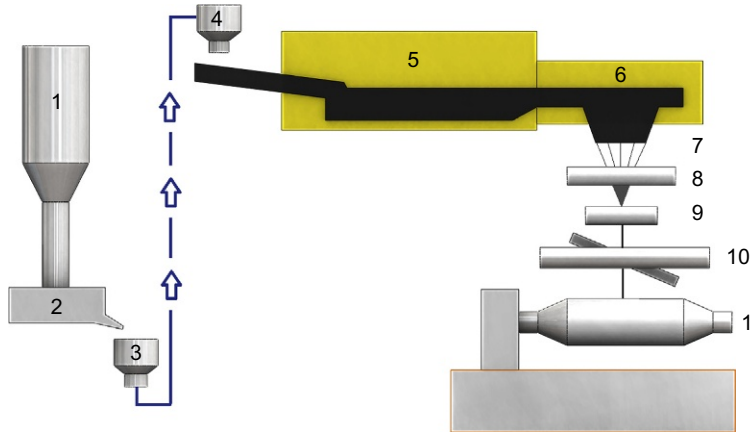

Fig. 8.2 Basalt fiber manufacturing procedure illustrates the following steps, (1) crushed stone silo, (2) loading station, (3) transport system, (4) batch charging station, (5) initial melt zone, (6) secondary heat zone with precise temperature control, (7) filament-forming bushings, (8) sizing applicator, (9) strand formation station, (10) fiber tensioning station, and (11) automated winding station.
Reproduced from Deák T, Czigány T. Chemical composition and mechanical properties of basalt and glass fibers: a comparison. Text Res J 2009;79(7):645–51. http://dx.doi.org/10.1177/0040517508095597.

basalt (d) fibers are all shown in Fig. 8.3. Basalt fibers are quite novel in the area of composite application. Due to its resistance to high temperature, basalt fiber is generally used for high-temperature applications such as flame-retardant materials, disk brakes, and heat-insulation applications.

8.3 Structural properties

Basalt fibers exhibit significant structural properties such as high strength, good modulus, and improved strain to failure and high-temperature resistance [3,5]. Besides these promising properties, basalt fibers can be used for specific materials because it is noncombustible. Moreover, basalt fibers show high thermal stability and good chemical resistance; it is nontoxic and has relatively low costs. Thus, basalt fiber is an effective alternative to glass fiber in the field [5]. Where mechanical properties are not crucial but the cost is critical, it is an effective alternative to carbon fiber. Mechanical and physical properties of four popular reinforcing fibers used in the composite industry are compared in Table 8.1.

As shown in Table 8.1, basalt fibers not only have good mechanical properties but also can be applied across a wider temperature range, withstanding heating up to 700°C. That can be a key point for the material selection process, especially for the aerospace industry. Materials with high thermal stability play a significant role in high-temperature conditions. In a study conducted by Hao and Yu [7], a thermal gravimetric analysis was performed to obtain the mass loss occurred over a temperature

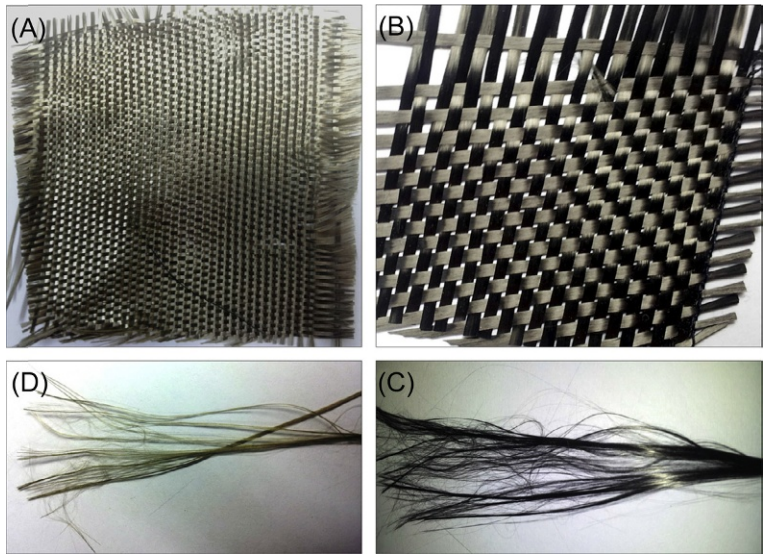

Fig. 8.3 Woven fabrics, (A) basalt fiber fabric, (B) carbon fiber fabric, (C) strands of carbon fiber, and (D) strands of basalt fiber.
Reproduced with permission from Dhand V, Mittal G, Rhee KY, Park S, Hui D. A short review on basalt fiber reinforced polymer composites. Compos Part B 2015;73:166–80. http://dx.doi.org/10.1016/j.compositesb.2014.12.011.

Table 8.1 Comparison of mechanical with physical properties of fibers [6]

Properties	Continuous basal fiber	Glass fiber (E-glass)	Glass fiber (S-glass)	Carbon fiber
Breaking strength (MPa)	3000–4840	3100–3800	4020–4650	3500–6000
Modulus of elasticity (GPa)	79.3–93.1	72.5–75.5	83–86	230–600
Breaking extension (%)	3.1	4.7	5.3	1.5–2.0
Fiber diameter (μm)	6–21	6–21	6–21	5–15
Linear density (tex)	60–4200	40–4200	40–4200	60–2400
Temperature withstand (°C)	−260…+700	−50…+380	−50…+300	−50…+700

range of between 200°C and 350°C for basalt and glass fibers. The analysis showed that basalt fiber has better thermal stability than glass fiber (Fig. 8.4).

Environmental conditions, such as being subjected to chemical attack, are also critical for materials. In 1981, Ramachandran et al. [8] studied the chemical durability of basalt fibers and reported that basalt fibers have perfect chemical resistance to alkaline attack but show poor resistance to acids. In addition, due to their good electric insulating properties, basalt fibers have been used in printed circuit boards [9]. Carmisciano et al. [10] conducted a study on the electric and interlaminar properties of basalt and glass fiber-reinforced, vinyl ester composites. The study showed similar measurements for the frequency dependence of the dielectric constant and the

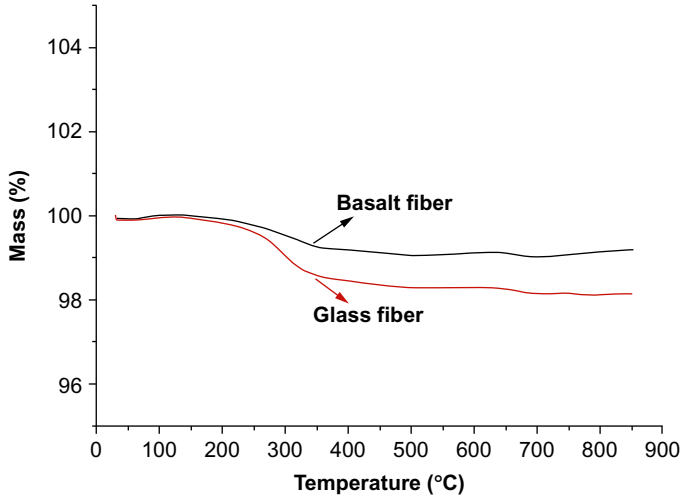

Fig. 8.4 TGA curves for basalt and glass fibers.
Reproduced with permission from Hao LC, Yu WD. Evaluation of thermal protective performance of basalt fiber nonwoven fabrics. J Therm Anal Calorim 2009;100(2):551–5. http://dx.doi.org/10.1007/s10973-009-0179-0.

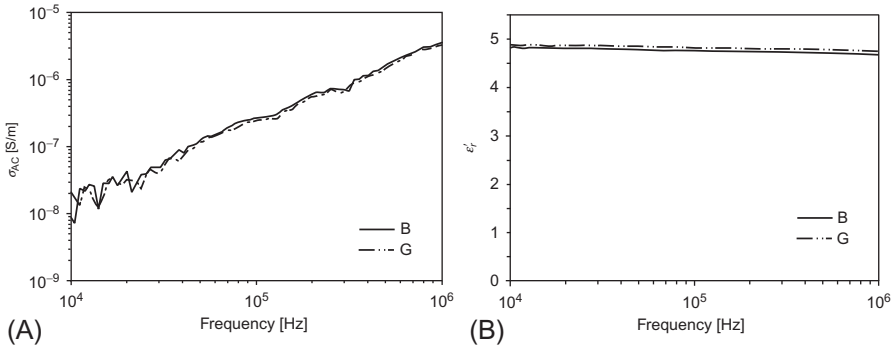

Fig. 8.5 (A) Frequency dependence of dielectric constant and (B) frequency dependence of ac conductivity for basalt (B) and glass (G) fiber-reinforced composites.
Reproduced with permission from Carmisciano S, Rosa IM, Sarasini F, Tamburrano A, Valente M. Basalt woven fiber reinforced vinylester composites: flexural and electrical properties. Mater Des 2011; 32(1):337–42. http://dx.doi.org/10.1016/j.matdes.2010.06.042.

effective conductivity of basalt and glass fiber composites. The results also confirmed the potential of basalt fiber in electronic applications (Fig. 8.5A and B).

8.4 Basalt fiber-reinforced composites

Basalt fibers have been used together with various thermoset and thermoplastic resins by several researchers in the past years, aimed at determining the effect of basalt fiber on a wide range of research areas. In one of the remarkable studies in research

literature, Park and Subramanian [11] studied the effect of a silane coupling agent on the interfacial properties of basalt fiber-reinforced epoxy composites in 1991. Czigány et al. [12] investigated basalt fiber-reinforced polypropylene composites using Junkers production technology. Another in-depth study by Czigány [13] focused on the mechanical properties of polypropylene reinforced with basalt, glass, carbon, and hemp fibers and also their basalt hybrid composites. The fibers were subjected to a surface treatment with a reaction mixture of maleic acid anhydride and sunflower oil in order to obtain good interfacial adhesion. A significant improvement on the mechanical properties of fiber-reinforced polypropylene composites was reported in each case compared with those of pristine polypropylene samples. Overall, the study showed the efficient hybridization of basalt fiber with other conventional fibers to give sufficient mechanical properties at relatively low cost.

Further research on the mechanical characterization of basalt fiber-reinforced composites was carried out by Liu et al. [14]. They investigated the mechanical sufficiency of basalt fiber for transportation applications via both experimental and statistical methods. The results showed a similar mechanical performance for basalt fiber with fiberglass. Next, Liu et al. investigated the aging behavior of basalt fiber composites used in transportation [15]. The tolerance of basalt fiber-reinforced epoxy composites immersed in brine was analyzed, along with moisture absorption, temperature, and moisture cycling. Based on the results, 240 days of aging in brine or water resulted in a significant decrease in Young's modulus and reduced tensile strength of the basalt composites.

The effect of fiber content on the mechanical properties was investigated by Öztürk [16]. Flexural, tensile, and impact strengths were all determined for basalt, hemp, and hemp/basalt fiber-reinforced phenol formaldehyde composites. The study showed an increased tensile strength for basalt fiber-reinforced composites with the fiber volume content up to a specific value but a reduced flexural strength with increased fiber content. In another study [17], the effect of a partial pyrolysis process—including simple curing at 250°C up to the treatment by total pyrolysis at a final temperature of 1000°C—on the mechanical properties of basalt fiber composites was investigated. The composite treated with partial pyrolysis at 650°C exhibited the highest flexural strength and a superior fracture resistance at room temperature. The composite pyrolyzed at 750°C was also reported to be more suitable for high-temperature applications due to its slower degradation.

The basalt fiber studies also considered nanoenhancement. Chen et al. [18] studied functionalized multiwalled carbon nanotubes (MWCNT)-modified and basalt fiber-reinforced epoxy composites. In the work performed by Wei et al. [19], coatings made from epoxy via the sol-gel method and SiO_2-based epoxy were synthesized in order to apply them to basalt fibers. It was reported that the hybrid coating formed on the surface of the fiber led to increased surface roughness and increased tensile strength in multifilament yarn.

Basalt fiber has been used in hybrid composite research because of its potential for good mechanical and thermal properties and relatively low costs. Researchers studied effects based on this potential by using it with traditional fibers in hybrid composite structures. Using this concept, Wang et al. [20] studied the low-velocity impact

behavior of interply and intraply hybrid basalt/aramid composites. Results showed that interply hybrid composites exhibited higher ductility, higher specific energy absorption, and lower peak load than intraply hybrids. The failure modes were also researched in order to examine the energy absorption capabilities of the hybrid composites. The results showed that whereas interply hybrids failed layer by layer with larger energy absorption, the failure in intraply hybrids reacted in a brittle way with lower energy absorption. Fiber hybridization offers multiple advances by delivering good combinations of properties in the structure.

In a study by Dehkordi et al. [21], basalt and nylon fibers were used in an intraply hybrid woven with different compositions. The low-velocity impact behavior of the hybrids and the homogeneous composites was investigated to determine parameters such as maximum force and deflection and total absorbed energy. It was reported that the impact behavior was significantly affected by the basalt/nylon fiber content. Thus, it is understood that the composition of fibers is a crucial parameter in terms of mechanical performance.

By contrast to the structural properties of hybrid composites, a cost optimization for the compositions is also critical work for large-scale industrial designs and applications. Currently, basalt fibers offer sufficient structural properties and low costs that make them a suitable hybridization fiber component. Other research literature includes articles that include basalt fiber hybridization with other fibers in intraply and interply hybrid forms [22–26].

8.5 Surface treatments of basalt fibers

As discussed in the previous section, the interface—or interphase—plays the most critical role in composite materials, and thus, the surface modification of the fiber and polymer is of great importance for the composite performance. In the context of this book, the surface modification of the fibers will be explained in-depth. In the glass fiber and carbon fiber chapters, it was explained that there has been tremendous research into modification of fibers. Since the discovery of glass fiber in 1937, there have been many important studies on the surface modification of glass. Also, as carbon fiber technology has been developing since the 1960s, there have been in-depth studies on the functionality in and the compatibility of carbon fiber for use in various polymer matrices. This area is studied by the fiber manufacturing companies in big research groups to manufacture state-of-the-art fibers that are much better in comparison with many other competing companies. Besides industrial research, this area is thoroughly studied by academia, as there are lots of material science challenges that have to be solved, and especially with the increased capability of characterization tools such as tensiometers, electron microscopes, and surface chemical analysis, this area has been investigated by many respected scientists. Furthermore, the recent, fast-growing nanotechnology area offers many new opportunities for these fiber technologies because the interface is greatly affected by nanoparticles like carbon nanotubes, graphene, and other nanostructures.

For glass fiber and carbon fiber, a polymeric emulsion called *sizing* has been used for many decades. This is where the fibers are passed through a water-based emulsion

tank, and the emulsion is dried in appropriate furnaces that enable the vaporization of the water on the surface. Sizing formulations have been trade secrets for a long time, and the details of these emulsions are still difficult to find in academic literature. Besides sizing, various surface modification techniques such as silane coupling agents, titanate coupling agents, and urethane coatings have been studied in-depth, especially for glass fiber.

At the beginning of the chapter, it was stated that basalt fibers have been commercially used since 1995, and it is quite new compared with conventional fibers like glass fiber (1937) and carbon fiber (1957), and thus, the surface modification of basalt fibers is quite new, and the studies are very limited.

Historically, maleic anhydride grafting appears to be the first surface modification of basalt fiber seen in literature to improve polypropylene composite performance. Two studies were conducted by Botev et al. [27] and Matkó et al. [28]. Botev et al. were the first to study the interfacial properties of basalt composites. While Matkó et al. studied maleic anhydride grafting on polypropylene, Bashtannik et al. [29] studied hydrochloric acid (HCl) and sodium hydroxide (NaOH) modifications to polyethylene matrices during the same time period, around 2003. Matkó et al. observed every minute changes in the impact fracture and tensile strength values. Bashtannik et al. showed that the adhesive forces were improved via these conventional and chemical modifications.

Literature on glass fiber shows that silane coupling agents have been used for basalt fiber composites with thermosetting polymer blends such as vinyl ester and epoxy. Czigány et al. [30] studied two different silane coupling agents with epoxy and vinyl functional groups. Depending on the polymer blend ratio, the performance of types of silane coupling agents differs. With suitable silane coupling agents, tensile strength and bending strength can be improved up to 50%. This study once more shows the importance of silane coupling agents. Although there are very many publications on silane treatment of various fibers and minerals in composites, there is only one study on basalt fibers, which shows that there is much to do in this area.

As the technologies for plasma physics have developed, awareness of their influence in the area of composites has also increased. Historically, Wang et al. [31] were the first group that published a plasma treatment for basalt fiber in 2007. They did not conduct composite tests; instead, they studied the fiber properties based on plasma modification. They used nonthermal plasma for the basalt fiber, and the effect of the plasma is shown in Fig. 8.6. The roughness was improved, but the mechanical performance of the fiber was reduced.

Kim et al. [32] studied oxygen plasma treatment on basalt fiber composites. They desized the basalt fiber and then used oxygen plasma for a specific time. They observed an increase in the wettability and an improvement in the mechanical performance by 16%. They investigated the contact angle of fibers, which was significantly different, and uniquely, they also performed energy release rates for the basalt fiber composites.

Kurniawan et al. [33] studied atmospheric glow-discharge plasma for basalt fiber-reinforced polylactic acid. This study was conducted with silane-treated fibers. They optimized irradiation time at 4.5 min, and they improved the tensile strength by 45% and the modulus value by 18%.

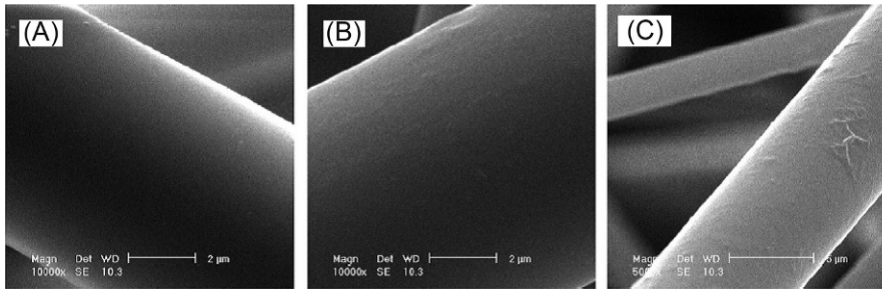

Fig. 8.6 The morphologies of different treatment time by plasma (A, 1 min; B, 3 min; and C, 10 min).
Reproduced with permission from Wang G, Liu Y, Guo Y, Zhang Z, Xu M, Yang Z. Surface modification and characterizations of basalt fibers with non-thermal plasma. Surf Coat Technol 2007;201(15):6565–8. http://dx.doi.org/10.1016/j.surfcoat.2006.09.069.

With new characterization tools in the area of nanotechnology, nanoparticles have become very critical for composite materials. The role of nanoparticles is addressed as a separate chapter in this book, but it still has influences on the basalt fiber composites as well. Chen et al. [18] were the first group that investigated the effect of nanoparticles on basalt fiber composites. They used multiwall carbon nanotubes to reinforce the basalt composites. The interphase region was significantly improved with an 8.72% increase in tensile strength and a 31.65% increase in the modulus value. They further investigated the results with micromechanical modeling.

During the same period in 2011, two important papers by Wei et al. [34] appeared on nanoenhanced basalt composites that use nanosize SiO_2. In the first study, they successfully demonstrated that the interlaminar shear strength (ILSS) values were increased with a silane coating on the basalt fiber. This increase was further improved with nanosize SiO_2 particles. The composite performance and ILSS values were improved one step further with silane coupling of the nanosize SiO_2. In the second study by Wei et al. [19], the percentage of the nanoparticles was optimized at 5%. These two studies provided very important results for composite materials research and for the composite industry.

A final study on nanoenhanced basalt composites was conducted by Ary Subagia et al. [35]. They utilized the semiprecious mineral tourmaline at the micron- and nano-scale level for basalt-epoxy composites. They improved the tensile strength value by 16% and the tensile modulus by 27%.

8.6 Applications of basalt fiber

Basalt fiber is a unique and natural material based on its high mechanical strength, high resistance to wear, impact and corrosion performance, good thermal endurance, light weight, relatively low cost, and eco-friendly nature. Therefore, basalt fibers and their derivatives have a wide range of engineering applications because of a proved high-performance level and desirable characteristics. Several researchers have mentioned the applications of composite materials based on basalt fibers so far [36,37].

Currently, it is one of the mostly preferred and frequently used materials in the aerospace and automotive industry, civil engineering, the chemical and petrochemical industry, manufacturing engineering, and the power engineering and electric industry.

8.6.1 Aerospace and automotive industry

In the aerospace and automotive industries, the competitive advantage of basalt fibers comes from properties like noise damping, acoustic absorption, high specific strength, and good ductility [38]. The use of basalt fiber in aircrafts and automobiles helps to reduce the undesired noise generated externally and by engines, and basalt fibers may be used as acoustic proofing in the aerospace industry. In addition, they are used in the manufacturing of aeronautical machines thanks to their frictional, chemical, and heat resistance. Moreover, basalt fibers are increasingly used in the automotive industry for production of car headliners, compressed natural gas (CNG) cylinders, brake pads, and clutch facings (Fig. 8.7) [36]. Basalt fibers also offer several benefits for use as fillers for car mufflers—having good sound-insulating properties and good resistance to thermal cycling. Hence, basalt products are extensively preferred in the aerospace and automotive industry.

8.6.2 Civil engineering

Composite materials such as fiber-reinforced polymer (FRP), glass FRP (GFRP), and carbon FRP (CFRP) have been used in the construction industry for three decades. Many construction codes and standards focus on the use of composite structures developed in the construction industry. By comparison with FRP, GFRP, and CFRP, the use of basalt fibers in construction applications is relatively new. However, the use of basalt fibers has greatly increased in civil engineering, and it has recently gained wide acceptance in the construction industry. Currently, many different construction materials based on basalt fibers—which might be an alternative to traditional construction materials—have been developed, and these innovative materials such as

Fig. 8.7 Basalt fiber-based CNG cylinder and ring specimens.
Reproduced with permission from Pavlovski D, Mislavsky B, Antonov A. CNG cylinder manufacturers test basalt fibre. Reinf Plast 2007;51(4):36–7. 39.

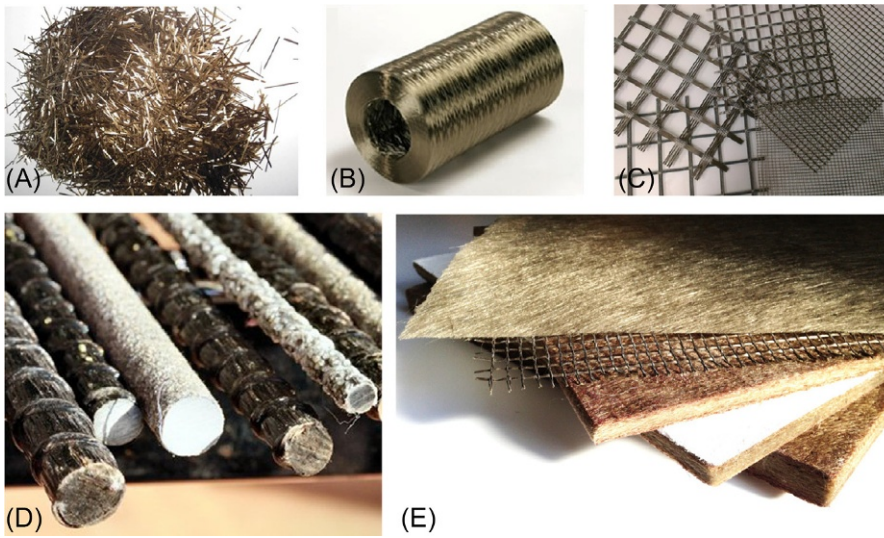

Fig. 8.8 Basalt-based materials, (A) chopped fibers, (B) roving, (C) grids, (D) rebars, and (E) insulating panels, net, and veil.
Reproduced with permission from Moretti E, Belloni E, Agosti F. Innovative mineral fiber insulation panels for buildings: thermal and acoustic characterization. Appl Energy 2016;169:421–32. http://dx.doi.org/10.1016/j.apenergy.2016.02.048.

rebars, laminates, panels, grids, chopped fibers, veils, and plates have delivered beneficial solutions in civil engineering applications (Fig. 8.8).

The experimental results from previous literature show that basalt rebars have the potential to replace steel in reinforced concrete structures wherever a corrosion problem exists because of the noncorrosive behavior of basalt rebars [41–44]. In addition, chopped basalt fibers might be used as a strengthening material for existing conventional building materials, such as concrete and mortar. Chopped fibers in concrete or mortar are effective additives that enhance the structural and mechanical performance of these materials [45,46]. Chopped basalt fibers are incorporated into concrete or mortar to improve certain material properties. By comparison with plain concrete, the mechanical properties of the chopped basalt fiber reinforcement increased with the addition of basalt fibers [46]. Furthermore, SEM images show a good bond is obtained between chopped basalt fibers and concrete (Fig. 8.9).

In addition to the rebars and chopped fibers, as an internal- and external-strengthening building material, basalt fiber-based laminates, panels, and plates have been widely used in existing structures to increase their load capacity and construction life. In the most common uses, masonry and concrete structures are fully or partially wrapped with continuous basalt laminates (Fig. 8.10) [47,49]. Furthermore, basalt fiber-based panels and laminates have been used as thermal and acoustic insulation in buildings, and they are successfully used in structures where corrosion has damaged the steel reinforcement and concrete due to environmental impacts.

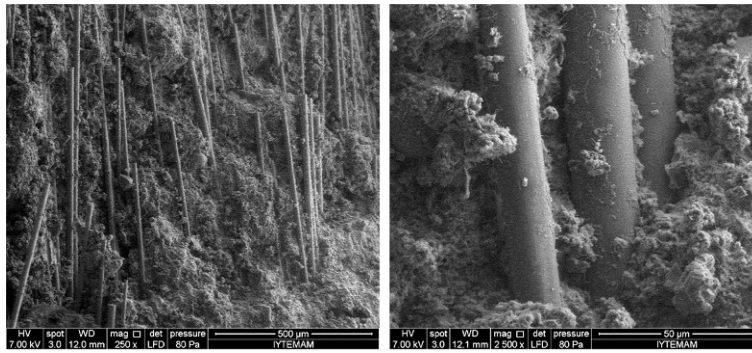

Fig. 8.9 SEM images of basalt fiber-reinforced concrete.

Fig. 8.10 External strengthening of the structures with basalt-based materials. Reproduced with permission from Campione G, La Mendola L, Monaco A, Valenza A, Fiore V. Behavior in compression of concrete cylinders externally wrapped with basalt fibers. Compos Part B 2015;69:576–86. http://dx.doi.org/10.1016/j.compositesb.2014.10.008; Marcari G, Basili M, Vestroni F. Experimental investigation of tuff masonry panels reinforced with surface bonded basalt textile-reinforced mortar. Compos Part B 2017;108:131–42. http://dx.doi.org/10.1016/j.compositesb.2016.09.094.

8.6.3 Chemical and petrochemical industry

Basalt fibers have high chemical and thermal stability and have effective thermal-, electric-, and sound-insulating properties. Thanks to their proved properties, basalt fibers are widely used in the chemical and petrochemical industry. Basalt fiber-based equipment such as tanks or pipes are among the most convenient materials for on-site transportation, collection, and storage of corrosive liquids and gases like hydrogen sulfide, acids, and alkali chemicals because of their resistance to corrosion and aggressive chemical compounds [3–5]. Basalt-based pipes may be used to transfer petroleum, oil, gas products, hot and cold water, aggressive liquids and loose materials from the reservoir to the end user. Moreover, basalt-based pipes are effective in the conveyance and storage of radioactive nuclear materials because of their

radiation-resistant properties. Since basalt fibers produce no chemical reactions in contact with other chemicals, they are widely used in many different applications such as hosing and crop watering, gas tubes, hydrocarbon pipelines, land drainage, and construction. The low thermal conductivity of basalt fibers helps to minimize unwanted deposition inside the pipes [50].

8.6.4 Manufacturing engineering

Basalt fibers have many advantages such as light weight, design flexibility, and relatively low cost. Moreover, basalt fibers are extremely strong and durable, which makes them ideal materials for manufacturing engineering. Due to their superior properties, basalt fibers have major applications in manufacturing engineering as well. Potential applications of basalt fibers in manufacturing engineering are widespread, ranging from small to large consumer products. During the past decades, basalt fibers have become commercially productive manufacturing materials with an increasing market potential. The use of basalt has the potential to reduce costs in industrial applications, and basalt fibers will undoubtedly constitute a greater portion of the total material market. In particular, they are industrially used for many different products, such as lightweight car and bicycle frames, motorcycle parts, golf clubs, skis, furniture, snowboards, containers, fishing rods, and sporting goods.

8.6.5 Power engineering and electrical industry

In power engineering, basalt fibers are used to produce wind turbine blades and lampposts due to their corrosion-resistant properties [50–53]. Moreover, basalt fibers are widely preferred in specialty power products because of their electric- and heat-insulating properties. Basalt, which has a good thermal conductivity and significant resistance to fire, allows woven tapes to be used for manufacturing fireproof power cables. Basalt fibers might be included on printed circuit boards (PCBs) providing special properties in comparison with ordinary components made of fiberglass. Basalt fibers are additionally used as a part of other electrospecialized applications, for example, in additional fireproof protection for electric links and underground conduits. There are other benefits in using basalt-based materials, including the disposal phases and its maintenance during the consequent portion of the postclosure phase.

8.7 Conclusion

As discussed in detail, basalt fibers are promising materials for the composite industry due to their low cost and superior structural properties. However, the most important characteristic of this material is its natural origin, which makes it eco-friendly. One of the most strategic perspectives is the amount of this natural resource. In some reports, it is stated that there are unlimited reserves of basalt rocks.

As technology develops more and more in the areas of composites and materials science, the need for basalt fiber will increase exponentially. The most important application will be its use in aerospace structures, which includes civil/military aircrafts and

also space shuttles that can carry a high loading with high-temperature resistance at an affordable price. Further studies conducted on the interface of the basalt fibers should make the composites much better. There is very good potential for military and health care applications, but these have not yet been realized. Besides these potential and current applications, basalt fiber research by researchers around the world is continuing to increase. The outstanding thermal properties, in particular, attract attention from high-tech engineering research concerned with thermal effects. Also, the structural properties of basalt fiber are being improved with sizing treatments, which is extremely important work leading to the production of superior basalt fibers. On the other hand, there are still many different polymers yet to be used as a matrix material and many traditional fibers to be used as a hybrid couple in hybrid composites.

References

[1] Tipping crucible for basalt furnaces. U.S. Patent Number, US1462446 A; 1923.
[2] Czigany T. Discontinuous basalt fiber-reinforced hybrid composites. In: Friedrich K, Fakirov S, Zhang Z, editors. Polymer composites: from nano- to macro-scale. London: Springer Science+Business Media; 2005. p. 309–28. http://dx.doi.org/10.1007/0-387-26213-X_17. ISBN: 978-0-387-24176-0 (Print) 978-0-387-26213-0.
[3] Dhand V, Mittal G, Rhee KY, Park S, Hui D. A short review on basalt fiber reinforced polymer composites. Compos Part B 2015;73:166–80. http://dx.doi.org/10.1016/j.compositesb.2014.12.011.
[4] Deák T, Czigány T. Chemical composition and mechanical properties of basalt and glass fibers: a comparison. Text Res J 2009;79(7):645–51. http://dx.doi.org/10.1177/0040517508095597.
[5] Fiore V, Scalici T, Bella GD, Valenza A. A review on basalt fibre and its composites. Compos Part B 2015;74:74–94. http://dx.doi.org/10.1016/j.compositesb.2014.12.034.
[6] Singha K. A short review on basalt fiber. Int J Text Sci 2012;1(4):19–28. http://dx.doi.org/10.5923/j.textile.20120104.02.
[7] Hao LC, Yu WD. Evaluation of thermal protective performance of basalt fiber nonwoven fabrics. J Therm Anal Calorim 2009;100(2):551–5. http://dx.doi.org/10.1007/s10973-009-0179-0.
[8] Ramachandran BE, Velpari V, Balasubramanian N. Chemical durability studies on basalt fibres. J Mater Sci 1981;16(12):3393–7. http://dx.doi.org/10.1007/bf00586301.
[9] Fiore V, Bella GD, Valenza A. Glass-basalt/epoxy hybrid composites for marine applications. Mater Des 2011;32(4):2091–9. http://dx.doi.org/10.1016/j.matdes.2010.11.043.
[10] Carmisciano S, Rosa IM, Sarasini F, Tamburrano A, Valente M. Basalt woven fiber reinforced vinylester composites: flexural and electrical properties. Mater Des 2011;32(1):337–42. http://dx.doi.org/10.1016/j.matdes.2010.06.042.
[11] Park J, Subramanian R. Interfacial shear strength and durability improvement by monomeric and polymeric silanes in basalt fiber/epoxy single-filament composite specimens. J Adhes Sci Technol 1991;5(6):459–77. http://dx.doi.org/10.1163/156856191x00602.
[12] Czigány T, Vad J, Pölöskei K. Basalt fiber as a reinforcement of polymer composites. Periodica Polytechnica ser Mech Eng 2005;49(1):3–14.
[13] Czigány T. Special manufacturing and characteristics of basalt fiber reinforced hybrid polypropylene composites: mechanical properties and acoustic emission study. Compos Sci Technol 2006;66(16):3210–20. http://dx.doi.org/10.1016/j.compscitech.2005.07.007.

[14] Liu Q, Shaw MT, Parnas RS, Mcdonnell A. Investigation of basalt fiber composite mechanical properties for applications in transportation. Polym Compos 2005; 27(1):41–8. http://dx.doi.org/10.1002/pc.20162.
[15] Liu Q, Shaw MT, Parnas RS, Mcdonnell A. Investigation of basalt fiber composite aging behavior for applications in transportation. Polym Compos 2006;27(5):475–83. http://dx.doi.org/10.1002/pc.20215.
[16] Öztürk S. The effect of fibre content on the mechanical properties of hemp and basalt fibre reinforced phenol formaldehyde composites. J Mater Sci 2005;40(17):4585–92. http://dx.doi.org/10.1007/s10853-005-1103-z.
[17] Černý M, Glogar P, Sucharda Z, Chlup Z, Kotek J. Partially pyrolyzed composites with basalt fibres—mechanical properties at laboratory and elevated temperatures. Compos A: Appl Sci Manuf 2009;40(10):1650–9. http://dx.doi.org/10.1016/j.compositesa.2009.08.002.
[18] Chen W, Shen H, Auad ML, Huang C, Nutt S. Basalt fiber-epoxy laminates with functionalized multi-walled carbon nanotubes. Compos A: Appl Sci Manuf 2009;40 (8):1082–9. http://dx.doi.org/10.1016/j.compositesa.2009.04.027.
[19] Wei B, Song S, Cao H. Strengthening of basalt fibers with nano-SiO_2-epoxy composite coating. Mater Des 2011;32(8–9):4180–6. http://dx.doi.org/10.1016/j.matdes.2011.04.041.
[20] Wang X, Hu B, Feng Y, Liang F, Mo J, Xiong J, et al. Low velocity impact properties of 3D woven basalt/aramid hybrid composites. Compos Sci Technol 2008;68(2):444–50. http://dx.doi.org/10.1016/j.compscitech.2007.06.016.
[21] Dehkordi MT, Nosraty H, Shokrieh MM, Minak G, Ghelli D. Low velocity impact properties of intra-ply hybrid composites based on basalt and nylon woven fabrics. Mater Des 2010;31(8):3835–44. http://dx.doi.org/10.1016/j.matdes.2010.03.033.
[22] Czigány T. Basalt fiber reinforced hybrid polymer composites. Mater Sci Forum 2005;473–474:59–66. http://dx.doi.org/10.4028/www.scientific.net/msf.473-474.59.
[23] Sarasini F, Tirillò J, Ferrante L, Valente M, Valente T, Lampani L, et al. Drop-weight impact behaviour of woven hybrid basalt-carbon/epoxy composites. Compos Part B 2014;59:204–20. http://dx.doi.org/10.1016/j.compositesb.2013.12.006.
[24] Subagia IA, Kim Y, Tijing LD, Kim CS, Shon HK. Effect of stacking sequence on the flexural properties of hybrid composites reinforced with carbon and basalt fibers. Compos Part B 2014;58:251–8. http://dx.doi.org/10.1016/j.compositesb.2013.10.027.
[25] Sarasini F, Tirillò J, Valente M, Ferrante L, Cioffi S, Iannace S, et al. Hybrid composites based on aramid and basalt woven fabrics: impact damage modes and residual flexural properties. Mater Des 2013;49:290–302. http://dx.doi.org/10.1016/j.matdes.2013.01.010.
[26] Dehkordi MT, Nosraty H, Shokrieh MM, Minak G, Ghelli D. The influence of hybridization on impact damage behavior and residual compression strength of intraply basalt/nylon hybrid composites. Mater Des 2013;43:283–90. http://dx.doi.org/10.1016/j.matdes.2012.07.005.
[27] Botev M, Betchev H, Bikiaris D, Panayiotou C. Mechanical properties and viscoelastic behavior of basalt fiber-reinforced polypropylene. J Appl Polym Sci 1999;74 (3):523–31. http://dx.doi.org/10.1002/(sici)1097-4628(19991017)74:33.0.co;2-r.
[28] Matkó S, Anna P, Marosi G, Szép A, Keszei S, Czigány T, et al. Use of reactive surfactants in basalt fiber reinforced polypropylene composites. Macromol Symp 2003;202 (1):255–68. http://dx.doi.org/10.1002/masy.200351222.
[29] Bashtannik PI, Kabak AI, Yakovchuk YY. The effect of adhesion interaction on the mechanical properties of thermoplastic basalt plastics. Mech Compos Mater 2003;39:85. http://dx.doi.org/10.1023/A:1022943823622.

[30] Czigány T, Deák T, Tamás P. Discontinuous basalt and glass fiber reinforced PP composites from textile prefabricates: effects of interfacial modification on the mechanical performance. Compos Interfaces 2008;15(7–9):697–707. http://dx.doi.org/10.1163/156855408786778302.
[31] Wang G, Liu Y, Guo Y, Zhang Z, Xu M, Yang Z. Surface modification and characterizations of basalt fibers with non-thermal plasma. Surf Coat Technol 2007;201(15):6565–8. http://dx.doi.org/10.1016/j.surfcoat.2006.09.069.
[32] Kim M, Kim M, Rhee K, Park S. Study on an oxygen plasma treatment of a basalt fiber and its effect on the interlaminar fracture property of basalt/epoxy woven composites. Compos Part B 2011;42(3):499–504. http://dx.doi.org/10.1016/j.compositesb.2010.12.001.
[33] Kurniawan D, Kim BS, Lee HY, Lim JY. Atmospheric pressure glow discharge plasma polymerization for surface treatment on sized basalt fiber/polylactic acid composites. Compos Part B 2012;43(3):1010–4. http://dx.doi.org/10.1016/j.compositesb.2011.11.007.
[34] Wei B, Cao H, Song S. Surface modification and characterization of basalt fibers with hybrid sizings. Compos A: Appl Sci Manuf 2011;42(1):22–9. http://dx.doi.org/10.1016/j.compositesa.2010.09.010.
[35] Subagia IA, Tijing LD, Kim Y, Kim CS, Iv FP, Shon HK. Mechanical performance of multiscale basalt fiber-epoxy laminates containing tourmaline micro/nano particles. Compos Part B 2014;58:611–7. http://dx.doi.org/10.1016/j.compositesb.2013.10.034.
[36] Jamshaid H, Mishra R. A green material from rock: basalt fiber—a review. J Text Inst 2015;107(7):923–37. http://dx.doi.org/10.1080/00405000.2015.1071940.
[37] Dalinkevich AA, Gumargalieva KZ, Marakhovsky SS, Soukhanov AV. Modern basalt fibrous materials and basalt fiber-based polymeric composites. J Nat Fibers 2009;6(3):248–71. http://dx.doi.org/10.1080/15440470903123173.
[38] Saravanan D. Spinning the rocks—basalt fibers. J Inst Eng (India) Text Eng Div 2006;86:39–45.
[39] Pavlovski D, Mislavsky B, Antonov A. CNG cylinder manufacturers test basalt fibre. Reinf Plast 2007;51(4):36–7. 39.
[40] Moretti E, Belloni E, Agosti F. Innovative mineral fiber insulation panels for buildings: thermal and acoustic characterization. Appl Energy 2016;169:421–32. http://dx.doi.org/10.1016/j.apenergy.2016.02.048.
[41] Fan X, Zhang M. Experimental study on flexural behaviour of inorganic polymer concrete beams reinforced with basalt rebar. Compos Part B 2016;93:174–83. http://dx.doi.org/10.1016/j.compositesb.2016.03.021.
[42] Lapko A, Urbański M. Experimental and theoretical analysis of deflections of concrete beams reinforced with basalt rebar. Arch Civ Mech Eng 2015;15(1):223–30. http://dx.doi.org/10.1016/j.acme.2014.03.008.
[43] Hassan M, Benmokrane B, ElSafty A, Fam A. Bond durability of basalt-fiber-reinforced-polymer (BFRP) bars embedded in concrete in aggressive environments. Compos Part B 2016;106:262–72. http://dx.doi.org/10.1061/(ASCE)CC.1943-5614.0000270.
[44] Elgabbas F, Vincent P, Ahmed EA, Benmokrane B. Experimental testing of basalt-fiber-reinforced polymer bars in concrete beams. Compos Part B 2016;91:205–18. http://dx.doi.org/10.1016/j.compositesb.2016.01.045.
[45] Zych T, Wojciech K. Brittle matrix composites: study on the properties of cement mortars with basalt fibres. Cambridge: Woodhead Publishing Ltd.; 2012.
[46] Jiang C, Fan K, Wu F, Chen D. Experimental study on the mechanical properties and microstructure of chopped basalt fibre reinforced concrete. Mater Des 2014;58:187–93. http://dx.doi.org/10.1016/j.matdes.2014.01.056.

[47] Campione G, La Mendola L, Monaco A, Valenza A, Fiore V. Behavior in compression of concrete cylinders externally wrapped with basalt fibers. Compos Part B 2015;69:576–86. http://dx.doi.org/10.1016/j.compositesb.2014.10.008.
[48] Marcari G, Basili M, Vestroni F. Experimental investigation of tuff masonry panels reinforced with surface bonded basalt textile-reinforced mortar. Compos Part B 2017;108:131–42. http://dx.doi.org/10.1016/j.compositesb.2016.09.094.
[49] Di Ludovico M, Prota A, Manfredi G. Structural upgrade using basalt fibers for concrete confinement. J Compos Constr 2010;14(5):541–52. http://dx.doi.org/10.1061/(ASCE)CC.1943-5614.0000114.
[50] van de Velde K, Kiekens P, van Langenhove L. Basalt fibres as reinforcement for composites, In: Proceedings of 10th international conference on composites/nano engineering, University of New Orleans, New Orleans, LO; 2003. p. 20–6.
[51] Wei B, Cao H, Song S. Tensile behavior contrast of basalt and glass fibers after chemical treatment. Mater Des 2010;31(9):4244–50. http://dx.doi.org/10.1016/j.matdes.2010.04.009.
[52] Kumbhar VP. An overview: basalt rock fibers—new construction material. Acta Eng Intl 2014;2(1):11–8.
[53] Thorhallsson ER. In: Basalt fibers, advanced materials for various applications, NordMin, information Day and Brokerage Event in Copenhagen, 13 November 2013; 2013.

This page intentionally left blank

Ceramic fibers

9

*Emre Yalamaç**, *Mucahit Sutcu*†, *Suat Bahar Basturk**
*Manisa Celal Bayar University, Manisa, Turkey, †Izmir Katip Çelebi University, Izmir, Turkey

9.1 Introduction

This chapter mainly focuses on the type of ceramic fibers, fabrication methods used to make ceramic fibers, and their application areas. Oxide and nonoxide ceramic fibers are being used as reinforcement materials for composites due to their unique properties of high elastic modulus and high-temperature durability. Their properties make them valuable to use in automotive, aerospace, and heat-resistant structural applications. Ceramic fibers are found in two forms, continuous (long length) and discontinuous (short length). Alumina- and silicate-based continuous oxide fibers are made by sol-gel process but short oxide fibers by melt-spinning route. On the other hand, silicon- and boron-based nonoxide ceramic fibers are currently being developed and produced by thermal conversion of polymer precursor process.

Metal matrix composites (MMCs) are generally reinforced with fibers having diameters >100 μm, in order to withstand thermal degradation in processes such as hot pressing (HP) and reactivity with the alloy matrix [1]. These fibers are processed by chemical vapor deposition (CVD) method. On the other hand, ceramic fibers are also used in ceramic matrix to make complex-shaped parts. In this case, ceramic matrix composites (CMCs) are generally used ceramic fibers with diameters <20 μm processed by precursor route. Therefore, these fine fibers can be woven [1].

9.2 Oxide fibers

Ceramic oxide fibers that are in the form of long length and short length have been commercially available since the 1970s. These fibers that mostly consist of alumina (Al_2O_3) and alumina-silica (Al_2O_3-SiO_2) mixtures due to their high melting points are generally used for high-temperature applications. During the last decade, these oxide fibers have an increasing interest for aerospace and power engineering applications because of their high corrosion resistance in corrosive atmospheres together with comparatively low costs [2–5]. Moreover, they are preferred in engineering applications due to their microstructural stability, good mechanical strength, and long-term creep performance at higher temperatures [6–8]. These superior properties result from the presence of crystalline phases such as alumina, mullite, yttria-doped alumina, and zirconia [3,7]. In this section, the physical properties of these oxide fibers will be reviewed.

Ceramic oxide fibers are used both as insulation and as reinforcement material. The mostly known examples for oxide ceramic fibers are composed of oxides such as silica (SiO_2), mullite ($3Al_2O_3{\cdot}2SiO_2$), alumina (Al_2O_3), and zirconia (ZrO_2) having

Fiber Technology for Fiber-Reinforced Composites. http://dx.doi.org/10.1016/B978-0-08-101871-2.00009-6

different characteristic properties. Their application areas depend on their melting points and maximum use temperatures. For example, silica-based glass fibers with a big sales market are not used at temperatures above 250°C. On the other hand, alumina-based fibers have been previously used as refractory insulation, up to 1600°C; however, they are also currently preferred as reinforcements for use up to and above 1000°C in the MMCs [3]. In general, oxide-based ceramic fibers have poor thermal and electric conduction properties and higher thermal expansion coefficients than nonoxide ceramic fibers. These fibers are generally used as high-temperature insulation materials due to their superior insulating properties. Oxide fiber materials have low thermal conductivities, excellent thermal-shock resistance, good electric resistivity, and acoustic properties. Furthermore, they are generally more dense than nonoxide ceramic fibers, while their density is relatively low as compared with metals [4].

Recently, different methods such as slurry spinning, sol-gel spinning, and single-crystal growth have been developed for manufacturing of oxide-based ceramic fibers [8]. The sol-gel spinning method is adopted for the production of oxide fibers that have high melting point [3]. Various aluminum precursors such as aluminum chloride, aluminum formoacetate, and aluminum nitroformoacetate can be used together with silica sols for the fabrication of alumina-based fibers. In order to adjust a suitable rheology for a good spinnability, different polymer-spinning aids such as poly(ethylene oxide), poly(vinylalcohol), and poly(vinylpyrrolidone) are added. This mixture is spun into green fibers and then dried and sintered at higher temperatures to obtain ceramic fibers [9].

Alumina (Al_2O_3)-based fibers are the most common of oxide fibers. These fibers exhibit excellent thermal, mechanical, and electric properties such as high-temperature strength, high thermal-shock and creep resistance, high dimensional stability, low thermal expansion coefficient, and good dielectric properties. In addition, alumina-based fibers are preferred because of their good chemical stability in oxidizing and reducing atmospheres up to 1000°C at high temperatures [8]. Alumina-based fibers find a wide application area from rocket boosters and race cars to industrial furnaces and fuel cells. These fibers are used in such varied applications as seals and gaskets, electric insulation, and composite reinforcement, as well as heat, flame, and impact shielding for aircraft and spacecraft [10]. The commercial ceramic fiber products used for high-temperature applications and structural reinforcement for composites are shown in Fig. 9.1.

Alumina-based fibers are often used as structural reinforcements in a variety of metal, ceramic, and polymer composites, making them stiffer and stronger [11,12]. They are suitable for load-bearing applications; resulting composites withstand higher temperatures than metals.

An important application of the alumina-based fibers is the usage as high-temperature insulating material in the form of blankets, mat, and textiles for fire protection, seals, and other heat-resistant components with a combination of low thermal conductivity, thermal-shock resistance, and electric resistance at high temperatures [13,14]. For thermal insulation, alumina fibers exhibit important advantages as compared with aluminosilicate fibers.

Comparison of the properties of some commercial alumina-based fibers is presented in Table 9.1. According to the table, fibers with high Al_2O_3 content have higher

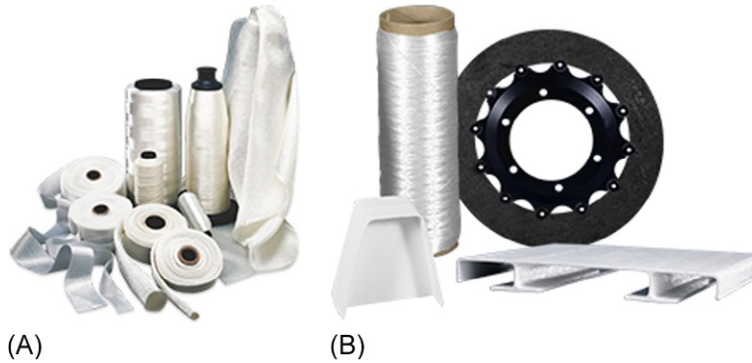

Fig. 9.1 Examples of 3M Nextel ceramic fiber products, (A) high-temperature applications and (B) structural reinforcement for composites [10].
Reproduced with permission from 3M Company.

elastic modulus. The addition of small amounts of silica to alumina increases its ability to be processed into fibers [2]. Therefore, aluminosilicate fibers are less expensive than alumina fibers. Some properties are significantly affected with the addition of silica. SiO_2-containing alumina fibers have greater tensile strength, but their elastic modulus values are lower.

Fiber FP with diameter of 20 μm, which is 99.9% α-Al_2O_3, is produced by slurry-spinning process. In the slurry process, alumina particles are dispersed in an aqueous suspension that contains aluminum chloride, organic polymers, and other additives. The aluminum chloride is polymerized into a viscous mix and spun into fibers [2,8]. The fibers are calcined around 800°C to remove the organics and finally sintered at temperatures up to 1800°C to obtain the polycrystalline alpha-phase alumina. Almax fiber process is similar to that of Fiber FP. Also, PRD-166 fiber that contains 85% Al_2O_3 and 15% ZrO_2 is produced by slurry process. The tensile strength of PRD-166 fiber with diameter of 20 μm is higher than that of Fiber FP [8]. Saphikon sapphire fiber is developed by single-crystal growth technique from a melt through a die. The currently available fiber diameter is between 70 and 250 μm [2].

In addition, commercial alumina-based fibers are produced by sol-gel spinning [15–17]. In the solution or sol-gel spinning process, firstly, fiber precursor solution is prepared and concentrated to remove excess solvent, and then, a viscous spin paste is obtained. Then, continuous fibers are extruded by spinning and pyrolysis to remove organic matter and then heat-treated above 800°C to crystallize and sintered the fibers [3].

A commercial fiber (Altex, Sumitomo) has been developed by solution process from organoaluminum compounds. This process involves a polyaluminoxane dissolved in an organic solvent combined with a silicon-containing compound to prepare a viscous spinning mix. These fibers are made by calcining green fibers spun from polyaluminoxane solutions [18].

The sol-gel spinning process has been also used to manufacture 3M Nextel fibers that contain Al_2O_3, SiO_2, and B_2O_3. Nextel ceramic fibers are manufactured from

Table 9.1 Properties of some commercial alumina-based fibers [2,5,7,8]

Fiber trade name	Manufacturer	Composition (wt%)	Diameter (μm)	Density (g/cm^3)	Tensile strength/elastic modulus (MPa/GPa)	Manufacturing process
Fiber FP	Du Pont	Al_2O_3, >99%	20	3.9	1400/380	Slurry spinning
Almax	Mitsui	Al_2O_3, >99.5%	10	3.6	1800/320	Slurry spinning
Saphikon	Saphikon	Al_2O_3, 100%	70–250	3.8	3100/380	Single-crystal growth
Nextel 610	3M	Al_2O_3, >99%	10–12	3.9	3100/380	Sol-gel spinning
Saffil RF	ICI	Al_2O_3, 95% SiO_2, 5%	1–5	3.3	2000/300	Solution spinning
Nextel 720	3M	Al_2O_3, 85% SiO_2, 15%	10–12	3.4	2100/260	Sol-gel spinning
Altex	Sumitomo	Al_2O_3, 85% SiO_2, 15%	9–17	3.2	1800/210	Sol-gel spinning
Nextel 550	3M	Al_2O_3, 73% SiO_2, 27%	10–12	3.03	2000/193	Sol-gel spinning
Nextel 312	3M	Al_2O_3, 62% SiO_2, 24% B_2O_3, 14%	10–12	2.7	1700/150	Sol-gel spinning
Nextel 440	3M	Al_2O_3, 70% SiO_2, 28% B_2O_3, 2%	10–12	3.05	2000/190	Sol-gel spinning
Nextel 650	3M	Al_2O_3, 89% ZrO_2, 10% Y_2O_3, 1%	10–12	4.1	2550/358	Sol-gel spinning
PRD-166	Du Pont	Al_2O_3, 85% ZrO_2, 15%	20	4.2	2070/380	Slurry spinning

continuous oxide composite grade fibers designed for load-bearing structural applications in metal, ceramic, and polymer matrices. Nextel fibers are spun, dried, and then sintered at high temperatures. 3M Nextel fibers with diameter of 10–12 μm have fine-grain size and smooth surface. The Nextel fibers contain different crystal phases after firing due to their chemical compositions given in Table 9.1. For example, Nextel 312 fibers are composed of 62% Al_2O_3, 24% SiO_2, and 14% B_2O_3, and their crystal phases are mullite and amorphous, or some of the fibers are amorphous [2]. The crystal content of Nextel 440 fibers is γ-alumina, mullite, and amorphous silica [2,8]. Most commercial fibers that contain silica or amorphous phases are detrimental to creep performance because they are viscous at high temperatures.

Nextel 610 and 720 fibers have crystal structures based on α-alumina and α-alumina/mullite, respectively. Nextel 610 fibers have higher strength at room temperature than Nextel 720 fibers. The strength of 610 type fibers having single phase decreases more than 720 at lower temperature due to grain growth of 610 fibers. Nextel 720 fibers are made from an α-alumina with silica added to have better strength retention at higher temperature due to reduced grain boundary sliding [19,20]. Fig. 9.2 indicates the cross section of the Nextel 720 fiber with a diameter of 12.5 μm. The Nextel 720 fibers based on alumina and mullite are commercial fibers with the most promising creep properties. Nextel 720 fiber has higher creep resistance than Nextel 610 due to the presence of the mullite phase [19].

Another commercial alumina-based fiber that is Nextel 650 was developed as composite reinforcement for high-temperature applications. Nextel 650 oxide fibers contain α-alumina and cubic zirconia phases [21]. Addition of ZrO_2 is used to decrease

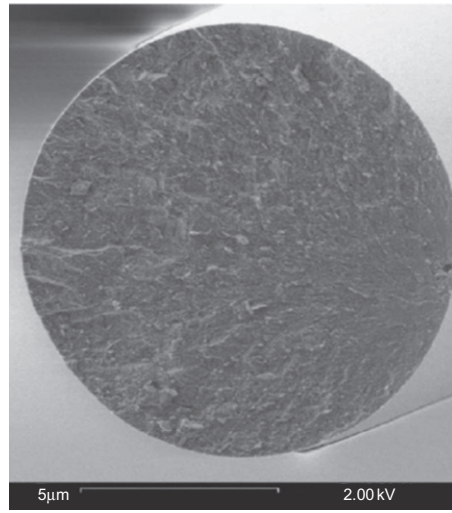

Fig. 9.2 Cross section of the Nextel 720 fiber.
From Deléglise F, Berger M, Bunsell A. Microstructural evolution under load and high temperature deformation mechanisms of a mullite/alumina fibre. J Eur Ceram Soc 2002;22:1501–12. http://dx.doi.org/10.1016/S0955-2219(01)00461-7.

grain growth; Y_2O_3 is added to reduce creep rate. Their creep rate is 10–100 times lower than that of Nextel 610 oxide fibers [21,22]. This indicates a development in high-temperature creep properties proportional to Nextel 610 fibers due to the reduced grain boundary diffusivity by the dopants [5]. Recently, some researchers prepared polycrystalline zirconia-toughened alumina fibers from aqueous solutions of aluminum hydroxide chloride 2.5-hydrate and zirconium oxychloride octahydrate via dry spinning, calcination, and then sintering processes. These ceramic fibers with diameter of 10 μm had an average tensile strength of 1010 MPa [6].

9.3 Nonoxide fibers

Production of nonoxide fibers is difficult due to their high melting points and resistance to densification. Oxidation resistance tends to be their main deficiency. For these fibers, extensive research has been conducted and reported in terms of processing, microstructure, mechanical, and thermal stability. These ceramic fibers are either fine or thick diameter [2].

9.3.1 Silicon carbide based fibers

Silicon carbide (SiC) fibers have an excellent combination of high strength, modulus, and thermal stability, including good oxidation resistance and mechanical properties (compressive-tensile strength) at high temperatures. Also they are able to display high creep resistance and good oxidation resistance. Although strength and modulus properties of the fibers show some deterioration at temperature above 1200°C, they can withstand temperatures up to 1800°C even under oxidizing conditions [8].

Silicon carbide based fibers are generally applied as continuous fiber in ceramic matrix. This type of CMCs is used in hot section of engines for power, etc.

Two different commercial continuous SiC fiber production methods exist: (1) substrate-based fibers by coating SiC on either a tungsten or a carbon monofilament by CVD and (2) spinning and heat treating chemically derived polymer-based precursors. In the first process, fine columnar-grained SiC is vapor deposited from methyltrichlorosilane (CH_3SiCl_3) on a small-diameter (∼30 μm) carbon filament (SiC-C fiber) or on small filament (∼13 μm) of tungsten (SiC-W fiber) in the temperature range of 1200–1400°C. The final SiC fibers produced via CVD currently display diameters greater than 100 μm. In the second process, fine ceramic fibers are based on SiC with small diameters (<15 μm), and in the form of continuous length, multifiber tows are produced by the pyrolysis of a polycarbosilane (PCS) precursor. Fig. 9.3A shows CVD-derived SiC fiber that is made of β-SiC layer deposited on a 33 μm carbon filament and is supplied as monofilament with diameter of 142 μm (SCS-6 and SCS-Ultra, Specialty Materials). Fig. 9.3B shows polymer-derived SiC ceramic fiber, which is produced from melt spinnable PCS [1].

SiC-carbon fibers were synthesized by the copyrolysis of polydimethylsilane and pitch. SiC-C fibers were produced by melt spinning of the precursors and then heat treatment up to 1400°C in vacuum atmosphere [23].

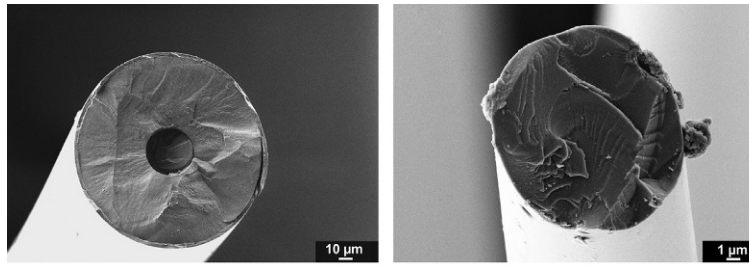

Fig. 9.3 Fracture surface of SiC-based fibers, (A) substrate-based fiber (SCS6) and (B) polymer-derived fiber (Hi-Nicalon).
From Flores O, Bordia RK, Nestler D, Krenkel W, Motz G. Ceramic fibers based on SiC and SiCN systems: current research, development, and commercial status. Adv Eng Mater 2014;16:621–36. http://dx.doi.org/10.1002/adem.201400069.

SiC/TiC ceramic fibers were also synthesized by polymer route. When Yajima et al. [24] continued the study on synthesis of SiC-based fibers from PCSs, they produced novel structure of polytitanocarbosilane (PTC) by cross-linking of PCS with titanium tetra-alkoxide. Pyrolysis of PTC above 1300°C and under nitrogen atmosphere resulted in crystallization of β-SiC and TiC with release of CO and SiO gases and formation of a SiO_2 and TiO_2 layer on the surface of the fiber [25].

Si-Ti-C-O fiber system (Tyranno Lox-M) was the first generation of commercial SiC fibers produced by Ube Industries. The resulting fiber had a tensile strength of 3.3 GPa and a tensile modulus of 187 GPa at room temperature [26].

Si-Zr-C-O fiber system (Tyranno ZMI) was the second generation of commercial SiC fibers also produced by Ube Industries. In order to reduce oxygen content of fibers (from 20 to 9 wt%) and improve the strength retention at high temperatures, titanium metal was replaced by zirconium in this product [1]. As a result, tensile modulus of the fiber is higher than that of Si-Ti-C-O fiber.

Si-Al-C-O fiber system (Tyranno SA3) was the third-generation SiC fiber from Ube Industries. In this product, aluminum was added into PCS chains to help the cross-linking of the polymeric fibers. In addition to tensile modulus, the creep resistance at high temperatures (>1300°C) of Si-Al-C-O fiber shows considerable improvement compared with the earlier Tyranno series [27].

Dow Corning, Inc. also produced SiC fiber (Sylramic) by using boron as sintering aid from PCS or polyorganosiloxane. The company also produced SiC fiber with smaller grains of TiB_2 and B_4C by oxidation and doping of PTC fiber with boron [28]. COI Ceramics expanded its ceramic SiC fiber study with the development of new fiber (Sylramic-iBN). They applied heat treatment process on the Sylramic fiber under nitrogen-containing gas atmosphere in order to diffuse the boron from the bulk to the fiber surface, where it reacts with nitrogen to form an *in situ* BN coating [29]. Composition and typical properties for the commercially available SiC fibers are given in Table 9.2.

Table 9.2 Composition and properties of SiC-based fibers [1,26]

Trade name	Manufacturer	Elemental composition (wt%)	Avg diameter (μm)/fibers per tow	Density (g/cm^3)	Tensile strength (GPa)	Elastic modulus (GPa)	Approx price (€)
SCS-6-9/ Ultra[a]	Specialty Materials	70 Si + 30 C + trace Si and C	70–140[b]	~3	~3.5/~6	390–350/390	3400/kg
Nicalon 200 N	Nippon Carbon	56 Si + 32 C +12 O	14/500	2.55	3.0	210	2650/kg
Hi-Nicalon	Nippon Carbon	69 Si + 37 C +0.5 O	14/500	2.74	2.8	270	8000/kg
Hi-Nicalon Type S	Nippon Carbon	69 Si + 31 C +0.2 O	12/500	3.05	2.6	420	11,500/kg
Tyranno Lox M	Ube Industries	55 Si + 32 C +10 O +2.0 Ti	11/800	2.48	3.3	187	1500/kg
Tyranno ZMI	Ube Industries	57 Si + 35 C +7.6 O +1.0 Zr	11/800	2.48	3.4	200	2000/kg
Tyranno SA3	Ube Industries	68 Si + 32 C + 0.6 Al	7.5/1600	3.02	2.8	380	8000/kg
Sylramic-iBN	COI Ceramics	Sylramic	10/800	3.2	3.2	~400	
Sylramic	COI Ceramics (Dow Corning)	67 Si + 29 C + 0.8 O +2.3 B + 0.4 N +2.1 Ti	10/800	3.2	3.2	~400	18,750/kg

[a]Except SCS-6-9/ultra fibers, all fibers are produced from derived polymer-based precursors.
[b]SCS-6-9/ultra fibers are mono filament.

9.3.2 SiCN based fibers

In the beginning of the 1970s, Verbeek [30] patented a homogeneous mixture of SiC fiber with silicon nitride (Si_3N_4) fiber by production of a meltable polycarbosilazane (PCSZ) resin. PCSZ was synthesized by heating at 520°C trichloromethylsilane with methylamine. The melt-spun precursor fiber was firstly heated up to 110°C under moisture air and then heated to 1500°C in inert atmosphere. His study was the milestone for research in the processing of ceramic fibers from SiCN systems. SiC-S_3N_4 fiber studies were continued by modifying Verbeek process (polymer precursors). Penn et al. produced a SiC-Si_3N_4 fiber with tensile strength of 0.7 GPa and modulus value of 200 GPa [31].

In order to commercialize ceramic SiCN(O) fibers, many studies concerning PCSZ were carried out. Dow Corning, Inc. developed a nitrogen-rich hydridopolysilazane (HPZ) ceramic fiber [32].

More detailed studies on polymer-derived ceramic SiCN fiber were done at Laboratoire des Composites Thermostructuraux (Bordeaux, France). Si-C-N-O monofilaments were spun from meltable novel PCSZ precursor, cured under oxygen/nitrogen at temperature range of 90–230°C and submitted to a pyrolysis treatment in argon between 1200°C and 1600°C. The mechanical characteristics after pyrolysis have a tensile strength of 1850 MPa and elastic modulus of 185 GPa for a curing temperature of 140°C [33].

Aoki et al. invented novel polymetallosilazanes that are useful in the manufacture of metal-containing silicon nitride ceramic fibers. In their study, polyaluminosilazane solution was mixed with poly(ethyl methacrylate). After the solvent-removing process, the spinning solution was then charged to a defoaming vessel of a dry-spinning device. Finally, precursor fibers were obtained with an average diameter of 10 μm. The fibers were then heated from room temperature to 1350°C at a heating rate of 180°C/h in a nitrogen atmosphere while applying a tension, thereby obtaining silicon nitride-based ceramic fibers that have a tensile strength of 2.75 GPa and Young's modulus of 255 GPa [34].

9.3.3 Boron-based fibers

Boron fibers are commercially produced by CVD techniques; boron is generally coated on a fine tungsten wire (~12 μm diameter) substrate. But a carbon substrate can also be used. Boron fiber with 100 μm diameter has a density of 2.6 g/cm^3. It has high melting point of 2040°C. The average tensile strength of boron fiber is 3–4 GPa, while its Young's modulus is between 380 and 400 GPa. Due to their superior mechanical properties and low density, they are used in military air crafts, space shuttle, and sports equipment such as golf shafts, tennis rackets, and bicycle frames [8]. Specialty Materials, Inc. produces trademark boron fibers (Hy-Bor) and epoxy resin prepreg tape with 50 vol% boron fiber [35].

There are two boron fiber fabrication processes: (1) thermal decomposition of a boron hydride and (2) reduction of boron halide. In the first method, process takes place at low temperature; therefore, carbon-coated glass fibers can be used as a

substrate. The produced fibers are weak and less dense due to the lack of adherence between boron and core and trapped gases [36]. In the second method, boron trihalide (BX_3) reduction takes place at high temperatures under hydrogen gas; therefore, high-melting-point metal tungsten is used as a substrate.

The boron is deposited on the core according to the reaction [37]:

$$2BX_3(g) + 3H_2(g) \rightarrow 2B(s) + 6HX(g) \quad (X: Cl, Br, I) \tag{9.1}$$

Boron fiber manufacturing process is described with more details in Section 9.4.1.

Boron fibers have a microcrystalline structure that is generally called amorphous because characteristic X-ray diffraction pattern shows a typical of amorphous material. But amorphous boron fiber is really composed of 2 nm nanocrystalline phase. Fig. 9.4 shows the morphology of fiber surface that resembles a "corncob" structure consisting of nodules separated by boundaries. The nucleation of boron occurred preferentially on the substrate and then grows outward in a conical form. Finally, the nodules are obtained [37].

Boron carbide (B_4C) fiber is produced directly from B_4C powders. Cellulose-based viscose mixture is prepared, and the powders are dispersed to form a boron-carbide-loaded slurry, and then, the slurry is spun, and green fiber is formed. The cellulose acts as a binder in the fiber-forming process. The green fiber is heat-treated at a low temperature about 500°C to produce excess carbon as a sintering aid. Afterward, the temperature increases to a high temperature (1800–2300°C) to form boron carbide fiber. The reaction forming B_4C fiber is defined as ($B_4C + C \rightarrow B_4C$) [38].

Boron nitride can be used in wide variety of applications especially in electric and electronic area due to its high electric resistivity coupled with its high thermal conductivity. It has also excellent thermal-shock resistance and high corrosion resistant [39].

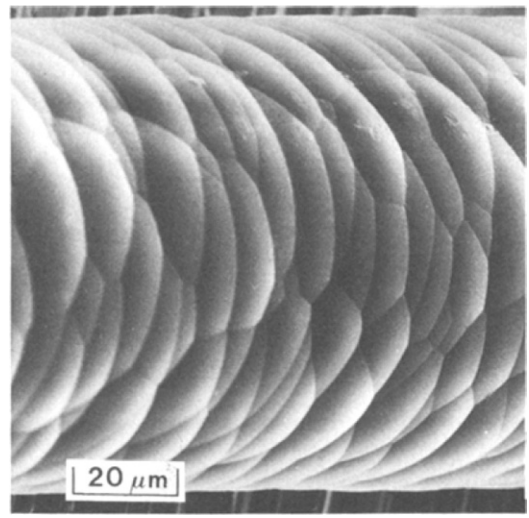

Fig. 9.4 Morphology of a boron fiber.
From Carlsson J. Review techniques for the preparation of boron fibres. J Mater Sci 1979;14:255–64.

Economy and Lin patented a BN fiber prepared by heating of boric oxide (B_2O_3) continuous multifilament (800 filaments/yarn) fiber made by melt spinning of B_2O_3 at temperatures (~800°C) in an ammonia (NH_3) atmosphere. Complex or series of reactions occurs between the B_2O_3 and NH_3, partially nitride boric oxide fiber, which consists essentially of boron (35%–55%), nitrogen (40%–50%), oxygen, and hydrogen.

They also found that when such a partially nitride fiber is heated in nitrogen atmosphere at a sufficiently high temperature (~2000°C), a further complex or series of reactions take place very rapidly within the fiber, and volatile substance is also dissipated, and then finally, partially nitride fiber is converted to essentially BN fiber. During the production of BN fibers, they were stretched at high temperatures and resulted in decreasing diameter of the fibers. The fiber (5 μm diameter) had Young's modulus of 235.8 GPa and a tensile strength 579 MPa [40].

9.3.4 Other fibers

There are lots of different nonoxide fiber types, in addition to abovementioned ones. Some important ones are also mentioned in this section.

Si-Al-O-N ceramic fibers were produced from a polyaluminocarbosilane (PACs), which were synthesized by reacting polycarbosilane and an aluminum alkoxide modified with an ester (ethyl acetoacetate). Amorphous Si-Al-O-N ceramic fibers were converted from the preceramic fibers after a pyrolysis process under flowing ammonia up to 1000°C. Afterward, the fibers were further fired in a graphite furnace under N_2 flow at 1200–1500°C for 1 h. At 1000°C nitridation temperature, values of tensile strength up to 1750 MPa have been measured for fibers having a diameter of 15 μm [41].

Another type of synthetic ceramic fiber is silicon oxynitride (SiNO). The polycarbosilane was melt-spun into polycarbosilane fibers at 310°C in a N_2; then, polycarbosilane fibers were cured by the oxidation at several temperatures (145–180°C); finally, they were heated from 1200°C to 1500°C in the NH_3 gas flow, and silicon oxynitride (SiNO) fibers with 11–13 μm diameter were obtained. Tensile strength of 1.5 GPa and Young's modulus of 125 GPa are heated at 1300°C. But by further heating, this silicon oxynitride is considered to decompose to silicon nitride and a gas phase of SiO and N_2 [42].

9.4 Production techniques of ceramic fibers

9.4.1 CVD technique

In the literature, the CVD is a very common primary technique to produce ceramic fibers. Many nonoxide fibers employed in CMCs, MMCs, and intermetallic composites (IMC) have been manufactured via CVD. This process is based on the deposition of a material's vapor phase on a core substrate that is in the form of a monofilament. Tungsten/wolfram (W) and carbon (C)-type monofilaments/wires are typically used as the core component due to their availability at higher temperatures [26].

In CVD route, the deposited material is the separation product of the gases in the vapor phase.

Boron (B) deposition occurs from the decomposition of boron trichloride (BCl_3) into boron and hydrogen (H) as seen below in the reaction (9.2): whether boron is coated on tungsten or carbon core fiber, the method for CVD of boron is similar. Fig. 9.5 shows a schematic of continuous production of boron filament. Tungsten wire (W) passes through hydrogen-reduction chamber and then through two boron deposition chambers. The wire is electrically heated under a gas mixture of H_2 and BCl_3; the mercury traps (M) also act as electric contact with the wire B, the finished boron filament [37,43]:

$$2BCl_3 + 3H_2 \rightarrow 2B + 6HCl \tag{9.2}$$

Reduction temperature and speed of the wire are critical for obtaining a boron fiber with optimum properties and structure. The critical temperature is about 1000°C. After deposition of boron on a tungsten substrate, a series of compounds such as W_2B, WB, W_2B_5, and WB_4 phases are formed by diffusion of boron into tungsten [36,37].

Generally, decomposition reaction forms from SiC filament fabrication in CVD process by using the silane-based precursors (e.g., alkylchlorosilane or methyltrichlorosilane). The reactive gas mixture as expressed in reaction (9.3) gets into the reactor from the inlet, and both of the reactor sides are sealed with mercury gaskets to inhibit the leakage. During this operation, the SiC fiber is stored as the vapor phase on the core that is heated up to 1300°C. Although the resultant fibers generally exhibit larger diameters (50–150 μm), which are not suitable for complex preform shaping, their strength (up to 6 GPa tensile strength) and stiffness (up to 390 GPa tensile modulus) properties are reasonably high. Final SiC filaments show very fine- and columnar-grained microstructures. The CVD is a fast high-temperature method without any hazardous effects; however, several important factors such as reactant gas types, applied pressure, ambient temperature, and concentration of the gas phase influence the final product due to the sensitivity of chemical precursors. The SiC fibers are inexpensive as compared with the boron fibers and show various surface compositions to promote the interaction with different composite matrices [26]:

$$CH_3SiCl_3 \rightarrow SiC + 3HCl \tag{9.3}$$

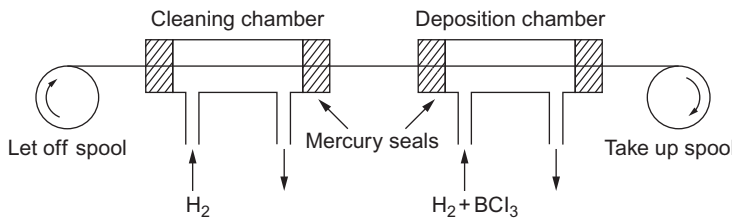

Fig. 9.5 A schematic of continuous production of boron filament.
From Carlsson J. Review techniques for the preparation of boron fibres. J Mater Sci 1979;14:255–64.

9.4.2 Melt spinning technique

In the traditional melt-spinning route, the precursor materials (e.g., oxides like Al_2O_3) are melted and subjected to spinning process. During spinning, the oxides in the molten state are forced throughout the nozzles at relatively high pressure and solidified by cooling. The produced fibers generally exhibit amorphous structure due to the high cooling rates that lead to the instability. The rapid viscosity change owing to the tremendous temperature variation causes the lack of diameter control. In addition to that, a number of parameters such as spinning speed, draw ratio, temperature, and environmental circumstances considerably affect the structures of fabricated fibers. Melt spinning is recently used as a part of preceramic polymer processing that utilizes inorganic polymers and will be described in the next sections [7,44].

9.4.3 Slurry spinning

This technique has been developed to avoid the handicaps of melt-spinning method. Both oxide and nonoxide fibers can be manufactured via extrusion (spinning) of ceramic slurries. In this process, the slurry is composed of three basic components: alumina particulates (either in solid or in aqueous form), suspension of alumina precursor (e.g., aluminum chlorohydroxide), and organic polymer. The polymer component provides the viscosity increase and facilitates the extrusion of slurry from the spinneret. The precursor used in this process promotes the densification during sintering. Once the slurry passes through the nozzles, the green (unfired) fibers are wrapped onto a roller and exposed to calcination (firing below sintering temperature) to eliminate water and volatiles and to control the shrinkage. Eventually, the calcined fibers are sintered to remove porosity and convert the alumina precursor to the stable α-alumina phase [45,46]. The average diameter of the manufactured fibers is approximately 20 μm in 200 filament tows. In many slurry-spinning applications, a silica-based compound is introduced to improve the strength properties and wettability of the filaments with the matrices. Although the tensile strength of the produced fibers is in the range of 1.40–1.55 GPa, α-alumina grains (∼0.5 μm size) agglomerate and act as defects, which cause strength decrease. The weaving of the fibers is also extremely difficult due to the brittle character of the fibers (410 GPa tensile modulus), and therefore, the availability of these filaments are very limited [4,47].

9.4.4 Chemical conversion

The chemical conversion/processing approach is based on the conversion of ceramic/inorganic precursor fibers into a different composition via chemical reactions by using an external compound. In this technique, the precursor fiber is subjected to the (atomic) deposition of the external compound that diffuses through the fiber surface. After the successful reaction of components, the final fiber exhibits the composition of desired chemical content [48]. The most common example of this process is the conversion of carbon precursor into the SiC fiber by utilizing Si or SiO agents

(carbide-forming material) in the vapor phase. The following reactions of this route are seen as below:

$$C + Si \rightarrow SiC \tag{9.4}$$

$$2C + SiO \rightarrow SiC + CO \tag{9.5}$$

Although the reactions shown in (9.4) and (9.5) exist theoretically, their practical existence and efficiency is very limited. However, activated carbon fiber (ACF) usage leads to a better conversion ratio as compared with the other attempts. ACF provides a wide nanoporous surface that allows more diffusivity along the fiber [4]. The other prevalent applications of this process are related with nitriding a metal, organometallic, or oxide precursor fiber with the introduction of nitrogen (N) or ammonia (NH_3). The conversion of neat boron (B) precursors into boron nitride (BN) fibers with the aid of NH_3 to generate nitride formation is a conversant example in the literature [48].

9.4.5 Preceramic polymer processing (polymer-derived precursor method)

A plenty of ceramic fibers including many types of elements such as silicon, carbon, nitrogen, boron, and titanium have been produced with this method. The idea of preceramic polymer processing is primarily based on the combination of two discrete techniques: melt or dry spinning and pyrolysis. Various polymeric materials are used as precursors like polycarbosilane (Ceramic Gr™ SiC fiber), polytitanocarbosilane (Tyranno™ Si-Ti-C-O fiber), and hydridopolysilazane (HPZ™ silicon carbonitride fiber). In the beginning of the process, the inorganic polymer precursors are subjected to melt or dry spinning to manufacture green fibers. Melt spinning is generally preferred instead of dry spinning because it does not require solvent during the production, and the resultant fibers exhibit better performance. In this route, the molten polymer in a thick viscous liquid state is pressed from the nozzles, and continuous filaments are obtained before solidification. Under an inert environment, these filaments are squeezed into more delicate fibers that are called as "green fibers" [46,49].

Curing of green fibers is carried out by thermal or chemical routes that provide effective cross-linking and prevent melting. The cured filaments are exposed to pyrolysis at high temperatures (between 800°C and 1800°C range) in an inert atmosphere. As far as the pyrolytic gases vacate the reaction, the unity of the fibers is maintained with a high degree of densification ratio. Several major factors such as purity of precursor polymer, flaw amount and the efficiency of spinning route, and curing and pyrolysis processes remarkably influence the mechanical and thermal properties of fabricated products. Consequently, the manufactured fibers generally show pretty good tensile strength, oxidation resistance, and thermal stability. However, initial cost of precursor, material loss during the operation, and the reduction of fiber length may be described as the significant disadvantages of this technique. In particular, the main reason for this length decrease is attributed to the high level of density increase related with extra carbonization [4,26]. Chloroorganosilicon compounds used to produce preceramic polymers

with mixed coordinations on tetravalent silicon, such as poly(silanes), poly(carbosilanes), poly(silazanes), poly(borosilazanes), poly(silsesquioxanes), and poly(carbosiloxanes), are displayed in Fig. 9.6 [50].

9.4.6 Sol-gel process

In the traditional processing techniques, the manufacturing of high-purity fibers and various compositions of mixed ceramic oxide filaments is relatively difficult. Particularly, the liquid immiscibility at the melting temperature and phase separation/crystallization during cooling are the main problems in those techniques. The sol-gel method is generally used to produce oxide-based ceramic fibers. Theoretically, the "sol" is composed of either colloidal particles, which may be crystalline or amorphous, or polymers in a solvent. The "gel" includes a three-dimensional (3-D) continuous network that covers a liquid phase, and in a colloidal gel, the stacking of particles leads to the formation of this network [51].

In a typical sol-gel route, low-molecular-weight metal alkoxides, which dissolve in a liquid, are used as the starting materials. After the hydrolysis and polycondensation

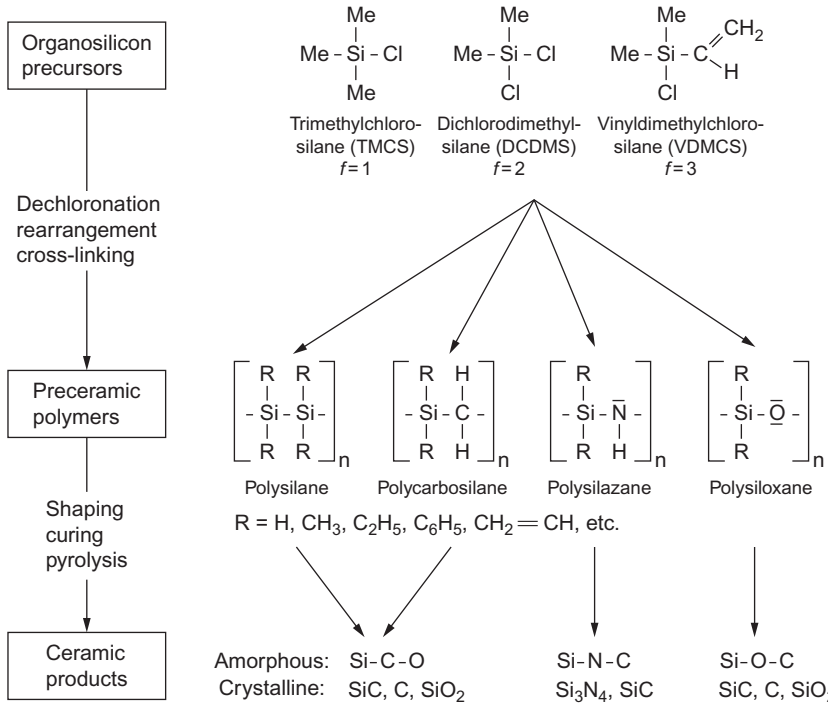

Fig. 9.6 Manufacturing steps of polymer-derived precursor method.
From Greil P. Active-filler-controlled pyrolysis of preceramic polymers. J Am Ceram Soc 1995;78:835–48. http://dx.doi.org/10.1111/j.1151-2916.1995.tb08404.x.

reactions, the solvent is removed, and fine particles come together to generate the 3-D network (gelation). During gelation the viscosity rising is observed significantly, and the viscous solution is exposed to dry-spinning process to form the fibers. The resultant fibers are dried (100–180°C), and a subsequent heating (500–800°C) leads to the elimination of volatiles with a series of chemical reactions and provides densification. It should be noted here that the control of drying step has a great importance due to the probability of crack formation and disintegration of the gelled structure. Furthermore, the solvent evaporation and shrinkage through drying may cause the dimensional variations of fibers. The porosity can be eliminated at relatively high temperatures (above 800°C) that also leads to the conversion from amorphous bodies into the polycrystalline products. However, extra-high-temperature treatment is the reason for excessive grain growth and the loss of fiber strength. Compared with the other processing techniques, relatively low operation temperatures are required during sol-gel route to fabricate silica, alumina, zirconia, titania, or mixed oxide fibers. In the literature, various alumina-based fiber compositions are valid, and their features depend on the portion of alumina and its phases (δ, γ, or α) and the amount of second phase [2,52].

The resultant properties of fibers (e.g., physical, mechanical, electric, and optical) can be modified with the addition of different oxides and metal components. The final diameter of the continuous filaments produced by sol-gel method is generally in the range of 10–20 μm where the elastic modulus of the products changes from 150 to 373 GPa [4].

9.4.7 Single-crystal fiber growth (edge-defined film-fed growth-EFG) technique

Single-crystal fiber production is generally used to fabricate specific type of products (filaments, wires, and whiskers) used in optical and electronic industries. Edge-defined film-fed growth (FED) is one of the most common techniques to manufacture single crystals with various shapes that grow from melt, solution, and vapor. Originally, the EFG method was firstly developed by LaBelle in 1971 to produce sapphire filaments, but it has been already applied for the growth of oxides such as Al_2O_3, $LiNbO_3$, TiO_2, and Si [53]. In a typical EFG process, a die (or tube) is immersed in a molten liquid that is fed with capillary action through an orifice in the die to form a local molten pool. The melt flows to the top surface of the die, so the vertical edges of the die determine the shape of the filament. The continuous interaction of the seed crystal, which is located on the top plane, and molten surface results in the formation of single-crystal fiber drawn. The elimination of the probable defects is achieved with a linear temperature distribution. The compatibility of the die material and ceramic melt is critical in order to avoid the possible hazardous reactions [46].

In terms of sapphire fibers, the final diameter of the filaments is generally in the range of 100–500 μm. The average tensile-strength values of a sapphire fiber with 250 μm diameter show 2.75 GPa along c-axis and 2.40–2.90 GPa range through the *a*-axis [54].

The schematic representation of an EFG process that includes the production route of Ga_2O_3 is given in Fig. 9.7A–C.

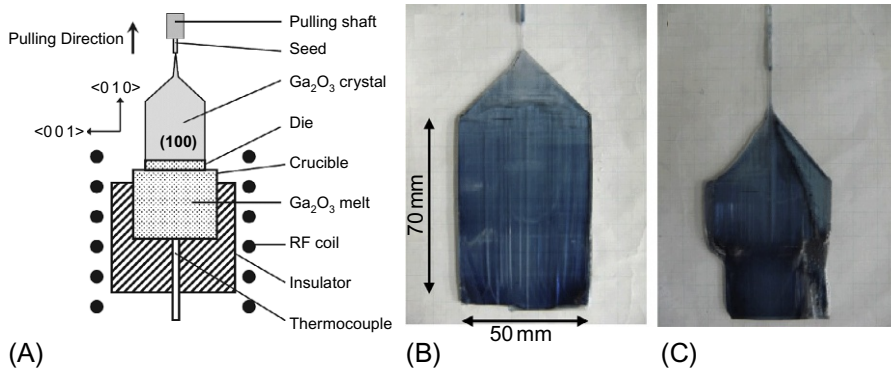

Fig. 9.7 (A) Schematic representation of EFG process, (B) as grown single-crystal β-Ga_2O_3 ribbon, and (C) polycrystalline β-Ga_2O_3 ribbon.
From Aida H, Nishiguchi K, Takeda H, Aota N, Sunakawa K, Yaguchi Y. Growth of B-Ga_2O_3 single crystals by the edge-defined, film fed growth method. Jpn J Appl Phys 2008;47:8506–9. http://dx.doi.org/10.1143/JJAP.47.8506.

9.5 Application of ceramic fibers

The use of ceramic fibers in the composite applications is taking attraction/attention since the last decades. In particular, continuous ceramic fibers/filaments are generally employed in high-temperature applications instead of metals due to their high thermal tolerance and corrosion resistance. Ceramic fibers may be produced in various forms like blankets, felts, bulk fibers, vacuum-formed or cast shapes, paper, and textiles depending on the application area [55]. The existence of ceramic fibers considerably improves both physical and mechanical properties of CMCs and satisfies the unity of the composites through matrix cracking that leads to the increase of composite's tolerance to failure. From the point of view of industrial implementation, ceramic-fiber-reinforced composites are utilized in many different commercial products such as aircraft engine components (turbine combustors, compressors, and exhaust nozzles), automotive and gas turbine elements, aerospace missiles, heat exchangers, hot gas filters, rocket nozzles, gasket, and wrapping insulations [55,56].

There are plenty of studies available in the literature that focus on the performance of various ceramic fibers in CMCs. Depending on the requirements (mechanical, physical, or thermal), oxide, nonoxide, or other types of ceramic filaments find applications in many cases.

A typical example for the ceramic-fiber-reinforced matrix composite is given in Fig. 9.8. The Nextel™ 610 (alumina-based) fibers and mullite matrix were integrated via classic lamination technique that is generally used for the fabrication of polymer matrix composites. As shown in Fig. 9.8A, the 0°/90° fabrics were systematically embedded in the ceramic phase, and the regular packing of alumina fibers is clearly observed in Fig. 9.8B [57].

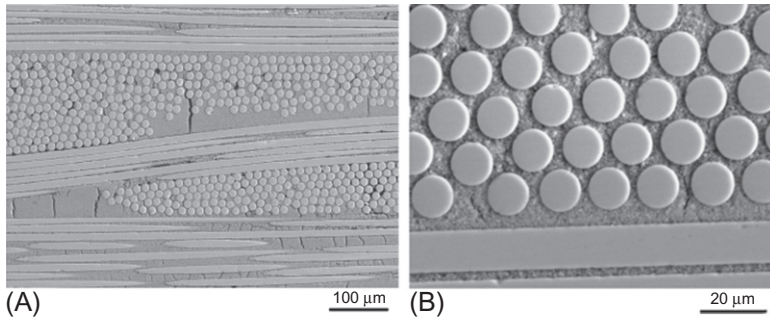

Fig. 9.8 SEM images of Nextel™ 610/mullite composites with 0/90 fiber orientation, (A) fiber bundles and (B) almost regular and dense packing of fibers within a bundle.
From Simon RA. Progress in processing and performance of porous-matrix oxide/oxide composites. Int J Appl Ceram Technol 2005;2:141–9. http://dx.doi.org/10.1111/j.1744-7402.2005.02016.x.

References

[1] Flores O, Bordia RK, Nestler D, Krenkel W, Motz G. Ceramic fibers based on SiC and SiCN systems: current research, development, and commercial status. Adv Eng Mater 2014;16:621–36. http://dx.doi.org/10.1002/adem.201400069.
[2] Weddell JK. Continuous ceramic fibres. J Text Inst 1990;81:333–59. http://dx.doi.org/10.1080/00405009008658717.
[3] Bunsell AR. Oxide fibers. In: Bansal N, editor. Handbook of ceramic composites. New York: Springer Science & Business Media; 2005. p. 3–31.
[4] National Research Council. Ceramic fibers and coatings: advanced materials for the twenty first century. Washington, DC: National Academy Press; 1998.
[5] Wilson DM, Visser LR. High performance oxide fibers for metal and ceramic composites. Compos A: Appl Sci Manuf 2001;32:1143–53.
[6] Pfeifer S, Demirci P, Duran R, Stolpmann H, Renfftlen A, Nemrava S, et al. Synthesis of zirconia toughened alumina (ZTA) fibers for high performance materials. J Eur Ceram Soc 2016;36:725–31. http://dx.doi.org/10.1016/j.jeurceramsoc.2015.10.028.
[7] Bernd Clau ß. Fibers for ceramic matrix composites. In: Krenkel W, editor. Ceramic matrix composites: fiber reinforced ceramics and their applications. Weinheim: Wiley-VCH Verlag GmbH & Co. KGaA; 2008. p. 1–19.
[8] Cooke TF. Inorganic fibers—a literature review. J Am Ceram Soc 1991;78:2959–78.
[9] Schawaller D, Clauß B, Buchmeiser MR. Ceramic filament fibers—a review. Macromol Mater Eng 2012;297:502–22. http://dx.doi.org/10.1002/mame.201100364.
[10] 3M. 3M™ Nextel™ Ceramic Fibers and Textiles. Web Page 2016. www.3m.com/ceramics.
[11] Zawada LP, Hay RS, Lee SS, Staehler J. Characterization and high-temperature mechanical behavior of an oxide/oxide composite. J Am Ceram Soc 2003;86:981–90. http://dx.doi.org/10.1111/j.1151-2916.2003.tb03406.x.
[12] Bin TH. Preparation of long alumina fibers by sol-gel method using tartaric acid. Int J Miner Metall Mater 2011;18:691–4. http://dx.doi.org/10.1007/s12613-011-0498-6.
[13] Sedaghat A, Taheri-Nassaj E, Naghizadeh R. An alumina mat with a nano microstructure prepared by centrifugal spinning method. J Non-Cryst Solids 2006;352:2818–28. http://dx.doi.org/10.1016/j.jnoncrysol.2006.02.068.

[14] Venkatesh R, Chakrabarty PK, Siladitya B, Chatterjee M, Ganguli D. Preparation of alumina fibre mats by a sol-gel spinning technique. Ceram Int 1999;25:539–43. http://dx.doi.org/10.1016/S0272-8842(97)00092-8.
[15] Chandradass J, Balasubramanian M. Sol-gel processing of alumina fibres. J Mater Process Technol 2006;173:275–80. http://dx.doi.org/10.1016/j.jmatprotec.2005.11.030.
[16] Zhang H, Hang Y, Qin Y, Yang J, Wang B. Synthesis and characterization of sol-gel derived continuous spinning alumina based fibers with silica nano-powders. J Eur Ceram Soc 2014;34:465–73. http://dx.doi.org/10.1016/j.jeurceramsoc.2013.08.015.
[17] Wilson DM. Spun (slurry and sol-gel) ceramic fibers. In: Mortensen A, editor. Concise encyclopedia of composite materials. Amsterdam: Elsevier; 2005. p. 823–6.
[18] Horikiri S, Tsuji K, Abe Y, Fukui A, Ichiki E. Process for producing alumina fiber or alumina-silica fiber. US Patent No. 4101615; 1978.
[19] Deléglise F, Berger MH, Jeulin D, Bunsell AR. Microstructural stability and room temperature mechanical properties of the Nextel 720 fibre. J Eur Ceram Soc 2001;21:569–80. http://dx.doi.org/10.1016/S0955-2219(00)00249-1.
[20] Deléglise F, Berger M, Bunsell A. Microstructural evolution under load and high temperature deformation mechanisms of a mullite/alumina fibre. J Eur Ceram Soc 2002;22:1501–12. http://dx.doi.org/10.1016/S0955-2219(01)00461-7.
[21] Wilson DM, Visser LR. Nextel™ 650 ceramic oxide fiber: new alumina-based fiber for high temperature composite reinforcement. In: 24th annual conference on composites, advanced ceramics, materials, and structures: b: ceramic engineering and science proceedings. John Wiley & Sons, Inc.; 2008. p. 363–73. http://dx.doi.org/10.1002/9780470294635.ch44.
[22] Poulon-Quintin A, Berger MH, Bunsell AR. Mechanical and microstructural characterisation of Nextel 650 alumina-zirconia fibres. J Eur Ceram Soc 2004;24:2769–83. http://dx.doi.org/10.1016/j.jeurceramsoc.2003.08.011.
[23] Hasegawa Y, Okamura K. Synthesis of precursors for SiC-C fibers by copyrolysis of polysilane and pitch. J Ceram Assoc Jpn 1987;95:109–13.
[24] Yajima S, Iwai T, Yamamura T, Okamura K, Hasegawa Y. Synthesis of a polytitano carbosilane and its conversion to inorganic compounds. J Mater Sci 1981;16:1349–55.
[25] Yamamura T, Ishikawa T, Shibuya M, Hisayuki T, Okamura K. Development of a new continuous Si-Ti-C-O fibre using an organometallic polymer precursor. J Mater Sci 1988;23:2589–94.
[26] DiCarlo JA, Yun H-M. Non-oxide (silicon carbide) fibers. In: Bansal NP, editor. Handbook of ceramic composites. New York: Springer Science & Business Media; 2005. p. 33–52.
[27] Ishikawa T, Kohtoku Y, Kumagawa K, Yamamura T, Nagasawa T. High-strength alkali-resistant sintered SiC fibre stable to 2200°C. Nature 1998;391:773–5.
[28] Lipowitz J, Rabe JA, Zangvil A, Xu Y. Structure and properties of Sylramic™ silicon carbide fiber—a polycrystalline, stoichiometric β-SiC composition. Ceram Eng Sci Proc 1997;18:147–57.
[29] DiCarlo JA, Yun H. Methods for producing silicon carbide architectural preforms. US7687016B1. 2010.
[30] Verbeek W. Production of shaped articles of homogeneous mixtures of silicon carbide and nitride. US Patent 3853567; 1974.
[31] Penn BG, Daniels JG, Ledbetter FE, Clemons JM. Preparation of silicon carbide-silicon nitride fibers by the pyrolysis of polycarbosilazane precursors: a review. Polym Eng Sci 1986;26:1191–4. http://dx.doi.org/10.1002/pen.760261705.
[32] Freeman HA, Langley NR, Li CT, Lipowitz J, Rabe JA. Polymer derived ceramic fibers having improved thermal stability. US Patent 5238742; 1993.

[33] Mocaer D, Chollon G, Pailler R, Filipuzzi L, Naslain R. Si-C-N ceramics with a high microstructural stability elaborated from the pyrolysis of new polycarbosilazane precursors. J Mater Sci 1993;28:2632–8. http://dx.doi.org/10.1007/BF00354712.
[34] Aoki H, Suzuki T, Katahata T, Haino M, Nishimura G, Kaya H, et al. Novel polymetallosilazanes useful in the manufacture of silicon nitride based ceramic fibers. EU Patent 0344870A2; 1989.
[35] Specialty Materials I. http://www.specmaterials.com/boronfiber.htm; 2016.
[36] Chawla KK. Composite materials science and engineering. 3rd. ed. New York: Springer Science & Business Media; 2012.
[37] Carlsson J. Review techniques for the preparation of boron fibres. J Mater Sci 1979;14:255–64.
[38] Mohammadi F, Cass RB. Boron Carbide Ceramic Fibers. US8536080B2, 2013.
[39] Lin RY, Economy J, Murty HH, Ohnsorg R. Preparation and characterization of high strength, high modulus continuous boron nitride fibers. Appl Polym Symp 1976;29:175–88.
[40] Economy J, Lin R-Y. High modulus boron nitride fibers. US Patent 3668059; 1972.
[41] Soraru GD, Mercadini M, Maschio RD, Taulelle F, Babonneau F. Si-Al-O-N fibers from polymeric precursor: synthesis, structural, and mechanical characterization. J Am Ceram Soc 1993;76:2595–600.
[42] Okamura K, Sato M, Hasegawa Y. Silicon nitride fibers and silicon oxynitride fibers obtained by the nitridation of polycarbosilane. Ceram Int 1987;13:55–61. http://dx.doi.org/10.1016/0272-8842(87)90038-1.
[43] Van Maaren AC, Schob O, Westerveld W. Boron filament: a light, stiff and strong material. Philips Tech Rev 1975;35:125–36.
[44] Motz G, Bernard S. Processing and applications. In: Colombo P, Riedel R, Soraru GD, Kleebe H-J, editors. Polymer derived ceramics: from nanostructure to applications. Pennsylvania: DEStech Publications; 2010. p. 344–5.
[45] Kelly A. Concise encyclopedia of composite materials. USA: Elsevier Science; 2006.
[46] Marzullo A. Boron, high silica, quartz and ceramic fibers. In: Peters ST, editor. Handbook of composites; Dordrecht: Springer Science & Business Media; 1998. p. 156–68.
[47] Birchall JD. Inorganic fibers. In: Brook RJ, editor. Concise encyclopedia of advanced ceramic materials. Oxford: Pergamon Press; 1991. p. 236–8.
[48] Rice RW. Ceramic fabrication technology. New York: Marcel Dekker Inc.; 2003.
[49] Baldus P, Jansen M, Sporn D. Ceramic fibers for matrix composites in high temperature engine applications. Science 1999;285:699–702.
[50] Greil P. Active-filler-controlled pyrolysis of preceramic polymers. J Am Ceram Soc 1995;78:835–48. http://dx.doi.org/10.1111/j.1151-2916.1995.tb08404.x.
[51] Varaprasad DV, Abhiraman AS. Sol-gel silica fiber forming investigations. Final project report. Georgia Institute of Technology School of Chemical Engineering, Atlanta, GA; 1987.
[52] Hench LL. Glasses from sol–gel monoliths. In: Brook RJ, editor. Concise encyclopedia of advanced ceramic materials. Oxford: Pergamon Press; 1991. p. p. 176–8.
[53] Aida H, Nishiguchi K, Takeda H, Aota N, Sunakawa K, Yaguchi Y. Growth of B-Ga_2O_3 single crystals by the edge-defined, film fed growth method. Jpn J Appl Phys 2008;47:8506–9. http://dx.doi.org/10.1143/JJAP.47.8506.
[54] Rudolph P, Fukuda T. Fiber crystal growth from the melt. Cryst Res Technol 1999;34:3–40.

[55] Saruhan B. Oxide based fiber-reinforced ceramic-matrix composites: principles and materials. Springer Science+Bussiness Media; 2003.
[56] Report on Carcinogens, 14th ed., National toxicology program. USA: Department of Health and Human Services; 2016.
[57] Simon RA. Progress in processing and performance of porous-matrix oxide/oxide composites. Int J Appl Ceram Technol 2005;2:141–9. http://dx.doi.org/10.1111/j.1744-7402.2005.02016.x.

This page intentionally left blank

Natural fibers

10

Ahmet Çağrı Kılınç[*], *Cenk Durmuşkahya*[†], *M. Özgür Seydibeyoğlu*[†]
*Dokuz Eylul University, Izmir, Turkey, †Izmir Katip Çelebi University, Izmir, Turkey

10.1 Introduction to natural fibers

10.1.1 Introduction

Plant fibers are one of the oldest natural materials in human history. In the beginning, people were collecting several wild plant species for their versatile fibers. After years, agriculture emerged and people started to cultivate fiber plants. Archeologists have found bits of fabric estimated to be 10,000 years old in both the Old and New worlds. Primitive civilizations explored plant fiber usage especially in textile weaving long before they began to refine metal or pottery making.

In the past, all fibers were very important because they had been used in many ways. Some of them were used to rope or yarn making that used in hunting, fishing, netting, climbing, carrying and others, for textile weaving. Perhaps one of the most important reasons for using fibers in the ancient time could be seen in the cloth making. Thousands of years ago, after the human expansion from Africa to Asia and Europe, humans faced with lower temperatures in the new habitats and for that reason they needed to protect their bodies from harsh winds and freezing temperatures. As a result of this condition, people begun to explore plant fibers as a textile material beside the animal peltries and wools to cope with cold weather.

In the beginning plant fibers were collected from the wild. Some barks, or some fibrous leaves could be used. But the discovery of cotton and hemp has changed the fate of the world. Then fibers from cultivated plants made many things easy because the production increased overwhelmingly. For this reason, in a short period of time, plant fibers took an indispensable place in the human life.

The history of spinning began when the first spinners rolled strands of fibers between their hands and realized that twisting gave strength to the yarn. Many researchers believe that these first yarns were spun from the long fibers of plant stems and then spinning short fibers, like cotton. With the early invention of the spindle and whorl, techniques of hand spinning were developed that endure even today in parts of the world. People everywhere have used the fibers from local native plants to make a variety of everyday and ceremonial fabrics, fishnets and bowstrings, floor mats, sheets, and blankets [1].

As societies became more complex, the need for certain kinds of fabrics greatly increased. For instance in the middle ages, shipping developed and sailcloth and rope rigging increased. Then after the invention of spinning wheel and mechanical spinning devices were invented, the use of natural fibers ascended. After the industrial revolution

Fiber Technology for Fiber-Reinforced Composites. http://dx.doi.org/10.1016/B978-0-08-101871-2.00010-2

plant fibers were the primary materials for clothing, bedding and towels, curtains, upholstery, flour and sugar bags, twines, tarpaulins, awnings, belts, hoses, etc.

But after the 1950s man made fibers were invented and in a short time due to their advantages these materials became more popular than natural fibers. Synthetic fibers were cheap and more durable and they had longer lasting features. Therefore today man made fibers are much more preferred. On the other hand, natural fibers began to be attractive in the different lanes such as biomaterials and bio composites. Nowadays many scientists research new usage of plant fibers in the emerging sectors and it is shown that natural fibers will serve to mankind for a long time [2,3].

10.1.2 History

Archeological evidence points to humans using natural fibers even before written history. Hemp is accepted as the first plant fiber by many scientists. According to archeological data from southwest Asia its use was started at about 4500 BC [4]. The Egyptians invented spinning and weaving using linen by 3400 BC [5].

Using plant species is as old as human history. Humans were used to plant species as a food source but after this point they explored unique features of plant species. After feeding, medicinal features of plants gave them long age and other uses of plants made daily life easier. Therefore our ancestor explored new features of plants day-by-day.

When it comes to ten millennia BC, man started to plant domestically and then agriculture emerged in several different parts of the world. At first Fertile Crescent in other words Mesopotamia became a starting point of agriculture. Chine and India followed it. In the west, Mexico and Mountain ranges played an important role in plant domestication. As a result of these movements, agriculture emerged in different places freely and naturally [6].

Many scientists accept that different fiber plants were domesticated freely in different parts of the world but main type of fibers were cotton, flax, hemp, and jute.

Cotton was first domesticated in the Kachi Plain of Balochistan, Pakistan about 7000 years ago. The earliest evidence was found in Neolithic occupation of Mehrgarh. First cotton species (*Gossiypium arboreum*) cultivation began in the Indus Valley of India and Pakistan and then eventually spread over Africa and Asia. After a short time, another cotton species (*Gossiypium herbaceous*) was cultivated in Arabia and Syria. These two species of cotton are genetically different species. Many botanists accept that *G. herbaceous* species originated from an African species but *G. arboreum* wild progenitor has not been found yet [7].

Up to now a lot of *G. arboreum* archeological evidence was found in Indus Valley. According to archeobotanists Indus Valley people formerly collected wild species from nature and then when they were depositing seeds of *G. arboreum*, they managed to farm it. In that region, archeologists found abundant samples of seed and fragments of cloths and cotton textiles, which have been found to date back to fourth millennium BC. This evidence showed that Mehrgarh city economy was based on cotton exportation.

Other important cotton producers were Jordan, Northern Caucasus in sixth millennia BC. Later in the first millennia BC, cotton fabrics were found in Iraq, Iran, and Greece. According to Assyrian records of Sennacherib, cotton was grown in Mosul but due to cold winter, production was not in huge amount.

In the same millennium cotton were cultivated in Persian Gulf, North Africa, Uzbekistan, and China. After Christ, between 9th and 10th centuries Arabs spread out cotton to Southwest Asia and Mediterranean Basin [8].

On the other hand *G. herbaceous* was limited in the Africa. This plant was taller than *G. arboreum* and had smaller fruit and thicker seed coats. For that reason *G. herbaceous* was not preferred too much and *G. herbaceous* won the selection competition.

Former, *G. hirsutum*, was cultivated in Mexico and latter *G. barbadense* was cultivated in Peru. According to botanists cotton was one of the first nonfood plants domesticated by the prehistoric inhabitants of the Americas.

In America first cottons were used to make fishing nets in the costal zones by American Indians because, the economy of the time consisted of marine based lifestyle.

Come as to *G. hirsutum*, the oldest evidence of this species were found in Tehaucan valley and has been dated between 3400 and 2300 BC. And also other ancient cotton samples were found in Yucatan Peninsula in the similar period [9].

Cotton were accepted as very valuable material by Maya and Aztecs and cotton products were given to noble visitors as gifts and army leaders as payment.

In the past, second important plant fiber was flax. Flax fibers were obtained from the stems of the plant *Linum usitatissimum* which today many of us know as a medicinal plant. The plant has been used for fiber production since prehistoric times. It grows best at northern temperate latitudes.

According to archeological researches first flax seeds were found in the Fertile Crescent about 11,000 years ago with wild wheat and barley. Perhaps, it was domesticated first for edible oil and, then later, for its fiber. Archeologists found earliest evidence for flax use in Abu Hureyra and Tell Mureybit in northern Syria. At the 8th millennium BC flax spread throughout the near East. In the 7th millennium BC flax seeds were found in sites on the Greek mainland. And then it found its way to Danube valley in Southwestern Germany. In the 6th millennium evidence for explicit fiber production were seen in Arbon Beiche settling in Switzerland [10].

On the other hand flax seeds reached China about 5000 years ago. At first in China people used it for edible oil too. After more years they explored it again as a fiber plant. In the first millennium BC in Scandinavia people saw that plant and they learned how to use it as a fiber [11].

Hemp is one of the most important plants for human beings. It has several different usages and therefore it is special. It is one of the important fiber plants, besides it is also an important food, medicinal, and narcotic plant.

Due to these features of hemp it is one of the oldest edible plants in human history.

The first identified coarse paper made from hemp therefore is really important. If our ancestor did not explore it, maybe we would have used still parchment.

In 1997, a hemp rope dating back to 26,900 BC was found in Czechoslovakia. it was the oldest evidence for hemp fiber. Botanist accepted that Cannabis plant originated in Central Asia. Archeological evidence showed that people used hemp clothing in China about 5 millennia BC. In China people used Cannabis plants: the root for medicine, the stem for textiles, rope, and paper making, the leaves and flowers for intoxication and medicine, and the seeds for food and oil.

From China farmers took Cannabis plant to Korea around 2 millennia BC. And after very short time it reached India. It was introduced to the middle East between 2000 and 1400 BC. Greeks were introduced to cannabis about 200 BC and finally during the 5th century it reached Britain with Anglo-Saxon invasions. The Spanish brought to Cannabis to the Americas in the mid 1500s.

Hemp was used for centuries to make rope, canvas, and paper. Long hemp fibers can be used like linen and can be spun and woven linen like fabric [12]. Due to low lignin content, in Europe hemp fibers are used mainly in the special paper industry [13].

Jute is another important plant fiber because of cheapness but it is a very new species as a fiber plant. When looked at antiquity there were no evidences related with jute. Therefore we can say it is a new fiber if it can be compared with cotton, flax, and hemp.

10.2 Plant fibers

10.2.1 Structure of plant fibers

Plant fibers are bundles of elongated dead plant cells cemented together by pectin and other noncellulosic compounds. Single fiber (single cell) composed of two walls [14]. Cell wall of growing plant cell is primary wall and this wall is composed of 90% polysaccharide (20%–30% cellulose and structure of remaining polysaccharides has not been completely defined) and 10% glycoproteins. The primary wall forms small proportion of whole fiber. Primary cell wall defines size, shape, and growth rate of cell [14]. Polymerization degree of cellulose in primary wall is lower if compared with secondary wall. Polymerization degree of cellulose in secondary wall is about 14,000. Cellulose crystallinity is higher in secondary wall and microfibrils of secondary walls are thicker [15]. Secondary cell wall (S) which is formed by successive deposition of cellulose layers consists of three sublayers (S1, S2, and S3). Each layer has distinct structure, chemical composition, microfibrillar arrangement, and wall thickness. S2 is the thickest part. S2 forms about 80% of whole secondary wall. Therefore, properties of fiber are mainly depends on properties of S2 layer. Plant fibers are considered as composite materials; rigid and crystalline cellulose microfibrils reinforcement embedded in amorphous hemicelluloses/lignin matrix [16]. Cellulose is main constituent of plant fibers. Crystalline cellulose microfibril is composed of aggregated β-4-linked D-glucan chains. Hemicellulose has short and branched chains. Branched chains containing pendant side groups cause the amorphous structure of hemicellulose. Rigidity of plant originates from lignin. Lignin is three-dimensional copolymer and is formed through a free-radical polymerization of phenolic alcohols (coniferyl, synapyl, and p-coumaryl alcohols) catalyzed by different peroxidases [17].

10.2.2 Seed and fruit fibers

10.2.2.1 Cotton

Cotton plant is a member of the Malvaceae family and belongs to genus Gossypium. The genus Gossypium consists of approximately 50 species of shrubs and small trees found worldwide in both tropical and subtropical areas but only four among them are

grown on a commercial scale in the world; *G. hirsutum*, *G. barbadense*, *G. herbaceum*, and *G. arboreum* [18]. Commercially annual cotton plants are grown and height of this plant only reaches 1.2 m. Seedling emergence normally takes place 4–14 days after planting and first flower buds (called squares) appear within about 35 days. First flower appears 60–80 days after planting and flowers only stay open for 24 h. The fruits which are called bolls begin to develop after pollination. The boll contains seeds of cotton and thus it is considered as fruit. After shedding of pink flowers, individual cells on the surface of the seeds start and these fibers grow, mature, and thicken forming a hollow cotton fiber inside the boll [19]. Fig. 10.1 shows mature cotton plant.

Cotton fibers have 25–60 mm length and 12–45 μm diameter [18]. Chemical and mechanical properties of cotton fibers are listed in Table 10.1. Although cotton is traditionally used to make various textile products [20], cotton reinforced composite materials for automobiles and graphene/cotton composite fabrics as flexible electrode materials for electrochemical capacitors are potential applications of cotton composites [21].

10.2.2.2 Kapok

Kapok belongs to Malvaceae family, formerly Bombacaceae family and botanically known as *Ceiba pentandra* L. Kapok originated in tropical India [23] and cultivated widely in Southeast Asia [24]. Kapok grows in the dry, humid, and very humid tropics. Kapok is a gigantic and fast-growing tree and the height of tree reaches 0.4–0.5 m in 2 years under ideal conditions and tropical species of the tree grows up to 30–60 m. A growing tree produces about 600–900 fruits (seed capsules) annually and these fruits are slender column in shape and usually 5 cm in diameter and 10–20 cm in length [25]. Kapok tree and the fruits are shown in Fig. 10.2A and B, respectively.

Fruits are harvested before full maturation and when the fruit is opened along the central axis fiber bundles are found. Each fruit produces 12–15 g fiber bundles. Extracted fiber bundles have umbrella structure whose one end is fluffy and other

Fig. 10.1 Mature cotton plant.
(From "Getty images" http://www.gettyimages.com/.)

Table 10.1 **Chemical and mechanical properties of cotton fibers [22]**

Chemical properties					Mechanical properties			
Cellulose (%)	**Hemicellulose (%)**	**Lignin (%)**	**Wax (%)**	**Moisture (%)**	**Density (g/cm^3)**	**Elongation (%)**	**Tensile strength (MPa)**	**Young's modulus (GPa)**
85–90	5.7	–	–	–	1.50–1.60	7–8	287–597	5.5–12.6

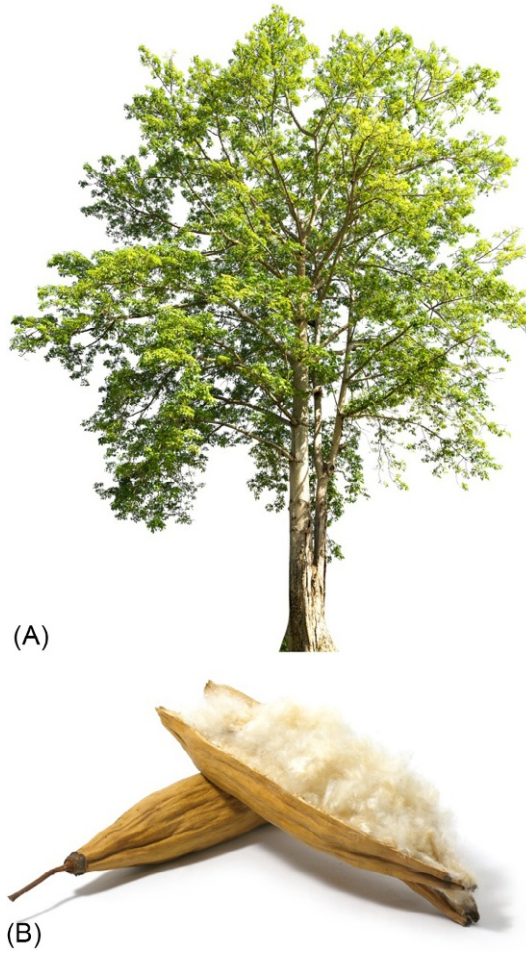

Fig. 10.2 (A) Kapok tree; (B) kapok fruit (seed capsule).
(From "Getty images" http://www.gettyimages.com/.)

end is ordered [26]. Fibers are isolated from the seeds and fruit cover manually by human labor [23]. Kapok fiber bundles are more than 17 mm in length with a diameter of 20–43 μm and this length tends to increase by increasing fruit size [26]. Chemical and mechanical properties of kapok fibers are listed in Table 10.2.

Low strength and inelasticity properties of kapok fibers made these fibers unsuitable for spinning process [27]. Waxy cutin content of fiber surface makes fiber hydrophobic (water repellent) and oleophilic (oil absorbent) and therefore kapok fibers are potential materials for oil removal applications [24]. Kapok fiber is also a sound and heat insulation material as well as a good filling and floating material [28] and the fiber is utilized as packing materials for pillows and quilts [23].

Table 10.2 **Chemical and mechanical properties of kapok fibers [20]**

Chemical properties					Mechanical properties			
Cellulose (%)	**Hemicellulose (%)**	**Lignin (%)**	**Wax (%)**	**Moisture (%)**	**Density (g/cm^3)**	**Elongation (%)**	**Tensile strength (MPa)**	**Young's modulus (GPa)**
35–50	22–45	15–22	2–3	–	1.474	1.2	93.3	4

10.2.3 Bast and leaf fibers

10.2.3.1 Abaca

Banana belongs to family of Musaceae and is botanically known as *Musa textilis*, which is known as Manila hemp, relative of banana [29]. The plant is native to Philippines and after World War II, abaca was successfully cultivated in Ecuador, which supplies 16% of the world market. Alluvial fertile soils having good moisture retention are the best places for the plantation of abaca plant [30]. The plant grows to a height of 3–8 m depending on its variety [31]. Abaca plant produces 12–20 stems (leaves) till harvesting [30]. The inner leaves of the abaca are narrower and contain less fiber and are finer than the outer leaves. Harvesting of the stalks usually takes place between 18 and 24 months from the first shoots. Fiber quantity changes from 1.5% to 3.5% depending on the extraction process; mechanical decortication process yields 3%–3.5% while spindle stripping process yields 1.5%–2% fiber [32]. Abaca plant and extracted abaca fibers are shown in Fig. 10.3A and B.

Extracted abaca fibers have 2–4 m length with a diameter of 150–260 μm [32]. Chemical and mechanical properties of abaca fibers are listed in Table 10.3 [32]. Abaca fibers are the strongest fibers among all commercial natural fibers [31]. Abaca fibers are generally used to make fishing lines, twines, and ropes and marine cordage. Because of its lightness and high strength, abaca fibers have been used as reinforcement for polypropylene matrix to produce automobile body parts [32] and also biocomposites are potential applications of abaca fibers [33,34].

10.2.3.2 Sisal

Sisal belongs to family of Asparagaceae and is botanically known as *Agave sisalana* [35]. The plant is native to Yucatan-Mexico [36] but its commercial potential has spread cultivation areas in tropical countries in Africa, the West Indies, and the Far East [18]. Sisal grows naturally wild on the hedges of fields and railway tracks [37]. The plant grows up to about 2 m high [18]. Flowering of sisal plant takes about 10 years, and after flowering, leaves production ceases. Therefore leaves can be cut from 2 or 3 years to 8 years after planting [36]. Sisal plant produces about 200–250 leaves and each leaf yields about 1000 fiber bundles [35]. This number corresponds to about 4% of a leaf and the remaining is waste. Fig. 10.4 shows (A) sisal plant and (B) extracted sisal fibers.

The lack of woody part makes sisal leaves suitable for fiber extraction. Hand decortication is a historical way of mechanical decortication, leaf is first pounded and then pulp is scraped away with a knife. With a development of mechanical decorticators, this time consuming process is no more used. In the mechanical decoration process, rotating wheel crushes and beats leaves with blunt knives, so that only fibers remain [38]. Sisal fibers are about 1.0–1.5 m in length having a diameter of 100–300 μm [35]. Chemical and mechanical properties of sisal fibers are listed in Table 10.4.

Fig. 10.3 (A) Abaca plant; (B) dried abaca fibers.
(From "Getty images" http://www.gettyimages.com/.)

10.2.3.3 Jute

C. capsularis and *C. olitorius* are two domesticated species of the genus Corchorus [40] in the family Malvaceae [41]. *C. capsularis* and *C. olitorius* are known as white and dark jute, respectively. Jute fibers are one of the most important fibers alongside the cotton [18]. Jute plant is native to tropical and subtropical regions throughout the

Table 10.3 **Chemical and mechanical properties of abaca fiber [32]**

Chemical properties				Mechanical properties			
Cellulose (%)	**Hemicellulose (%)**	**Lignin (%)**	**Moisture (%)**	**Density (g/cm^3)**	**Elongation (%)**	**Tensile strength (MPa)**	**Young's modulus (GPa)**
68.32	19.0	12–13	10–11	1.5	1.1	980	41

Fig. 10.4 (A) Sisal plant and (B) extracted sisal fibers.
(From "Getty images" http://www.gettyimages.com/.)

world [41] and Thailand, Nepal, Indonesia, India, and China are main producers of raw fibers and finished products of jute [42]. Also fiber processing, and spinning and weaving mills all make a very important contribution to the economies of several of these countries [18]. Stalks of jute plants are harvested when height of plant reaches to 3–4 m with a diameter of 2–3 cm [43]. Dried jute plants are shown in Fig. 10.5.

Extraction of jute fibers can be done by water retting which is the most common method for jute retting. Extracted dry fibers by weight are about 4%–4.5% of the green crop [43] and fibers have 1.5–3 m length. Chemical and mechanical properties of jute fibers are listed in Table 10.5. Biodegradability, fire, and heat resistance properties of jute fibers make it suitable for use in various industries such as fashion, travel, luggage, furnishings, and carpets and other floor coverings [18].

10.2.3.4 Flax

L. usitatissimum L. belonging to Linaceae family is the botanical name of flax. Although it has been proposed that Southwest Asia and Mediterranean are the center of origin, flax is grown in a wide range of countries such as China, India,

Table 10.4 **Chemical and mechanical properties of sisal fibers [39]**

Fiber	Chemical properties					Mechanical properties			
	Cellulose (%)	Hemicellulose (%)	Lignin (%)	Wax (%)	Moisture (%)	Density (g/cm^3)	Elongation (%)	Tensile strength (MPa)	Young's modulus (GPa)
Sisal	60–78	10.0–14.2	8–14	2.0	10–22	1.5	2–2.5	511–635	9–22

Fig. 10.5 Dried jute plants.
(From "Getty images" http://www.gettyimages.com/.)

Argentina, Canada, and USA [18,44]. According to data of 2004, flax was grown in 47 countries [44].

Flax is an annual herbaceous plant and it is primarily cultivated for the purpose of seed/oil and fiber production. Distinct varieties have been developed for oilseed and fiber flax. Oilseed flax varieties are highly branched and short and also have high oil content of about 40%–45% while fiber flax varieties are unbranched and tall [45]. Flax plant contains approximately 25% seed, 75% stem, and leaves [46]. Twenty percent of flax stem is fibers and these bast fibers can be produced from only 75% of the plant height. Flax plant grows to a height of 80–150 cm depending on its variety. Extraction of flax fibers can be done by different retting methods such as water retting, dew retting, and enzyme retting. Purpose of retting is separation of technical fiber bundles from the woody tissue. In this process the pectin that holds the fiber bundles together and attached to the central core of the stem is dissolved [18]. Flax plant illustration and field retting of flax are shown in Fig. 10.6A and B, respectively.

Extracted flax fibers have 60–140 cm length with a diameter of 40–80 μm [18]. Each bundle consists of 10–40 individual fibers. Chemical and mechanical properties of flax fibers are listed in Table 10.6 [47]. Abundancy, renewability, and biodegradable properties of flax fiber extend its usage area. Beside the conventional applications of flax fiber such as carpets, towels, ropes, fabrics; it has value added applications such as composites. Flax mat/polypropylene composites were used to produce exterior floor panel for automobiles and also studies of biocomposites containing flax fibers were reported [48,49].

10.2.3.5 Hemp

Cannabis sativa L. belonging to Cannabaceae family is botanical name of hemp plant. Hemp plant is native to Central Asia [18], however it is a widely grown global plant and grown mostly in China satisfying the one third of total hemp demand [50], Philippines, Central Asia, and EU [51]. Rich in nitrogen and nonacidic well-drained soils

Table 10.5 **Chemical and mechanical properties of jute fibers [22]**

Chemical properties			Mechanical properties			
Cellulose (%)	**Hemicellulose (%)**	**Lignin (%)**	**Density (g/cm^3)**	**Elongation (%)**	**Tensile strength (MPa)**	**Young's modulus (GPa)**
61–71	14–20	12–13	1.30	1.5–1.8	393–773	26.5

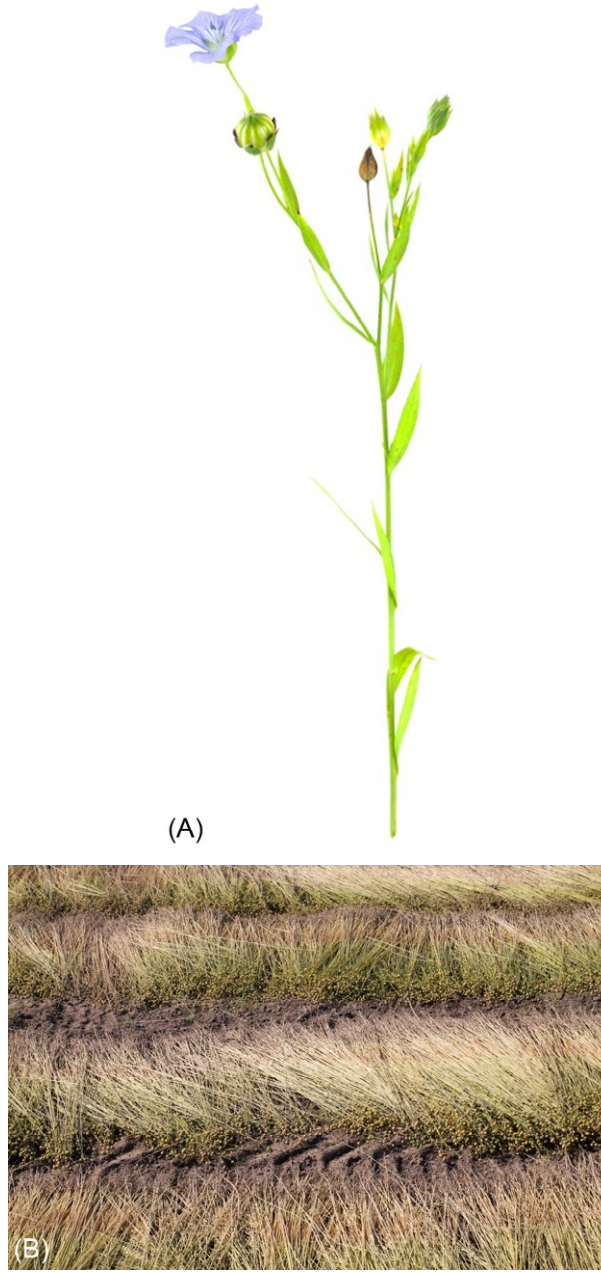

Fig. 10.6 (A) Flax plant illustration; (B) field retting of flax.
(From "Getty images" http://www.gettyimages.com/.)

Table 10.6 **Chemical and mechanical properties of flax fibers [46]**

Chemical properties					Mechanical properties			
Cellulose (%)	Hemicellulose (%)	Lignin (%)	Wax (%)	Moisture (%)	Density (g/cm^3)	Elongation (%)	Tensile strength (MPa)	Young's modulus (GPa)
81	16.7–20.6	13	3	10–22	1.5	2.7–3.2	345–1035	27.6

are best places for plantation of hemp plants. Hemp is annual plant and grown rate of hemp plant from seed is impressive [18]. About 70–90 days after plantation are required for harvesting of the plant for fiber production [51]. Hemp plant grows to a height of 2–4 m without branching and fiber yield is usually 15%–25% [52]. Hemp plant is shown in Fig. 10.7.

The most common and least costly method for extraction of hemp bast fibers is dew retting. Hemp stems are left in a field for up to 5 weeks for this retting method [53]. Extracted hemp fibers have about 1.8 m length or longer [18] with a diameter ranging from 50 to 100 μm [54]. Chemical and mechanical properties of hemp fibers are listed in Table 10.7. Hemp fibers are used in a wide range of products, including fabrics and textiles, yarns and spun fibers, paper, carpeting, home furnishings, construction and insulation materials, auto parts, and composites [55].

10.2.3.6 Henequen

Agave fourcroydes belonging to Liliaceae family is botanical name of henequen plant [57]. The plant is native to Yucatan-Mexico and relative of sisal plant [58]. Life cycle of henequen plant is about 20 years and the plant produces flowers toward the end of its life. Henequen grows in shallow infertile soils [59] and height of plant can reach about 3–8 m [60] and gray leaves of the plant are 76–150 cm long [61]. Henequen plant is shown in Fig. 10.8.

Fig. 10.7 Hemp plant.
(From "Getty images" http://www.gettyimages.com/.)

Table 10.7 **Chemical and mechanical properties of hemp fibers [56]**

Chemical properties				Mechanical properties			
Cellulose (%)	**Hemicellulose (%)**	**Lignin (%)**	**Wax (%)**	**Density (g/cm^3)**	**Elongation (%)**	**Tensile strength (MPa)**	**Young's modulus (GPa)**
68	15	10	0.8	1.47	2–4	690	70

Fig. 10.8 Henequen plant.
(From "Getty images" http://www.gettyimages.com/.)

Leaves can be cut from 6 to maximal 10 years after planting [62]. Fiber yield of henequen leaves are about 3.5%–5% of the weight of the leaves [61]. Extracted henequen fibers are greater than 1 m and diameter of fiber vary from 340 to 470 μm [63]. Chemical and mechanical properties of henequen fibers are listed in Table 10.8.

10.2.3.7 Kenaf

Hibiscus cannabinus L. belonging to Malvaceae family is the botanical name of kenaf. Kenaf is a warm season annual canelike bast fiber crop. The plant is native to northern Africa but the plant can be grown in a wide range of soil types, from sandy desert soils to high organic peat soils however best yields occur on well-drained fertile sites and also abundant soil moisture is necessary to growth of the plant [65]. Kenaf's ability to absorb nitrogen and phosphorus in the soil and ability to accumulate carbon dioxide at a clearly high rate are main two reasons of very high interest in kenaf cultivation [66]. Kenaf plant generally grows to height of 2.5–4.2 m and the diameters of the stalks are in the range of 1.9–3.8 cm in a growing season of 4–5 months. Kenaf plant is composed of 74% stalks and 26% leaves by dry weight and the average composition of the kenaf stalk is 65% woody core and 35% bark [67]. Kenaf stalks consist of two

Table 10.8 Chemical and mechanical properties of henequen fibers [64]

Chemical properties				Mechanical properties		
Cellulose (%)	**Hemicellulose (%)**	**Lignin (%)**	**Wax (%)**	**Elongation (%)**	**Tensile strength (MPa)**	**Young's modulus (GPa)**
60	25	8	2	4.8	500	13.2

Fig. 10.9 Kenaf field.
(From "Getty images" http://www.gettyimages.com/.)

kinds of fiber: an outer fiber (bast) which are long and situated in the cortical layer and an inner fiber (core) which are short and located in the ligneous zone [18]. Fiber yield of kenaf stalks change from 17% to 28% for bast fiber and 20% to 40% for core fiber [68]. Kenaf field is shown in Fig. 10.9.

Kenaf fibers are usually extracted by water retting or dew retting. Extracted kenaf bast fibers are commonly longer than 1 m [68]. Chemical and mechanical properties of kenaf fibers are listed in Table 10.9. Kenaf fibers are generally used to make sacking, canvas, and ropes. Also the plant has been used as alternative raw material in paper and pulp industries to avoid destruction of forests [69].

10.3 Conclusion and future outlook

Various common plant fibers such as jute, flax, hemp, banana, sisal, etc. have been investigated by many researchers because of their availability and properties. Some other studies advance the feasibility to use novel natural fibers as reinforcement for composite materials. Properties of these novel natural fibers are given in Table 10.10.

Good specific modulus values, low density, considerable toughness properties of plant fibers, abundance (and therefore low cost), recyclability, nontoxicity properties are main advantages of natural fibers if compared with other synthetic fibers such as glass and carbon fibers. But on the contrary high moisture absorption, fluctuation of fiber properties depending on the source and age of the plant, poor compatibility between fibers and matrix in composite materials are main disadvantages of plant fibers [75]. To overcome these problems some physical and chemical surface treatments must be used to enhance fiber-matrix adhesion to develop mechanical properties of natural fiber reinforced polymer composites and new genetic researches focusing on the producing high quality fibers having high cellulose content and aiming to reduce the fluctuation of fiber properties must be highlighted.

Table 10.9 **Chemical and mechanical properties of sisal fibers [57]**

Chemical properties				Mechanical properties			
Cellulose (%)	**Hemicellulose (%)**	**Lignin (%)**	**Wax (%)**	**Density (g/cm^3)**	**Elongation (%)**	**Tensile strength (MPa)**	**Young's modulus (GPa)**
31–72	20.3–21.5	8–19	–	1.45	1.6	930	53

Table 10.10 Properties of novel natural fibers

Fiber name	Cellulose (%)	Hemicellulose (%)	Lignin (%)	Density (g/cm^3)	Elongation (%)	Tensile strength (MPa)	Young's modulus (GPa)	Reference
Pennisetum purpureum	46	34	20	–	1.40 ± 0.23	73 ± 6	5.68 ± 0.14	[70]
Sansevieria ehrenbergii	80	11.25	7.8	0.887	2.8–21.7	50–585	1.5–7.67	[71]
Arundo donax	43.2	20.5	17.2	1.168	3.24	248	9.4	[49]
Ferula communis	53.3	8.5	1.4	1.24	4.2 ± 0.2	475.6 ± 15.7	52.7 ± 3.7	[72]
Lygeum spartum L.	–	–	–	1.4997 ± 0.0031	1.49–3.74	64.63–280.03	4.47–13.27	[73]
Althea officinalis L.	44.6	13.5	2.7	1.18	3.9	415.2	65.4	[74]

References

[1] Buchanan R. A weaver's garden: growing plants for natural dyes and fibers. Loveland, CO: Interweave Press; 1987.

[2] Arthanarieswaran VP, Kumaravel A, Kathirselvam M. Evaluation of mechanical properties of banana and sisal fiber reinforced epoxy composites: influence of glass fiber hybridization. Mater Des 2014;64:194–202.

[3] Zakikhani P, Zahari R, Sultan MTH, Majid DL. Extraction and preparation of bamboo fibre-reinforced composites. Mater Des 2014;63:820–8.

[4] Thedinger S. Prohibition in the United States: International and US regulation and control of industrial hemp. Colo J Int'l Envtl L Pol'y 2005;17:419.

[5] Venugopal P, Giasuddin B, Sivaji J. Ethics and social responsibility in Indian textile industry (a Study on Textile Industries of Coimbatore and Tirupur, Tamil Nadu). Chanakya Int J Bus Res 2015;1(1):62–7.

[6] Fisher CH. History of natural fibers. J Macromol Sci—Chem 1981;15(7):1345–75.

[7] Moulherat C, Tengberg M, Haquet J-F, Mille Bt. First evidence of cotton at Neolithic Mehrgarh, Pakistan: analysis of mineralized fibers from a copper bead. J Archaeol Sci 2002;29(12):1393–401.

[8] Bouchaud C, Tengberg M, Dal Prà P. Cotton cultivation and textile production in the Arabian Peninsula during antiquity; the evidence from Madâ'in Sâlih (Saudi Arabia) and Qal'at al-Bahrain. Veg Hist Archaeobotany 2011;20(5):405–17.

[9] Wendel JF, Grover CE. Taxonomy and evolution of the cotton genus, *Gossypium*. Madison, WI: American Society of Agronomy, Inc., Crop Science Society of America, Inc., Soil Science Society of America, Inc; 2015. p. 25–44.

[10] Diamond J. Evolution, consequences and future of plant and animal domestication. Nature 2002;418(6898):700–7.

[11] Liu FH, Chen X, Long B, Shuai RY, Long CL. Historical and botanical evidence of distribution, cultivation and utilization of Linum usitatissimum L. (flax) in China. Veg Hist Archaeobotany 2011;20(6):561.

[12] Manaila E, Stelescu MD, Craciun G, Surdu L. Effects of benzoyl peroxide on some properties of composites based on hemp and natural rubber. Polym Bull 2014;71(8):2001–22.

[13] Kalia S, Kaith BS, Kaur I, editors. Cellulose fibers: bio-and nano-polymer composites: green chemistry and technology. Springer Science & Business Media; 2011.

[14] McNeil M, Darvill AG, Fry SC, Albersheim P. Structure and function of the primary cell walls of plants. Annu Rev Biophys 1984;53(1):625–63.

[15] Harris PJ. Primary and secondary plant cell walls: a comparative overview. N Z J For Sci 2006;36(1):36.

[16] Northcote DH. Chemistry of the plant cell wall. Annu Rev Plant Physiol 1972;23 (1):113–32.

[17] Radotić K, Simić-Krstić J, Jeremić M, Trifunović M. A study of lignin formation at the molecular level by scanning tunneling microscopy. Biophys J 1994;66(6):1763.

[18] Bismarck A, Mishra S, Lampke T. Plant fibers as reinforcement for green composites. In: Mohanty AK, Misra M, Drzal L, editors. Natural fibers, biopolymers and biocomposites. Boca Raton, FL: CRC Press Tailor and Francis Group; 2005.

[19] DeJoode DR, Wendel JF. Genetic diversity and origin of the Hawaiian Islands cotton, *Gossypium tomentosum*. Am J Bot 1992;1311–9.

[20] Smole MS, Hribernik S, Stana Kleinschek K, Kreže T. Plant fibres for textile and technical applications. Adv Agrophys Res 2013;10:52372.

[21] Holbery J, Houston D. Natural-fiber-reinforced polymer composites in automotive applications. JOM 2006;58(11):80–6.
[22] Xu L-L, Guo M-X, Liua S, Bian S-W. Graphene/cotton composite fabrics as flexible electrode materials for electrochemical capacitors. RSC Adv 2015;5(32):25244–9.
[23] Hori K, et al. Excellent oil absorbent kapok [*Ceiba pentandra* (L.) Gaertn.] fiber: fiber structure, chemical characteristics, and application. J Wood Sci 2000;46(5):401–4.
[24] Chaiarrekij S, et al. Kapok I: characteristics of Kapok fiber as a potential pulp source for papermaking. Bioresources 2011;7(1):0475–88.
[25] Brown SH. Ceiba pentandra Family: Malvaceae. http://lee.ifas.ufl.edu/hort/GardenPubsAZ/Ceiba_pentandra.pdf.
[26] Wu HY, Wang FM, Tan F. Study on Java Kapok fruit and fiber length. Adv Mater Res 2011;332. Trans Tech Publications.
[27] Huang X, Lim T-T. Performance and mechanism of a hydrophobic-oleophilic kapok filter for oil/water separation. Desalination 2006;190(1):295–307.
[28] Ding Y, et al. The adsorption character of kapok fiber and reactive dyeing technology on modified kapok fiber. Ratio 2014;100:1.
[29] Lacuna-Richman C. The role of abaca (*Musa textilis*) in the household economy of a forest village. Small-scale For Econ Manage Policy 2002;1(1):93–101.
[30] Bande MM. Ecophysiological and agronomic response of Abaca (*Musa textilis*) to different resource conditions in Leyte Island, Philippines. Diss. University of Hohenheim; 2012.
[31] Spencer JE. The abaca plant and its fiber, Manila hemp. Econ Bot 1953;7(3):195–213.
[32] Vijayalakshmi K, et al. Abaca fibre. Trans Eng Sci 2014;2:16–9.
[33] Shibata M, et al. Biocomposites made from short abaca fiber and biodegradable polyesters. Macromol Mater Eng 2003;288(1):35–43.
[34] Shibata M, et al. Biodegradable polyester composites reinforced with short abaca fiber. J Appl Polym Sci 2002;85(1):129–38.
[35] Li Y, Mai Y-W, Lin Y. Sisal fibre and its composites: a review of recent developments. Compos Sci Technol 2000;60(11):2037–55.
[36] Hartemink AE, Wienk JF. Sisal production and soil fertility decline in Tanzania. Outlook Agric 1995;24:91.
[37] Mukherjee PS, Satyanarayana KG. Structure and properties of some vegetable fibres. J Mater Sci 1984;19(12):3925–34.
[38] de Andrade Silva F, Chawla N, de Toledo Filho RD. Tensile behavior of high performance natural (sisal) fibers. Compos Sci Technol 2008;68(15):3438–43.
[39] Indran S, Edwin Raj R, Sreenivasan VS. Characterization of new natural cellulosic fiber from *Cissus quadrangularis* root. Carbohydr Polym 2014;110:423–9.
[40] Kundu A, et al. Origins of white (*Corchorus capsularis* L.) and dark (*C. olitorius* L.) jute: a reevaluation based on nuclear and chloroplast microsatellites. J Plant Biochem Biotechnol 2013;22(4):372–81.
[41] Olawuyi PO, et al. Chromosome studies in jute plant (*Corchorus olitorius*). Eur J Biotechnol Biosci 2014;2(1):1–3.
[42] Ahmed Z, Akhter F. Jute retting: an overview. Online J Biol Sci 2001;1:685–8.
[43] Campbell JK. Dibble sticks, donkeys, and diesels: machines in crop production. Manila, Philippines: International Rice Research Institute; 1990.
[44] Jhala AJ, Hall LM. Flax (*Linum usitatissimum* L.): current uses and future applications. Aust J Basic Appl Sci 2010;4(9):4304–12.
[45] Ehrensing DT. Flax. Corvallis, OR: Extension Service, Oregon State University; 2008.
[46] Kurt O. Ketenin (*Linum usitatissimum* L.) Üretimi ve Kullanım Alanları. OMÜZF Dergisi 1996;11(1):189–94.

[47] Kumar R, Yakubu MK, Anandjiwala RD. Biodegradation of flax fiber reinforced poly lactic acid. Express Polym Lett 2010;4(7):423–30.
[48] Li X, et al. Thermal diffusivity, thermal conductivity, and specific heat of flax fiber-HDPE biocomposites at processing temperatures. Compos Sci Technol 2008;68(7):1753–8.
[49] Fiore V, Scalici T, Valenza A. Characterization of a new natural fiber from *Arundo donax* L. as potential reinforcement of polymer composites. Carbohydr Polym 2014; 106:77–83.
[50] Hu R, Lim J-K. Fabrication and mechanical properties of completely biodegradable hemp fiber reinforced polylactic acid composites. J Compos Mater 2007;41(13):1655–69.
[51] Shahzad A. Hemp fiber and its composites—a review. J Compos Mater 2012;46 (8):973–86.
[52] Pervaiz M, Sain MM. Carbon storage potential in natural fiber composites. Resour Conserv Recycl 2003;39(4):325–40.
[53] Karus M, Vogt D. European hemp industry: cultivation, processing and product lines. Euphytica 2004;140(1–2):7–12.
[54] Fan M. Characterization and performance of elementary hemp fibres: factors influencing tensile strength. Bioresources 2010;5(4):2307–22.
[55] Indran S, Edwin Raj R, Sreenivasan VS. Characterization of new natural cellulosic fiber from *Cissus quadrangularis* root. Carbohydr Polym 2014;110:423–9.
[56] Johnson R. Hemp as an agricultural commodity. Washington, DC: Library of Congress, Congressional Research Service; 2014.
[57] Infante D, et al. Asexual genetic variability in *Agave fourcroydes*. Plant Sci 2003;164 (2):223–30.
[58] Rendón-Salcido LA, et al. Azúcares y subproductos alcohólicos de henequén (*Agave fourcroydes*) en función de la edad de la planta y el clima. Rev Fitotec Mex 2009;32 (1):39–44.
[59] MartÍNez-Torres J, et al. Ethanol production from two varieties of henequen (*Agave fourcroydes* Lem). GCB Bioenergy 2011;3(1):37–42.
[60] Piven NM, et al. Reproductive biology of henequen (*Agave fourcroydes*) and its wild ancestor *Agave angustifolia* (Agavaceae). I. Gametophyte development. Am J Bot 2001;88(11):1966–76.
[61] No, Cırcular. Sısal And Henequén, Plants Yıeldıng Fıber For Bınder Twıne.
[62] Nobel PS. PAR, water, and temperature limitations on the productivity of cultivated *Agave fourcroydes* (henequen). J Appl Ecol 1985;157–73.
[63] Cazaurang-Martinez MN, et al. Physical and mechanical properties of henequen fibers. J Appl Polym Sci 1991;43(4):749–56.
[64] Seki Y, et al. Extraction and properties of *Ferula communis* (chakshir) fibers as novel reinforcement for composites materials. Compos Part B Eng 2013;44(1):517–23.
[65] Webber III CL, Bhardwaj HL, Bledsoe VK. Kenaf production: fiber, feed, and seed. Trends in new crops and new uses. Alexandria, VA: ASHS Press; 2002. p. 327–339.
[66] Bazen EF, Roberts RK, English BC. Economic feasibility of kenaf production in three Tennessee counties. J Agribusiness 2006. 24(2):135.
[67] Webber III CL, Bledsoe VK. Kenaf yield components and plant composition. Trends New Crops New Uses 2002;348–57.
[68] Sanadi AR, et al. Renewable agricultural fibers as reinforcing fillers in plastics: mechanical properties of kenaf fiber-polypropylene composites. Ind Eng Chem Res 1995;34 (5):1889–96.
[69] Akil HM, et al. Kenaf fiber reinforced composites: a review. Mater Des 2011;32 (8):4107–21.

[70] Ridzuan MJM, et al. Characterisation of natural cellulosic fibre from *Pennisetum purpureum* stem as potential reinforcement of polymer composites. Mater Des 2016;89:839–47.
[71] Sathishkumar TP, et al. Characterization of new cellulose *Sansevieria ehrenbergii* fibers for polymer composites. Compos Interface 2013;20(8):575–93.
[72] Seki Y, et al. Extraction and properties of *Ferula communis* (chakshir) fibers as novel reinforcement for composites materials. Compos Part B Eng 2013;44(1):517–23.
[73] Belouadah Z, Ati A, Rokbi M. Characterization of new natural cellulosic fiber from *Lygeum spartum* L. Carbohydr Polym 2015;134:429–37.
[74] Sarikanat M, et al. Determination of properties of *Althaea officinalis* L. (Marshmallow) fibres as a potential plant fibre in polymeric composite materials. Compos Part B Eng 2014;57:180–6.
[75] Fiore V, Di Bella G, Valenza A. The effect of alkaline treatment on mechanical properties of kenaf fibers and their epoxy composites. Compos Part B: Eng 2015;68:14–21.

This page intentionally left blank

The use of biotechnology for green composites

11

Metehan Atagür, M. Özgür Seydibeyoğlu
Izmir Katip Çelebi University, Izmir, Turkey

11.1 Introduction to green composites

11.1.1 Introduction

Green chemistry and green materials have been one of the most important areas for the scientific community to reduce the wastes with increased environmental problems. Moreover, the consumers are also quite cautious for the energy and materials they consume, and they prefer biobased materials, and this is also reflected in the area of materials/composites and polymers [1]. The worldwide interest in green composites has accelerated due to the desire and need to find eco-friendly material. As indicated by ISI Web of Sciences and Thomas Innovations, there is a tremendous increase in the number of publication and publication citations on green composites in recent years, as shown in Fig. 11.1.

Furthermore, the green composites have been the top priority areas in the polymeric materials. The growth rate for the green plastics is around 18% for the United States and 14% for Europe [1]. The Ministry of Energy in the United States is planning to increase the use of natural-resourced materials to 10% until 2020 and to 50% until 2050 [2]. By the year 2020, it is expected that annual consumption of bioplastics will be around 3.1 million ton and that is close to 5% of the whole plastic industry [2]. The main application areas for the green polymers are packaging, biomedical, automotive, textile, and construction.

In this chapter, detailed explanations for the biopolymers will be given, the latest research on biotechnology for green composites will be explained, and some of the applications will be briefly shown. Before explaining these, an important topic for the bioplastics and biocomposites is the life-cycle assessment, which will be explained in the following section.

11.1.2 Life-cycle assessment

As stated above, environmental problems, global warming, and increased carbon footprint necessitate the use of environmentally friendly materials and the increased use of natural resources [3]. In this area, a very tool named as life-cycle assessment has been developed, and it has been used for 30 years, and there is still a continuous improvement in the method [4].

Fiber Technology for Fiber-Reinforced Composites. http://dx.doi.org/10.1016/B978-0-08-101871-2.00011-4

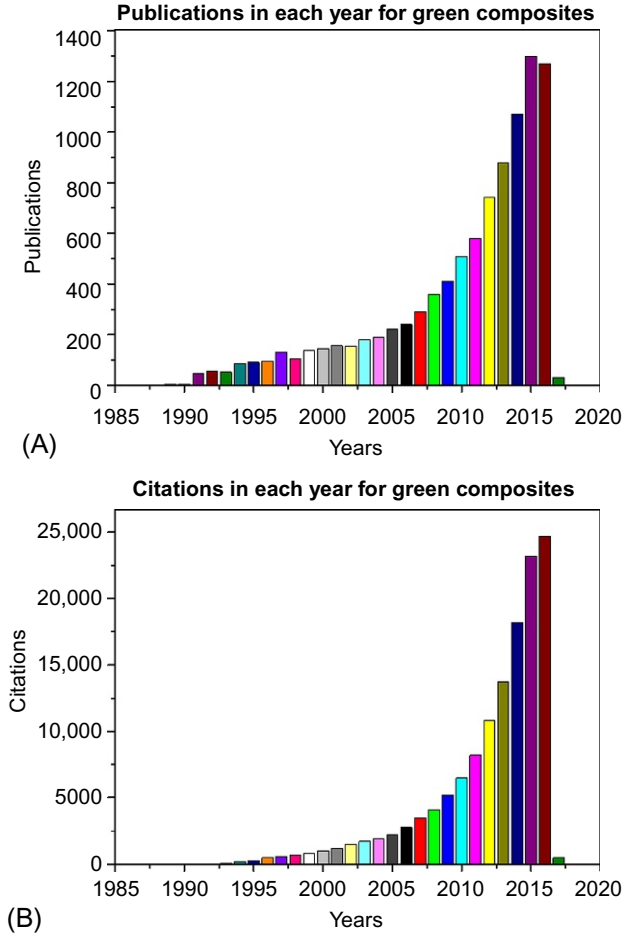

Fig. 11.1 (A) Number of publications on green composites in recent years. (B) Number of citations on green composites in recent years.
Source: ISI Web of Science.

Life-cycle assessment (LCA) is a systematic method to evaluate, manage, and report the environmental effects of a product or service during the entire chain including the raw materials, production, transportation, and consumer usage. Fig. 11.2 shows the schema of LCA [5].

With LCA, the whole environmental effects including the usage of energy and the volume of water used are all considered for manufacturing a piece of item. In this way, all the risks and opportunities are determined in a holistic approach. As the use of LCA increases, it will be easier to build a sustainable environment with optimized natural resources and optimized financing [6].

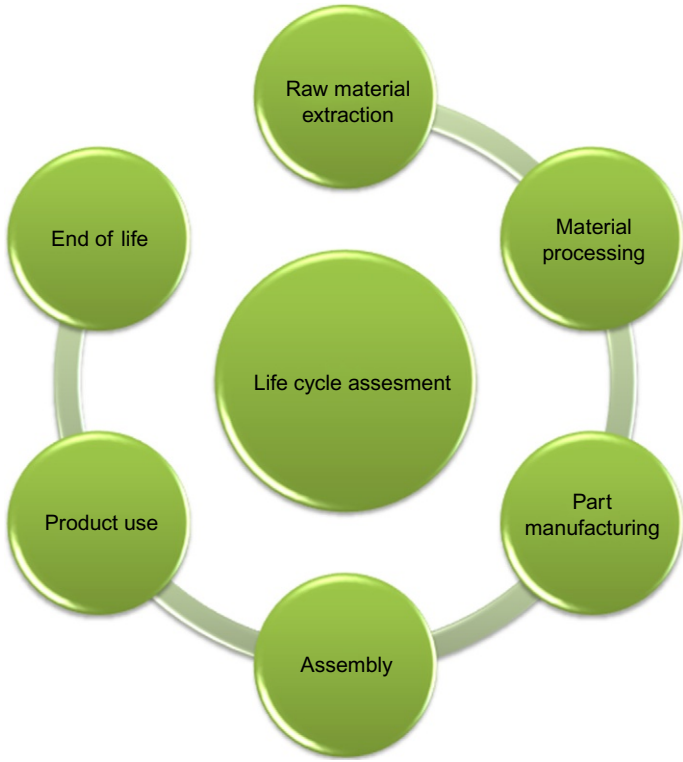

Fig. 11.2 Stages of LCA.

11.1.3 LCA's of composite materials

One of the most important factors affecting the development of polymeric composites was the performance characteristics such as high rigidity expected from studies. The importance of the life-cycle in the design of composite materials has begun in recent years for the production of recyclable materials and the work done for durability analyzes [7].

The benefits of using environmentally friendly materials instead of fossil-fuel-based raw materials and the reduction of greenhouse gas emissions have been a driving force in the production, development, and use of new biologically based materials by attracting great interest from scientists, politicians, and industry. In order to make strategic decisions, the environmental impacts of biomass materials should be analyzed in a comprehensive and effective manner compared with the fossil- or mineral-based counterparts already in use. Life-cycle analyzes are applied to many biobased materials that can be found in the literature [8–14].

For example, the energy intensity of carbon-fiber-reinforced composites used in passenger cars is calculated in the study made by Suzuki and Takahashi. Energy intensity and cost calculations of carbon fibers showed that there are impediments for the

application [8]. The energy use and carbon emission of a rooftop wind turbine were investigated by Rankine et al., and the results showed that lowering carbon emission may be ensured by microgeneration with the usage of small generators in the house [12]. The life-cycle cost of all-composite suspension bridge was analyzed by Meiarashi et al., and they compared conventional steel bridges with composite ones [13]. The use of biodegradable fibers and resins in place of synthetic fibers and resins has gained considerable interest, and accelerating the work in this field has been supported in recent years in the literature [15,16].

11.2 Natural polymer sources

Natural polymers can be found in living organisms or are the type of polymers that can be created by them. The polymer can be synthesized from renewable sources using bioresources for bioplastic production. It is possible to collect natural polymers under two headings, living organisms and renewable sources. They can be directly living organisms such as carbon hydrates or proteins, or they can be synthesized with the help of sources such as renewable lactic acid and triglycerides [17].

Interest in natural polymers is increasing day by day as synthetic polymers are not environmentally friendly, and the oil resources are limited, and their production is far from being sustainable. Natural polymers have been found suitable to substitute petroleum-based polymers. Scientists have concentrated on the production and development of micro- and nanosized high-performance materials in their work. Studies of recent years have shown that natural polymers are of great interest due to their morphological and physical advantages compared with synthetic polymers [18].

11.2.1 Polylactic acid

Polylactic family is a group of polymers with various copolymers. Polylactic acid (PLA) is the biggest biopolymer in terms of the quantity produced annually in the world reaching a price close to polypropylene. PLA is a semicrystalline material with an aliphatic backbone (Fig. 11.3). This polymer has properties close to polyethylene terephthalate and polypropylene, which are very much used in the polymer industry [19]. PLA like other biopolymers such as starch and sugar beet is biodegradable under certain composting environment. Besides being environmentally friendly, it is also biocompatible, which enables it to be used in many biomedical applications. It is commonly used in the packaging area, agricultural films, and biomedical applications [20].

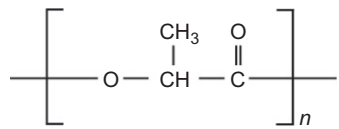

Fig. 11.3 General chemical structure of polylactic acid.

Studies on increasing the mechanical properties of PLA-based composites and a specific purpose of use are found in the literature. The production of PLA-based biofiber-reinforced composite materials was made using production techniques such as compression and injection molding [21]. Many authors have worked on studies to improve the physical and thermal properties of PLA-based composites and studies to improve the mechanical properties of the fibers as an advantage of providing high toughness of the fibers [22–26].

11.2.2 Polyhydroxyalkanoates

Polyhydroxyalkanoates (PHA) are very important biopolymers, which were first discovered in 1927 as a food storage in certain bacteria. In the 1950s, it was discovered that it has thermoplastic properties. In the 1980s and 1990s, research on PHA was accelerated. This class of polymers is produced using bacteria, *Alcaligenes eutrophus*. Polyhydroxy butyrate (PHB) is the homopolymer form of this family, but it is brittle. To avoid the brittleness and to have better processing, copolymers of PHB with valeric acid, polyhydroxybutyrate-co-valerate copolymers, have been produced [27,28]. Among many different types, PHA has a linear long-chain structure with 3-hydroxy fatty-acid functional groups in the main backbone [29]. General chemical structure of PHA was shown in Fig. 11.4.

PHA matrix composites are comparatively new for composite world. The studies continue in the literature in order to modify the properties of PHA matrix, especially for improving the mechanical properties. There are many research about the composites, which includes PHA matrix; for example, Choi et al. investigated PHBV/montmorillonite nanocomposites prepared by melt intercalation method. There is a nucleating effect of organoclay, and this made an increase in temperature and crystallization rate of PHBV. Furthermore, the nanocomposites displayed meaningful increases in tensile strength and thermal stability [30]. Sanchez-Garcia et al. focused on the structure and barrier properties of PHB and PHB/clay nanocomposites. Intergallery swollen organomodified montmorillonite clays added to the PHB matrix and a high dispersion of filler are obtained; however, this addition makes instability in melt of the biopolymer [31].

11.2.3 Cellulose acetate

Biopolymers can be derived by reaction under certain conditions by using cellulose as a natural polymer. For this reason, cellulose esters can be seen as a convenient and suitable biodegradable polymer source. Cellulose-derived polymers used in the

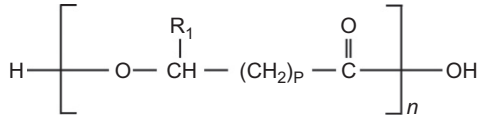

Fig. 11.4 General chemical structure of polyhydroxyalkanoates.

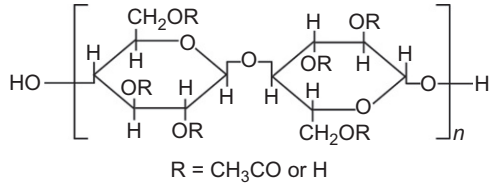

Fig. 11.5 General chemical structure of cellulose acetates.

production of polymer-based composites are generally cellulose acetate (CA) (Fig. 11.5), cellulose acetate propionate (CAP), and cellulose acetate butyrate (CAB) [32]. Green composites include cellulose esters that can be produced by extrusion production method and formed by compression, injection, blow, or rotational molding.

There are many studies made by using cellulose esters to produce green composite materials [33–39]. Glasser et al. [40] used different types of fibers, which are discontinuous water-extracted steam-exploded fibers, alkali-extracted fibers, untreated oat fibers, and acetylated fiber, in order to produce CAB matrix green composite. Acetylated lignocellulosic fibers showed good adhesion in comparison to chemically unmodified fiber because a decrease in the fiber pull-out phenomena is observed. Mohanty et al. [41] have indicated a study about green composites that include CAB and CAP as matrix phase and single fibers of flax and ramie as dispersed phase. Single-fiber fragmentation testing for composites was made. It was found that flax fibers provide better adhesion to CAB compared with ramie fibers. Furthermore, they showed that reinforcement effect of the fibers is considerably high in terms of improvement in the tensile and flexural properties of the biocomposites and for their shear storage modulus.

11.2.4 Thermoplastic starch

Starch is one of the most abundant natural polymers found in nature. It has begun to be used in the development of many new materials including biocomposites. It is a raw material used for the production of thermoplastic starch (TPS). It is known that the production of TPS is made with the help of plasticizers by interrupting molecular chain interactions under certain conditions. Water and glycerol are some of the plasticizer additives commonly used in TPS production [42].

TPS has become a common polymer used as a matrix material as it can be easily manufactured like other thermoplastic materials with temperature and pressure. However, when compared with other thermoplastics, TPS has disadvantages such as being water soluble and having low mechanical properties [43]. There has been research to improve mechanical properties with different reinforcing materials [43–47] and the combination with other thermoplastics [48–52]. Maksimov et al. have made nanocomposite production using unmodified montmorillonite and starch and obtained water-resistant and low water vapor permeability composite material by adding low

amount of clay [53]. Ma et al. used multiwalled carbon nanotubes as reinforcing material and processing with TPS matrix to reduce the tensile strength of nanocomposite production and increase tensile strength and modulus. The composites displayed restrained retrogradation [54].

11.2.5 Biobased polyethylene

In recent years, polyolefin resins, especially polyethylene (PE) and polypropylene (PP), have been synthesized from biodegradable monomers instead of petroleum-derived monomers to avoid the problems created by petrochemical plastics [55,56]. Along with the developing technology, biodegradable PE (bio-PE) bioethanol was synthesized at industrial scale by catalytic dehydrated to ethylene [55]. Structure of bioethanol, bioethylene, and biopolyethylene was shown in Fig. 11.6.

The production cost of bio-PE is more than fossil PE. Because it is an eco-friendly resource produced from biomass, bio-PE is more advantageous for some special applications [57].

There are only a few publications in the literature on biobased polyethylene composites and blends [58,59]. Castro et al. have been subjected to bending, impact, DMTA, and TG and DSC tests on HDPE-based composites produced from HDPE synthesized from sugarcane ethanol and lignocellulosic curuaua fibers. Impact modifier and hydroxyl-terminated polybutadiene (LHPB) were also used as coupling agent. Some properties such as flexural strength and bending modulus of the curuaua fibers have been approached to the properties of polyethylenes. LHPB addition has been shown to improve impact strength of composites [59].

11.2.6 Polybutylenesuccinate

Polybutylenesuccinate (PBS) is chemically synthesized by polycondensation of 1,4-butanediol with succinic acid (Fig. 11.7). PBS is a commercially available aliphatic thermoplastic polyester because of its thermal and chemical resistance, melt

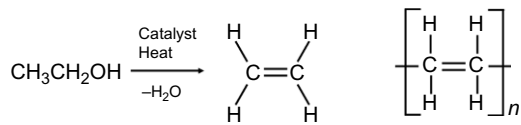

Fig. 11.6 Structure of bioethanol, bioethylene, and biopolyethylene.

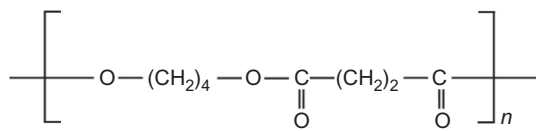

Fig. 11.7 General chemical structure of polybutylene succinate.

processability, and biodegradability [60]. Unlike other conventional thermoplastic polymers such as PP and PE, PBS is quite expensive and has lower mechanical properties [61].

In order to reduce cost and modify properties of PBS-based materials, starch [62,63], strain protein [64,65], and many different plant fibers [66–69] are blended with PBS or produced as a composite. Moreover, blending with fibers is an efficient, easy, and economical method [70]. Liu et al. evaluated the effect of different fiber surface modifications using a coupling agent in flax-reinforced PBS-based biocomposites. As a result of using the coupling agent, tensile strength and modulus values of the composites increased, and the values of the elongation at break decreased [71].

11.2.7 Others

Chitin and chitosan are natural aminopolysaccharide polymers used in biomedical and many other areas with unique structural and multidimensional properties [72–74]. At the same time, chitin and chitosan polymers have found many different application areas due to their sustainable, biocompatible, biodegradable, antimicrobial, and nontoxic properties [75–77]. Ojagh et al. produced a new biodegradable film from chitosan and cinnamon essential oil. The properties of CEO-added chitosan film have been improved with the result of cross-linking with chitosan and cinnamon oil [78].

Alginates are linear polysaccharides found in nature. They are synthesized from soil bacteria and brown seaweed [79]. Sodium alginates are the most commonly used alginates, and the industry is frequently used since it is known to be the first by-product of algal purification [80]. Alginates have many applications such as stabilizers and gel-forming, film-forming, or water-binding agents in the industry [81]. These applications vary from textile dyeing to ceramic production in many ranges. They can also be used from the production of welding rods to water treatment. The polymer is soluble in cold water and may form a thermostable gel [82–84]. These features also make it possible to use it in the food industry as well, for example, in custard creams or in reconstituted foods. The polymer can also act as a stabilizer in beverages, ice creams, emulsions, and sauces [85].

In the presence of the heterogeneous catalysis system, propylene oxide and carbon dioxide produce a regular alternating copolymer poly(propylene carbonate) PPC, which is a biodegradable aliphatic polyester [86,87]; PPC polymer is a melt processable, has high transparency, and may be biodegradable in soil and buffer solution. In the literature, biodegradable composites formed by PPC matrix-reinforced unmodified granular cornstarch have been studied [88,89]. Ge et al. blend starch-g-poly(methyl acrylate) (S-g-PMA) copolymer containing 28.6 wt% PMA with PPC in order to develop the dispersed phase and PPC matrix phase [90].

11.3 Applications

For about half a century, vast amount of research is being carried in the field of bioplastics and biocomposites, which illustrates their significance. However, research and development is just part of a product life-cycle. The real engineering starts when

the science that is developed is being applied to a specific application. Thus, the engineering process either introduces a new material (or product) into the market or supplements an existing one. Some of the applications that bioplastics and/or biocomposites are applied include packaging, civil, construction and building, biomedical, and automotive [91].

11.3.1 Packaging applications

Among the total plastic usage, "packaging" occupies the top position with 41%, of which about 20% is used in food industry. Packaging waste is one of the most wastes in the landfills because most of the packaging materials are made of synthetic plastics and not renewable or degradable natural resources [91].

The Biotec research team developed a film called Bioflex. This film is made from TPS granules and is manufactured using the extrusion process. The research study showed that Bioflex film has good barrier properties against water vapor permeability. Bioflex film can be used instead of traditional foil [92]. Avérous et al. [45] examined the plasticized wheat straw (PWS) and cellulose fiber composites in their packaging applications. PWS has been found to have a significant increase in durability values when blended with cellulose fibers [93].

11.3.2 Automotive applications

In recent years, the automotive industry has been accelerating cost- and weight-reduction efforts on car parts by using low-density reinforcements. In these works, it is aimed to provide performance with natural fiber usage instead of using glass, aramid, or carbon fiber. In this context, the fibers used in the interior parts of cars with the help of the fibers obtained from renewable sources have gained a good reputation day by day. In 1996, Mercedes-Benz used jute reinforcement in epoxy matrix in E-class vehicles [94]. Green composites were used in Audi A2 middle-class cars in the interior panels of polyurethane doors reinforced with flax/sisal fiber mixture at the beginning of the 2000s [95]. Toyota has declared its leadership about adaptation of environmentally friendly bioplastic materials in the brand. In RAUM 2003 model, natural rubber-filled composite material is used in the spare tire cover. The PLA-based matrix material obtained from the sugarcane and sweet potato was reinforced with the kenaf plant [96]. In the past years, Ford has used the Flex 2010 parachute in the storage bin and on the inner lid of wheat straw reinforcement. BMW has used prepreg natural fiber mats and a thermosetting acrylic copolymer for the bottom door panel in 7 Series sedan vehicles [97].

11.4 Conclusion and future outlook

As the need for environmentally friendly materials increases, the need for green chemistry and greener materials increases; the use of biobased polymers with affordable costs will be the primary subject for the whole industry including packaging,

automotive, construction, textile, and biomedical. Improved processing conditions and tailored degradability/compostability with reduced prices will be the key issues for the new technologies. The use of nonfood resources is of great importance such as the use of CO_2 and marine resources is becoming more important. Carbon footprint analysis, LCA, and other systematic approaches will show the main advantages of these polymers. Instead of using toxic chemical to make oxodegradable films, environmentally friendly biologically resourced biodegradable polymers should be more commonly used.

References

[1] Ashori A. Wood–plastic composites as promising green-composites for automotive industries! Bioresour Technol 2008;99(11):4661–7.
[2] Wolf O, Crank M, Patel M, Marscheider-Weidemann F, Schleich J, Hüsing B, et al. Technical report EUR 22103 EN. Europe: Techno-economic Feasibility of Large-scale Production of Bio-based Polymers.
[3] Finnveden G, Hauschild MZ, Ekvall T, Guinée J, Heijungs R, Hellweg S, et al. Recent developments in life cycle assessment. J Environ Manag 2009;91(1):1–21.
[4] Guinee JB, Heijungs R, Huppes G, Zamagni A, Masoni P, Buonamici R, et al. Life cycle assessment: past, present, and future†. Environ Sci Technol 2010;45(1):90–6.
[5] ISO. ISO 14040 International Standard. Environmental management—life cycle assessment—principles and framework. In: Geneva, Switzerland: International Organisation for Standardization; 2006.
[6] Fava J, Hall J. Why take a life cycle approach. Life cycle initiative; 2004.
[7] Leterrier Y. 2.33—life cycle engineering of composites A2—Kelly, Anthony. In: -Zweben C, editor. Comprehensive composite materials. Pergamon: Oxford; 2000. p. 1073–102.
[8] Suzuki T, Takahashi J. Prediction of energy intensity of carbon fiber reinforced plastics for mass-produced passenger cars. In: Ninth Japan International SAMPE Symposium JISSE-9, Tokyo, Japan; 2005.
[9] Dhingra R, Overly JG, Davis GA. Life-cycle environmental evaluation of aluminum and composite intensive vehicles, In: Center for Clean Products and Clean Technologies, University of Tennessee; 1999.
[10] Das S. The cost of automotive polymer composites: a review and assessment of DOE's lightweight materials composites research. Oak Ridge, TN: Oak Ridge National Laboratory; 2001.
[11] Kasai J. Life cycle assessment, evaluation method for sustainable development. JSAE Rev 1999;20(3):387–94.
[12] Rankine R, Chick J, Harrison G. Energy and carbon audit of a rooftop wind turbine proceedings of the institution of mechanical engineers, Part A. J Power Energy 2006; 220(7):643–54.
[13] Meiarashi S, Nishizaki I, Kishima T. Life-cycle cost of all-composite suspension bridge. J Compos Constr 2002;6(4):206–14.
[14] Ehlen MA. Life-cycle costs of fiber-reinforced-polymer bridge decks. J Mater Civ Eng 1999;11(3):224–30.
[15] Pervaiz M, Sain MM. Carbon storage potential in natural fiber composites. Resour Conserv Recycl 2003;39(4):325–40.

[16] Corbière-Nicollier T, Laban BG, Lundquist L, Leterrier Y, Månson J-A, Jolliet O. Life cycle assessment of biofibres replacing glass fibres as reinforcement in plastics. Resour Conserv Recycl 2001;33(4):267–87.
[17] Stevens ES. Green plastics: an introduction to the new science of biodegradable plastics. Princeton, NJ: Princeton University Press; 2002.
[18] John MJ, Thomas S, editors. Natural polymers: composites, vol. 1. Royal Society of Chemistry; 2012.
[19] Henton DE, Gruber P, Lunt J, Randall J. Polylactic acid technology. Nat Fibers Biopolym Biocompos 2005;16:527–77.
[20] Gupta B, Revagade N, Hilborn J. Poly (lactic acid) fiber: an overview. Prog Polym Sci 2007;32(4):455–82.
[21] Kasuga T, Ota Y, Nogami M, Abe Y. Preparation and mechanical properties of polylactic acid composites containing hydroxyapatite fibers. Biomaterials 2000;22(1):19–23.
[22] Nam JY, Sinha Ray S, Okamoto M. Crystallization behavior and morphology of biodegradable polylactide/layered silicate nanocomposite. Macromolecules 2003;36(19):7126–31.
[23] Iannace S, Ali R, Nicolais L. Effect of processing conditions on dimensions of sisal fibers in thermoplastic biodegradable composites. J Appl Polym Sci 2001;79(6):1084–91.
[24] Meinander K, Niemi M, Hakola JS, Selin JF. Polylactides-degradable polymers for fibres and films macromolecular symposia. Hoboken, NJ: Wiley Online Library; 1997. p. 147–53.
[25] Van de Velde K, Kiekens P. Biopolymers: overview of several properties and consequences on their applications. Polym Test 2002;21(4):433–42.
[26] Bleach N, Nazhat S, Tanner K, Kellomäki M, Törmälä P. Effect of filler content on mechanical and dynamic mechanical properties of particulate biphasic calcium phosphate—polylactide composites. Biomaterials 2002;23(7):1579–85.
[27] Anderson AJ, Dawes EA. Occurrence, metabolism, metabolic role, and industrial uses of bacterial polyhydroxyalkanoates. Microbiol Rev 1990;54(4):450–72.
[28] Van Loosdrecht M, Pot M, Heijnen J. Importance of bacterial storage polymers in bioprocesses. Water Sci Technol 1997;35(1):41–7.
[29] Madison LL, Huisman GW. Metabolic engineering of poly (3-hydroxyalkanoates): from DNA to plastic. Microbiol Mol Biol Rev 1999;63(1):21–53.
[30] Mook Choi W, Wan Kim T, Ok Park O, Keun Chang Y, Woo Lee J. Preparation and characterization of poly (hydroxybutyrate-co-hydroxyvalerate)-organoclay nanocomposites. J Appl Polym Sci 2003;90(2):525–9.
[31] Sanchez-Garcia M, Gimenez E, Lagaron J. Morphology and barrier properties of solvent cast composites of thermoplastic biopolymers and purified cellulose fibers. Carbohydr Polym 2008;71(2):235–44.
[32] Mohanty A, Misra M, Drzal L. Sustainable bio-composites from renewable resources: opportunities and challenges in the green materials world. J Polym Environ 2002; 10(1–2):19–26.
[33] Toriz G, Arvidsson R, Westin M, Gatenholm P. Novel cellulose ester-poly(furfuryl alcohol)-flax fiber biocomposites. J Appl Polym Sci 2003;88(2):337–45.
[34] Matsumura H, Sugiyama J, Glasser WG. Cellulosic nanocomposites. I. Thermally deformable cellulose hexanoates from heterogeneous reaction. J Appl Polym Sci 2000;78 (13):2242–53.
[35] Seavey KC, Ghosh I, Davis RM, Glasser WG. Continuous cellulose fiber-reinforced cellulose ester composites. I. Manufacturing options. Cellulose 2001;8(2):149–59.
[36] Seavey KC, Glasser WG. Continuous cellulose fiber-reinforced cellulose ester composites. II. Fiber surface modification and consolidation conditions. Cellulose 2001;8 (2):161–9.

[37] Franko A, Seavey KC, Gumaer J, Glasser WG. Continuous cellulose fiber-reinforced cellulose ester composites III. Commercial matrix and fiber options. Cellulose 2001;8 (2):171–9.
[38] Romero RB, Leite CAP, Gonçalves MdC. The effect of the solvent on the morphology of cellulose acetate/montmorillonite nanocomposites. Polymer 2009;50(1):161–70.
[39] Zhou C-H, Zhang D, Tong D-S, Wu L-M, Yu W-H, Ismadji S. Paper-like composites of cellulose acetate-organo-montmorillonite for removal of hazardous anionic dye in water. Chem Eng J 2012;209:223–34.
[40] Glasser WG, Taib R, Jain RK, Kander R. Fiber-reinforced cellulosic thermoplastic composites. J Appl Polym Sci 1999;73(7):1329–40.
[41] Mohanty AK, Misra M, Drzal LT, editors. Natural fibers, biopolymers, and biocomposites. CRC Press; 2005.
[42] Martins IMG, Magina SP, Oliveira L, Freire CSR, Silvestre AJD, Neto CP, et al. New biocomposites based on thermoplastic starch and bacterial cellulose. Compos Sci Technol 2009;69(13):2163–8.
[43] Curvelo AAS, de Carvalho AJF, Agnelli JAM. Thermoplastic starch-cellulosic fibers composites: preliminary results. Carbohydr Polym 2001;45(2):183–8.
[44] Carvalho AJF, Job AE, Alves N, Curvelo AAS, Gandini A. Thermoplastic starch/natural rubber blends. Carbohydr Polym 2003;53(1):95–9.
[45] Avérous L, Fringant C, Moro L. Plasticized starch-cellulose interactions in polysaccharide composites. Polymer 2001;42(15):6565–72.
[46] Funke U, Bergthaller W, Lindhauer MG. Processing and characterization of biodegradable products based on starch. Polym Degrad Stab 1998;59(1):293–6.
[47] Wollerdorfer M, Bader H. Influence of natural fibres on the mechanical properties of biodegradable polymers. Ind Crop Prod 1998;8(2):105–12.
[48] Arvanitoyannis I, Kolokuris I, Nakayama A, Aiba S-i. Preparation and study of novel biodegradable blends based on gelatinized starch and 1,4-trans-polyisoprene (gutta percha) for food packaging or biomedical applications. Carbohydr Polym 1997;34 (4):291–302.
[49] Averous L, Moro L, Dole P, Fringant C. Properties of thermoplastic blends: starch-polycaprolactone. Polymer 2000;41(11):4157–67.
[50] Griffin GJL. Starch polymer blends. Polym Degrad Stab 1994;45(2):241–7.
[51] St-Pierre N, Favis BD, Ramsay BA, Ramsay JA, Verhoogt H. Processing and characterization of thermoplastic starch/polyethylene blends. Polymer 1997;38(3):647–55.
[52] Yang Z, Bhattacharya M, Vaidya UR. Properties of ternary blends of starch and maleated polymers of styrene and ethylene propylene rubber. Polymer 1996;37(11):2137–50.
[53] Maksimov RD, Lagzdins A, Lilichenko N, Plume E. Mechanical properties and water vapor permeability of starch/montmorillonite nanocomposites. Polym Eng Sci 2009;49 (12):2421–9.
[54] Ma X, Yu J, Wang N. Glycerol plasticized-starch/multiwall carbon nanotube composites for electroactive polymers. Compos Sci Technol 2008;68(1):268–73.
[55] Chen G-Q, Patel MK. Plastics derived from biological sources: present and future: a technical and environmental review. Chem Rev 2011;112(4):2082–99.
[56] Queiroz AUB, Collares-Queiroz FP. Innovation and industrial trends in bioplastics. Polym Rev 2009;49(2):65–78.
[57] Nagakawa Y, Yunoki S, Saito M. Liquid scintillation counting of solid-state plastic pellets to distinguish bio-based polyethylene. Polym Test 2014;33:13–5.
[58] Brito GF, Agrawal P, Araújo EM, de Mélo TJA. Polylactide/biopolyethylene bioblends. Polímeros 2012;22:427–9.

[59] Castro DO, Ruvolo-Filho A, Frollini E. Materials prepared from biopolyethylene and curaua fibers: composites from biomass. Polym Test 2012;31(7):880–8.
[60] Ratto JA, Stenhouse PJ, Auerbach M, Mitchell J, Farrell R. Processing, performance and biodegradability of a thermoplastic aliphatic polyester/starch system. Polymer 1999;40 (24):6777–88.
[61] Wang J, Yang K, Lu S. Preparation and characteristic of novel silicone rubber composites based on organophilic calcium sulfate whisker. High Perform Polym 2011;23(2):141–50.
[62] Li J, Luo X, Lin X, Zhou Y. Comparative study on the blends of PBS/thermoplastic starch prepared from waxy and normal corn starches. Starch-Starke 2013;65(9–10):831–9.
[63] Tran T, Lee B-H, Yang H-S, Chotineeranat S, Sriroth K, Kim H-J. Use of starch granules melting to control the properties of bio-flour filled polypropylene and poly(butylene succinate) composites: physico-chemical properties. Starch-Starke 2011;63(10):649–54.
[64] Reddy MM, Mohanty AK, Misra M. Biodegradable blends from plasticized soy meal, polycaprolactone, and poly(butylene succinate). Macromol Mater Eng 2012;297(5):455–63.
[65] Bonham S, Misra M, Mohanty AK. Effect of co-rotation and counter-rotation extrusion processing on the thermal and mechanical properties, and morphology of plasticized Soy protein isolate and poly(butylene succinate) blends. Macromol Mater Eng 2011;296(9):788–801.
[66] Nam TH, Ogihara S, Nakatani H, Kobayashi S, Song JI. Mechanical and thermal properties and water absorption of jute fiber reinforced poly (butylene succinate) biodegradable composites. Adv Compos Mater 2012;21(3):241–58.
[67] Faruk O, Bledzki AK, Fink H-P, Sain M. Biocomposites reinforced with natural fibers: 2000–2010. Prog Polym Sci 2012;37(11):1552–96.
[68] Frollini E, Bartolucci N, Sisti L, Celli A. Poly (butylene succinate) reinforced with different lignocellulosic fibers. Ind Crop Prod 2013;45:160–9.
[69] Nam TH, Ogihara S, Tung NH, Kobayashi S. Effect of alkali treatment on interfacial and mechanical properties of coir fiber reinforced poly(butylene succinate) biodegradable composites. Compos Part B 2011;42(6):1648–56.
[70] Luo X, Li J, Feng J, Yang T, Lin X. Mechanical and thermal performance of distillers grains filled poly(butylene succinate) composites. Mater Des 2014;57:195–200.
[71] Liu L, Yu J, Cheng L, Qu W. Mechanical properties of poly(butylene succinate) (PBS) biocomposites reinforced with surface modified jute fibre. Compos A: Appl Sci Manuf 2009;40(5):669–74.
[72] Aoi K, Takasu A, Tsuchiya M, Okada M. New chitin-based polymer hybrids. 3. Miscibility of chitin-graft-poly(2-ethyl-2-oxazoline) with poly(vinyl alcohol). Macromol Chem Phys 1998;199(12):2805–11.
[73] Chandy T, Sharma CP. Chitosan-as a biomaterial. Biomater Artif Cells Artif Organs 1990;18(1):1–24.
[74] Paul W, Sharma C. Chitosan, a drug carrier for the 21 st century: a review. STP Pharma Sci 2000;10(1):5–22.
[75] Harish Prashanth KV, Tharanathan RN. Chitin/chitosan: modifications and their unlimited application potential—an overview. Trends Food Sci Technol 2007;18(3):117–31.
[76] Rinaudo M. Chitin and chitosan: properties and applications. Prog Polym Sci 2006;31 (7):603–32.
[77] Rinaudo M. Main properties and current applications of some polysaccharides as biomaterials. Polym Int 2008;57(3):397–430.
[78] Ojagh SM, Rezaei M, Razavi SH, Hosseini SMH. Development and evaluation of a novel biodegradable film made from chitosan and cinnamon essential oil with low affinity toward water. Food Chem 2010;122(1):161–6.

[79] Draget KI, Skjåk-Bræk G, Smidsrød O. Alginate based new materials. Int J Biol Macromol 1997;21(1–2):47–55.
[80] Draget K. 29—Alginates. Handbook of hydrocolloids. 2nd ed. Cambridge: Woodhead Publishing; 2009. p. 807–28.
[81] Ertesvåg H, Valla S. Biosynthesis and applications of alginates. Polym Degrad Stab 1998;59(1):85–91.
[82] Qin Y, Cai L, Feng D, Shi B, Liu J, Zhang W, et al. Combined use of chitosan and alginate in the treatment of wastewater. J Appl Polym Sci 2007;104(6):3581–7.
[83] Xie Z-P, Huang Y, Chen Y-L, Jia Y. A new gel casting of ceramics by reaction of sodium alginate and calcium iodate at increased temperatures. J Mater Sci Lett 2001;20 (13):1255–7.
[84] Babu RP, O'Connor K, Seeram R. Current progress on bio-based polymers and their future trends. Prog Biomater 2013;2(1):8.
[85] Brownlee IA, Seal CJ, Wilcox M, Dettmar PW, Pearson JP. Applications of alginates in food. In: Rehm BHA, editor. Alginates: biology and applications. Berlin, Heidelberg: Springer; 2009. p. 211–28.
[86] Chisholm MH, Navarro-Llobet D, Zhou Z. Poly(propylene carbonate). 1. More about poly(propylene carbonate) formed from the copolymerization of propylene oxide and carbon dioxide employing a zinc glutarate catalyst. Macromolecules 2002;35(17):6494–504.
[87] Chisholm MH, Zhou Z. Concerning the mechanism of the ring opening of propylene oxide in the copolymerization of propylene oxide and carbon dioxide to give poly(propylene carbonate). J Am Chem Soc 2004;126(35):11030–9.
[88] Peng S, Wang X, Dong L. Special interaction between poly(propylene carbonate) and corn starch. Polym Compos 2005;26(1):37–41.
[89] Ge XC, Li XH, Zhu Q, Li L, Meng YZ. Preparation and properties of biodegradable poly(propylene carbonate)/starch composites. Polym Eng Sci 2004;44(11):2134–40.
[90] Ge XC, Xu Y, Meng YZ, Li RKY. Thermal and mechanical properties of biodegradable composites of poly(propylene carbonate) and starch-poly(methyl acrylate) graft copolymer. Compos Sci Technol 2005;65(14):2219–25.
[91] Pilla S. Handbook of bioplastics and biocomposites engineering applications. Boca Raton, FL: John Wiley & Sons; 2011.
[92] Lörcks J. Properties and applications of compostable starch-based plastic material. Polym Degrad Stab 1998;59(1):245–9.
[93] Moroa L. Starch-based biodegradable materials suitable for thermoforming packaging. Starch-Starke 2001;53:368–71.
[94] Suddell B, Evans W. Natural fiber composites in automotive applications. In: Mohanty AK, Misra M, Drzal TL, editors. Natural fibers, biopolymers, and biocomposites. CRC Press; 2005.
[95] Mohanty AKMM, Drzal TL, Selke SE, Harte BR, Hinrichsen G. Naturalfibers, biopolymers, and biocomposites: an introduction. In: Mohanty AK, Misra M, Drzal TL, editors. Natural fibers, biopolymers, and biocomposites. Boca Raton: CRC Press-Taylor & Francis Group; 2005. p. 1–36.
[96] Koronis G, Silva A, Fontul M. Green composites: a review of adequate materials for automotive applications. Compos Part B 2013;44(1):120–7.
[97] Stewart R. Automotive composites offer lighter solutions. Reinf Plast 2010;54(2):22–8.

Nanofibers for fiber-reinforced composites

12

Nesrin Horzum, Nehir Arik*, Yen Bach Truong†*
*Izmir Katip Çelebi University, Izmir, Turkey, †Commonwealth Scientific and Industrial Research Organization (CSIRO), Clayton, VIC, Australia

12.1 Introduction and historical perspective

The presence of nanomaterials in nature provides an inspiring way of bridging nanoscience into the classroom. Discovering that common natural materials such as paper and clay or materials such as feathers and spider silk have properties that depend not only on their chemistry but also their nanostructure is especially stimulating. Controlling of the surface chemistry of functional fibers has become an active research field in the last two decades, because of the increasing interest in fabricating fiber-reinforced composites (FRCs) with superior properties crucial in many applications.

12.1.1 Micro- and nanofibers

From past to present, the research on the fabrication of synthetic fibers has been increasing. The need for the improvement of both chemical and physical properties of fibers and being their use in many different application areas have led to the rapid development of fiber technology. The fibers that has the linear density lower than 1 dtex are generally accepted as microfibers. The traditional engineering microsized fibers such as glass, carbon, and Kevlar fibers are being used as reinforcing materials in composites [1]. FRCs can provide better structural properties having high modulus of elasticity and strength to weight ratios. On the other hand, fibers having diameters below 0.5 μm are considered as nanofibers, which will ultimately find significant applications in the fabrication of nanocomposites. Compared with microfibers as reinforcement materials, the nanofiber-reinforced composites have more superior mechanical performance and structural properties.

12.1.2 Methods used to form micro- and nanofibers

Traditional methods used to obtain micro- or nanofiber webs include melt spinning, solution spinning, and melt blowing [2]. The melt spinning process is based on the drawing down extruded strands of polymer melt [3]. However, this technology can only be applied to viscoelastic materials that can undergo strong deformations to

Fiber Technology for Fiber-Reinforced Composites. http://dx.doi.org/10.1016/B978-0-08-101871-2.00012-6

withstand the developing stresses during drawing [1]. Typically, fibers having diameters greater than 2 μm can be produced by melt spinning [4]. Islands-in-the-sea (fibers within fibers) process, which is a variation of melt spinning, involves production of several individual strands of a polymer component (island) within a larger single strand of a second polymer component (sea). The bicomponent strands are extruded through dies, cooling, or attenuating of fibers by high-velocity air streams. This process allows to produce fibers with a diameter ranging from 0.1 to 5 μm [5]. The main restriction for this technique is that the removal of sea component from the fibers, which often creates an environmental issue due to the need for solvents, and consequently, a limited number of polymers can be processed [6].

Solution spinning includes dry-spinning, wet-spinning, and gel-spinning processes [7,132]. In both dry and wet spinning, a viscous solution of polymer passes through fine holes of a spinneret to form fibers. In dry-spinning case, the solvent is evaporated using a heated column where the polymer solidifies. In wet spinning, the polymer solution is pushed through a spinneret into a chemical bath in which the polymer is precipitated by dilution or chemical reaction to form fibers. It is possible to draw fibers with diameters ranging 100 μm to over a millimeter [132]. Gel spinning can also be described as dry-wet spinning, since the filaments pass through the air and then are cooled in a liquid bath. High-strength polyethylene and aramid fibers are produced by gel spinning [8].

Since the 1990s, there has been a growing interest in electrospinning due to its applicability to a variety of polymers and easy fabrication of ultrafine fibers. Electrospun fibers are produced from polymer melt or solution by electrostatic forces. This process is able to produce fibers with diameters in the range from 40 nm to 2 μm [9].

Melt blowing is another method for the fabrication of nonwoven network of fibers, based on the extrusion of molten polymer through an orifice, attenuated by heated high-velocity air stream. This method has been used to produce microfibers ranging in diameters from 1 to 50 μm [4,10].

A novel solution blow spinning (SBS) method is the combination of both electrospinning and melt blowing technologies. Micro- and nanofibers with diameters ranging from a few tenths of nanometers to several microns can be produced [3,133].

12.2 Electrospinning

12.2.1 The fundamental aspects

The uses of nanofiber materials have attracted quite extensive attention over the last 25 years with the increasing popularity of the simple electrospinning technique [9], which has now become a scalable fabricating technique. Although electrospinning is mostly a technique that is biased to laboratory-scale work, the ever increasing number of commercial electrospinning companies instills confidence that the future will see industrial-scale usage of nanofiber materials. Nanofiber materials have found uses in many areas including composite reinforcements, filters, tissue engineering, battery

cells and capacitors, drug delivery, smart textiles, protective clothing, catalysts, wound dressings, sensors, and cosmetics [11].

A thorough history of electrospinning can be found in a review paper by researchers in New Zealand [12]. Although there are discrepancies on the exact origin of electrospinning, most of the patents were filed between 1931 and 1944 by Anton Formhals. The "Taylor" cone commonly used to describe the theory of electrospinning by many novices and experts originated from Sir Geoffrey Ingram Taylor, who between 1964 and 1969 developed the theoretical underpinnings of electrospinning by mathematical modeling of the shape of a cone formed by a fluid droplet under the effect of an electric field.

Electrospinning is a technique for producing fibers from submicron down to nanometer in diameter with high surface area. The technique can be further divided into two main categories: solution electrospinning and melt electrospinning. In solution electrospinning, the polymer(s) and other additive materials are firstly dissolved in a suitable solvent at an optimized concentration before electrospinning, whereas in melt electrospinning, the polymer is heated to an optimized temperature to form a melt. In either case, a high electric field is applied to the droplet of fluid coming out of the tip of a die or spinneret, which acts as one of the electrodes. When the electric field supply is strong enough, it will lead to the droplet formation and finally to the ejection of a charged jet from the tip of the cone accelerating toward the counter electrode leading to the formation of fibers. While solution electrospinning relies on evaporation of the solvent to produce fiber, melt electrospinning requires cooling of the polymeric jet [13].

In its simplest form, electrospinning can be carried out using a single spinneret system (monoaxial using pump 1 only) with one polymer dissolved in a solvent at the right concentration, for example 20% polyurethane in *N*,*N*-dimethyl formamide solution and processing parameter of 0.2 mL/h pump rate, 23 gauge needle spinneret size, at gap distance and applied potential of 20 kV [14]. The collector geometry used in this study was a rotating drum and by changing the drum speed from 1 to 9 m/s, while keeping all other material and process variables constant, membranes in which the fibers were randomly distributed or aligned were fabricated (Fig. 12.1).

Functional additives and mixtures of two or more polymers dissolved in a solvent or mixture of solvents can also be electrospun monoaxially using a single spinneret. However, there are different variations on the simple monoaxial electrospinning described above. The most commonly described variation is coaxial electrospinning where two different solutions can be coelectrospun without direct mixing, using two concentrically aligned spinnerets. The same voltage is applied to both spinnerets, and it deforms the compound droplet. A jet is generated on the tip of the deformed droplet and, in an ideal case, a core-shell nanofiber is formed. This type of electrospinning is mainly used in developing structures with higher strength using stronger core, drug delivery products using sheath and core materials degrading at different rates, and better tissue engineering products obtained by coating a less biocompatible but desirable material with a more biocompatible one [15].

The incorporation of active agents, such as drugs to nanofibers has been heavily pursued by either simply mixing or blending the active compound with the polymer

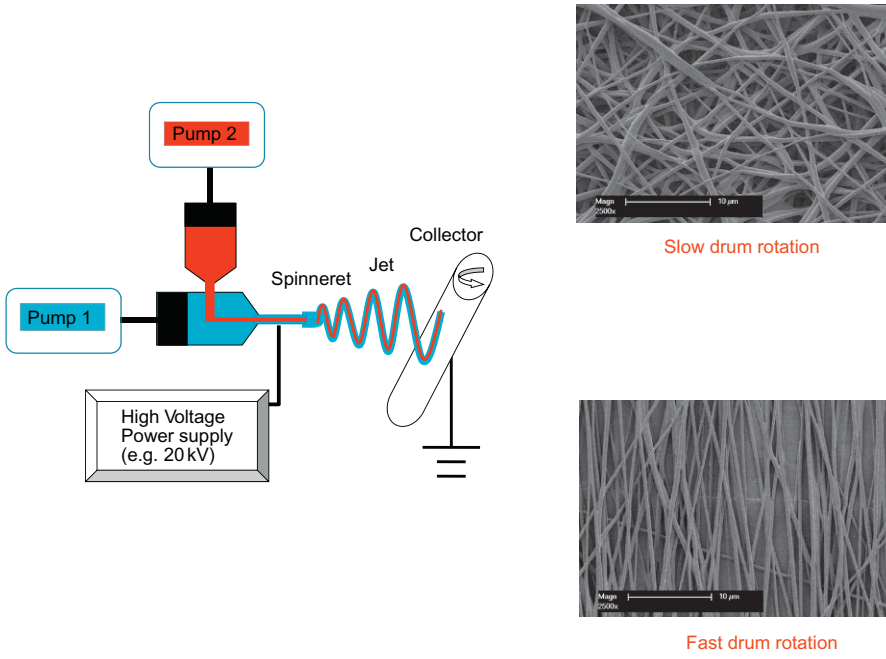

Fig. 12.1 A schematic view of electrospinning setup (monoaxial without pump 2 and inner red spinneret) or coaxial with both pumps.

solution prior to electrospinning or by adding the additives that are prefixed to a holder type material to attain controlled release [16]. Other methods of incorporating active compounds or to add functionality to the nanofibers are to perform post treatment of the electrospun nanofibers by different coating treatments or by performing surface functionalization to change the existing functional groups [17].

Industrial-scale eletrospun production is becoming a reality [18] with several companies including Inovenso and Elmarco offering industrial-scale electrospinning machines. An exhaustive list of companies currently supplying electrospinning products can also be found in Persano et al. review paper [18], and some of the more prominent companies include Donaldson, DuPont, and Finetex Technology. With such knowledge at hand, it can be said that nanofibers fabricated by electrospinning have a promising future in materials manufacturing for numerous and varied applications.

12.2.2 Factors affecting fiber formation

Variables that can affect electrospinning can be classified into two categories; the material variables relating to the polymer and choice of solvents and the process variables pertaining to equipment and processing parameters. The material and process variables listed in Table 12.1 can affect both the ability of producing nanofibers and the quality of the nanofibers.

Table 12.1 Material and process variables in electrospinning

Material variables	Process variables
A: Polymer solution or melt • Concentration • Solvent choice • Additives B: Environment • Temperature • Humidity C: Collector • Geometry • Dielectric properties	D: Applied potential E: Pump rate F: Spinneret properties G: Gap distance

During electrospinning, the concentration of polymer solution is one of the most important parameters in the fiber formation. It should be noted that surface tension and viscosity have a significant role in the determination of the concentration range, which continuous fibers can be fabricated by electrospinning. As the concentration is too low, electrospraying occurs in the form of macro/nanoparticles instead of electrospinning, due to the low viscosity and high surface tension of the solution. If the polymer concentration is not adequate for electrospinning, beaded fibers are obtained. For solution of low viscosity ($\eta < 1$ poise), surface tension has a dominant effect on fiber morphology. At very high viscosities ($\eta > 20$ poise), the ejection of jet from the solution becomes difficult [19]. If the solution has a suitable viscosity, continuous fibers can be obtained. Polymer concentration does affect not only the electrospinnability but also the fiber diameter. In general, increasing the concentration of electrospinning solution results in larger fiber diameter.

Another parameter is the selection of solvent in terms of its viscosity, surface tension, dielectric constant, and vapor pressure. Supaphol and coworkers reported that smooth polystyrene (PS) fibers were fabricated from the as-prepared PS solutions that have high polarity, conductivity, boiling point, low viscosity, and surface tension [20]. The effect of solvent system on the morphology of fibers was also studied for electrospinning of polyvinylpyrrolidone (PVP) solutions. Continuous fibers were produced from PVP solutions in ethanol because of higher dielectric constant and lower surface tension of the solvent [21].

The existing literature on the effect of additives such as inorganic salt and surfactant is extensive and focuses particularly on the fiber morphology and diameter. By changing the conductivity and surface tension of the solutions, the elimination of beads is possible.

By increasing the conductivity, density of net charge increases; then, accordingly, the jet is stretched under viscoelastic force, which in turn leads to formation of bead-free fibers. Fallahi et al. investigated the fabrication of uniform PS fibers by incorporating salt (LiCl) and nonionic surfactant (polyether modified polysiloxane).

They claimed that increasing the amount of surfactant resulted in larger bead and thinner fiber formation, whereas increment in fiber diameter was observed with addition of salt into the solution [22]. Addition of increasing amount of NaCl and LiCl into the polyamide-6 solution in formic acid, resulted in increase in fiber diameter due to the increase in both viscoelastic force and mass flow [23]. Similar results were reported with the addition of triethylbenzylammonium chloride to a polyurethane/DMF solution [24].

Ambient temperature and relative humidity strongly affect electrospinning. As for the temperature, high temperature promotes solvent evaporation rate but reduces viscosity of the solution, thus thinner fibers are obtained. De Vrieze et al. reported these two opposing effects on the average fiber diameter of PVP nanofibers as a function of temperature [25]. At higher temperatures, the fiber formation process can be completed by rapid solidification of the jet because of higher solvent evaporation rate. The polymer chains move more freely, leading to lower solution viscosity and thus producing higher stretching rate and thinner fibers. The inverse relationship between the solvent evaporation rate and solution viscosity has been also proved for polyamide-6 fibers that had thinner fiber diameter with the increase in temperature [23]. The humidity of the electrospinning environment affects the fiber diameter depending on the chemistry of the polymer. De Vrieze et al. have observed that as the humidity increased, the average fiber diameter of cellulose acetate nanofibers increased, whereas average diameter of PVP fibers decreased. The different trends in diameter was explained not only by the variations in chemical and molecular interaction but also by its effect on the solvent evaporation rate [25]. In general, at high humidity, water condenses on the fiber surface preventing the fiber drying during the nanofiber jet flight, and this may have an influence on the morphology of the fiber particularly when the polymer is dissolved in volatile solvents. On the contrary, at low humidity, the rate of evaporation increases and fiber formation occurs. Recently, Liang et al. have demonstrated that increasing the relative humidity to a critical point (73% RH) resulted in self-alignment of nanofibers into a 3-D honeycomb-like structure. Above the critical point, no structure was observed, only few nanofibers was obtained because of the slow evaporation rate [26].

The structuration of the nanofiber mat is also possible for particular applications depending on the geometry and dielectric properties of the collectors. There are two basic approaches currently being adopted in research into the collectors. One is the use of mobile collectors that can provide fiber alignment onto a rotating drum or disk. The other induces a modification of electric forces on the charged fibers reaching to the collector. Furthermore, tuning the local differences of the dielectric properties by using different dielectric materials for the collector is another way for nanofiber mat structuration. Lavielle et al. [27] produced "microwoven" PCL scaffolds with good mechanical properties using various collectors with microscopic patterns prepared by photolithography.

In regard to the process variables, a critical voltage value exists, which if exceeded, a stable polymer jet can be obtained. However, further increasing applied voltage results in higher instability and stretching of the jet, leading generally to thinner fibers. A decrease in tip-to-collector distance increases the electric field, thus semisolidified

and bead-defected fibers can be formed. At constant electric potential and tip-to-collector distance, fiber diameter gradually increases with increasing feed rate of the polymer solution. If the feed rate is too low, nonuniform fibers with broad diameter distribution are obtained. It is worth mentioning that the diameter or length of needle may affect the fiber diameter. Macossay et al. fabricated poly(methyl methacrylate) (PMMA) fibers using needles with different internal diameters. No correlation between the needle diameter and the average fiber diameter has been observed, but the fibers obtained using thinner needle diameter have a broader diameter range [28].

12.2.3 Nanofibers containing nanoparticles

The combination of electrospun nanofibers and inorganic nanoparticles in one object yields hybrid materials that are intrinsically porous and possess higher chemical and thermal stability. Although nanoparticles have a larger surface area than nanofibers of the same diameter, nanoparticles are usually difficult to separate from the reaction media due to the lack of mechanical integrity. In this respect, polymer fibers can be used as supports to place inorganic particles in a structural template, in an isolated and nonaggregated fashion [29]. The different strategies to produce hybrid electrospun fibers were categorized as (i) electrospinning of precursors followed by heat treatment, (ii) electrospinning of ex situ synthesized inorganic materials, (iii) surface crystallization on electrospun fibers, and (iv) combination of these methods.

Table 12.2 summarizes the recent studies related to nanofibers containing nanoparticles. Although the most common method is the heat treatment of polymer/inorganic precursor fibers, the resulting fibrous materials after this process are often brittle and lose their mechanical strength [41]. On the other hand, simultaneous electrospinning of ex situ synthesized nanoparticles and polymer leads to the reduction of the performance of available active sites due to the polymer shielding [42,43]. Hence, the fabrication of nanofiber/nanoparticle composites by the in situ formation of the nanoparticles on the surface of electrospun fibers allows the possibility of synthesis at lower temperature without any additional heat treatment and a controlled nanoparticle formation on the surface of the fibrous template. Surface treatment of electrospun fibers is also advantageous in terms of prevention of nanoparticle aggregation and providing uniform distribution of the nanoparticles on the fibers.

12.2.4 Fiber-reinforced composites

FRCs consist of fibers and matrix [44]. High-strength, high-stiffness structural fibers and low cost, lightweight, environmentally resistant polymers are combined to make a composite [45]. Fibers or other reinforcing materials strengthen the polymeric matrix [44]. The mechanical properties and durability of the composites become better than plain polymer [45]. The matrix holds the fibers, provides load transfer, whereas the fibers contribute to the strength and stiffness [44]. In the 1960s and 1970s, fibrous materials such as boron, carbon, and aramid were commercialized due to their higher strength and stiffness and lower density to meet the higher-performance challenges of space exploration and air travel. Initially, fabrication of composites made up of fibers

Table 12.2 The recent literature on nanofiber-nanoparticle composites

Nanofiber	Nanoparticle	Composite	Strategy	Application	Reference
Polycaprolactone (PCL)	Fluorescent polystyrene (PS)	Nanoparticle/ nanofiber composite	Electrospinning of polymer blend with ex situ synthesized inorganic materials	Cell adhesion	[30]
Polyacrylonitrile (PAN)	Magnesium oxide (MgO)	PAN-MgO nanofiber	Electrospinning of polymer blend with ex situ synthesized inorganic materials	Air filtration	[31]
Amphiphilic block copolymer [poly [methoxy poly(ethylene glycol)methacrylate]-block-poly(butyl acrylate) (PMPEGMA-b-PBA)], phenolic resin, and polyethylene oxide (PEO)	Nickel (Ni)	Ni/NiO/MnO_x/ Carbon nanofiber	Electrospinning of precursors followed by carbonization	Lithium-ion battery anode	[32]
Polyvinyl pyrrolidone (PVP)	TiO_2	TiO_2 nanofiber	Electrospinning of precursors followed by calcination	Photoanode	[33]
Polyacrylonitrile (PAN)	SiO_2	SiO_2/PAN hybrid nanofiber	Electrospinning of solution containing a sol–gel precursor and a polymer	Membrane separator for lithium-ion battery	[34]
Polyacrylonitrile (PAN)	SnO_x and ZnO	SnO_x-ZnO/ carbon nanofiber	Electrospinning of precursors followed by carbonization	Lithium-ion battery anode	[35]

Polyvinylpyrrolidone (PVDF)	SiO_2	PVDF-SiO_2 nanofiber	Electrospinning of polymer blend with ex situ synthesized inorganic materials	Forward osmosis desalination	[36]
Polyvinyl pyrrolidone (PVP)	Fe_2O_3	Fe_2O_3 nanofiber	Electrospinning of precursors followed by calcination	Chromate adsorption from waste waters	[37]
Polyvinyl alcohol (PVA)	CuO	CuO nanoparticle	Electrospinning of precursors followed by calcination	Hydrazine hydrate electrooxidation	[38]
Polyvinyl alcohol (PVA)	CuO	CuO nanoparticle	Electrospinning of precursors followed by calcination	Hydrazine hydrate electrooxidation	[38]
Polyvinyl pyrrolidone (PVP)/ polyacrylonitrile (PAN)	$NiCO_2O_4$	$NiCo_2O_4$ NPs-decorated N-doped carbon nanofiber	Electrospinning of precursors followed by multi-step heat treatment	Lithium-ion battery cathode	[39]
Polyvinyl alcohol (PVA)/chitosan oligosaccharide (COS)	Ag	PVA/ COS-AgNPs nanofiber	Electrospinning of precursors	Wound healing	[40]

that have superior properties were too costly. Therefore, researchers have studied on this problem until now, and they achieved to produce cheaper fibers that are used in current studies [45].

The key aspects of effective reinforcement can be listed as high aspect ratio, uniform dispersion, alignment, and interfacial stress transfer [46]. The aspect ratio of the fibers is an important factor that contributes to the properties of new types of composites. Homogeneous dispersion of fibers prevents agglomeration and provides efficient load transfer minimizing the presence of stress concentration centers. The difficulty in controlling fiber alignment decreases the efficiency of reinforcement, structural, or functional performance [47]. The orientation and length of fibers should be considered for a particular application [48]. In engineering applications, various types of fibers with different orientations and lengths have been used for decades. The fiber-reinforced plastics for commercial use have attracted great attention in the aviation industry in the 1930s [49]. The other significant requirement for FRCs is the applied external stress to the composite that is transferred to the fibers. Thus, it allows them to take a disproportionate share of the load affecting the performance of composites.

Nowadays, FRCs are commonly used in aerospace, marine, armored vehicles, automobile, railways, civil engineering applications, sporting goods, etc. due to their high specific strength and hardness [50]. Glass fiber is widely used as a reinforcement due to its low cost, high tensile and impact strength, light weight, and having a corrosion resistance. Furthermore, polyester resin reinforced with glass fiber is the material of many application areas such as marine, constructions, automobile, and railway industry. Another example is vapor-grown carbon nanofiber-reinforced polymer composites having improved mechanical properties through better interfacial adhesion and fiber alignment. Hossain et al. [50] investigated the use of carbon nanofibers (CNFs) as nanofillers in woven glass fiber-reinforced polyester composites. They observed 0.2 wt% CNFs-loaded polyester resin had better dispersion of CNFs. The results of this investigation show that the incorporation of even low amount of CNFs improved mechanical properties of the composite system. Besides enhanced mechanical strength, it is possible to fabricate conductive polymer composite by the addition of carbon fibers. The increment in volume fraction of carbon fibers results in higher effective electric conductivity of the composite [51].

12.3 Carbon nanotubes/nanofibers

Conductive nanofiller/polymer fibers are functional nanomaterials since they have remarkable electrical, thermal, and mechanical properties. The successful combination of high aspect ratio and one-dimensional conductive nanofillers, including carbon nanotubes (CNTs) and CNFs with the various electrospun nanofibers, leads to significant enhancement in the aforementioned properties. The tensile strength and modulus of elasticity depend on the polymer matrix, and types, synthesis method, dispersion and concentration of carbon nanofillers in the polymer matrix [52].

The preparation of CNT/polymer solution for electrospinning involves mixing polymer solution and nanotube dispersion to obtain homogeneously oriented CNTs in the resultant fibers. To date, CNTs have been embedded into various polymer

matrices including chitosan [53,54], epoxy [55], nylon 6,6 [56], polyacrylonitrile [52,57–61], polyaniline [62], polycaprolactone [63], polycarbonate [64], poly(ethylene oxide) [65–67], polylactic acid [68], polymethyl methacrylate [69,70], polystyrene [71], polyurethane [72], poly(vinyl alcohol) [73–75], and regenerated silk [76,77].

Apart from considering different polymer matrices, extensive research has been conducted to demonstrate the application potential of various types of carbon nanomaterials, mainly single-walled (SW) and multiwalled (MW) carbon nanotubes and vapor-grown carbon nanofibers (VGCNFs), as reinforcements in polymer matrices. CNTs can be produced by arc discharge, laser evaporation/ablation, thermal and plasma-enhanced chemical vapor deposition (CVD) [78]. Depending on the manufacturing methods, the diameter of SWCNTs can be close to 1 nm, and MWCNT can have a diameter larger than a few nanometers. Besides this, VGCNFs, which are also termed MWCNTs, typically have diameters in the range of 50–200 nm [79]. VGCNFs can be synthesized by catalytic CVD of a hydrocarbon gas, such as acetylene and propane, or carbon monoxide using metals, usually Fe, Ni, Co, Au, or metal alloy catalysts at temperatures around 500–1500°C [78]. Although carbon nanomaterials differ from one another not only in their size but in their also electric and mechanical properties, very few related works have been reported. Ashrafi et al. studied on the influence of CNT types in improving the mechanical properties of epoxy resins [80]. A comparative study between SWCNT- and MWCNT-modified laminated composites showed that SWCNTs are more effective in enhancing the mechanical performance of the composites. The flammability behavior of SWCNT and MWCNT membranes (buckypaper) and carbon nanofiber (CNF) paper on the epoxy/carbon fiber composite surface was investigated by Wu et al. [81]. The flame-retardant efficiency of MWCNT-based buckypaper was correlated with its high-temperature thermo-oxidation and dense network. CNF paper composite showed low flame-retardant efficiency due to its large pore size and thus high gas permeability.

Uniform dispersion and orientation of carbon nanomaterials within the polymer matrix are two other significant parameters in preparation of composites. Because of strong van der Waals interaction and small size, CNTs or CNFs tend to aggregate to form bundles preventing uniform dispersion within the polymeric resins, which results in lower physical and mechanical properties of the composite material [82]. In order to improve the carbon nanomaterial dispersion, several approaches have been followed, including solution-evaporation methods with high-energy sonication [83] and surfactant-assisted processing [84,85]. Furthermore, deposition of carbon nanotubes suspension under an electric [86] or a magnetic field [87], onto a chemically modified substrate [88], solution casting [89], melt processing [90], and in situ polymerization [91,92] are the most commonly used techniques.

It is worth mentioning that the length and concentration of carbon nanomaterials also affect dispersion behavior and, therefore, electrical, thermal, and mechanical properties of nanocomposites. Abu Al-Rub et al. reported that low concentration long CNTs (10–30 μm) are more effective than high volume of short CNTs (1.5 μm) in filling nanosized voids leading to enhancement in the packing density of the cementitious

composite. It was also shown that the Young's modulus increases as the concentration of long CNTs decreases, whereas the increment in the concentration of short CNTs results in higher modulus of elasticity. Both the flexural strength and ductility increased while using short 0.2 wt% MWCNTs or long 0.1 wt% MWCNTs as reinforcements for the nanocomposites [93]. Recently, MWCNTs/PVP composite nanofibers were fabricated by electrospinning. Effects of MWCNTs concentration on the electric conductivity, complex permittivity, and electromagnetic interference shielding effectiveness (EMI SE) of the nanocomposite were investigated. Total EMI SE was found to be ~42 dB at 10 wt% MWCNTs/PVP nanofibers [94]. In another study, electrospun nanofibers of the MWCNTs/P(St-co-GMA) were embedded into an epoxy matrix for exploring the reinforcing abilities. The flexural modulus of the nanofiber-reinforced composite increased even positioning a single layer of MWCNTs/P(St-co-GMA) nanofibrous mats of 1%, 1.5%, and 2% CNT weight fraction. This increase was attributed to the well-dispersed MWCNTs in addition to the modified chemistry of the nanofibers with epoxide moieties enabling cross-linking between the polymer matrix and the fibers [95].

12.4 Cellulose nanofibers

Cellulose is one of the most important biopolymers. Having many features such as biocompability, biological degradability, availability, and sustainability, it is commonly preferred to use [96]. This polysaccharide is found in everywhere and plenty in nature, given its industrial use in sails, timber, ropes, and paper. For example, wood is the most commercially utilized natural resource containing cellulose [97]. Like wood, plants, marine animals (tunicates), algae, and bacteria can be counted as cellulose source materials. Cellulose has a nonbranched chain of variable length of 1–4-linked β-D-anhydroglucopyranose units. Fig. 12.2 shows the structure of cellulose repeating unit. The hydrogen bonding between hydroxyl groups and oxygens of adjacent molecules stabilizes the glycosidic linkage resulting in the linear configuration of the cellulose chain. Intermolecular hydrogen bonds and van der Waals forces promote parallel stacking of cellulose chains aggregating into the repeated crystalline structure to form microfibrils (5–50 nm in diameter and several microns in length) in the plant cell wall [98].

Cellulose nanofibers are usually insulated from lignocellulosic plants [99]. They can also be produced from annual plants and agricultural by-products, and they have widely renewable resources [100]. Because cellulose nanofibers have semicrystalline structure, their thermal expansion coefficient is close to that of quartz [101]. The

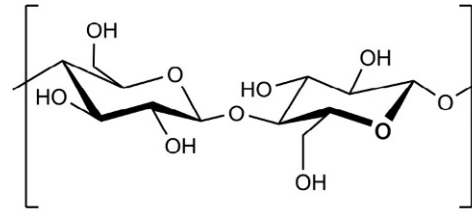

Fig. 12.2 The repeating unit of cellulose in chair conformation.

fibrillated cellulose with a nanoscale structure is generally composed by some combination of chemical, enzymatic, and/or mechanical improvements of lignocellulosic materials [102,103]. Cellulose nanofibers are characterized by a large surface area ($\sim$800 m^2 g^{-1}), high strength (2–3 GPa), high elastic modulus ($\sim$140 GPa) [104], low weight, biodegradability, and biocompatibility [105,106].

The natural nanostructured cellulose has been the main field of many research areas and has been used by different industries, particularly in biomedical and pharmaceutical applications [102]. Moreover, cellulose nanofiber-reinforced composites have potential applications in food packaging, paper, thin components in the electric and electronic devices, etc. [107].

12.4.1 Nanocellulose for fiber-reinforced composites

Cellulose nanofiber-based materials establish a comparatively new class of naturally sourced reinforcements. Due to their high mechanical properties, incorporation of cellulose nanofibers into the composites has gained significant interest. Furthermore, good transparency, barrier properties, and dimensional stability are advantages of cellulose nanofiber-based composites [103]. Cellulose nanofibers have been widely used with various polymers to produce nanocomposites.

Recent studies have been performed on the production of cellulose nanofiber-reinforced epoxy composites. The mechanical performance and thermal stability of the cellulose nanofiber-reinforced composites increase with the reinforcement loading [107]. Masoodi et al. performed assessment of swelling and tension/fracture behavior of bio-derived epoxy composites [108]. The preparation of high-nanocellulose-content biocomposites from well-dispersed nanofibrillated cellulose in epoxy matrix was also described by Ansari et al. [109]. The successful combination of nanocellulose and epoxy provided high strength, modulus of elasticity, and ductility, and moisture stability for a cellulose-based biocomposite. In another study, epoxy has been used for surface modification of cellulose nanofibers used as a reinforcement in a polyvinyl alcohol (PVA) matrix. The chemically functionalized cellulose nanofiber-reinforced PVA showed higher elastic modulus, strength, and strain compared with the composite prepared by unmodified cellulose nanofibers [110].

Nanocomposites are usually reinforced with low percentage of cellulose nanofibers (usually $<$10%) in contrast with the high level of fibers (40%–60%) used in common composites [107]. Petersson et al. produced the nanocomposites by incorporating 5 wt% of the different cellulose nanowhiskers into a poly(lactic acid) matrix [111]. The effect of various cellulose nanofiber percentages by mass in the epoxy matrix was evaluated [107]. The authors showed that the addition of 0.25% and 0.5% cellulose nanofibers was homogeneously dispersed in the polymeric matrix, whereas agglomeration of the nanofibers was detected in the matrix with 0.75% content. Although there are still many obstacles remaining for usage of cellulose nanofibers, they have great potential for use as reinforcement in polymer matrices [111]. The main problem is the dispersion of highly hydrophilic nanocellulose into the hydrophobic polymer matrices. The homogeneous distribution of cellulose nanofibers in a polymer is too difficult on account of their high surface energy and the existence of hydroxyl groups on the surface; thereby,

it has strong hydrogen bonding. Different chemical modifications have been applied to overcome this problem. The dispersibility of nanofibers in a polymer matrix and dimensional stability of the final composite can be enhanced by acetylation. In acetylation process, hydroxyl groups on the cellulose react with the chemical; accordingly, hydrophilic surface of the cellulose is modified and becomes hydrophobic [99,106]. The other process is topochemical trimethylsilylation. Grunert and Winter reported the preparation of nanocomposites with a cellulose acetate butyrate matrix using trimethylsilylated cellulose whiskers [112]. However, these modifications not only are complicated to perform but also have negative effect on the properties of the composite, from using modified cellulose nanofibers. It has been found that the unmodified nanofibers showed better mechanical and reinforcing performance than the modified ones [112,113]. Besides the difficulty in dispersion of cellulose nanostructures, they are not commercially available, and their production is time-consuming, resulting in a low yield [111].

12.5 Applications

The advanced nanofiber-reinforced polymer composites (NFRCs) contribute to enhancing the development of new resin composite materials for a wide range of applications. Fig. 12.3 shows a survey of publications related to the applications of NFRCs.

The data clearly demonstrate that the improvement of durability and longevity of the materials constitutes the major application area, and hence, the NFRCs can be applied to design constructions such as aircraft, automotive industry, buildings, bridges, and railways. However, most of the studies conducted are focused mainly on the characterization and mechanical properties of the composite materials. The applications of NFRCs can also be extended to the electric and electronic field starting from flexible electrodes to conductive support materials. Through the use of NFRCs in fuel cells [114,115], dye-sensitized solar cells [116], lithium-ion batteries [117,118], and supercapacitors [119,120]; it seems to be possible to promote energy storage and efficiency. Furthermore, NFRCs are one of the extensively used membranes for

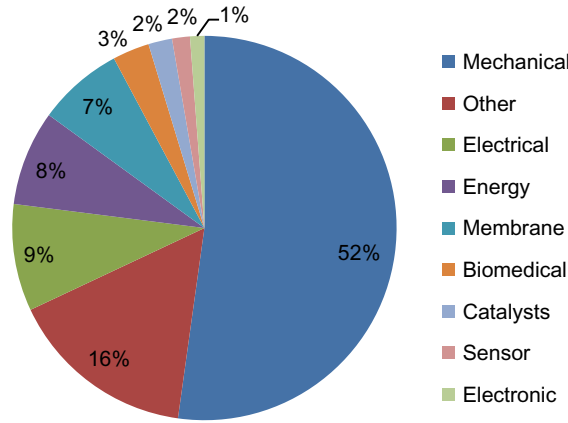

Fig. 12.3 Publication distribution showing application fields of nanofiber-reinforced composites (data analysis of publications was done using the Web of Science at 07 Nov. 2016).

separation and filtration applications such as water treatment and food processing [121–123]. In addition, NFRCs are finding potential applications in biomedical engineering, particularly in the areas of drug delivery systems [124] and scaffolds for tissue/bone [125,126]. Recently, the interest on nanofibers as reinforcing agent in dentistry has been rapidly growing [127,128]. Currently, available resin composites are made of fibers at a larger scale. Although nanoscale fibers that can be used to make resin composite stringer and tougher are desirable for their benefits, there are no commercially available nanofiber materials in dental applications. Moreover, the use of natural nanofibers such as cellulose, chitin, and chitosan is highly promising to develop new bio-based composites for regeneration/remineralization in endodontics or drug delivery systems for periodontal diseases [129]. NFRCs can also be used as supports for catalysts and sensors [130,131]. In the near future, NFRCs will be applied to a wide variety of applications as novel materials/tailored structures, since the properties of the composites can be adjusted by changing the parameters of the fiber such as fiber type, volume fraction, and diameter.

12.5.1 Future trends

The field of nanofiber-reinforced composites has been growing considerably in recent years. Both the use of electrospun fibers within the polymer matrix and incorporation of nanomaterials including fibers, particles, and tubes into the polymer fibers lead to improvements in mechanical strength, modulus of elasticity, and conductivity of the composite. Considerable work is still required including the successful incorporation of nanomaterials into polymer matrix with a high loading content, understanding of the structure-property relationship, and fabrication of low-cost nanofiber-reinforced composite at a large scale. A significant issue to be considered is nanosafety for the safe and sustainable development of advanced composites. Although it is not known which side effects nanomaterials can have on living cells so far, necessary precautions should be taken while using nanomaterials in laboratory and industrial scale. To this respect, development of natural fiber-reinforced biocomposites based on green polymer forms one of the emergent areas in material science raising awareness for use in a variety of applications.

References

[1] Huang ZM, Zhang YZ, Kotaki M, Ramakrishna S. A review on polymer nanofibers by electrospinning and their applications in nanocomposites. Compos Sci Technol 2003;63:2223–53. http://dx.doi.org/10.1016/S0266-3538(03)00178-7.

[2] Jayaraman K, Kotaki M, Zhang Y, Mo X, Ramakrishna S. Recent advances in polymer nanofibers. J Nanosci Nanotechnol 2004;4(1–2):52–65. http://dx.doi.org/10.1166/jnn.2004.078.

[3] Medeiros ES, Glenn GM, Klamczynski AP, Orts WJ, Mattoso LHC. Solution blow spinning: a new method to produce micro- and nanofibers from polymer solutions. J Appl Polym Sci 2009;113(4):2322–30. http://dx.doi.org/10.1002/app.30275.

[4] Ellison CJ, Phatak A, Giles DW, Macosko CW, Bates FS. Melt blown nanofibers: fiber diameter distributions and onset of fiber breakup. Polymer 2007;48(11):3306–16. http://dx.doi.org/10.1016/j.polymer.2007.04.005.
[5] Fedorova N, Pourdeyhimi B. High strength nylon micro- and nanofiber based nonwovens via spunbonding. J Appl Polym Sci 2007;104(5):3434–42. http://dx.doi.org/10.1002/app.25939.
[6] Wang D, Gang S, Chiou BS. A high-throughput, controllable, and environmentally benign fabrication process of thermoplastic nanofibers. Macromol Mater Eng 2007;292(4):407–14. http://dx.doi.org/10.1002/mame.200600460.
[7] Kotek R, Jung D, Tonelli AE, Vasanthan N. Novel methods for obtaining high modulus aliphatic polyamide fibers. J Macromol Sci Polym Rev 2005;45(3):201–30. http://dx.doi.org/10.1081/MC-200067716.
[8] Barham PJ, Keller A. High-strength polyethylene fibers from solution and gel spinning. J Mater Sci 1985;20(7):2281–302. http://dx.doi.org/10.1007/BF00556059.
[9] Reneker DH, Chun I. Nanometre diameter fibres of polymer, produced by electrospinning. Nanotechnology 1996;7(3):216–23. http://dx.doi.org/10.1088/0957-4484/7/3/009216.
[10] Shambaugh RL. A macroscopic view of the melt-blowing process for producing microfibers. Ind Eng Chem Res 1988;27(12):2363–72. http://dx.doi.org/10.1021/ie00084a021.
[11] Lu P, Ding B. Applications of electrospun fibers. Recent Pat Nanotechnol 2008;2(3):169–82. http://dx.doi.org/10.2174/187221008786369688.
[12] Tucker N, Stanger JJ, Staiger MP, Razzaq H, Hofman K. The history of the science and technology of electrospinning from 1600 to 1995. J Eng Fiber Fabr 2012;7:63–73. https://www.researchgate.net/publication/236621149.
[13] Dalton PD, Grafahrend D, Klinkhammer K, Klee D, Moller M. Electrospinning of polymer melts: phenomenological observations. Polymer 2007;48(23):6823–33. http://dx.doi.org/10.1016/j.polymer.2007.09.037.
[14] Truong YB, Glattauer V, Lang G, Hands K, Kyratzis IL, Werkmeister JA, et al. A comparison of the effects of fibre alignment of smooth and textured fibres in electrospun membranes on fibroblast cell adhesion. Biomed Mater 2010;5(2). http://dx.doi.org/10.1088/1748-6041/5/2/025005.
[15] Moghe AK, Gupta BS. Co-axial electrospinning for nanofiber structures: preparation and applications. Polym Rev 2008;48(2):353–77. http://dx.doi.org/10.1080/15583720802022257.
[16] Venugopal J, Prabhakaran MP, Low S, Choon AT, Deepika G, Dev VRG, et al. Continuous nanostructures for the controlled release of drugs. Curr Pharm Des 2009;15(15):1799–808. http://dx.doi.org/10.2174/138161209788186344.
[17] Yoo HS, Kim TG, Park TG. Surface-functionalized electrospun nanofibers for tissue engineering and drug delivery. Adv Drug Deliv Rev 2009;61(12):1033–42. http://dx.doi.org/10.1016/j.addr.2009.07.007.
[18] Persano L, Camposeo A, Tekmen C, Pisignano D. Industrial upscaling of electrospinning and applications of polymer nanofibers: a review. Macromol Mater Eng 2013;298(5):504–20. http://dx.doi.org/10.1002/mame.201200290.
[19] Deitzel JM, Kleinmeyer J, Harris D, Tan NCB. The effect of processing variables on the morphology of electrospun nanofibers and textiles. Polymer 2001;42(1):261–72. http://dx.doi.org/10.1016/S0032-3861(00)00250-0.
[20] Supaphol P, Mit-uppatham C, Nithitanakul M. Ultrafine electrospun polyamide-6 fibers: effects of solvent system and emitting electrode polarity on morphology and average fiber diameter. Macromol Mater Eng 2005;290(9):933–42. http://dx.doi.org/10.1002/mame.200500024.

[21] Nasouri K, Shoushtari AM, Mojtahedi MRM. Thermodynamic studies on polyvinylpyrrolidone solution systems used for fabrication of electrospun nanostructures: effects of the solvent. Adv Polym Technol 2015;34(3). http://dx.doi.org/10.1002/adv.21495.
[22] Fallahi D, Rafizadeh M, Mohammadi N, Vahidi B. Effect of LiCI and non-ionic surfactant on morphology of polystyrene electrospun nanofibers. E-Polymers 2008;056:1618–7229. http://dx.doi.org/10.1515/epoly.2008.8.1.644.
[23] Mit-uppatham C, Nithitanakul M, Supaphol P. Ultrafine electrospun polyamide-6 fibers: effect of solution conditions on morphology and average fiber diameter. Macromol Chem Phys 2004;205(17):2327–38. http://dx.doi.org/10.1002/macp.200400225.
[24] Demir MM, Yilgor I, Yilgor E, Erman B. Electrospinning of polyurethane fibers. Polymer 2002;43(11):3303–9. http://dx.doi.org/10.1016/S0032-3861(02)00136-2.
[25] De Vrieze S, Van Camp T, Nelvig A, Hagstrom B, Westbroek P. The effect of temperature and humidity on electrospinning. J Mater Sci 2009;44(5):1357–62. http://dx.doi.org/10.1007/s10853-008-3010-6.
[26] Liang T, Parhizkar M, Edirisinghe M, Mahalingam S. Effect of humidity on the generation and control of the morphology of honeycomb-like polymeric structures by electrospinning. Eur Polym J 2014;61:72–82. http://dx.doi.org/10.1016/j.eurpolymj.2014.09.020.
[27] Lavielle N, Hebraud A, Mendoza-Palomares C, Ferrand A, Benkirane-Jessel N, Schlatter G. Structuring and molding of electrospun nanofibers: effect of electrical and topographical local properties of micro-patterned collectors. Macromol Mater Eng 2012;297(10):958–68. http://dx.doi.org/10.1002/mame.201100327.
[28] Macossay J, Marruffo A, Rincon R, Eubanks T, Kuang A. Effect of needle diameter on nanofiber diameter and thermal properties of electrospun poly(methyl methacrylate). Polym Adv Technol 2007;18(3):180–3. http://dx.doi.org/10.1002/pat.844.
[29] Horzum N, Muñoz-Espí R, Glasser G, Demir MM, Landfester K, Crespy D. Hierarchically structured metal oxide/silica nanofibers by colloid electrospinning. ACS Appl Mater Interfaces 2012;4(11):6338–45. http://dx.doi.org/10.1021/am301969w.
[30] Nicolini AM, Toth TD, Yoon JY. Tuneable nanoparticle-nanofiber composite substrate for improved cellular adhesion. Colloids Surf B Biointerfaces 2016;145:830–8. http://dx.doi.org/10.1016/j.colsurfb.2016.05.079.
[31] Dehghan SF, Golbabaei F, Maddah B, Latifi M, Pezeshk H, Hasanzadeh M, et al. Optimization of electrospinning parameters for polyacrylonitrile-MgO nanofibers applied in air filtration. J Air Waste Manage Assoc 2016;66(9):912–21. http://dx.doi.org/10.1080/10962247.2016.1162228.
[32] Bhaway SM, Chen YM, Guo YH, Tangvijitsakul P, Soucek MD, Cakmak M, et al. Hierarchical electrospun and cooperatively assembled nanoporous Ni/NiO/MnO_x/carbon nanofiber composites for lithium ion battery anodes. ACS Appl Mater Interfaces 2016;8(30):19484–93. http://dx.doi.org/10.1021/acsami.6b05592.
[33] Balkan T, Guler Z, Morozova M, Dytrych P, Solcova O, Sarac AS. The effect of deposition on electrochemical impedance properties of TiO_2/FTO photoanodes. J Electroceram 2016;36(1–4):102–11. http://dx.doi.org/10.1007/s10832-016-0021-6.
[34] Yanilmaz M, Lu Y, Zhu JD, Zhang XW. Silica/polyacrylonitrile hybrid nanofiber membrane separators via sol-gel and electrospinning techniques for lithium-ion batteries. J Power Sources 2016;313:205–12. http://dx.doi.org/10.1016/j.jpowsour.2016.02.089.
[35] Joshi BN, An S, Jo HS, Song KY, Park HG, Hwang S, et al. Flexible, freestanding, and binder-free SnOx-ZnO/carbon nanofiber composites for lithium ion battery anodes. ACS Appl Mater Interfaces 2016;8(14):9446–53. http://dx.doi.org/10.1021/acsami.6b01093.

[36] Obaid M, Ghouri ZK, Fadali OA, Khalil KA, Almajid AA, Barakat NAM. Amorphous SiO_2 NP-incorporated poly(vinylidene fluoride) electrospun nanofiber membrane for high flux forward osmosis desalination. ACS Appl Mater Interfaces 2016;8(7):4561–74. http://dx.doi.org/10.1021/acsami.5b09945.

[37] Nalbandian MJ, Zhang ML, Sanchez J, Choa YH, Nam J, Cwiertny DM, et al. Synthesis and optimization of Fe_2O_3 nanofibers for chromate adsorption from contaminated water sources. Chemosphere 2016;144:975–81. http://dx.doi.org/10.1016/j.chemosphere.2015.08.056.

[38] Hosseini SR, Kamali-Rousta M. Preparation of electro-spun CuO nanoparticle and its application for hydrazine hydrate electro-oxidation. Electrochim Acta 2016;189:45–53. http://dx.doi.org/10.1016/j.electacta.2015.12.070.

[39] Xue HR, Mu XW, Tang J, Fan XL, Gong H, Wang T, et al. A nickel cobaltate nanoparticle-decorated hierarchical porous N-doped carbon nanofiber film as a binder-free self-supported cathode for nonaqueous Li-O-2 batteries. J Mater Chem A 2016;4(23):9106–12. http://dx.doi.org/10.1039/c6ta01712f.

[40] Li CW, Wang Q, Li J, Hu M, Shi SJ, Li ZW, et al. Silver nanoparticles/chitosan oligosaccharide/poly(vinyl alcohol) nanofiber promotes wound healing by activating TGF beta 1/Smad signaling pathway. Int J Nanomed 2016;11:373–87. http://dx.doi.org/10.2147/IJN.S91975.

[41] Horzum N, Mari M, Wagner M, Fortunato G, Popa AM, Demir MM, et al. Controlled surface mineralization of metal oxides on nanofibers. RSC Adv 2015;5(47):37340–5. http://dx.doi.org/10.1039/c5ra02140e.

[42] Neubert S, Pliszka D, Thavasi V, Wintermantel E, Ramakrishna S. Conductive electrospun PANi-PEO/TiO_2 fibrous membrane for photo catalysis. Mater Sci Eng B Adv Functional Solid-State Mater 2011;176(8):640–6. http://dx.doi.org/10.1016/j.mseb.2011.02.007.

[43] Roso M, Sundarrajan S, Pliszka D, Ramakrishna S, Modesti M. Multifunctional membranes based on spinning technologies: the synergy of nanofibers and nanoparticles. Nanotechnology 2008;19(28). http://dx.doi.org/10.1088/0957-4484/19/28/285707.

[44] Rathod AP, Vora TP. Fiber reinforced polymer reinforcement for construction-state of the art review. Int J Res Eng Technol 2015;04(2):2319–22. http://dx.doi.org/10.15623/ijret.2015.0402101.

[45] Bakis CE, Bank LC, Brown VL, Cosenza E, Davalos JF, Lesko JJ, et al. Fiber-reinforced polymer composites for construction-state-of-the-art review. J Compos Constr 2002;6(2):73–87. http://dx.doi.org/10.1061/(ASCE)1090-0268(2002)6:2(73).

[46] Coleman JN, Khan U, Blau WJ, Gun'ko YK. Small but strong: a review of the mechanical properties of carbon nanotube-polymer composites. Carbon 2006;44(9):1624–52. http://dx.doi.org/10.1016/j.carbon.2006.02.038.

[47] Thostenson ET, Li CY, Chou TW. Nanocomposites in context. Compos Sci Technol 2005;65(3–4):491–516. http://dx.doi.org/10.1016/j.compscitech.2004.11.003.

[48] Balasubramanian M. Composite materials and processing. Boca Raton, FL: CRC Press; 2013.

[49] Riechers K. Synthetic resins in aircraft construction—their composition, properties, present state of development and application to light structures. UNT Digit Libr 1937;4(8):14.

[50] Hossain MK, Hossain ME, Hosur MV, Jeelani S. Flexural and compression response of woven E-glass/polyester-CNF nanophased composites. Compos Part A Appl Sci Manuf 2011;42(11):1774–82. http://dx.doi.org/10.1016/j.compositesa.2011.07.033.

[51] Pal G, Kumar S. Multiscale modeling of effective electrical conductivity of short carbon fiber-carbon nanotube-polymer matrix hybrid composites. Mater Des 2016;89:129–36. http://dx.doi.org/10.1016/j.matdes.2015.09.105.
[52] Hou HQ, Ge JJ, Zeng J, Li Q, Reneker DH, Greiner A, et al. Electrospun polyacrylonitrile nanofibers containing a high concentration of well-aligned multiwall carbon nanotubes. Chem Mater 2005;17(5):967–73. http://dx.doi.org/10.1021/cm0484955.
[53] Numnuam A, Thavarungkul P, Kanatharana P. An amperometric uric acid biosensor based on chitosan-carbon nanotubes electrospun nanofiber on silver nanoparticles. Anal Bioanal Chem 2014;406(15):3763–72. http://dx.doi.org/10.1007/s00216-014-7770-3.
[54] Shokrgozar MA, Mottaghitalab F, Mottaghitalab V, Farokhi M. Fabrication of porous chitosan/poly(vinyl alcohol) reinforced single-walled carbon nanotube nanocomposites for neural tissue engineering. J Biomed Nanotechnol 2011;7(2):276–84. http://dx.doi.org/10.1166/jbn.2011.1284.
[55] Allaoui A, Bai S, Cheng HM, Bai JB. Mechanical and electrical properties of a MWNT/epoxy composite. Compos Sci Technol 2002;62(15):1993–8. http://dx.doi.org/10.1016/S0266-3538(02)00129-X.
[56] Baji A, Mai YW, Wong SC, Abtahi M, Du XS. Mechanical behavior of self-assembled carbon nanotube reinforced nylon 6,6 fibers. Compos Sci Technol 2010;70(9):1401–9. http://dx.doi.org/10.1016/j.compscitech.2010.04.020.
[57] Ge JJ, Hou HQ, Li Q, Graham MJ, Greiner A, Reneker DH, et al. Assembly of well-aligned multiwalled carbon nanotubes in confined polyacrylonitrile environments: electrospun composite nanofiber sheets. J Am Chem Soc 2004;126(48):15754–61. http://dx.doi.org/10.1021/ja048648p.
[58] Kedem S, Schmidt J, Paz Y, Cohen Y. Composite polymer nanofibers with carbon nanotubes and titanium dioxide particles. Langmuir 2005;21(12):5600–4. http://dx.doi.org/10.1021/la0502443.
[59] Lam H, Ye H, Gogotsi Y, Ko F. Structure and properties of electrospun single-walled carbon nanotubes reinforced nanocomposite fibrils by coelectrospinning. Polym Prepr 2004;45:124–5.
[60] Titchenal NL, Naguib N, Ye HH, Gogotsi Y, Liu J, Ko FK. Next-generation carbon fibers by electrospinning PAN and MWNT nanocomposite. In: Abstracts of Papers of The American Chemical Society, vol. 226. Part: 2 Meeting Abstract: 573-POLY; 2003. p. U443.
[61] Ye HH, Lam H, Titchenal N, Gogotsi Y, Ko F. Reinforcement and rupture behavior of carbon nanotubes-polymer nanofibers. Appl Phys Lett 2004;85(10):1775–7. http://dx.doi.org/10.1063/1.1787892.
[62] Simotwo SK, DelRe C, Kalra V. Supercapacitor electrodes based on high-purity electrospun polyaniline and polyaniline-carbon nanotube nanofibers. ACS Appl Mater Interfaces 2016;8(33):21261–9. http://dx.doi.org/10.1021/acsami.6b03463.
[63] Deshpande HD, Dean DR, Thomas V, Clem WC, Jose MV, Nyairo E, et al. Carbon nanofiber reinforced polycaprolactone fibrous meshes by electrostatic co-spinning. Curr Nanosci 2012;8(5):753–61.
[64] Kim GM, Michler GH, Potschke P. Deformation processes of ultrahigh porous multiwalled carbon nanotubes/polycarbonate composite fibers prepared by electrospinning. Polymer 2005;46(18):7346–51. http://dx.doi.org/10.1016/j.polymer.2005.06.008.
[65] Bao JX, Clarke LI, Gorga RE. Effect of constrained annealing on the mechanical properties of electrospun poly(ethylene oxide) webs containing multiwalled carbon nanotubes. J Polym Sci Part B-Polym Phys 2016;54(8):787–96. http://dx.doi.org/10.1002/polb.23960.

[66] Lim JY, Lee CK, Kim SJ, Kim IY, Kim SI. Controlled nanofiber composed of multi-wall carbon nanotube/poly(ethylene oxide). J Macromol Sci Part A Pure Appl Chem 2006;43 (4–5):785–96. http://dx.doi.org/10.1080/10601320600598936.
[67] Su ZQ, Li JF, Li Q, Ni TY, Wei G. Chain conformation, crystallization behavior, electrical and mechanical properties of electrospun polymer-carbon nanotube hybrid nanofibers with different orientations. Carbon 2012;50(15):5605–17. http://dx.doi.org/10.1016/j.carbon.2012.08.017.
[68] Ko F, Gogotsi Y, Ali A, Naguib N, Ye HH, Yang GL, et al. Electrospinning of continuous carbon nanotube-filled nanofiber yarns. Adv Mater 2003;15(14):1161. http://dx.doi.org/10.1002/adma.200304955.
[69] Kim DO, Nam JD, Lee DH, Lee JY, Park JJ, Kim JM. Morphological characteristics of electrospun poly(methyl methacrylate) nanofibers containing multi-walled carbon nanotubes. Mol Cryst Liq Cryst 2007;464:719–26. http://dx.doi.org/10.1080/15421400601030761.
[70] Sundaray B, Babu VJ, Subramanian V, Natarajan TS. Preparation and characterization of electrospun fibers of poly(methyl methacrylate)—single walled carbon nanotube nanocomposites. J Eng Fiber Fabr 2008;3(4):39–45.
[71] Macossay J, Ybarra AVR, Arjamend FA, Cantu T, Eubanks TM, Chipara M, et al. Electrospun polystyrene-multiwalled carbon nanotubes: imaging, thermal and spectroscopic characterization. Des Monomers Polym 2012;15(2):197–205. http://dx.doi.org/10.1163/156855511X615065.
[72] Sen R, Zhao B, Perea D, Itkis ME, Hu H, Love J, et al. Preparation of single-walled carbon nanotube reinforced polystyrene and polyurethane nanofibers and membranes by electrospinning. Nano Lett 2004;4(3):459–64. http://dx.doi.org/10.1021/nl035135s.
[73] Rakesh GR, Ranjit GS, Karthikeyan KK, Radhakrishnan P, Biji P. A facile route for controlled alignment of carbon nanotube-reinforced, electrospun nanofibers using slotted collector plates. Express Polym Lett 2015;9(2):105–18. http://dx.doi.org/10.3144/expresspolymlett.2015.12.
[74] Salimbeygi G, Nasouri K, Shoushtari AM, Malek R, Mazaheri F. Fabrication of polyvinyl alcohol/multi-walled carbon nanotubes composite electrospun nanofibres and their application as microwave absorbing material. Micro Nano Lett 2013;8(8):455–9. http://dx.doi.org/10.1049/mnl.2013.0381.
[75] Zhou WP, Wu YL, Wei F, Luo GH, Qian WZ. Elastic deformation of multiwalled carbon nanotubes in electrospun MWCNTs-PEO and MWCNTs-PVA nanofibers. Polymer 2005;46(26):12689–95. http://dx.doi.org/10.1016/j.polymer.2005.10.114.
[76] Pan H, Zhang YP, Hang YC, Shao HL, Hu XC, Xu YM, et al. Significantly reinforced composite fibers electrospun from silk fibroin/carbon nanotube aqueous solutions. Biomacromolecules 2012;13(9):2859–67. http://dx.doi.org/10.1021/bm300877d.
[77] Wei K, Xia JH, Kim BS, Kim IS. Multiwalled carbon nanotubes incorporated bombyx mori silk nanofibers by electrospinning. J Polym Res 2011;18(4):579–85. http://dx.doi.org/10.1007/s10965-010-9451-z.
[78] Parveen S, Rana S, Fangueiro R. A review on nanomaterial dispersion, microstructure, and mechanical properties of carbon nanotube and nanofiber reinforced cementitious composites. J Nanomater 2013. http://dx.doi.org/10.1155/2013/710175.
[79] Ma HM, Zeng JJ, Realff ML, Kumar S, Schiraldi DA. Processing, structure, and properties of fibers from polyester/carbon nanofiber composites. Compos Sci Technol 2003;63(11):1617–28. http://dx.doi.org/10.1016/S0266-3538(03)00071-X.
[80] Ashrafi B, Guan JW, Mirjalili V, Zhang YF, Chun L, Hubert P, et al. Enhancement of mechanical performance of epoxy/carbon fiber laminate composites using

single-walled carbon nanotubes. Compos Sci Technol 2011;71(13):1569–78. http://dx.doi.org/10.1016/j.compscitech.2011.06.015.

[81] Wu Q, Zhu W, Zhang C, Liang ZY, Wang B. Study of fire retardant behavior of carbon nanotube membranes and carbon nanofiber paper in carbon fiber reinforced epoxy composites. Carbon 2010;48(6):1799–806. http://dx.doi.org/10.1016/j.carbon.2010.01.023.

[82] Dror Y, Salalha W, Khalfin RL, Cohen Y, Yarin AL, Zussman E. Carbon nanotubes embedded in oriented polymer nanofibers by electrospinning. Langmuir 2003;19(17):7012–20. http://dx.doi.org/10.1021/la034234i.

[83] Qian D, Dickey EC, Andrews R, Rantell T. Load transfer and deformation mechanisms in carbon nanotube-polystyrene composites. Appl Phys Lett 2000;76(20):2868–70. http://dx.doi.org/10.1063/1.126500.

[84] Bandyopadhyaya R, Nativ-Roth E, Regev O, Yerushalmi-Rozen R. Stabilization of individual carbon nanotubes in aqueous solutions. Nano Lett 2002;2(1):25–8. http://dx.doi.org/10.1021/nl010065f.

[85] Vigolo B, Penicaud A, Coulon C, Sauder C, Pailler R, Journet C, et al. Macroscopic fibers and ribbons of oriented carbon nanotubes. Science 2000;290(5495):1331–4. http://dx.doi.org/10.1126/science.290.5495.1331.

[86] Subagia IDGA, Jiang Z, Tijing LD, Kim Y, Kim CS, Lim JK, et al. Hybrid multi-scale basalt fiber-epoxy composite laminate reinforced with electrospun polyurethane nanofibers containing carbon nanotubes. Fibers Polym 2014;15(6):1295–302. http://dx.doi.org/10.1007/s12221-014-1295-4.

[87] Jia XL, Li WS, Xu XJ, Li WB, Cai Q, Yang XP. Numerical characterization of magnetically aligned multiwalled carbon nanotube-Fe_3O_4 nanoparticle complex. ACS Appl Mater Interfaces 2015;7(5):3170–9. http://dx.doi.org/10.1021/am507583r.

[88] Schlittler RR, Seo JW, Gimzewski JK, Durkan C, Saifullah MSM, Welland ME. Single crystals of single-walled carbon nanotubes formed by self-assembly. Science 2001;292(5519):1136–9. http://dx.doi.org/10.1126/science.1057823.

[89] Yuan W, Chan-Park MB. Covalent cum noncovalent functionalizations of carbon nanotubes for effective reinforcement of a solution cast composite film. ACS Appl Mater Interfaces 2012;4(4):2065–73. http://dx.doi.org/10.1021/am300038d.

[90] Manchado MAL, Valentini L, Biagiotti J, Kenny JM. Thermal and mechanical properties of single-walled carbon nano tubes-polypropylene composites prepared by melt processing. Carbon 2005;43(7):1499–505. http://dx.doi.org/10.1016/j.carbon.2005.01.031.

[91] Kausar A. Polyamide-grafted-multi-walled carbon nanotube electrospun nanofibers/epoxy composites. Fibers Polym 2014;15(12):2564–71. http://dx.doi.org/10.1007/s12221-014-2564-y.

[92] Zhao CG, Hu GJ, Justice R, Schaefer DW, Zhang SM, Yang MS, et al. Synthesis and characterization of multi-walled carbon nanotubes reinforced polyamide 6 via in situ polymerization. Polymer 2005;46(14):5125–32. http://dx.doi.org/10.1016/j.polymer.2005.04.065.

[93] Abu Al-Rub RK, Ashour AI, Tyson BM. On the aspect ratio effect of multi-walled carbon nanotube reinforcements on the mechanical properties of cementitious nanocomposites. Constr Build Mater 2012;35:647–55. http://dx.doi.org/10.1016/j.conbuildmat.2012.04.086.

[94] Nasouri K, Shoushtari AM, Mojtahedi MRM. Theoretical and experimental studies on EMI shielding mechanisms of multi-walled carbon nanotubes reinforced high performance composite nanofibers. J Polym Res 2016;23(4). http://dx.doi.org/10.1007/s10965-016-0943-3.

[95] Ozden YE, Menceloglu YZ, Papila M. MWCNTs/P(St-co-GMA) composite nanofibers of engineered interface chemistry for epoxy matrix nanocomposites. ACS Appl Mater Interfaces 2012;4(2):777–84. http://dx.doi.org/10.1021/am2014162.

[96] Chen W, Yua H, Liu Y, Chen P, Zhang M, Hai Y. Individualization of cellulose nanofibers from wood using high-intensity ultrasonication combined with chemical pretreatments. Carbohydr Polym 2011;83(4):1804–11. http://dx.doi.org/10.1016/j.carbpol.2010.10.040.
[97] Eichhorn SJ, Baillie CA, Zafeiropoulos N, Mwaikambo LY, Ansell MP, Dufresne A, et al. Review: current international research into cellulosic fibres and composites. J Mater Sci 2001;36(9):2107–31. http://dx.doi.org/10.1023/A:1017512029696.
[98] Moon RJ, Martini A, Nairn J, Simonsen J, Youngblood J. Cellulose nanomaterials review: structure, properties and nanocomposites. Chem Soc Rev 2011;40(7):3941–94. http://dx.doi.org/10.1039/c0cs00108b.
[99] Babaeea M, Jonoobi M, Hamzeha Y, Ashori A. Biodegradability and mechanical properties of reinforced starch nanocomposites using cellulose nanofibers, Carbohydr Polym 2015;132:1–8. http://linkinghub.elsevier.com/retrieve/pii/S0144861715005500.
[100] Gindl W, Keckes J. All-cellulose nanocomposite. Polymer 2005;46(23):10221–5. http://dx.doi.org/10.1016/j.polymer.2005.08.040.
[101] Iwatake A, Nogi M, Yano H. Cellulose nanofiber-reinforced polylactic acid. Compos Sci Technol 2008;68(9):2103–6. http://dx.doi.org/10.1016/j.compscitech.2008.03.006.
[102] Bettaieb F, Nechyporchuk O, Khiari R. Effect of the oxidation treatment on the production of cellulose nanofiber suspensions from *Posidonia oceanica*: the rheological aspect. Carbohydr Polym 2015;134:664–72. http://dx.doi.org/10.1016/j.carbpol.2015.07.091.
[103] Qamhia II, Sabo RC, Elhajjar RF. Static and dynamic characterization of cellulose nanofibril scaffold-based composites. BioResources 2014;9(1):381–92. http://dx.doi.org/10.15376/biores.9.1.381-392.
[104] Kobe R, Yoshitani K, Teramoto Y. Fabrication of elastic composite hydrogels using surface-modified cellulose nanofiber as a multifunctional crosslinker. J Appl Polym Sci 2016;133(4). http://dx.doi.org/10.1002/app.42906.
[105] Kiziltas A, Nazari B, Kiziltas EE, Gardner DJS, Han Y, Rushing TS. Cellulose nanofiber-polyethylene nanocomposites modified by polyvinyl alcohol. J Appl Polym Sci 2016;133(6). http://dx.doi.org/10.1002/app.42933.
[106] Lavoratti A, Cristine L, José A. Dynamic-mechanical and thermomechanical properties of cellulose nanofiber/polyester resin composites. Carbohydr Polym 2016;136:955–63. http://dx.doi.org/10.1016/j.carbpol.2015.10.008.
[107] Yusra AFI, Khalil HPSA, Hossain MS, Davoudpour Y, Astimar AA, Zaidon A, et al. Characterization of plant nanofiber-reinforced epoxy composites. Bioresources 2015;10(4):8268–80.
[108] Masoodi R, El-Hajjar RF, Pillai KM, Sabo R. Mechanical characterization of cellulose nanofiber and bio-based epoxy composite. Mater Des 2012;36:570–6. http://dx.doi.org/10.1016/j.matdes.2011.11.042.
[109] Ansari F, Galland S, Johansson M, Plummer C, Berglund LA. Cellulose nanofiber network for moisture stable, strong and ductile biocomposites and increased epoxy curing rate. Compos Part A 2014;63:35–44. http://dx.doi.org/10.1016/j.compositesa.2014.03.017.
[110] Virtanen S, Vuoti S, Heikkinen H, Lahtinen P. High strength modified nanofibrillated cellulose-polyvinyl alcohol films. Cellulose 2014;21(5):3561–71. http://dx.doi.org/10.1007/s10570-014-0347-7.
[111] Petersson L, Kvien I, Oksman K. Structure and thermal properties of poly(lactic acid)/cellulose whiskers nanocomposite materials. Compos Sci Technol 2007;67(11–12):2535–44. http://dx.doi.org/10.1016/j.compscitech.2006.12.012.
[112] Grunert M, Winter WT. Nanocomposites of cellulose acetate butyrate reinforced with cellulose nanocrystals. J Polym Environ 2002;10(1–2):27–30.

[113] Nair KG, Dufresne A, Gandini A, Belgacem MN. Crab shell chitin whiskers reinforced natural rubber nanocomposites. 3. Effect of chemical modification of chitin whiskers. Biomacromolecules 2003;4(6):1835–42. http://dx.doi.org/10.1021/bm030058g.
[114] Lee HJ, Lim JM, Kim HW, Jeong SH, Eom SW, Hong YT, et al. Electrospun polyetherimide nanofiber mat-reinforced, permselective polyvinyl alcohol composite separator membranes: a membrane-driven step closer toward rechargeable zinc-air batteries. J Membr Sci 2016;499:526–37. http://dx.doi.org/10.1016/j.memsci.2015.10.038.
[115] Park AM, Wycisk RJ, Ren XM, Turley FE, Pintauro PN. Crosslinked poly(phenylene oxide)-based nanofiber composite membranes for alkaline fuel cells. J Mater Chem A 2016;4(1):132–41. http://dx.doi.org/10.1039/c5ta06209h.
[116] Li Y, Lee DK, Kim JY, Kim B, Park NG, Kim K, et al. Highly durable and flexible dye-sensitized solar cells fabricated on plastic substrates: PVDF-nanofiber-reinforced TiO_2 photoelectrodes. Energy Environ Sci 2012;5(10):8950–7. http://dx.doi.org/10.1039/c2ee21674d.
[117] Dubal DP, Ayyad O, Ruiz V, Gomez-Romero P. Hybrid energy storage: the merging of battery and supercapacitor chemistries. Chem Soc Rev 2015;44(7):1777–90. http://dx.doi.org/10.1039/c4cs00266k.
[118] Xu J, Wang LB, Guan J, Yin S. Coupled effect of strain rate and solvent on dynamic mechanical behaviors of separators in lithium ion batteries. Mater Des 2016;95:319–28. http://dx.doi.org/10.1016/j.matdes.2016.01.082.
[119] Devarayan K, Lei DY, Kim HY, Kim BS. Flexible transparent electrode based on PANi nanowire/nylon nanofiber reinforced cellulose acetate thin film as supercapacitor. Chem Eng J 2015;273:603–9. http://dx.doi.org/10.1016/j.cej.2015.03.115.
[120] Miao YE, Yan JJ, Huang YP, Fan W, Liu TX. Electrospun polymer nanofiber membrane electrodes and an electrolyte for highly flexible and foldable all-solid-state supercapacitors. RSC Adv 2015;5(33):26189–96. http://dx.doi.org/10.1039/c5ra00138b.
[121] Feng Y, Xiong TR, Xu HB, Li CG, Hou HQ. Polyamide-imide reinforced polytetrafluoroethylene nanofiber membranes with enhanced mechanical properties and thermal stabilities. Mater Lett 2016;182:59–62. http://dx.doi.org/10.1016/j.matlet.2016.06.074.
[122] Liu CL, Li XF, Liu T, Liu Z, Li NN, Zhang YF, et al. Microporous CA/PVDF membranes based on electrospun nanofibers with controlled crosslinking induced by solvent vapor. J Membr Sci 2016;512:1–12. http://dx.doi.org/10.1016/j.memsci.2016.03.062.
[123] Tian M, Wang R, Goh K, Liao Y, Fane AG. Synthesis and characterization of high-performance novel thin film nanocomposite PRO membranes with tiered nanofiber support reinforced by functionalized carbon nanotubes. J Membr Sci 2015;486:151–60. http://dx.doi.org/10.1016/j.memsci.2015.03.054.
[124] Pachuau LS. A mini review on plant-based nanocellulose: production, sources, modifications and its potential in drug delivery applications. Mini-Rev Med Chem 2015;15(7):543–52. http://dx.doi.org/10.2174/1389557515666150415150327.
[125] Gao X, Song JL, Ji P, Zhang XH, Li XM, Xu X, et al. Polydopamine-templated hydroxyapatite reinforced polycaprolactone composite nanofibers with enhanced cytocompatibility and osteogenesis for bone tissue engineering. ACS Appl Mater Interfaces 2016;8(5):3499–515. http://dx.doi.org/10.1021/acsami.5b12413.
[126] Nakhoda HM, Dahman Y. Mechanical properties and biodegradability of porous polyurethanes reinforced with green nanofibers for applications in tissue engineering. Polym Bull 2016;73(7):2039–55. http://dx.doi.org/10.1007/s00289-015-1592-0.
[127] Sun W, Cai Q, Li P, Deng XL, Wei Y, Xu MM, et al. Post-draw PAN-PMMA nanofiber reinforced and toughened Bis-GMA dental restorative composite. Dent Mater 2010;26(9):873–80. http://dx.doi.org/10.1016/j.dental.2010.03.022.

[128] Vidotti HA, Manso AP, Leung V, do Valle AL, Ko F, Carualho RM. Flexural properties of experimental nanofiber reinforced composite are affected by resin composition and nanofiber/resin ratio. Dent Mater 2015;31(9):1132–41. http://dx.doi.org/10.1016/j.dental.2015.06.018.
[129] Tanimoto Y. Dental materials used for metal-free restorations: recent advances and future challenges. J Prosthodont Res 2015;59(4):213–5. http://dx.doi.org/10.1016/j.jpor.2015.07.003.
[130] Al-Saleh MH, Sundararaj U. A review of vapor grown carbon nanofiber/polymer conductive composites. Carbon 2009;47(1):2–22. http://dx.doi.org/10.1016/j.carbon.2008.09.039.
[131] Fu Y, Zhong WH. Cure kinetics behavior of a functionalized graphitic nanofiber modified epoxy resin. Thermochim Acta 2011;516(1–2):58–63. http://dx.doi.org/10.1016/j.tca.2011.01.016.
[132] Berry SM, Harfenist SA, Cohn RW, Keynton RS. Characterization of micromanipulator-controlled dry spinning of micro- and sub-microscale polymer fibers. J Micromech Microeng 2006;16:1825–32. http://dx.doi.org/10.1088/0960-1317/16/9/010.
[133] da Silva Parize DD, Foschini MM, de Oliveira JE, Klamczynski AP, Glenn GM, Marconcini JM, et al. Solution blow spinning: parameters optimization and effects on the properties of nanofibers from poly(lactic acid)/dimethyl carbonate solutions. J Mater Sci 2016;51:4627–38. http://dx.doi.org/10.1007/s10853-016-9778-x.

Further Reading

Aoyagi Y, Yamashita K, Doi Y. Thermal degradation of poly[(R)-3-hydroxybutyrate], poly[ε-caprolactone], and poly[(S)-lactide]. Polym Degrad Stab 2002;76(1):53–9. http://www.sciencedirect.com/science/article/pii/S0141391001002658.
Bagherpour S. Fibre reinforced polyester composites. Intech; 2012135–66. http://dx.doi.org/10.5772/48697.
Brown E, Sottos NR, White SR. Fracture testing of a self-healing polymer composite. Exp Mech 2002;42(4):372–9. http://dx.doi.org/10.1177/001448502321548193.
Degée P, Dubois P, Jérôme R. Bulk polymerization of lactides initiated by aluminium isopropoxide. Thermal stability and viscoelastic properties. Macromol Chem Phys 1997;198:1985–95. http://dx.doi.org/10.1002/macp.1997.021980624.
Esser-Kahn AP, Thakre PR, Dong HF, Patrick JF, Vlasko-Vlasov VK, Sottos NR, et al. Three-dimensional microvascular fiber-reinforced composites. Adv Mater 2011;23(32):3654–8. http://dx.doi.org/10.1002/adma.201100933.
Kessler MR, Sottos NR, White SR. Self-healing structural composite materials. Compos Part A Appl Sci Manuf 2003;34(8):743–53. http://dx.doi.org/10.1016/S1359-835X(03)00138-6.
Lee YJ, Joo HJ, Radovic LR. Preferential distribution and oxidation inhibiting/catalytic effects of boron in carbon fiber reinforced carbon (CFRC) composites. Carbon 2003;41(13):2591–600. http://dx.doi.org/10.1016/S0008-6223(03)00372-5.
Mallick PK. Fibre-reinforced composites: materials, manufacturing and design. CRC Press; 2007.
Nishida H, Mori T, Hoshihara S, Fan YJ, Shirai Y, Endo T. Effect of tin on poly(l-lactic acid) pyrolysis. Polym Degrad Stab 2003;81(3):515–23. http://dx.doi.org/10.1016/S0141-3910(03)00152-6.

Noda M, Okuyama H. Thermal catalytic depolymerization of poly(L-lactic acid) oligomer into LL-lactide: effects of Al, Ti, Zn and Zr compounds as catalysts. Chem Pharm Bull 1999;47 (4):467–71. http://dx.doi.org/10.1248/cpb.47.467.

Scott MB, Harfenist SA, Cohn RW, Keynton RS. Characterization of micromanipulator-controlled dry spinning of micro- and sub-microscale polymer fibers. J Micromech Microeng 2006;16:1825–32. http://dx.doi.org/10.1088/0960-1317/16/9/010.

Thostenson ET, Li WZ, Wang DZ, Ren ZF, Chou TW. Carbon nanotube/carbon fiber hybrid multiscale composites. J Appl Phys 2002;91(9):6034–7. http://dx.doi.org/10.1063/1.1466880.

White SR, Caruso MM, Moore JS. Autonomic healing of polymers. MRS Bull 2008;33 (8):766–9. http://dx.doi.org/10.1557/mrs2008.163.

Zhang CQ, Li YP, Wang W, Zhan NQ, Xiao N, Wang S, et al. A novel two-nozzle electrospinning process for preparing microfiber reinforced pH-sensitive nano-membrane with enhanced mechanical property. Eur Polym J 2011;47 (12):2228–33. http://dx.doi.org/10.1016/j.eurpolymj.2011.09.015.

This page intentionally left blank

The use of nanotechnology for fibre-reinforced polymer composites

13

Sibel Demiroglu[*], *Vivekanandhan Singaravelu*[†], *M. Özgür Seydibeyoğlu*[*], *Manjusri Misra*[‡], *Amar K. Mohanty*[‡]
[*]Izmir Katip Çelebi University, Izmir, Turkey, [†]VHNSN College, Virudhunagar, India, [‡]University of Guelph, Guelph, ON, Canada

13.1 Introduction

Polymer composites receive significant interest in the last two decades not only due to their enhanced material performance but also due to their commercial potential in various fields [1]. These materials are capable of substituting various types of metallic or ceramic materials in many applications including automotive, aerospace, marine, civil, household appliances, advanced electronics, and sport articles [1,2]. The global market of the composite materials in 2015 was around US $69.50 billion, and it has been predicted that it will reach up to US $105.26 billion by 2021 with the compound annual growth rate (CAGR) of 7.04% [3]. A wide range of polymers have been extensively explored as the matrix, including thermoplastics, thermosets, and elastomers [4]. Likewise, numerous materials that belong to different categories including metals, metal oxides, carbon allotropes, and natural products in particulate or fibrous nature have been extensively used as reinforcements for the fabrication of composite materials [4–6]. In order to meet the specific requirements of many industrial applications, composites have been made with the combinations of various filler/reinforcements and polymers [7]. Among them, polymer matrix composites fabricated with fiber reinforcements receive significant attention due to their enhanced physicochemical performance, functional properties, low temperature processing, cost-effectiveness, and commercial potential. Carbon, glass, and natural fibers are the common fibrous materials that are used in composite fabrication.

13.1.1 Fibre-reinforced polymer composites

Fiber reinforcement into polymer matrix leads to the formation of composite materials with enhanced mechanical properties due to the effective load transfer mechanism between the fiber and the matrix [8,9]. They also offer many advantages such as lower weight, high stiffness/strength to weight ratios, improved durability, and cost benefits compared with their matrix counterpart [5,10]. Even the traditional engineering fibers such as carbon and glass fibers were explored for many commercial applications;

Fiber Technology for Fiber-Reinforced Composites. http://dx.doi.org/10.1016/B978-0-08-101871-2.00013-8

lignocellulosic fibers receive extensive attention in recent years due to their lower density, environmental friendliness, abundance in nature, and biodegradability [8]. As the global demand expands for the sustainable and eco-friendly materials, biopolymers also receive increased consideration along with natural fibers for composite fabrication [11]. Thus, extensive efforts have been made in increasing the commercial potential of these bio-based composite materials in many felid including automotive, packaging, agriculture, biomedical, and consumer products [12,13]. The mechanical properties of the fiber-reinforced composite materials are not only due to the properties of fibers and resins but also based on the physical/chemical nature of their interphase [14]. Thus, the key challenge in composite fabrication is the enhancement of compatibility between polymer matrix and the fiber surface, which enables the effective stress transfer [15–17]. Countless approaches have been incorporated, increasing the fiber-matrix adhesion in modifying both matrix and fiber [15–17]. This includes both matrix and fiber modification by employing various physical and chemical activities. Common method is the use of suitable compatibilizers depending on the chemical nature of fiber and matrix, which creates effective chemical bonding during the composite processing [18,19]. From an engineering fiber perspective, several methods have been used for their surface modification, which involves oxidation processes, formation of silicon carbide whiskers, ammonia plasma treatments, and sizing with various chemical compounds [14]. Similarly, surface treatments of the natural fibers include alkaline/silane treatments, grafting of monomers, acetylation/benzoylation, and modification with coupling agents [15]. The coupling agents are commonly known to be tetrafunctional organometallic compounds, which are based on silicon, titanium, and zirconium [15]. The challenges involved in the abovementioned traditional matrix and fiber modification processes are the execution of many processing steps and the need of specific modification strategy for individual matrix-fiber combination. In this context, the recent advancements in nanoscience offer key benefits in modifying both matrix and fiber, which ultimately improves their compatibility.

13.1.2 Nanotechnologies for fibre-reinforced polymer composites

The recent developments in nanotechnology facilitate the new innovations in fabricating advanced materials with enhanced physicochemical and custom-fitted functional properties, which can be effectively explored in many fields [20]. Especially in polymer composites, integration of various nanostructured materials and the nanofabrication techniques has created a platform for developing new class of materials termed as “nanocomposites” that could effectively fulfill the demand of many industrial/manufacturing sectors [21]. A wide range of nanostructured materials that include nanoparticles (metal/metal oxides/carbon), fiber carbon/cellulose, and two-dimensional (2-D) materials (clay/talc/graphene) have been extensively explored for the fabrication of composite materials. Nanocomposites are recently being utilized in various fields as these materials have excellent properties such as lightweight, thermal/structural stability, electric conductivity, improved barrier performance,

and durability [22–24]. The enormous advantages of nanocomposites compared with their respective virgin polymer or micro/macro reinforcements have triggered an impressive press over the previous decade. Thus, a wide range of polymer nanocomposites by compiling various polymer matrixes and nanostructured reinforcements have been developed and explored for numerous potential applications [4]. Owing to the desired properties, some applications of the nanocomposites are uniquely appropriate, which includes energy storage, packaging, biotechnology, electronics, cosmetics, communication, and security sectors. Along with the fabrication of nanocomposites made with nanofillers or reinforcements, the advanced nano-enabled processing or fabrication techniques also enhance the performance of various other fiber-/particulate-reinforced composite materials [25–27]. In particular, with fiber-reinforced composite materials, nanotechnology can be integrated with both the matrix and fiber in order to improve the overall performance of the composite material. The aim of this chapter is to review and summarize the recent developments in the area of nano-enhanced polymer composites with fiber reinforcement.

13.2 Nanotechnologies for matrix modification

The modification of matrix with nanostructured materials could enrich their physicochemical properties including dielectric constant, modulus, thermal, and mechanical strength. The purpose of this section is to summarize the various research accomplishments in matrix modification by reinforcing various nanostructured materials, which includes hyperbranched polymers, polyhedral oligomeric silsesquioxane (POSS), and nanoparticles.

13.2.1 Matrix modification with hyperbranched polymers

Hyperbranched polymers are considered as organic nanostructures that can be structurally defined as highly branched macromolecules (Fig. 13.1). This enables the hyperbranched polymers to have a three-dimensional (3-D) dendritic architecture [28,29]. Because of this architecture, hyperbranched polymers have a large degree of functional terminal groups and free area for its structure to develop the toughness of epoxy matrix. They can also be utilized to enhance the processability by accomplishing a superior filler dispersal [30]. For instance, carbon nanofibers have been used to improve mechanical and electric properties of composites, but carbon nanofibers require a homogenous scattering inside a polymer network. To enhance the dispersibility of carbon nanofibers inside a polymer matrix, a hyperbranched polyol/carbon nanofiber composite was developed by Rhodes et al. [31]. Also, a few studies have been conducted on hyperbranched polymers to study their impact on fracture toughness and mechanical properties of the fiber-reinforced composites. Wong et al. investigated the impact of hyperbranched polymer on the poly(L-lactic acid)-flax fiber composites. They demonstrated that when the hyperbranched polymer was utilized as additive, the fracture toughness of fiber-reinforced composite was

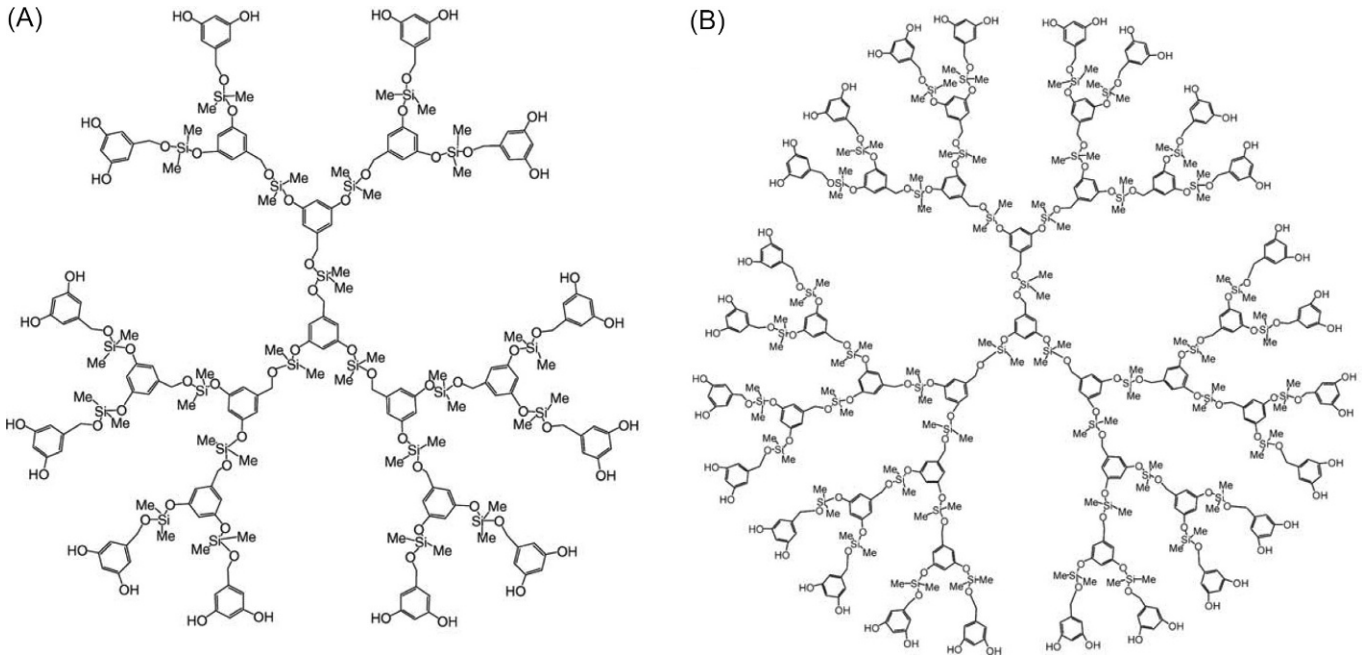

Fig. 13.1 Schematic representation of third (A) and fourth (B) generation of hyperbranched dendritic structures.
Adapted from Bourrier O, Butlin J, Hourani R, Kakkar AK. Aggregation of 3,5-dihydroxybenzyl alcohol based dendrimers and hyperbranched polymers, and encapsulation of DR1 in such dendritic aggregates. Inorg Chim Acta 2004;357:3836–46, Elsevier, copyright © 2004.

increased [32]. In another study, Li et al. [33] showed that epoxy/hyperbranched polymers with amino terminal groups/glass fiber composites had remarkable development in elongation at break, impact resistance, and tensile strength in comparison with the unmodified epoxy/polyamide thermosets.

13.2.2 Matrix modification by POSS

POSS is the nanostructured organic and inorganic matter with the empirical formula of $RSiO_{1.5}$, where R can be H atom or any organic functional group such as, acrylate, alkyl, alkaline, hydroxyl, and epoxide. POSS consists of silica-based cage core with the abovementioned organic functional groups at the corners of the cage. Incorporating POSS with polymer matrix, it offers capability to reinforce polymers and enables the effective reinforcement of fibers and particulates [34]. Nanomaterials like carbon nanotubes (CNTs), nanoclays, and carbon nanofibers can be effortlessly dispersed in POSS-based composites, subsequently encouraging the improvement of some properties such as porosity, modulus, and heat resistance [35]. Two types of POSS coatings were utilized for long carbon fiber-reinforced polyarylacetylene (PAA) matrix, and the interlaminar shear strength was evaluated to understand the impact of coating. This work exhibits the capability of utilizing POSS to improve the carbon fiber/polymer interface. Therefore, their impact resistant was increased significantly [36]. Zhang et al. reported the effect of POSS addition on the graphene oxide (GO)-grafted carbon fiber (CF). The addition of POSS to the fiber-reinforced composite improved their interfacial adhesion and enhanced their mechanical performance. Fig. 13.2 shows the scanning electron microscopic (SEM) images of the fractured surface of (a) desired carbon fiber, (b) CF-GO, and (c) CF-GO-POSS. In Fig. 13.2A, the fractured surface of carbon fiber composites presented several holes because of carbon fiber pull out from the matrix resin. This image showed that the interfacial adhesion among fiber and matrix was poor. Interestingly, better interfacial adhesion between fibre and matrix was seen in Fig. 13.2B, which is due to the modification of carbon fibre surface with POSS [37].

13.2.3 Nanoparticle reinforcement for matrix enhancement

Nanomaterials have been effectively explored as the potential additives for the increment of physical and mechanical facilities of fiber-reinforced composites. Thus, a great deal of research has been made to improve the resin properties and solve its deficiencies by reinforcing nanomaterials such as carbon nanofibers, graphene, nanocellulose, and CNTs [35,36]. For instance, Gonjy et al. [38] showed that the interlaminar shear strength of the glass fiber-reinforced composites were enhanced by utilizing low amounts of CNTs. While most of the studies regarding nanocomposites have been limited to just two-stage nanocomposites (carbon nanofiber-dispersed polymer), the merge of nanomaterials into the polymers is relied upon to enhance the mechanical properties, for example, the compressive strength (Fig. 13.3) [39].

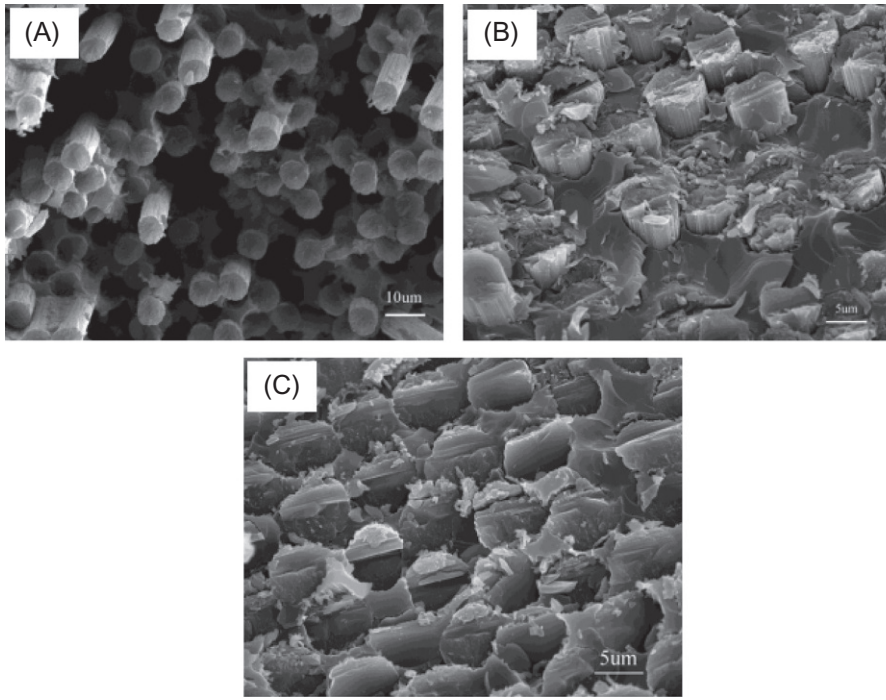

Fig. 13.2 SEM images of the fractured composite surface made with (A) pristine carbon fiber, (B) CF-GO, and (C) CF-GO-POSS.
Adapted from Zhang R, Gao B, Du W, Zhang J, Cui H, Liu L, et al. Enhanced mechanical properties of multiscale carbon fiber/epoxy composites by fiber surface treatment with graphene oxide/polyhedral oligomeric silsesquioxane. Compos A: Appl Sci Manuf 2016;84:455–63, Elsevier, copyright © 2016.

It has been shown that the increased use of nanoparticles such as SiO2 [40,41] for the effective enhancement of the tribological performance of traditional polymer composites reinforced with carbon fibers. Zhang et al. [42] demonstrated the dispersion of silica nanoparticles into epoxy-based polymer composites loaded with different fillers such as CNTs, short glass fibers, and short carbon fibers. The results showed that the nanoparticles improved the tribological behavior of composites when they were dispersed into nano-enhanced epoxy matrix. It is also observed that the incorporation of nanoclays into the fiber-reinforced epoxy composite can enhance the mechanical properties. Chowdhury et al. [43] utilized nanoclays in carbon fiber-reinforced polymer matrix composites at very low concentrations to enhance the thermal and flexural properties of the fabricated composites. Flexural test results showed the highest improvement in modulus and strength values around 14% and 9%, respectively. Further the dynamic mechanical analysis (DMA) results indicated the excellent progress in storage modulus by around 52% and an increase in Tg (glass transition temperature) values by around 13°C [43].

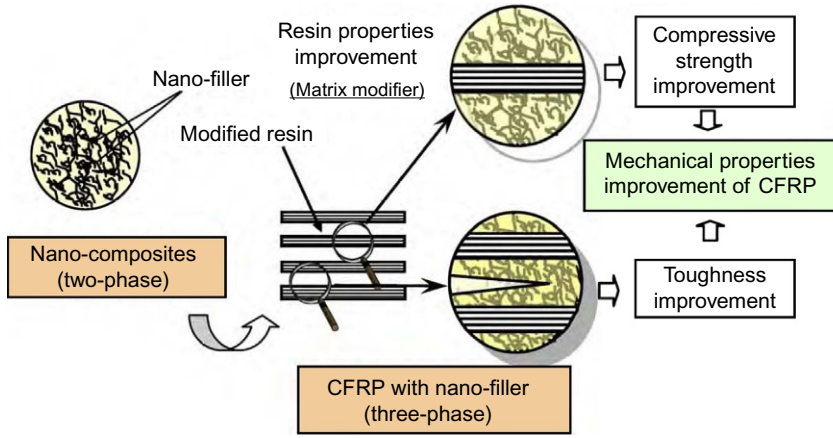

Fig. 13.3 Scenario of mechanical property improvement of CFRP (carbon fiber-reinforced polymer) by incorporation of nanofillers.
Adapted from Yokozeki T, Iwahori Y, Ishiwata S. Matrix cracking behaviors in carbon fiber/epoxy laminates filled with cup-stacked carbon nanotubes (CSCNTs). Compos A: Appl Sci Manuf 2007;38:917–24, Elsevier, copyright © 2006.

13.3 Nanotechnologies for fibre modification

Various nanofabrication techniques have been explored for the surface modification/functionalization of fibrous materials, which includes natural, carbon, and glass fibers aiming to enhance their composite performance such as thermal, mechanical, thermomechanical, electric, and functional properties. One of the key features of the surface modification of fibrous materials used in composite fabrication is the improvement of their interfacial adhesion between fiber and matrix and enhances their mechanical properties. This section summarizes the various nanotechnological strategies in fiber modification and their contribution in composite fabrications.

13.3.1 Nanomodification on natural fibres

13.3.1.1 Natural fibre modification with CNTs

Tzounis et al. [44] reported the effective fabrication of high-performance natural rubber composites employing short jute fibers (JFs) modified with CNT as hierarchical reinforcement. The surface modification of JFs with CNT network created a hierarchical structure that enables a promising reinforcing effect and improved the mechanical performance of the composite materials significantly. The obtained hierarchical structure of the JFs-CNT network enhances the wetting of the natural rubber on reinforcement and also enhances their interfacial mechanical interlocking [44]. Fig. 13.4 schematically illustrates the preparation and the interaction mechanism between the JFs and multiwalled carbon nanotubes (MWCNTs) and the TEM image of NR/JF-CNT

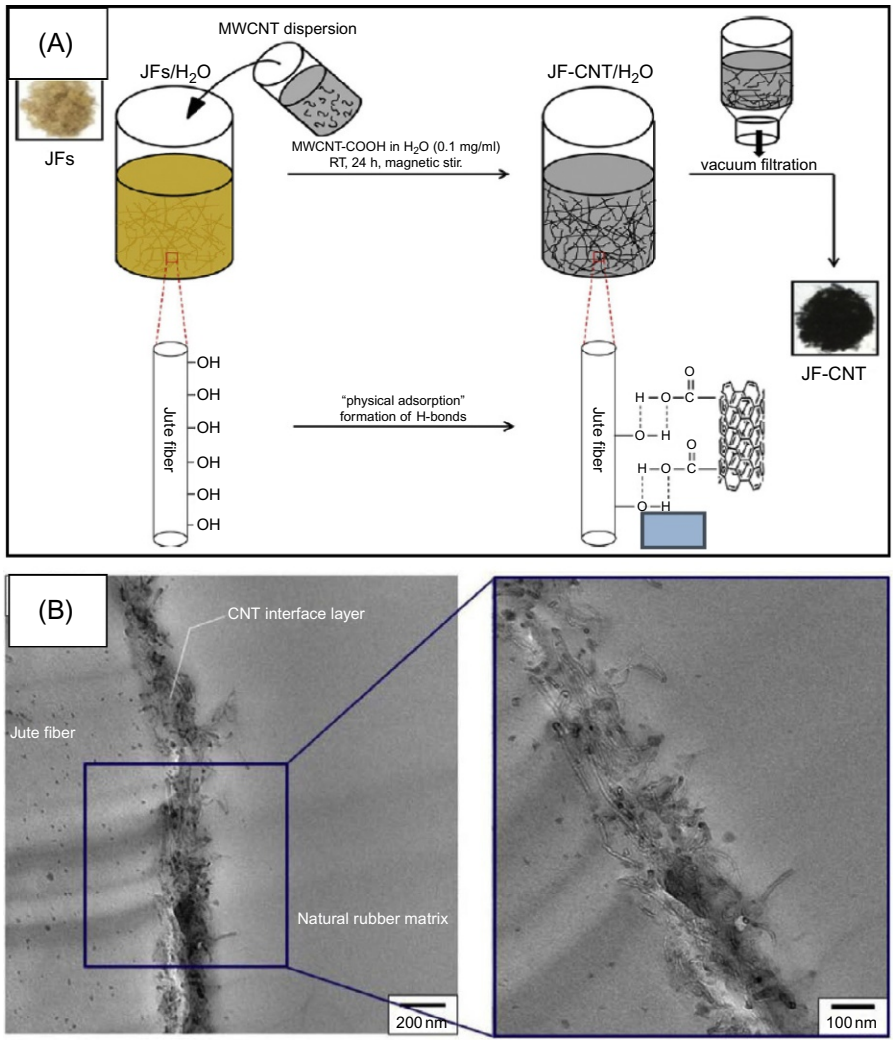

Fig. 13.4 (A) Schematic illustration of the preparation and the interaction mechanism between a-JFs and MWCNTs and (B) TEM interphase cross section image of the NR/JF-CNT hierarchical composite and the selected area at a higher magnification.
Adapted from Tzounis L, Debnath S, Rooj S, Fischer D, Mäder E, Das A, et al. High performance natural rubber composites with a hierarchical reinforcement structure of carbon nanotube modified natural fibers. Mater Des 2014;58:1–11, Elsevier, copyright © 2014.

hierarchical composite. Li et al. [45] demonstrated the fabrication of epoxy-based natural fiber composite employing flax fiber coated with CNTs. The result showed the improved mechanical properties, which suggested the effective interfacial bonding between fiber and matrix due to the nailing effect of CNTs that binds the fibers and

matrix. The incorporation of CNTs not only stiffened flax fiber but also played vital role in reinforcing its interface with epoxy [45].

13.3.1.2 Natural fibre modification with nano cellulose

One of the key issues in fabrication of biocomposite with natural fiber reinforcement is the poor adhesion between plant fibers (polar) and polymer matrices (nonpolar). Many approaches have been made and reported to overcome these issues. One of the green techniques is the modification of natural fiber surfaces with nanoscale bacterial cellulose to improve the interfacial interaction. Juntaro et al. [46] demonstrated the effective modification of hemp and sisal surfaces with bacterial cellulose. The surface-modified natural fibers were further reinforced into the biopolymers such as poly-L-lactic acid (PLLA) and cellulose acetate butyrate (CAB). SEM micrographs of the composite show the enhanced interfacial adhesion between the surface modified natural fibers and polymer matrix. Their tensile strength was found to increase significantly, especially with the PLLA matrix [46]. Pommet and researchers reported the surface modification of natural fibers by depositing bacterial cellulose using *Acetobacter xylinum*, which enables their effective adhesion to the polymer matrix [47]. Fig. 13.5 shows the photograph and their respective SEM image of the surface-modified sisal fiber covered with bacterial cellulose network. The developed "hierarchical fiber" has been effectively used for the fabrication of nanocomposites using CAB and poly(L-lactic acid) as matrix. The surface-modified natural fibers significantly increased interfacial adhesion and resulted in the enhancement of their mechanical properties [47]. Lee et al. [48] also reported the development of bacterial cellulose-modified sisal fiber for the fabrication hierarchical polymer composites employing acrylated epoxidized soybean oil (AESO) as matrix. Blaker et al. [49] reviewed the research work on the fabrication of hierarchical composites that are completely made from renewable resources, which discuss the surface modification of natural fiber with bacterial cellulose in extensive manner.

13.3.1.3 Natural fibre modification with metal and metal oxide nanoparticles

Natural fibers have been explored for composite application due to their renewable nature, abundance, cost-effectiveness, and low density [50]. However, their higher water absorbing capacity, lower dimensional stability, and also the compatibility-related issues lead to significant limitations for the product development [51]. Extensive efforts have been made in order to overcome these issues, and nanotechnology also provides better opportunity to improve their performance [15,52]. Functionalization of natural fibers with metal and metal oxide nanostructures receives significant attention in recent years as they offer enhanced composite performance and additional functional properties. Chowdhury and others reported the surface modification of empty fruit bunch fibers of oil palm with Cu nanoparticles [43]. They found that the strength and durability of Cu nanoparticle-modified empty fruit bunch fibers were improved significantly. Ramli et al. [53] explored the utilization of Cu

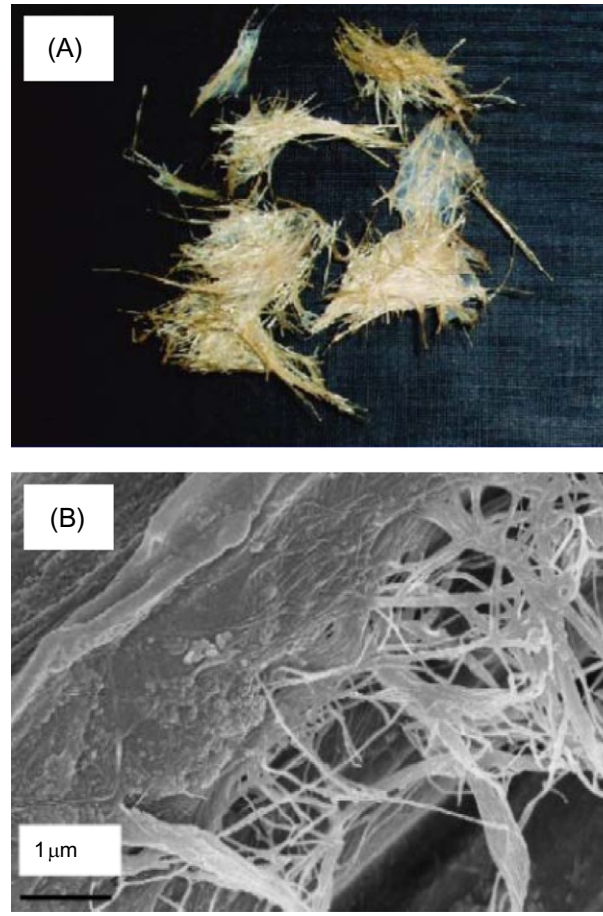

Fig. 13.5 Photograph (A) and their respective SEM image (B) of the surface-modified sisal fiber covered with bacterial cellulose network. Adapted from Pommet M, Juntaro J, Heng JY, Mantalaris A, Lee AF, Wilson K, et al. Surface modification of natural fibers using bacteria: depositing bacterial cellulose onto natural fibers to create hierarchical fiber reinforced nanocomposites. Biomacromolecules 2008;9:1643–51, American Chemical Society, copyright © 2018.

nanoparticle-impregnated oil palm empty fruit bunch fibers for the fabrication of composite using unsaturated polyester resin and found their enhanced composite properties. Vivekanandhan et al. [54] reported the green chemical approach using plant extract as reducing agent for the functionalization of microcrystalline cellulose (MCC) with silver nanoparticles and their effective reinforcement into PLA. The fabricated nanocomposite film exhibited effective antimicrobial activity against *Bacillus stearothermophilus* [54]. In addition to the antimicrobial property, the functionalized MCC also showed improved thermal stability due to the impregnation of Ag nanoparticles.

Wang et al. [55] grafted the flax fiber yarn with nanosized TiO_2 for the fabrication of epoxy-based composites and investigated their tensile and bonding properties of the single fibers. The incorporation of TiO_2 nanoparticles (~2.34 wt%) grafted flax fibers into the epoxy matrix improved the tensile

strength and the interfacial shear strength (IFSS) by 23.1% and 40.5%, respectively [55]. Foruzanmehr et al. [56] explored the sol-gel dip-coating technique for the formation of TiO_2 film on the surface of flax fibers. The PLA matrix was reinforced with TiO_2-coated fibers, and the impact resistance of the fabricated composite increased threefold compared with neat PLA. They also found that the water sorption of composite material decreased by 18% due to the effective adhesion between the TiO_2-modified fibers and the matrix [56]. Recently, Boulos et al. [57] performed the surface modification of flax fibers with ZrO_2 by sol-gel process and investigated the wetting performance and surface characterization of modified fibers. Their study demonstrated that the flax fibers modified with ZrO_2 significantly reduced the water uptake capacity of the composite [57].

13.3.2 Nanomodification on carbon fibres

13.3.2.1 Growth/deposition of CNTs on carbon fibre

Sharma and Lakkad reported the effect of CNTs growth on carbon fibers and their reinforcement into epoxy/amine polymer matrix for the fabrication of unidirectional composites [58]. The fabricated composite materials exhibited 69% increment in their tensile strength compared with their pristine carbon fiber composite, which is attributed to the CNTs grown on the carbon fiber surface [58]. An et al. [59] developed a novel process in order to grow vertically aligned CNT arrays on the carbon fiber fabric for the reinforcement of the epoxy resin/phthalic anhydride/benzyl dimethylamine matrix (Fig. 13.6). They found that the synthesized CNTs are about 20 μm in height with a mean outer diameter of 5.5 nm, exhibiting excellent hydrophobicity confirmed by its contact angle of 145 degrees [59]. The detailed investigation suggests that the CNT grown carbon fiber showed tensile strength degradation by about 10% compared with their pristine fibers, while the fiber modulus has not been changed much. Employing single-fiber pull-out tests, the IFSS of the fabricated microdroplet composites was found to be 135 MPa, whereas IFSS value of pristine carbon fiber composite was only 65 MPa, due to the increased surface area of the CNT grown carbon fiber [59]. Bedi et al. [60] investigated the chemical vapor deposition (CVD) process for the development of CNT-coated carbon fiber as the reinforcement for epoxy composite. Tensile testing of the single carbon fiber/epoxy composite materials indicates the significant improvement in their strength due to the CNT growth on the carbon fiber [60].

Zhang et al. [61] investigated the fabrication of CNT/carbon fiber hybrid structures by employing electrophoretic deposition (EPD) process. Prior to the composite fabrication, the developed CNT/carbon fiber hybrid structures were undergone sizing process employing poly(phthalazinone ether ketone) (PPEK) in order to enhance their interfacial strength in composites. The composites made with CNT/carbon fiber hybrid structures result in the enhancement of IFSS by 35.6% compared with nonfunctionalized CF-reinforced composites with PPEK sizing [61]. Deng et al. [62]

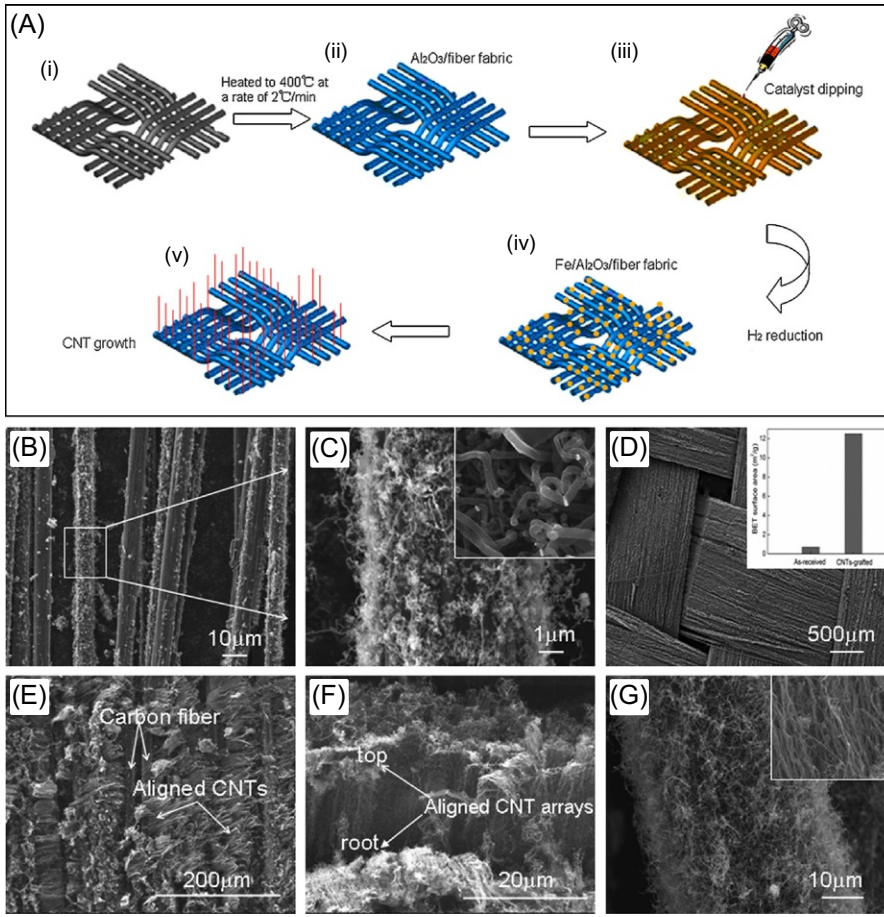

Fig. 13.6 (A) Schematic representation of the preparing CNTs grown onto carbon fiber fabric and (B–G) SEM images of vertically aligned CNT arrays grown onto carbon fiber fabric. Adapted from An F, Lu C, Guo J, He S, Lu H, Yang Y. Preparation of vertically aligned carbon nanotube arrays grown onto carbon fiber fabric and evaluating its wettability on effect of composite. Appl Surf Sci 2011;258:1069–76, Elsevier, copyright © 2011.

investigated the influence of CNT-coated carbon fiber on the properties of epoxy composites. CNT-coated carbon fiber was prepared with oxidative treatments followed by EPD. In order to investigate the mechanical properties of the CNT-coated carbon fiber-epoxy composites, the four flat panels of $15 \times 10\,cm^2$ were fabricated by employing vacuum-assisted resin transfer molding (VARTM) process. The investigation proved that the CNT-deposited carbon fibers via EPD deteriorates the mechanical properties of composites [62]. From these investigations, it was found that the CNT growth on the carbon fiber offers improved mechanical properties rather the CNT-deposited carbon fiber.

13.3.2.2 Carbon fibre modification with graphene oxide

Graphene-reinforced polymer composites exhibit great potential due to their enhanced physicochemical and functional properties. Integrating graphene with the fibrous structures enables the creation of hierarchical structure and provides extensive improvements on their composite properties. Recently, interest in the carbon fiber modification shifts into their surface functionalization with graphene and graphene oxides. The creation of graphene structures on the surface of carbon fibers enhances the wetting mechanism, which also improves fiber-matrix adhesion leading to their property enhancement. Zhang et al. [63] reported the fabrication of graphene oxide-grafted carbon fiber for epoxy-based composite application and investigated its effect on the mechanical properties. Graphene oxide-grafted carbon fiber increases the surface energy and surface functional groups, which results in improving the IFSS of its composites by 36.4%. The improved performance of the functionalized fibers is attributed to the effective reinforcement of graphene oxide entangled with the carbon fiber with matrix resin [63]. Wang et al. [64] fabricated the graphene oxide-decorated continuous carbon fibers by employing EPD process. They suggested that the graphene oxide sheets filled the defects on the carbon fiber surface and effectively suppressed crack propagation.

13.3.2.3 Carbon fibre modification with CNT and graphene oxide hybrids

Gao and his coworkers [65] developed the new class of hierarchical carbon fibers cografted with graphene oxide/CNTs for the fabrication of composites. Grafting the graphene oxide/CNTs on the carbon fibers could potentially increase their polar functionality and surface energy and improve the interlaminar shear strength and the IFSS by 48.12% and 83.39%, respectively [65]. Fig. 13.7 shows the schematic representation of grafting process along with SEM images of grafted carbon fibers and their respective composite interfacial structures. $CFNH_2$ was functionalized GO; then, the carbon fiber grafted with GO (CF-GO) was reacted with CNTs to obtain CF-GO-CNTs. It was found that the cografted carbon fiber exhibited better interfacial adhesion over their individual counterpart [65].

13.3.3 Nanomodification of glass fibres

Glass fibers (GFs) have been explored as cost-effective reinforcement material for polymer matrix, which also possess better mechanical and thermal properties. In order to improve the performance of glass fiber-reinforced composites, it is necessary to increase the wettability of the fiber. Recent developments in nanotechnology created a platform for the effective modification of glass fiber surfaces with nanostructured materials such as CNTs and graphene oxides [66–69]. These grafted nanostructured materials enable the effective interfacial adhesion between the glass fiber and the polymer matrix and further enhance their composite performance.

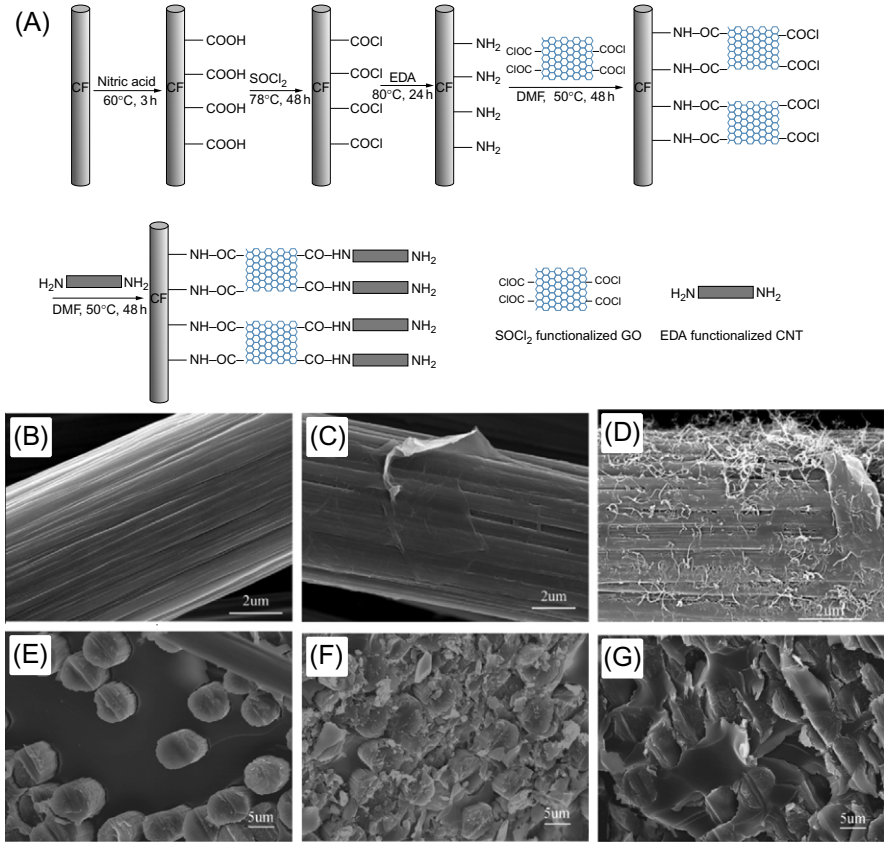

Fig. 13.7 (A) The functionalization of carbon fiber, (B–D) the SEM images of various carbon fibers, (B) desized carbon fiber, (C) CF-graphene oxide, and (D) CF-graphene oxide CNTs and (E–G) the fractured surface of composites: (E) desized carbon fiber, (F) CF-graphene oxide, and (G) CF-graphene oxide CNTs.
Adapted from Gao B, Zhang R, He M, Sun L, Wang C, Liu L, et al. Effect of a multiscale reinforcement by carbon fiber surface treatment with graphene oxide/carbon nanotubes on the mechanical properties of reinforced carbon/carbon composites. Compos A: Appl Sci Manuf 2016;90:433–40, Elsevier, copyright © 2016.

13.3.3.1 Growth/deposition of CNTs on carbon fibre

In recent years, surface modification of glass fiber with CNTs has received significant attention in order to enhance the fiber/matrix interface during the composite fabrication. Rahmanian and researchers demonstrated the floating catalyst CVD process for the growth of CNTs on the surface of glass fibers and CNTs [66]. The newly developed CNT-GF hierarchical fibers were reinforced with polypropylene matrix, and the obtained composites were exhibited improved mechanical (tensile, flexural, and impact) properties compared with their respective virgin short fiber composites [66].

Jamnani et al. [67] reported the effective deposition of CNT over glass fiber by employing dip-coating method using Nafion as binding agent. They performed single-fiber tensile test and found that the elastic modulus of CNT-coated glass fibers was unchanged, whereas its tensile strength was found to increase up to 38%. As another approach, Warrier et al. [68] reported the surface modification of glass fibers with CNTs by incorporating them into the sizing formulation. The epoxy composite fabricated with the CNT-modified fiber and matrix showed the increased glass transition temperature, fracture toughness, and coefficient of thermal expansion [68].

13.3.3.2 Glass fibre modification with graphene oxide

Chen et al. [69] reported the modification of glass fibers with graphene oxide for the fabrication of high-performance epoxy resin composites. The covalent immobilization of graphene oxides onto surface of glass fiber involves the effective formation of ester with the carboxylic functional groups of graphene oxide as shown in Fig. 13.8A. First, the glass fiber (GF) surface was modified using amino group, and then, the graphene oxide was grafted onto glass fibers by amidation reaction between the GF-NH_2 and the carboxy groups of graphene oxide. Fig. 13.8B and C shows the SEM images of amino grafted and the graphene oxide-coated glass fibers, respectively [69]. Also, Fig. 13.8D and E indicates the SEM images of the composite fracture surfaces, reinforced with commercial and graphene oxide-coated glass fibers. The results displayed that graphene oxide modification of the glass fibers improves the interfacial adhesion with polymer matrix and enhances the strength and toughness of the composite materials [69]. In addition, Mahmood and his team [70] employed the EPD process for the fabrication of graphene oxide-coated glass fibers used in epoxy composites. The synthesized graphene oxide via modified Hummer's method was deposited on the glass fiber through EPD process with various deposition voltages. They found that the deposition of graphene oxide on glass fiber improved the fiber-matrix IFSS of the epoxy composites by 219%. Similarly, EPD process has been explored by Pegoretti et al. [71] for the surface modification of glass fiber with graphene oxide. The modified fibers were explored for the fabrication of epoxy composites, and the fiber-matrix IFSS showed improved 220% compared with the IFSS of unmodified glass fiber.

13.4 Future perspectives

As the technology develops significantly, the use of nanotechnology will be the key issue for many new products development. For fiber-reinforced composites, there are many recent studies that utilize nanotechnology as explained in detail in this chapter. Nano-enhanced composites will find new applications in wind turbines, solar cells, smart materials, actuators, and many other structural applications. The conventional composites will be replaced with nano-enhanced systems to reduce the number of layers in the fiber-reinforced composites resulting in lower density of the final product. Some examples including bicycle frames, glass frames, and aerospace structures that prevent lightning striking are already developed, and they are soon to be

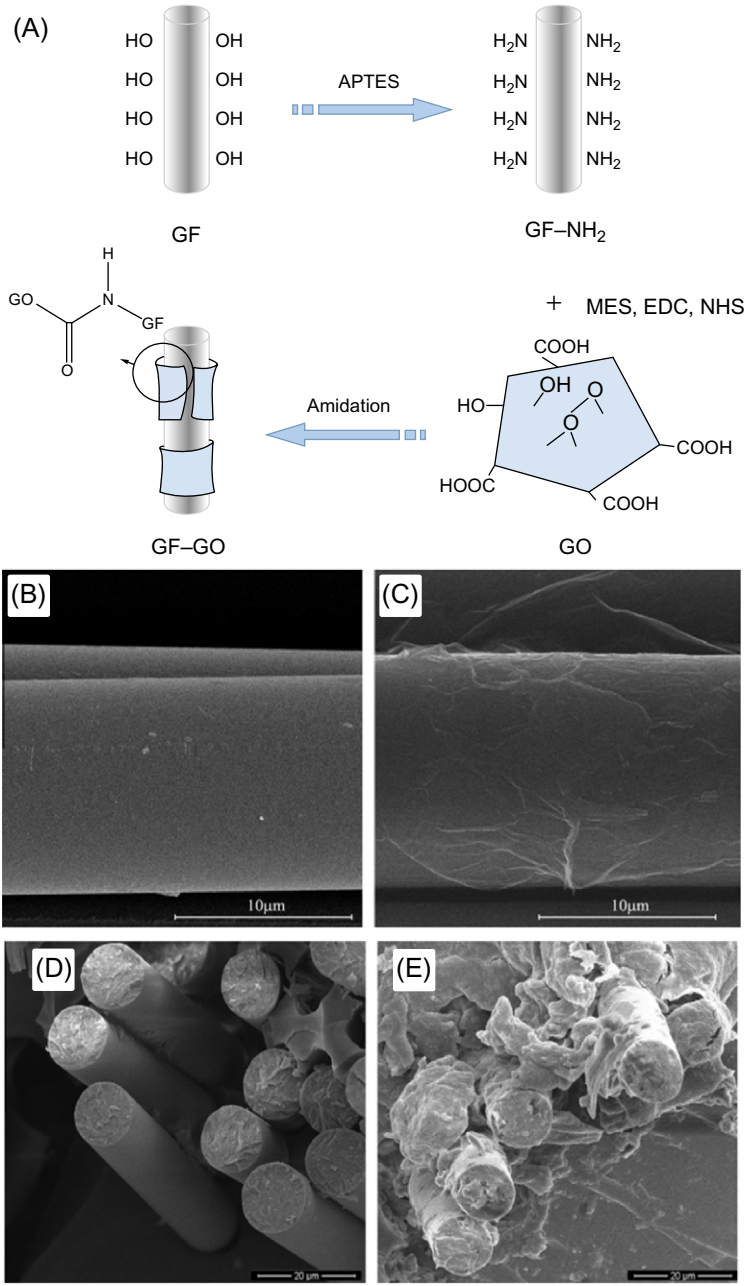

Fig. 13.8 Schematic representation of chemical routes to the synthesis of GO-g-GF (A), SEM images of NH_2 (B) and GO-modified (C) glass fibers and SEM images of the fractured surfaces of composites with the commercial (D) and GO-modified (E) glass fiber.
Adapted from Chen J, Zhao D, Jin X, Wang C, Wang D, Ge H. Modifying glass fibers with graphene oxide: towards high-performance polymer composites. Compos Sci Technol 2014;97:41–5, Elsevier, copyright © 2014.

commercialized. This chapter indicates that higher-quality products in sporting goods, aerospace, and automotive applications will replace conventional products via the use of nanotechnology for fiber-reinforced epoxy composites. It is apparent that the incorporation of nanomaterials into the polymeric matrices will help the researchers and composite industry for high-performance materials. Moreover, modification of fiber surfaces with nanotechnology will open new dimensions in the fiber composite industry, and it will be of great influence in many applications including biomedical and defense industries.

13.5 Conclusions

This chapter presented an overview of recent developments in fiber-reinforced composites within the context of nanotechnological developments. As the nanotechnology has a great impact in many different disciplines, it is shown that it also has a great influence on fiber-reinforced composites by enhancing their interfacial adhesion. Moreover, nanotechnology plays a critical role in new generation materials including the modification of matrices and fiber surfaces and offers various functional properties such as self-healing, flame retardant, and radiation shielding. Furthermore, the laboratory success of nano-enhanced matrix and fiber-based composite materials needs to be transformed into various products through scale-up activities. Polymers derived from natural resources open new dimensions for the composite industry and more opportunities as promising materials for future technologies. This area is still an open platform for basic and applied research that can create new products for the industrial applications.

Acknowledgments

The authors would like to thank the Ontario Research Fund—Research Excellence program, Round-7 (ORF-RE07) from the Ontario Ministry of Research and Innovation (MRI), currently known as the Ontario Ministry of Research, Innovation, and Science (MRIS) (Project # 052644 and # 052665); the Ontario Ministry of Agriculture, Food, and Rural Affairs (OMAFRA)—University of Guelph Bioeconomy—Industrial Uses theme (Project # 200283, 200001, 200600, and 200369); and the Natural Sciences and Engineering Research Council (NSERC) Canada Discovery Grants (Project # 401111 and 400320).

References

[1] Thakur VK, Thakur MK. Processing and characterization of natural cellulose fibers/thermoset polymer composites. Carbohydr Polym 2014;109:102–17.
[2] Abd-El-Messieh SL, Basta AH, El-Saied H. Electrical properties of cellulose ethers chelated with some metal salts. J Polym Mater 2001;18:279–85.
[3] Composites Market worth 105.26 Billion USD by 2021, Markets and markets.
[4] Reddy MM, Vivekanandhan S, Misra M, Bhatia SK, Mohanty AK. Biobased plastics and bionanocomposites: current status and future opportunities. Prog Polym Sci 2013;38:1653–89.

[5] Dhand V, Mittal G, Rhee KY, Park S-J, Hui D. A short review on basalt fiber reinforced polymer composites. Compos Part B 2015;73:166–80.
[6] Vivekanandhan S, Mohanty A, Misra M, Zarrinbakhsh N. Coproducts of biofuel industries in value-added biomaterials uses: a move towards a sustainable bioeconomy. Croatia: INTECH Open Access Publisher; 2013.
[7] Thakur VK, Thakur MK, Gupta RK. Review: raw natural fiber-based polymer composites. Int J Polym Anal Charact 2014;19:256–71.
[8] Herrera-Franco P, Valadez-Gonzalez A. Mechanical properties of continuous natural fibre-reinforced polymer composites. Compos A: Appl Sci Manuf 2004;35:339–45.
[9] Carolan D, Ivankovic A, Kinloch A, Sprenger S, Taylor A. Toughened carbon fibre-reinforced polymer composites with nanoparticle-modified epoxy matrices. J Mater Sci 2017;52:1767–88.
[10] Hult J, Rammerstorfer FG. Engineering mechanics of fibre reinforced polymers and composite structures. New York: Springer; 2014.
[11] Mohanty A, Misra M, Drzal L. Sustainable bio-composites from renewable resources: opportunities and challenges in the green materials world. J Polym Environ 2002;10:19–26.
[12] Gurunathan T, Mohanty S, Nayak SK. A review of the recent developments in bio-composites based on natural fibres and their application perspectives. Compos A: Appl Sci Manuf 2015;77:1–25.
[13] Bajpai PK, Singh I, Madaan J. Development and characterization of PLA-based green composites: a review. J Thermoplast Compos Mater 2014;27:52–81.
[14] Delamar M, Desarmot G, Fagebaume O, Hitmi R, Pinsonc J, Savéant J-M. Modification of carbon fiber surfaces by electrochemical reduction of aryl diazonium salts: application to carbon epoxy composites. Carbon 1997;35:801–7.
[15] Li X, Tabil LG, Panigrahi S. Chemical treatments of natural fiber for use in natural fiber-reinforced composites: a review. J Polym Environ 2007;15:25–33.
[16] Dilsiz N. Plasma surface modification of carbon fibers: a review. J Adhes Sci Technol 2000;14:975–87.
[17] Ishida H, Koenig J. The reinforcement mechanism of fiber-glass reinforced plastics under wet conditions: a review. Polym Eng Sci 1978;18:128–45.
[18] Pracella M, Chionna D, Anguillesi I, Kulinski Z, Piorkowska E. Functionalization, compatibilization and properties of polypropylene composites with hemp fibres. Compos Sci Technol 2006;66:2218–30.
[19] Bourmaud A, Riviere J, Le Duigou A, Raj G, Baley C. Investigations of the use of a mussel-inspired compatibilizer to improve the matrix-fiber adhesion of a biocomposite. Polym Test 2009;28:668–72.
[20] Bhushan B. Springer handbook of nanotechnology. Berlin: Springer Science & Business Media; 2010.
[21] Moniruzzaman M, Winey KI. Polymer nanocomposites containing carbon nanotubes. Macromolecules 2006;39:5194–205.
[22] Podsiadlo P, Kaushik AK, Arruda EM, Waas AM, Shim BS, Xu J, et al. Ultrastrong and stiff layered polymer nanocomposites. Science 2007;318:80–3.
[23] Potts JR, Dreyer DR, Bielawski CW, Ruoff RS. Graphene-based polymer nanocomposites. Polymer 2011;52:5–25.
[24] Jordan J, Jacob KI, Tannenbaum R, Sharaf MA, Jasiuk I. Experimental trends in polymer nanocomposites—a review. Mater Sci Eng A 2005;393:1–11.
[25] Andrews R, Weisenberger M. Carbon nanotube polymer composites. Curr Opinion Solid State Mater Sci 2004;8:31–7.
[26] Stankovich S, Dikin DA, Dommett GH, Kohlhaas KM, Zimney EJ, Stach EA, et al. Graphene-based composite materials. Nature 2006;442:282–6.

[27] Eichhorn SJ, Dufresne A, Aranguren M, Marcovich N, Capadona J, Rowan S, et al. Review: current international research into cellulose nanofibres and nanocomposites. J Mater Sci 2010;45:1.
[28] Bourrier O, Butlin J, Hourani R, Kakkar AK. Aggregation of 3,5-dihydroxybenzyl alcohol based dendrimers and hyperbranched polymers, and encapsulation of DR1 in such dendritic aggregates. Inorg Chim Acta 2004;357:3836–46.
[29] Gao C, Yan D. Hyperbranched polymers: from synthesis to applications. Prog Polym Sci 2004;29:183–275.
[30] Sörensen K, Pettersson B, Boogh L, Månson J. Dendritic polyester macromolecule in thermosetting resin matrix. PCT Pat./SE94/04440; 1994.
[31] Rhodes SM, Higgins B, Xu Y, Brittain WJ. Hyperbranched polyol/carbon nanofiber composites. Polymer 2007;48:1500–9.
[32] Wong S, Shanks RA, Hodzic A. Mechanical behavior and fracture toughness of poly (L-lactic acid)-natural fiber composites modified with hyperbranched polymers. Macromol Mater Eng 2004;289:447–56.
[33] Li S, Wu Q, Cui C, Zhu H, Hou H, Lin Q, et al. Synergetic reinforcements of epoxy composites with glass fibers and hyperbranched polymers. Polym Compos 2017, http://dx.doi.org/10.1002/pc.24280.
[34] Ayandele E, Sarkar B, Alexandridis P. Polyhedral oligomeric silsesquioxane (POSS)-containing polymer nanocomposites. Nanomaterials 2012;2:445–75.
[35] Iyer P, Mapkar JA, Coleman MR. A hybrid functional nanomaterial: POSS functionalized carbon nanofiber. Nanotechnology 2009;20:325603.
[36] Zhang X, Huang Y, Wang T, Liu L. Effects of polyhedral oligomeric silsesquioxane coatings on the interface and impact properties of carbon-fiber/polyarylacetylene composites. J Appl Polym Sci 2006;102:5202–11.
[37] Zhang R, Gao B, Du W, Zhang J, Cui H, Liu L, et al. Enhanced mechanical properties of multiscale carbon fiber/epoxy composites by fiber surface treatment with graphene oxide/polyhedral oligomeric silsesquioxane. Compos A: Appl Sci Manuf 2016;84:455–63.
[38] Gojny FH, Wichmann MH, Fiedler B, Bauhofer W, Schulte K. Influence of nano-modification on the mechanical and electrical properties of conventional fibre-reinforced composites. Compos A: Appl Sci Manuf 2005;36:1525–35.
[39] Yokozeki T, Iwahori Y, Ishiwata S. Matrix cracking behaviors in carbon fiber/epoxy laminates filled with cup-stacked carbon nanotubes (CSCNTs). Compos A: Appl Sci Manuf 2007;38:917–24.
[40] Österle W, Dmitriev A, Wetzel B, Zhang G, Häusler I, Jim B. The role of carbon fibers and silica nanoparticles on friction and wear reduction of an advanced polymer matrix composite. Mater Des 2016;93:474–84.
[41] Zhang G, Sebastian R, Burkhart T, Friedrich K. Role of monodispersed nanoparticles on the tribological behavior of conventional epoxy composites filled with carbon fibers and graphite lubricants. Wear 2012;292:176–87.
[42] Zhang L, Zhang G, Chang L, Wetzel B, Jim B, Wang Q. Distinct tribological mechanisms of silica nanoparticles in epoxy composites reinforced with carbon nanotubes, carbon fibers and glass fibers. Tribol Int 2016;104:225–36.
[43] Chowdhury M, Beg MDH, Khan MR, Mina M. Modification of oil palm empty fruit bunch fibers by nanoparticle impregnation and alkali treatment. Cellulose 2013;20:1477–90.
[44] Tzounis L, Debnath S, Rooj S, Fischer D, Mäder E, Das A, et al. High performance natural rubber composites with a hierarchical reinforcement structure of carbon nanotube modified natural fibers. Mater Des 2014;58:1–11.

[45] Li Y, Chen C, Xu J, Zhang Z, Yuan B, Huang X. Improved mechanical properties of carbon nanotubes-coated flax fiber reinforced composites. J Mater Sci 2015;50:1117–28.
[46] Juntaro J, Pommet M, Mantalaris A, Shaffer M, Bismarck A. Nanocellulose enhanced interfaces in truly green unidirectional fibre reinforced composites. Compos Interfaces 2007;14:753–62.
[47] Pommet M, Juntaro J, Heng JY, Mantalaris A, Lee AF, Wilson K, et al. Surface modification of natural fibers using bacteria: depositing bacterial cellulose onto natural fibers to create hierarchical fiber reinforced nanocomposites. Biomacromolecules 2008;9:1643–51.
[48] Lee K-Y, Ho KK, Schlufter K, Bismarck A. Hierarchical composites reinforced with robust short sisal fibre preforms utilising bacterial cellulose as binder. Compos Sci Technol 2012;72:1479–86.
[49] Blaker JJ, Lee K-Y, Bismarck A. Hierarchical composites made entirely from renewable resources. J Biobased Mater Bioenergy 2011;5:1–16.
[50] Saheb DN, Jog JP. Natural fiber polymer composites: a review. Adv Polym Technol 1999;18:351–63.
[51] Bledzki A, Reihmane S, Gassan J. Properties and modification methods for vegetable fibers for natural fiber composites. J Appl Polym Sci 1996;59:1329–36.
[52] Xie Y, Hill CA, Xiao Z, Militz H, Mai C. Silane coupling agents used for natural fiber/polymer composites: a review. Compos A: Appl Sci Manuf 2010;41:806–19.
[53] Ridzuan R, Maksudur Rahman K, Najmul Kabir C, Mohammad Dalour Hossen B, Rohaya Mohamed H, Astimar Abdul A, et al. Development of Cu nanoparticle loaded oil palm fibre reinforced nanocomposite. Adv Nanopart 2013;2:358–65.
[54] Vivekanandhan S, Christensen L, Misra M, Mohanty AK. Green process for impregnation of silver nanoparticles into microcrystalline cellulose and their antimicrobial bionanocomposite films. J Biomed Nanotechnol 2012;3:371–6.
[55] Wang H, Xian G, Li H. Grafting of nano-TiO_2 onto flax fibers and the enhancement of the mechanical properties of the flax fiber and flax fiber/epoxy composite. Compos A: Appl Sci Manuf 2015;76:172–80.
[56] Foruzanmehr M, Vuillaume PY, Elkoun S, Robert M. Physical and mechanical properties of PLA composites reinforced by TiO_2 grafted flax fibers. Mater Des 2016;106:295–304.
[57] Boulos L, Foruzanmehr MR, Tagnit-Hamou A, Elkoun S, Robert M. Wetting analysis and surface characterization of flax fibers modified with zirconia by sol-gel method. Surf Coat Technol 2017;313:407–16.
[58] Sharma S, Lakkad S. Effect of CNTs growth on carbon fibers on the tensile strength of CNTs grown carbon fiber-reinforced polymer matrix composites. Compos A: Appl Sci Manuf 2011;42:8–15.
[59] An F, Lu C, Guo J, He S, Lu H, Yang Y. Preparation of vertically aligned carbon nanotube arrays grown onto carbon fiber fabric and evaluating its wettability on effect of composite. Appl Surf Sci 2011;258:1069–76.
[60] Bedi HS, Padhee SS, Agnihotri PK. On the nature of interface of carbon nanotube coated carbon fibers with different polymers. In: IOP conference series: materials science and engineering, vol. 139. IOP Publishing; 2016. 012014.
[61] Zhang S, Liu W, Hao L, Jiao W, Yang F, Wang R. Preparation of carbon nanotube/carbon fiber hybrid fiber by combining electrophoretic deposition and sizing process for enhancing interfacial strength in carbon fiber composites. Compos Sci Technol 2013;88:120–5.
[62] Deng C, Jiang J, Liu F, Fang L, Wang J, Li D, et al. Influence of carbon nanotubes coatings onto carbon fiber by oxidative treatments combined with electrophoretic deposition on interfacial properties of carbon fiber composite. Appl Surf Sci 2015;357:1274–80.

[63] Zhang R, Gao B, Ma Q, Zhang J, Cui H, Liu L. Directly grafting graphene oxide onto carbon fiber and the effect on the mechanical properties of carbon fiber composites. Mater Des 2016;93:364–9.
[64] Wang C, Li J, Sun S, Li X, Zhao F, Jiang B, et al. Electrophoretic deposition of graphene oxide on continuous carbon fibers for reinforcement of both tensile and interfacial strength. Compos Sci Technol 2016;135:46–53.
[65] Gao B, Zhang R, He M, Sun L, Wang C, Liu L, et al. Effect of a multiscale reinforcement by carbon fiber surface treatment with graphene oxide/carbon nanotubes on the mechanical properties of reinforced carbon/carbon composites. Compos A: Appl Sci Manuf 2016;90:433–40.
[66] Rahmanian S, Thean K, Suraya A, Shazed M, Salleh MM, Yusoff H. Carbon and glass hierarchical fibers: influence of carbon nanotubes on tensile, flexural and impact properties of short fiber reinforced composites. Mater Des 2013;43:10–6.
[67] Jamnani BD, Hosseini S, Rahmanian S, Rashid SA, Balavandy SK. Grafting carbon nanotubes on glass fiber by dip coating technique to enhance tensile and interfacial shear strength. J Nanomater 2015;16:306.
[68] Warrier A, Godara A, Rochez O, Mezzo L, Luizi F, Gorbatikh L, et al. The effect of adding carbon nanotubes to glass/epoxy composites in the fibre sizing and/or the matrix. Compos A: Appl Sci Manuf 2010;41:532–8.
[69] Chen J, Zhao D, Jin X, Wang C, Wang D, Ge H. Modifying glass fibers with graphene oxide: towards high-performance polymer composites. Compos Sci Technol 2014;97:41–5.
[70] Mahmood H, Tripathi M, Pugno N, Pegoretti A. Enhancement of interfacial adhesion in glass fiber/epoxy composites by electrophoretic deposition of graphene oxide on glass fibers. Compos Sci Technol 2016;126:149–57.
[71] Pegoretti A, Mahmood H, Pedrazzoli D, Kalaitzidou K. Improving fiber/matrix interfacial strength through graphene and graphene-oxide nano platelets. In: IOP conference series: materials science and engineering, vol. 139. IOP Publishing; 2016. 012004.

This page intentionally left blank

Design and optimization of fiber composites

14

*Levent Aydin**, Hatice Seçil Artem*[†]
*Izmir Katip Çelebi University, Izmir, Turkey, [†]Izmir Institute of Technology, Izmir, Turkey

14.1 Introduction

In engineering, design, and optimization processes are very important issues to establish sustainable engineering systems. Compared to isotropic materials, it is necessary to deal with more complicated mathematical models that address the material anisotropy for fiber-reinforced composites. Due to the unique characteristics of fiber-reinforced composite materials such as different directional properties, interlaminar stresses, less notch sensitivity, and having positive and negative coefficients of thermal expansion, they require more material constants for characterization of the hygrothermomechanical responses. Therefore, the design process of composites for the effort required or the benefit desired has to be systematic, which includes innovative approaches to synthesize alternative solutions. In this regard, the main goal of all such attempt is relevant to reach minimizing the effort required or to maximize the desired benefit. Conceptually, "best design" for fiber-reinforced composites refers to optimization of the structural material. The process is quite different from the design approaches that are traditionally used for metals such as aluminum and steel. For example, by only material point of view, the designer has to choose the reinforcement type (short, long, particulate, micro, nano, etc.), the matrix, and also the process for curing in terms of performance and cost. Hence, in other words, the optimization of fiber-reinforced composites often means having (i) the lowest weight with limitations on the stiffness properties, (ii) the minimum cost with prescribed strength limits, or (iii) the maximum stiffness with prescribed resources.

In recent years, thanks to advanced computers and commercial programs, optimization methods are rapidly being used in many engineering design applications such as manufacturing processes, aerospace structures, and automotive. Moreover, optimization methods, coupled with modern tools of CAD (computer-aided design), are also being used to provide major improvement in the structural design of engineering systems [1,2].

In the formulation of the design problems, engineers utilize the design variables that directly change the properties of the material. Hence, best design (or optimization) of the considered structures has acquired a meaning. So as to develop better structural performance of the fiber-reinforced composites and satisfy the conditions of a specific design case, the thermophysical properties of the material can be tailored in addition to structural dimensions Gurdal et al. [1]. However, some of the

Fiber Technology for Fiber-Reinforced Composites. http://dx.doi.org/10.1016/B978-0-08-101871-2.00014-X

configurations designed to tailor the material properties are not manufactural even if there are many different production methods to obtain a composite part or a structure. Therefore, engineers do indeed work under some limited conditions that configurations are manufactural, thereby limiting the performance gains, which can be established through the use of fiber composites. Because of their anisotropic nature, unfortunately, it might not possible to find an efficient composite structural design that satisfies all the prescribed conditions by only sizing the cross-sectional areas and member thicknesses. In these cases, determining (i) the stacking sequence of a laminate, (ii) the material properties of each layers, and (iii) the number of layers becomes more of an issue for fiber composites.

14.2 Structural design

Only some specific structural design criteria, loading cases, components, and units have been carried out in almost all studies on the optimization of fiber-reinforced composite structures such as pressure vessels, bars, and disks. It should be noted that the structural optimization of a fiber-reinforced composite under different limitations qualifies as a fundamental problem in both structural design and strength analysis [3]. Structural design also ought to have the possibility of being extended to deal with anisotropic nature of fiber composites. It would be great if the following design requirements are valid for the fiber-reinforced composite structures: (i) high strength, (ii) long fatigue life, (iii) high stiffness, (iv) specified amounts of energy absorption, (v) light weight, (vi) low cost, (vii) dimensional stability, (viii) manufacturability, (ix) high natural frequency, and (x) high fracture toughness. However, in some circumstances, only one requirement is utilized to describe required properties. Generally, real-life applications of the engineering design problems on fiber composites are very complicated, and also two or more design requirements such as low weight-low cost, stiffness-low weight-low cost, and high fracture toughness-low weight-low cost have to be considered simultaneously. Hence, the designer has become some advantages and disadvantages when the number of inputs of a structural engineering system is high. For instance, it is effective to study with many inputs (design variables), since the engineers need to control the behavior of the fiber-reinforced composite structures satisfying the design constraints. However, it is very difficult to select and reach the correct (optimum) design variables and their corresponding values. It can be established only if it is based upon a systematic and/or mathematical approach. In these cases, design optimization of fiber composites becomes a suitable tool, and therefore, different solution methodologies should be taken into account.

14.3 Material selection

The general performance of an engineering system is limited by the physical properties of its material. Therefore, one of the most important tasks in engineering is to describe the factors and procedures to select the appropriate material for a specific structural application. After the material-selection step of an engineering component, the process follows two interrelated problems: (i) specifying the shape of the unit and (ii) choosing a manufacturing process [4]. Performance of the fiber-reinforced

composites depends on combination of physical properties, and then, the best material can be selected by maximizing one or more performance indices. Three fundamental questions are often helpful to select a composite material:

1. What are the factors governing the selection of the fiber (carbon, glass, kevlar, etc.)?
2. What are the factors essential for selection of the matrix (epoxy or polyester polypropylene)?
3. What are the overall factors about selection of the fiber-reinforced composite material?

The designer performs a series of selection stages. On each stage, a pair of fiber and matrix properties is specified.

14.3.1 Fiber selection factors

Fiber selection process for composites has to be attuned to design requirements of the engineering applications. Most important issues are (i) strength or stiffness, (ii) hygrothermomechanical properties, (iii) the thickness of a ply/availability of tow size, (iv) ply flexibility, (v) sizing and surface treatments, (vi) wetting, bonding, and material compatibility, and (vii) cost and availability.

Appropriate selection of the fiber and matrix will produce a fiber-reinforced composite system that (i) satisfies the conditions on design, (ii) facilitates manufacturing processes, and (iii) minimizes program risks (cost and schedule).

14.3.2 Matrix selection factors

The selection of appropriate matrix for a fiber-reinforced composite material is crucial and also involves many factors since the matrix links in all properties of a two-phase fiber composite material. The main considerations include (i) ability of the matrix to wet the fiber, (ii) fiber sizing compatibility, (iii) ease of processing, (iv) toxicity and health concerns, (v) cost and availability, (vi) prepeg handling characteristics, (vii) laminate quality, (viii) environmental resistance, (ix) moisture absorption, (x) composite glass transition temperature, (xi) tooling expansion, (xii) density, (xiii) flow characteristics, (xiv) tensile strength, (xv) diffusivity, and (xvi) microcracking. In Table 14.1, the principle properties of matrix materials: polymer, metal, carbon, and ceramic are given.

Table 14.1 Elements for matrix selection

Elements for selection	Rating of matrix materials			
	Worst	**Applicable**	**Good**	**Best**
Laminate quality	Ceramic	Carbon	Metal	Polymer
Fiber wetting	Ceramic	Metal	Carbon	Polymer
Processing ease	Ceramic	Metal	Carbon	Polymer
Strain-to-failure	Ceramic	Carbon	Metal	Polymer
Environmental resistance	Polymer	Metal	Carbon	Ceramic
Density	Metal	Ceramic	Carbon	Polymer
Cost	Metal	Carbon	Ceramic	Polymer

Based on Jones RM. Mechanics of composite materials. 2nd ed. Philadelphia: Taylor & Francis; 1999.

14.4 Optimization

Essentially, optimization of a structure can be defined as finding the best design or elite designs by minimizing the specified single objective or multiobjectives that satisfy all the constraints. Single-objective and multiobjective optimizations are the main approaches used in structural design problems. In single-objective approach, an optimization problem consists of a single-objective function, constraints, and bounds. However, the design of practical composite structures often requires the maximization or minimization of multiple, often conflicting, two or more objectives, simultaneously [5]. In such a case, multiobjective formulation is used, and a set of solutions are obtained with a different trade-off called Pareto optimality. Only one solution is to be chosen from the set of solutions for practical engineering usage. There is no such thing as the best solution with respect to all objectives in multiobjective optimization. Optimization techniques can be classified as traditional and nontraditional. Traditional optimization techniques, such as constrained variation and Lagrange multipliers, are analytic and find the optimum solution of only continuous and differentiable functions. Since composite design problems are very complex and have discrete search spaces, the traditional optimization techniques cannot be used in this area. In these cases, the use of stochastic optimization methods such as particle swarm (PS), genetic algorithms (GA), generalized pattern search algorithm (GPSA), and simulated annealing (SA) are appropriate. In composite laminate design problems, derivative calculations or their approximations are impossible to obtain or often costly. Therefore, stochastic search methods have also the advantage of requiring no gradient information of the objective functions and the constraints [6]. In the fiber-reinforced composite design and optimization studies, fiber orientation angles, and thickness are considered as the main design variables. In some optimization problems, lamina thicknesses [7–11] and/or fiber orientation angles [12,13] are also given as design variables [55].

14.4.1 Single-objective optimization

A standard mathematical formulation of the single-objective optimization consists of an objective function, equality and/or inequality constraints, and design:

$$\begin{aligned} &\text{minimize} \quad f(\theta_1, \theta_2, \ldots, \theta_n) \\ &\text{such that} \quad g_i(\theta_1, \theta_2, \ldots, \theta_n) \geq 0 \quad i = 1,2,\ldots,r \\ &\qquad\qquad p_j(\theta_1, \theta_2, \ldots, \theta_n) = 0 \quad j = 1,2,\ldots,m \end{aligned}$$

where f is the objective function, $\theta_1, \theta_2, \ldots, \theta_n$ are the design variables, and g and p are the constraints of the problem. In composite design and optimization problems, mass, stiffness, displacements, residual stresses, thickness, vibration frequencies, buckling loads, and cost are used as objective functions Gurdal et al. [1].

14.4.2 Multiobjective optimization

A multiobjective optimization problem can be stated as follows:

$$\begin{aligned} &\text{minimize} \quad f_1(\theta_1, \theta_2, \ldots, \theta_n), f_2(\theta_1, \theta_2, \ldots, \theta_n), \ldots, f_t(\theta_1, \theta_2, \ldots, \theta_n) \\ &\text{such that} \quad g_i(\theta_1, \theta_2, \ldots, \theta_n) \geq 0 \quad i = 1,2,\ldots,r \\ &\qquad\qquad p_j(\theta_1, \theta_2, \ldots, \theta_n) = 0 \quad j = 1,2,\ldots,m \end{aligned}$$

where $f_1, f_2, \ldots, f_t$ represent the objective functions to be minimized simultaneously. The main difficulties in multiobjective optimization problems are to minimize the distance of the generated solutions to the Pareto set and to maximize the diversity of the developed Pareto set. Detailed analysis of multiobjective optimization can be found in Deb [14].

14.4.3 Stochastic optimization algorithms

Stochastic optimization methods are optimization algorithms based on probabilistic elements, either in the objective function with the constraints or in the algorithm itself or both of them. GA, particle swarm optimization (PSO), ant colony optimization (ACO), SA, tabu search, harmony search, and GPSA are examples of the stochastic search techniques used in engineering applications. In composite laminate design problems, derivative calculations or their approximations are impossible to obtain or is often costly. Therefore, stochastic search methods have the advantage of requiring no gradient information of the objective functions and the constraints. In the following subsections, steps of the widely used algorithms are briefly overviewed.

14.4.4 Genetic algorithm

The GA is a stochastic optimization and search technique that allows obtaining alternative solutions for some of the complex engineering problems such as increasing composite strength and developing dimensionally stable and lightweight structures. GA method utilizes the principles of genetics and natural selection. This method is simple to understand and uses three simple operators: selection, crossover, and mutation. GA always considers a population of solutions instead of a single solution at each of iteration. It has some advantages in parallelism and robustness of GA. It also improves the chance of finding the global optimum point and helps to avoid local stationary point. However, GA is not guaranteed to find the global optimum solution to a problem. GA has been applied to the design of a variety of composite structures ranging from simple rectangular plates to complex geometries Aydin and Artem [5].

14.4.5 Generalized pattern search algorithm

GPSA has been defined for derivative-free unconstrained optimization of functions by Torczon [15] and later extended to take nonlinear constrained optimization problems into account. GPSA is a direct search method, which determines a sequence of points

that approach the optimal point. Each of iteration is divided into two phases: the search phase and the poll phase. In the search phase, the objective function is evaluated at a finite number of points on a mesh. The main task of the search phase is to find a new point that has a lower objective function value than the best current solution, which is called the incumbent. In the poll phase, the objective function is evaluated at the neighboring mesh points, so as to see whether a lower objective function value can be obtained. GPSA has some collection of vectors that form the pattern and has two commonly used positive basis sets; the maximal basis with $2N$ vectors and the minimal basis with $N+1$ vectors Aydin and Artem [5].

14.4.6 Simulated annealing

SA is a random search technique, and it is based on the simulation of thermal annealing of heated solids to achieve the minimum function value in a minimization problem. It is possible to solve mixed integer, discrete, or continuous optimization problems by using SA. In this algorithm, a new point is randomly generated at each iteration, and the algorithm stops when any of the stopping criteria are satisfied. The distance of the new point from the current point or the extent of the search is based on Boltzmann's probability distribution. The distribution implies the energy of a system in thermal equilibrium at temperature T.

Boltzmann's probability distribution can be written in the following form [2,5]:

$$P(E) = e^{-E/kT} \tag{14.1}$$

where $P(E)$ represents the probability of achieving the energy level E, k is the Boltzmann's constant, and T is temperature.

SA algorithm has the following steps:

1. Start with an initial vector x_1 and assign a high temperature value to the function.
2. Generate a new design point randomly and find the difference in function values.
3. Determine whether the new point is better or worse than the current point.
4. If the value of a randomly generated number is larger than $e^{-\Delta E/kT}$, accept the point x_{i+1}.
5. If the point x_{i+1} is rejected, then the algorithm generates a new design point x_{i+1} randomly.

However, it should be noted that the algorithm accepts a worse point based on acceptance probability [2].

14.4.7 Particle swarm optimization

The PSO algorithm resembles the character of social beings such as swarm of ants and flock of birds. PSO algorithm searches the solution and at the same moment, agents (swarming search points) share their information or feedbacks among themselves. When we compare PSO's certain features with other frequently used stochastic search algorithms in optimization problems such as GA, PSO is proved to be more effective. In most of these problems, PSO is also demonstrated to have tremendous computational abilities. Moreover, it does not follow any gradient types of information. In

a brief computation time, PSO can adapt universal and local exploration and exploitation abilities by incorporating a well-organized and also flexible mechanism. This method efficiently overcomes large and complex search spaces. For example, to understand clearly about the mechanism as model, it can be given a similar behavior from a flock of bird. When a food (target; maximum of the objective function) is located by one bird, this information is instantly passed to all other birds. Then, those birds head toward the target but not directly. While this happens, it should be considered that all birds have independent behavior with having their past memory. While Kennedy and Eberhart proposed the PSO algorithm in Ref. [16], its effectiveness is reported in an experimental study, which is about using the PSO algorithm for the optimal design of ply arrangement, by Kovacs et al. [17].

14.4.8 Differential evolution methods

Differential evolution (DE) is a stochastic optimization and search technique, which permits to gain alternative solutions for some of the complex engineering problems such as increasing frequency, frequency separation, and obtaining lightweight design. DE includes four main stages: initialization, mutation, crossover, and selection. The algorithm is checked by three parameters: scaling factor, crossover, and population size. The detailed description of the DE can be found in Ref. [56]. As in GA method, differential evolution methods (DEM) always considers a population of solutions instead of a single solution at each of iteration. Although the DEM is computationally expensive, it is relatively robust and efficient in finding global optimum and to avoid local minimum irrespective of initial points. However, DEM is not guaranteed to find the global optimum solution to a problem. DEM has been implemented to the design of a sort of fiber composite structures ranging from simple rectangular plates to complex geometries.

14.4.9 Ant colony optimization

Dorigo and Gambardella [18] presented the study on the solution of the traveling salesman problem by artificial ant colony. Furthermore, this algorithm has been able to be adapted on many integrated problems such as job-shop scheduling and vehicle routing [19,20]. ACO, which was developed by Dorigo and his collaborators in 1992, is directly based on real ant colonies that have the ability to find the shortest route from their nest to source of food without thrusting their visual cues but pheromone information. Pheromone of each ant is used by next ant following the same route by the probability of the trail of this chemical clue. By increasing the usage of same route, trails of pheromone raises on the route, which attracts more ants to follow same way. However, the pheromone deposited on the route evaporates in time. This character is described in the algorithm as three fundamental operations, which are known as "state transition," "local updating," and "global updating," and regulates to build a solution in a constructive approach. Graph representations are frequently used in most problems solved with ACO method. For this process, values that are defined for each

couple of elements or location of elements in the solution define the pheromone function. As a result, all or some of these elements form the final solution for the problem.

14.4.10 Topology (layout) optimization of fiber reinforced composites

In structural systems and constitutes, the selection of the best configuration is handled by layout or topology optimization. Topology optimization is the simultaneous selection of "the optimal layout," which is spatial sequence of members and joints, "geometry" being the location of joints and "cross-sectional dimensions" being sizing of a structure. Ideal layouts are supported on the use of isotropic materials being inside of the framework of classical black-white or 0-1 structures. Initial improvements in studies for topology optimization were about employment of composite material, which is described as interpolation of void and whole material. These early developments were based on a theoretical work leading an apprehension, which is the issue of existence of solutions resolved by increasing in extent of the design space to consist of relaxed designs, for the form of composites [57].

In order to submit composites as a part of the solution method in layout design, it is required to mind with a number of branches of material science and especially the methods for computing the effective material parameters of composites. After, it should be dealt with the limits on the possible behavior of effective material and straightly gives the knowledge gathered on the optimal use of local material properties. Therefore, this layout design named as the *homogenization approach* generates the principals for many studies. Individuating between the use of the methodology being generally as a tool for interpolation of properties and studies where existence of solutions means central aspect can be performed.

One can be sure that the importance/value of designing with composites as a study area is quite high. This design includes such variables that are the optimum orientation and the optimal layup of each ply of an orthotropic material. If one desires to find the optimal design, which can include any material, it is possible to select to work with an entirely free parametrization of the stiffness tensor.

Being orthotropic (anisotropic) materials, one can generally enter the angle of rotation of the directions of orthotropy as a design parameter in terms of desired transformation formulas for frame rotations in the design of composites. One should know that the density of the material is a function of many design variables describing the geometry of the holes at the microlevel. Moreover, it is also necessary to optimize the variables. Therefore, complexity of the problem will increase depending on spatial point or mesh element. Then, in order to create optimal structure, one can expect to find density values of 0 and 1 in major areas. In addition to these, one is also able to find detailed information about layout optimization for fiber-reinforced composite material structures in the reference being Bendsøe et al. [21].

In Table 14.2, a short review on design optimization of fiber-reinforced composite structures is given, including optimization methods, fiber types, and composites.

Table 14.2 Examples of engineering optimization problems for fiber-reinforced composite structures

Authors	Optimization problem	Optimization methods	Composite material	Fiber type
Aydin and Artem [5]	Design the stacking sequence of the laminated composites that have low coefficient of thermal expansion and high elastic moduli	Generalized pattern search, simulated annealing (SA), and genetic algorithm (GA)	Carbon-epoxy	Unidirectional long
Kaveh et al. [22]	Minimum thickness design of laminated composite plates under in plain loading	Charged system search algorithm	Graphite-epoxy	Unidirectional long
Koide and Luersen [23]	Maximization of fundamental frequency of laminated composite cylindrical shells	Ant colony	Graphite-epoxy	Unidirectional long
Walker et al. [24]	Design of laminated cylindrical shells for maximum torsional and axial buckling loads	Golden section	T300/5208 graphite epoxy	Unidirectional long
Lopatin and Morozov [25]	Buckling of the composite orthotropic clamped-clamped cylindrical shell loaded by transverse inertia forces	Finite element analysis by using Galerkin method	Glass fiber-reinforced polymeric composite	Unidirectional long
Mingfa et al. [26]	Design and structural optimization of specifically shaped composite tanks with complex loading conditions	Adaptive SA algorithm	Values are given without material name	Unidirectional long
Jafari and Rohani [27]	Optimization of perforated composite plates under tensile stress	GA	1. CE9000 glass-epoxy 2. Woven glass-epoxy 3. Plywood 4. Carbon-epoxy	1. Thin long 2. Woven 3. Thin long 4. Thin long

Continued

Table 14.2 Continued

Authors	Optimization problem	Optimization methods	Composite material	Fiber type
Li and Chandrashekhar [28]	Structural optimization of laminated composite hydrokinetic turbine blades	Particle swarm optimization (PSO)	E-glass/epoxy as facesheet and shear web with foam core (core is ignored for optimization process)	Long continuous
Manne and Tsai [29]	Optimization of minimum weight, layup, and thickness taper for quadrilateral plates having cutouts	Nelder-Mead	Graphite-epoxy *ASIH3501*	Unidirectional long
Hu and Fis [30]	Optimization of nonlinear composite materials and structures at multiple scales	Ant colony	Noncrimp fabric composite	Unidirectional long fiber
Aydin et al. [6]	Design and optimization of dimensionally stable composites	Efficient global optimization	Carbon/epoxy	Unidirectional long
Tabakov [31]	Design optimization of the pressure vessel subjected to Tsai-Hill failure criterion	Big Bang-Big Crunch algorithm	T300/5208 graphite epoxy	Unidirectional long
Deveci et al. [32]	Buckling optimization of composite plates under Puck failure criterion	Hybrid genetic and trust-region-reflective algorithms	Given values without material name	Unidirectional long
Thompson et al. [33]	Optimization of fiber-reinforced polymer composite bridge deck panels	Reliability-based optimization	Glass-epoxy	Unidirectional long
Madhusudhanan and Giri [34]	Design optimization of hybrid composite leaf spring	Firefly algorithm	1. Steel 2. Jute/E-glass/epoxy 65Si7	Woven E-glass
Lakshmi and Rao [35]	Optimization of fundamental frequency for 64-ply hybrid laminate plate	Multipopulation-based harmony search algorithm	Design 1: Graphite-epoxy Design 2: Graphite and	Unidirectional long

		with dynamic interaction of population	glass-epoxy as hybrid composite	
Paia et al. [36]	Optimization of the stacking sequence of a laminate for buckling response, matrix cracking, and strength requirements	Tabu search	Graphite-epoxy	Unidirectional long
Rao and Arvind [37]	**(a)** Thermal buckling optimization of laminated composite plates **(b)** Optimization of hybrid laminate composite panels for weight and cost with frequency and buckling constraints	Scatter search	**(a)** Graphite-epoxy (AS/3501) **(b)** Graphite-epoxy and glass-epoxy (generic S-glass/epoxy)	Unidirectional long
Fang and Springer [38]	Optimizing symmetrical fiber-reinforced composite laminates such that the weight is minimum and the Tsai-Wu strength failure criterion is satisfied	Monte Carlo	E-glass/epoxy composite	Unidirectional long
Chernivov et al. [39]	Optimum postimpact vibration control of an electrically conductive carbon fiber-reinforced composite plate subjected to an uncertain, or stochastic, impact load	Two-stage stochastic partial differential equation-constrained optimization methodology	Carbon fiber-reinforced composite	Thin long unidirectional fiber
Duy et al. [40]	Lightweight design optimization of laminated composite plates subjected to frequency constraints	Adaptive elitist differential evolution algorithm	Carbon-bismaleimide	Unidirectional long
Liu and Paavola [41]	Lightweight design of composite laminated structure with frequency constraint	Gradient projection algorithm	Carbon-bismaleimide	Unidirectional long

Continued

Table 14.2 Continued

Authors	Optimization problem	Optimization methods	Composite material	Fiber type
Vosoughi and Nikoo [42]	Multiobjective optimization of laminated composite plates for maximum natural frequency and thermal buckling temperature.	New hybrid differential quadrature, nondominated sorting genetic algorithm II, and Young bargaining model algorithm	Graphite-epoxy	Unidirectional long
Hemmatian et al. [43]	Multiobjective optimization of hybrid laminates for minimum weight and cost with fundamental frequency constraint	Elitist ant system	Graphite-epoxy Glass-epoxy	Unidirectional long
Omkar et al. [44]	Multiobjective optimization of laminated composite plates for minimum cost and weight	MPI-based parallel synchronous vector Evaluated PSO	Carbon-epoxy	Unidirectional long
Jiang et al. [45]	Design the stacking sequence of the laminated composites for maximum stiffness	Interval number programming method	Glass-epoxy	Unidirectional long
Jing et al. [46]	Stacking sequence optimization of composite laminates for maximum buckling load	Permutation search algorithm	Graphite-epoxy	Unidirectional long
Liu et al. [47]	Design the stacking sequence of the laminated composites for maximum buckling load	Permutation GA	Graphite-epoxy	Unidirectional long
Chang et al. [48]	Stacking sequence optimization of composite laminate	Permutation discrete PSO		Unidirectional long
Fakhrabadi et al. [49]	Multiobjective optimization of laminated composite plates for minimum cost and weight under different failure criteria	Discrete shuffled frog-leaping algorithm	Carbon-epoxy	Unidirectional long

Shin [50]	Design of a stiffened laminated plate for maximum buckling load	Homotopy method	Graphite-epoxy	Unidirectional long
Kalantari et al. [51]	A multiobjective robust optimization hybrid composites for minimize cost and weight under flexural loading	NSGA-II	Carbon-epoxy Glass-epoxy	Unidirectional long
Topal [52]	Multiobjective optimization of laminated cylindrical shells to maximize a weighted sum of the frequency and buckling load under external load	Modified feasible direction method	Graphite-epoxy	Unidirectional long
Omkar et al. [53,54]	Multiobjective optimization of laminated composite plates for minimum cost and weight under different failure criteria	Vector-evaluated artificial bee colony	Carbon-epoxy	Woven E-glass

References

[1] Gurdal Z, Haftka RT, Hajela P. Design and optimization of laminated composite materials. Hoboken, NJ: John Wiley & Sons; 1999.

[2] Rao SS. Engineering optimization: theory and practice. 4th ed. Hoboken, NJ: John Wiley & Sons; 2009.

[3] Karpov YS. Structural optimization of composite material for aircraft panels with strength, stability, and deflection restrictions. Strength Mater 2004;36(6):570–81.

[4] Jones RM. Mechanics of composite materials. 2nd ed. Philadelphia: Taylor&Francis; 1999.

[5] Aydin L, Artem HS. Comparison of stochastic search optimization algorithms for the laminated composites under mechanical and hygrothermal loadings. J Reinf Plast Compos 2011;30(14):1197–212.

[6] Aydin L, Aydin O, Artem HS, Mert A. Design of dimesionally stable composites using efficient global optimization method. Proc Inst Mech Eng L J Mater Des Appl 2016. http://dx.doi.org/10.1177/1464420716664921.

[7] Tauchert TR, Adibhatla S. Design of laminated plates for maximum stiffness. J Compos Mater 1984;18:58–69.

[8] Massard TN. Computer sizing of composite laminates of strength. J Reinf Plast Compos 1984;3:300–27.

[9] Martin PMJW. Optimum design of anisotropic sandwich panels with thin faces. Eng Optim 1997;11:3–12.

[10] Watkins RI, Morris AJ. A multi-criteria objective function optimization scheme for laminated composites for use in multilevel structural optimization schemes. Comput Methods Appl Mech Eng 1987;60:233–51.

[11] Walker M, Smith RE. A technique for the multi-objective optimization of laminated composite structures using genetic algorithms and finite element analysis. Compos Struct 2003;62:123–8.

[12] Park JH, Hwang JH, Lee CS, Hwang W. Stacking sequence design of composite laminates for maximum strength using genetic algorithms. Compos Struct 2001;52:217–31.

[13] Bruyneel M, Fleury C. Composite structures optimization using sequential convex programming. Adv Eng Softw 2002;33:697–711.

[14] Deb K. Multi-objective optimization using evolutionary algorithms. Chichester: John Wiley & Sons; 2001.

[15] Torczon V. On the convergence of pattern search algorithms. SIAM J Optim 1997;7:1–25.

[16] Kennedy J, Eberhart RC. Particle swarm optimization. In: Proceedings of the IEEE international conference on neural networks, IEEE Service Center, Piscataway; 1995.

[17] Kovacs G, Groenwold AA, J'Armai K, Farkas J. Analysis and optimum design of fibre-reinforced composite structures. Struct Multidiscip Optim 2004;28:170–9.

[18] Dorigo M, Gambardella LM. Ant colonies for the travelling salesman problem. Biosystems 1997;43:73–81.

[19] Talbi EG, Roux O, Fonlupt C, Robillard D. Parallel ant colonies for the quadratic assignment problem. Futur Gener Comput Syst 2001;17(4):441–9.

[20] Kolahan F, Abachizadeh M, Soheili S. An ant colony optimization for single-machine weighted tardiness scheduling with sequence-dependent setups. Proceedings of the 6th WSEAS international conference on simulation, modelling and optimization, Lisbon, Portugal; 2006. p. 19–23.

[21] Bendsøe MP, Sigmund O. Topology optimization. Berlin; Heidelberg: Springer-Verlag; 2004.

[22] Kaveh A, Soudmand BH, Sheikholeslami R. Optimal design of laminated composite structures via hybrid charged system search and particle swarm optimization. Asian J Civ Eng 2013;14(4):587–604.
[23] Koide RM, Luersen MA. Maximization of fundamental frequency of laminated composite cylindrical shells by ant colony algorithm. J Aerosp Technol Manag 2013;5(1):75–82.
[24] Walker M, Reis T, Adali S. Multiobjective design of laminated cylindrical shells for maximum torsional and axial buckling loads. Comput Struct 1997;62:237–42.
[25] Lopatin AV, Morozov EV. Buckling of the composite orthotropic clamped –clamped cylindrical shell loaded by transverse inertia forces. Compos Struct 2013;95:471–8.
[26] Mingfa R, Fanzi BU, Li T. Structural optimization approach for specially shaped composite tank in spacecrafts. J Mech Sci Technol 2015;29(4):1429–35.
[27] Jafari M, Rohani A. Optimization of perforated composite plates under tensile stress using genetic algorithm. J Compos Mater 2015;12540:1–9.
[28] Li H, Chandrashekhara K. Particle swarm-based structural optimization of laminated composite hydrokinetic turbine blades. J Mech Sci Technol Eng Optim 2015;47(9):3–19.
[29] Manne PM, Tsai SW. Design optimization of composite plates: part II—structural optimization by plydrop tapering. J Compos Mater 1998;32(6):1–27.
[30] Hu N, Fish J. Enhanced ant colony optimization for multiscale problems. Comput Mech 2016;57(3):447–63. http://dx.doi.org/10.1007/S00466-015-1245-z.
[31] Tabakov PY. Big bang—Big Crunch optimization method in optimum design of complex composite laminates. World Acad Sci Eng Technol 2011;5(5):927–31.
[32] Deveci HA, Aydin L, Artem HS. Buckling optimization of composite laminates using a hybrid algorithm under puck failure criterion constraint. J Reinf Plast Compos 2016;35(16):1233–47.
[33] Thompson MD, Eamon C, Rohani MR. Reliability-based optimization of fiber-reinforced polymer composite bridge deck panels. J Struct Eng 2006;132(12):1898–906.
[34] Madhusudhanan P, Giri R. Design optimization analysis of hybrid composite leaf spring using firefly algorithm. In: International conference on advances in materials, manufacturing and applications; 2015. p. 176.
[35] Lakshmi K, Rao ARM. Optimal design of laminate composite plates using dynamic hybrid adaptive harmony search algorithm. J Reinf Plast Compos 2015;34(6):493–518.
[36] Paia N, Kawa A, Weng M. Optimization of laminate stacking sequence for failure load maximization using tabu search. Compos Part B 2003;34:405–13.
[37] Rao ARM, Arvind N. A scatter search algorithm for stacking sequence optimisation of laminate composites. Compos Struct 2005;70:383–402.
[38] Fang C, Springer GS. Design of composite laminates by a Monte Carlo method. J Compos Mater 1993;27(7):721–53.
[39] Chernivov D, Krokhmal P, Zhupanska OI, Pasiliao CL. A two-stage stochastic PDE-constrained optimization approach to vibration control of an electrically conductive composite plate subjected to mechanical and electromagnetic loads. Struct Multidiscip Optim 2015;52(2):337–52. http://dx.doi.org/10.1007/s00158-015-1238-8.
[40] Duy TV, Huu VH, Thi TDD, Trung HD, Thoi TN. A global numerical approach for lightweight design optimization of laminated composite plates subjected to frequency constraints. Compos Struct 2017;159:646–55.
[41] Liu Q, Paavola J. Lightweight design of composite laminated structures with frequency constrain. Compos Struct 2016;156:356–60.
[42] Vosoughi AR, Nikoo MR. Maximum fundamental frequency and thermal buckling temperature of laminated composite plates by a new hybrid multi-objective optimization technique. Thin-Walled Struct 2015;95:408–15.

[43] Hemmatian H, Fereidoon A, Sadollah A, Bahreininejad A. Optimization of laminate stacking sequence for minimizing weight and cost using elitist ant system optimization. Adv Eng Softw 2013;57:8–18.
[44] Omkar SN, Venkatesh A, Mudigere M. MPI-based parallel synchronous vector evaluated particle swarm optimization for multi-objective design optimization of composite structures. Eng Appl Artif Intell 2012;25:1611–27.
[45] Jiang C, Han X, Liu GP. Uncertain optimization of composite laminated plates using a nonlinear interval number programming method. Comput Struct 2008;86:1696–703.
[46] Jing Z, Xueling Fan B, Sun Q. A stacking sequence optimization of composite laminates for maximum buckling load using permutation search algorithm. Compos Struct 2015;121:225–36.
[47] Liu B, Haftka RT, Akgun MA, Todoroki A. Permutation genetic algorithm for stacking sequence design of composite laminates. Comput Methods Appl Mech Eng 2000;186:357–72.
[48] Chang N, Wang W, Yang W, Wang J. Ply stacking sequence optimization of composite laminate by permutation discrete particle swarm optimization. Struct Multidiscip Optim 2010;41:179–87.
[49] Fakhrabadi MMS, Rastgoo A, Samadzadeh M. Multi-objective design optimization of composite laminates using discrete shuffled frog leaping algorithm. J Mech Sci Technol 2013;27(6):1791–800.
[50] Shin YS. Optimal design of stiffened laminated plates using a homotopy method. KSME J 1993;7(4):399–407.
[51] Kalantari M, Dong C, Davies IJ. Multi-objective robust optimization of unidirectional carbon/glass fibre reinforced hybrid composites under flexural loading. Compos Struct 2016;138:264–75.
[52] Topal U. Multi-objective optimization of laminated composite cylindrical shells for maximum frequency and buckling load. Mater Des 2009;30:2584–94.
[53] Omkar SN, Naik NG, Kiran P, Mudigere M. Vector evaluated and objective switching approaches of artificial bee colony algorithm (ABC) for multi-objective design optimization of composite plate structures. Int J Appl Metaheuristic Comp Archiv 2011;2(3):1–26.
[54] Omkar SN, Senthilnath J, Khandelwal R, Naik GN, Gopalakrishnan S. Artificial bee colony (ABC) for multi-objective design optimization of composite structures. Appl Soft Comput 2011;11:489–99.
[55] Akbulut M, Sönmez FÖ. Design optimization of laminated composites using a new variant of simulated annealing. Comput Struct 2011;89:1712–24.
[56] Storn R, Price K. Differential evolution – a simple and efficient heuristic for global optimization over continuous spaces. J Global Optim 1997;11:341–59.
[57] Rozvany GIN, Bendsøe MP, Kirsch U. Appl Mech Rev 1995;48(2):41–119.

Further Reading

[1] Abachizadeh M, Tahani M. An ant colony optimization approach to multi-objective optimal design of symmetric hybrid laminates for maximum fundamental frequency and minimum cost. Struct Multidiscip Optim 2009;37:367–76.
[2] Chetwynd DG. Selection of structural materials for precision devices. Precis Eng 1987;9:3–6.

[3] Hammoudi A, Djeddou F. Composite differential evolution algorithm: mixed variable structural optimization problem. J Chem Mater Res 2015;3:3–8.
[4] Rangarajan A, D′Mello RJ, Sundararaghavan V, Waas AM. Minimization of thermal expansion of symmetric, balanced, angle ply laminates by optimization of fiber path configurations. Compos Sci Technol 2011;71:1105–9.
[5] Rao MRA, Lakshimi K. Discrete hybrid PSO algorithm for design of laminate composites with multiple objectives. J Reinf Plast Compos 2011;30(20):1703–27.
[6] Trias D, Maimi P, Blanco N. Maximization of fundamental frequency of plates and cylinders. Compos Struct 2015;57(3):447–63 [in press, corrected proof].
[7] Yoo DG, Kim JH, Geem ZW. Overview of harmony search algorithm and its applications in civil engineering. Evol Intel 2014;7(1):3–16.

This page intentionally left blank

Concluding remarks and future outlook

15

M. Özgür Seydibeyoğlu[*], *Amar K. Mohanty*[†], *Manjusri Misra*[†]
*Izmir Katip Çelebi University, Izmir, Turkey, †University of Guelph, Guelph, ON, Canada

Although the composite materials have been used for long centuries, polymeric composites and fiber-reinforced composite materials are very new compared with many other material classes. This new area is a multidisciplinary area that can be considered even as a new undergraduate university degree offering many new research areas.

The new developments in the composite materials are on the following issues:

a. New weaving technologies including 3-D braiding and knitting techniques for the present fibers
b. New automation techniques well integrated with industry revolution 4.0
c. Use of simulation programs to model and design new composite structures
d. Structural long-fiber thermoplastic composites
e. Joining thermoplastic-based fiber composites
f. 3-D printing technology for the composite materials
g. Smart composites
h. The use of bioplastics for the composites
i. The use of natural fibers in the area, especially the use of long fibers in the thermoplastic resins
j. The use of nanotechnology and nanofibers for the fiber-reinforced composites

Besides composite materials, there are numerous research projects going on for the fiber technologies in the following areas:

a. The use of new low-cost precursors for carbon fiber
b. Effective utilization of basalt fibers
c. New natural fibers from different parts of the Earth
d. Surface modification of fibers
e. New sizing formulations with nanosized reinforcing particles
f. Nanosize reinforcing particle-reinforced fibers
g. Development of new technologies for nanosized fiber formation

The book provides an in-depth information on the fiber technology, specifically for the composite materials. Besides fibers, a solid mechanical analysis and design criteria are written by mechanical engineering faculty members. The conventional fibers are explained by the research scientists at the manufacturing plant including glass fiber and carbon fiber. The recent trends in biotechnology and nanotechnology are presented by the researchers. A final remark on the new developing fiber and composite technologies is listed above.

Fiber Technology for Fiber-Reinforced Composites. http://dx.doi.org/10.1016/B978-0-08-101871-2.00015-1

We hope that this book will be very helpful for the undergraduate and graduate students. The most distinctive usage will be from the industry people. As the market reports are given in the first section, the composite industry is growing with a very fast pace. However, there is a very limited information on the fiber technology for this very critical industry. It is very critical for energy applications, transportation applications, and military applications. The lack of information on this important technology brings many problems to the production lines. The use of appropriate fibers, the choice of suitable sizing agents, and the design calculations are of great importance for this industry to grow much better.

We therefore are very much pleased to present this important book, and we hope that it will be very helpful for the future research projects, for the industry, and for the educational purposes in the academy. With our expertise on fiber technology, carbon fiber technology, biocomposites, biotechnology, composite interface, and composite processing, we believe that we gathered many important scientists in this area, and we believe that it will be a key book.

Index

Note: Page numbers followed by *f* indicate figures, and *t* indicate tables.

A

Abaca fibers, 217, 218*f*, 219*t*
Acrylated epoxidized soybean oil (AESO), 285
Acrylic polymers, 128
Ant colony optimization (ACO), 305–306
Aramid fibers
  applications, 158–163
  fiber and product forms, 158
  formation, 154–155
  properties, 155–158, 156*t*
  spinning, 154–155
  structure, 155–158
  synthesis, 153–154
Autoclave process, 66, 67*f*
Automated fiber placement (AFP), 61–63, 68
Automated tape laying (ATL), 68

B

Basalt fibers
  aerospace industry, 178
  automotive industry, 178
  chemical industry, 180–181
  civil engineering, 178–179
  electrical industry, 181
  manufacturing engineering, 181
  petrochemical industry, 180–181
  power engineering, 181
  preparation, 170–171
  reinforced composites, 173–175
  structural properties, 171–173, 172*t*
  surface treatments, 175–177
Bernoulli-Euler-type equation, 42–43
Biocides, 115–116
Biodegradable PE (bio-PE), 243
Boron fibers, 195–197, 196*f*
  carbide, 196
  CVD techniques, 195
  morphology, 196, 196*f*
  nitride, 196
Boyd (CHU) model, 17–18
Brodnyan model, 21
Bulk molding compounds (BMC), 63, 107

C

Carbon-carbon (C/C) composites, 59, 148
Carbon fiber (CF)
  atomic structure, 123–124
  carbonization processes
    cellulosic precursors, 139–140
    PAN precursor, 133–138, 134*f*
    pitch based precursor, 138
  cellulose precursors, 131–132, 139–140
  developments and trends, 124–125, 140–141
  general purpose, 124
  high-performance applications, 124
  high strength, 124
  intermediate modulus, 124
  PAN precursors, 126–129, 126*f*, 133–138, 134*f*
  pitch precursors, 126*f*, 129–131, 138
  polyacrylonitrile fibers, 123
  polymer-matrix composites, 141–148
  types, 124
Carbon fiber grafted with GO (CF-GO), 289
Carbon fiber reinforced plastics (CFRP), 55–56, 178–179
Carbonization, 133–140
  cellulosic precursors, 139–140
  PAN precursor, 133–138, 134*f*
  pitch based precursor, 138
Carbon nanofiber (CNF), 260–261
Carbon nanotubes (CNTs), 3, 51, 57, 260–262, 281, 287–289
  fibre modification, 289
  growth/deposition, 287–288, 290–291
  multiwalled, 261
  nailing effect, 283–285
  natural fibre modification, 283–285
  single-walled, 261
  VGCNFs, 261

Cellulose acetate (CA), 241–242
Cellulose acetate butyrate (CAB), 241–242, 285
Cellulose acetate propionate (CAP), 241–242
Cellulose nanofibers
  lignocellulosic plants, 262–263
  natural nanostructured, 263
Ceramic fibers
  application, 203
  chemical conversion, 199–200
  composites
    manufacturing methods, 147–148
    polymeric matrices, 144–146
    reinforcements, 142–144
    uses, 148–150
  CVD technique, 197–198
  melt spinning technique, 199
  nonoxide
    boron fibers, 195–197
    Si-Al-O-N ceramic fibers, 197
    SiCN fibers, 195
    silicon carbide fibers, 192–194, 194*t*
  oxide, 187–192
  polymer-derived precursor method, 200–201, 201*f*
  single-crystal fiber growth technique, 202, 203*f*
  slurry spinning, 199
  sol-gel process, 201–202
  technology, developments and trends, 140–141
Ceramic matrix composites (CMCs), 59, 187
  physical and mechanical properties, 203
CFRP. *See* Carbon fiber reinforced plastics (CFRP)
Chantler model, 17–18
Chemical conversion approach, 264–265
Chemical vapor deposition (CVD) method, 187, 197–198, 261, 287
Chopped strands
  direct chopping process, 107
  dry chopping process, 107
  semiwet chopping process, 107
Closed molding process
  compression molding, 148
  extrusion, 148
  injection molding, 148
  light RTM, 147
  pultrusion, 147–148
  resin transfer molding, 147
  thermoforming, 148
  vacuum-assisted RTM, 147
  vacuum bagging, 148
Close proximity indirect exposure (CPIE), 141
Compound annual growth rate (CAGR), 1, 277
Compressed natural gas (CNG), 178, 178*f*
Computer-aided design (CAD), 299
Constitutive equations, 22–25
Continuous fiber-reinforced composites
  macromechanical analysis, 6–10
  micromechanical analysis, 11
Cotton fibers, 212–213, 213*f*, 214*t*
Cup-stacked carbon nanotubes (CSCNTs), 283*f*
Curved composites, 27–33
Cyanate esters (CE), 144

D

Damping analysis, 47–48
Differential evolution methods (DEM), 305
Dimethylacetamide (DMAc), 127–128
Dimethylformamide (DMF), 126–127
Dimethyl sulfoxide (DMSO), 127–128
Dynamic behavior
  damping analysis, 47–48
  longitudinal vibrations, composite bars, 40–42
  transverse vibration
    of composite beams, 42–44
    of orthotropic plates, 44–47
Dynamic mechanical analysis (DMA), 282

E

Electromagnetic interference shielding effectiveness (EMI SE), 261–262
Electrophoretic deposition (EPD), 287–288
Electrospinning
  fiber formation, 254–257
  fundamentals, 252–254
  nanoparticles, 257
Epoxy resins, 144–145
Eshelby's models, 11
Esterification treatment methods, 91
Excimer UV laser, 87

F

Fabric
  definition, 143
  knitted, 143
  unidirectional, 143
  woven, 143
Fiber composites
  characteristics, 299
  continuous fiber-reinforced composites
    macromechanical analysis, 6–10
    micromechanical analysis, 11
  curved composites, 27–33
  dynamic behavior, 40–48
  engineering optimization problems, 307–311*t*
  interface mechanics, 26–27
  material selection
    fiber selection factors, 301
    matrix selection factors, 301, 301*t*
  optimization
    ACO, 305–306
    DE methods, 305
    genetic algorithm, 303
    GPSA, 303–304
    multiobjective, 303
    PSO, 304–305
    simulated annealing, 304
    single-objective, 302
    stochastic optimization methods, 303
    topology, 306–311
  short fiber-reinforced composites
    law of mixtures, 12
    semi empirical models, 15–21
    Shear lag model, 12–15, 13*f*
  strength failure theories
    orthotropic lamina, 37–38
    orthotropic materials, 33–36
    properties and stress-strain relations, 33
  structural design, 300
  woven fabric composites, 22–25
Fiber modification methods
  alkaline treatments, 88
  biochemical treatments, 92
  esterification treatment methods, 91
  excimer UV laser, 87
  gamma radiation, 86
  graft copolymerization, 90
  heat treatment, 86
  isocyanate treatment, 92
  maleated coupling, 91–92
  ozone treatment, 86–87
  permanganate treatment, 89
  peroxide treatment, 89–90
  plasma treatment, 82–85
  silane treatments, 88–89
  sizing
    carbon fibers, 93
    glass fibers, 93–94
  UV treatment, 85–86
Fiber reinforced composites (FRCs)
  analyses, 73
  applications, 53–54, 264–265
  CAGR, 1, 277
  carbon nanotubes, 260–262
  cellulose nanofibers, 262–264
  CMCs, 59
  CNFs, 260
  current and future market outlook, 55–56
  definitions, 51–53
  electrospinning
    fiber formation, 254–257
    fundamentals, 252–254
    nanoparticles, 257
  FST
    nonoxidative, 75
    oxidative, 75
  load transfer mechanism, 277–278
  manufacturing process
    autoclave process, 66, 67*f*
    automated fiber placement, 68
    automated tape laying, 68
    centrifugal casting, 68
    compression molding, 63
    filament winding technique, 67, 68*f*
    hand lay-up process, 64, 64*f*
    injection molding, 69
    joining methods, 72
    machining operations, 70–71
    prepreg process, 70, 71*f*
    pultrusion method, 68, 69*f*
    reaction injection molding, 69–70
    recycling, 72
    resin transfer molding, 65–66, 66*f*
    sandwich construction, 70, 71*f*
    spray-up technique, 64, 65*f*
    thermoforming, 70

Fiber reinforced composites (FRCs) *(Continued)*
vacuum assisted resin transfer molding, 65–66
vacuum bagging, 66, 67*f*
vacuum infusion technique, 64, 65*f*
matrix adhesion, 60–61
microfibers, 251–252
MMCs, 59–60
nano-enhanced systems, 291–293
nanofibers, 251–252
nanotechnologies, 278–279
PMCs, 59
properties, 61
reinforcements, 56–58
testing, 73–74
Fiber-reinforced polymer (FRP), 178–179
Fiber selection process, 301
Fiber surface treatments (FSTs), 75
nonoxidative, 75
oxidative, 75
Fiber technology
energy applications, 318
military applications, 318
transportation applications, 318
Filament winding technique, 67, 68*f*
Film-fed growth (FED), 202
Flax fibers, 220–222, 224*f*, 225*t*

G

Gamma radiation, 86
Generalized pattern search algorithm (GPSA), 303–304
Genetic algorithm (GA), 303
Glass fibers, 93–94, 317
composite interphase
thermoplastics, 117–119
thermosets, 116–117
history of, 99
manufacturing process, 99–103, 100*f*
products
assembled rovings, 109
chopped and continuous strand mats, 109
chopped strands, 107–108
direct draw rovings, 108
sizing
antioxidizing agents, 114–115
antistatic agents, 114
biocides, 115–116
coupling agents, 112–113
emulsifying agents, 113–114
film forming agents, 111–112
lubricating agents, 113
plastifying agents, 115
surface active agents, 113–114
types of, 103–106, 104*t*
Glass FRP (GFRP), 178–179
Glass mat thermoplastic (GMT), 119
Gold model, 18–19
Graft copolymerization, 90
Green composites
applications
automotive, 245
packaging, 245
life-cycle assessment, 237–238, 239*f*
natural polymer
biobased polyethylene, 243
cellulose acetate, 241–242, 242*f*
polybutylenesuccinate, 243–244
polyhydroxyalkanoates, 241, 241*f*
polylactic acid, 240–241, 240*f*
thermoplastic starch, 242–243
Guth model, 18–19, 21

H

Halpin-Tsai model, 15–16, 19, 20*f*
Hemp fibers, 222–226, 226*f*, 227*t*
Henequen fibers, 226–228, 228*f*, 228*t*
High-density PE (HDPE), 146
Hooke's law, 13
Hummer's method, 291
Hu model, 17–18
Hydridopolysilazane (HPZ) ceramic fiber, 195
Hyperbranched polymers, 279–281, 280*f*

I

Interfacial shear strength (IFSS), 286–287
Interlaminar shear strength (ILSS), 84, 177
Intermetallic composites (IMC), 197
Interpenetrating polymer network (IPN), 117

J

Junkers method, 170
Jute fibers (JFs), 218–220, 222*f*, 223*t*, 283–285

K

Kapok fibers, 213–216, 215*f*, 216*t*
Kenaf fibers, 228–229, 229*f*
Kevlar, 155, 157

L

Lewis-Nielsen model, 16–17, 18*f*
Life-cycle assessment (LCA), 237–238, 239*f*
  composite materials, 239–240
Light RTM (LRTM), 147
Lignin, 132–133
Limiting oxygen index (LOI), 155
Linear low-density PE (LLDPE), 146
Long fiber thermoplastic (LFT), 119
Low-density PE (LDPE), 146
Lyocell fibers, 132

M

Macromechanical analysis, 6–10
  constitutive equations, 6–10
Maleated coupling, 91–92
Matrix selection factors, 301, 301*t*
Melt spinning technique, 199
Meta-aramid fibers, 159–161
Metal matrix composites (MMCs), 59, 187
Micro fibers, 251–252
Micromechanical analysis, 11
Modified Halpin-Tsai model, 19–20
Mooney equation, 21
Multiobjective optimization, 303
Multiwalled carbon nanotubes (MWCNTs), 174, 261, 283–285, 284*f*

N

Nanocellulose, 263–264
Nanofiber-reinforced polymer composites (NFRCs), 264
  applications, 264–265
  catalysts and sensors, 264–265
Nanofibers, 251–252
Nanoparticle reinforcement, 281–282
Nanotechnologies
  carbon fibre modification
    CNT, 289
    graphene oxide, 289
    graphene oxide hybrids, 289
    growth/deposition, 287–288, 288*f*
  glass fibre modification
    graphene oxide, 291
    growth/deposition, 290–291
  matrix modification
    hyperbranched polymers, 279–281, 280*f*
    nanoparticle reinforcement, 281–282
    POSS, 281
  natural fibre modification
    CNTs, 283–285
    metal and metal oxide nanoparticles, 285–287
    nano cellulose, 285
Natural fibers
  abaca, 217, 218*f*, 219*t*
  cotton, 212–213, 213*f*, 214*t*
  flax, 220–222, 224*f*, 225*t*
  hemp, 222–226, 226*f*, 227*t*
  henequen, 226–228, 228*f*, 228*t*
  history, 210–212
  jute, 218–220, 222*f*, 223*t*
  kapok, 213–216, 215*f*, 216*t*
  kenaf, 228–229, 229*f*
  properties, 231*t*
  sisal, 217, 220*f*, 221*t*, 230*t*
  structure, 212–229
Natural polymer
  biobased polyethylene, 243
  cellulose acetate, 241–242, 242*f*
  polybutylenesuccinate, 243–244
  polyhydroxyalkanoates, 241, 241*f*
  polylactic acid, 240–241, 240*f*
  thermoplastic starch, 242–243
N-benzylpyrazinium hexafluoroantimonate (BPH), 144–145
N-methyl-pyrrolidone (NMP), 153–154
Nomex, 153, 156*t*
Nonoxide fibers
  boron, 195–197
  CMCs, 197
  MMCs, 197
  Si-Al-O-N ceramic, 197
  SiCN, 195
  silicon carbide, 192–194, 194*t*
Nonspherical particulate systems
  Brodnyan model, 21
  Guth model, 21
  Halpin-Tsai model, 19, 20*f*
  modified Halpin-Tsai model, 19–20

O

Open-molding processes, 147
Optimization
  ACO, 305–306
  DE methods, 305
  genetic algorithm, 303
  GPSA, 303–304
  multiobjective, 303
  PSO, 304–305
  simulated annealing, 304
  single-objective, 302
  stochastic optimization methods, 303
  topology, 306–311
Orthotropic lamina
  biaxial strength criteria
    Hoffman failure criterion, 39
    Tsai-Hill failure criterion, 39
    Tsai-Wu tensor failure criterion, 39–40
  stiffness and strength, 37–38
Ozone treatment, 86–87

P

PAN-based precursor, 126–129
  spinning method, 128
Para-aramid fibers
  ballistic protection, 163
  composites, 161–162
  protective clothing, 162–163
Particle swarm optimization (PSO), 304–305
Permanganate treatment, 89
Peroxide treatment, 89–90
Phenolic resins, 145
1,4-Phenylenediamine (PPD), 153–154
Pitch, 129–131
  coal-tar, 130
  isotropic, 130
  melt spinning, 130–131
  mesophase, 130
Plasma treatment, 82–85
Poly(m-phenylene isophthalamide) (MPDI), 153
Poly(p-phenylene terephthalamide) (PPTA), 153–154
  PPD, 153–154
  TDC, 153–154
Poly(phthalazinone ether ketone) (PPEK), 287–288
Poly(propylene carbonate) (PPC), 244
Polyaluminocarbosilane (PACs), 197
Polyarylacetylene (PAA), 281
Polybutylenesuccinate (PBS), 243–244
Polycarbosilane (PCS), 192
Polyethylene glycol (PEG), 113–114
Polyhedral oligomeric silsesquioxane (POSS), 279, 281
Polyhydroxyalkanoates (PHA), 241, 241*f*
Polyhydroxy butyrate (PHB), 241
Polyimide resins, 145
Polylactic acid (PLA), 240–241, 240*f*
Poly-L-lactic acid (PLLA), 285
Polymer-derived precursor method, 200–201, 201*f*
Polymeric composites materials, 317
Polymer matrix composites (PMCs), 59, 141–148
  carbon fiber, 141–148
Polyvinyl alcohol (PVA), 263
p-phenylenediamine (PDA), 154
Prepreg process, 70, 71*f*
Printed circuit boards (PCBs), 181
Pultrusion method, 68, 69*f*, 147–148

R

Rayon, 139
Reaction injection molding (RIM), 69–70
Reinforced composites, 173–175
Reinforced reaction injection molding (RRIM), 69–70
Resin transfer molding (RTM), 61–63, 65–66, 147

S

Scanning electron microscopic (SEM), 281
S-combining rule, 17, 18*f*
Semi empirical models
  nonspherical particulate systems, 19–21
  spherical particulate systems, 15–19
Shear lag model, 12–15, 13*f*
Sheet molding compounds (SMC), 63, 99, 148
Short fiber-reinforced composites
  law of mixtures, 12
  semi empirical models, 15–21
  Shear lag model, 12–15, 13*f*
Si-Al-C-O fiber system, 193
SiC-carbon fibers, 192

SiCN fiber, 195
SiC/TiC ceramic fibers, 193
Silane treatments, 88–89
Silicon carbide (SiC) fibers, 192–194
Simulated annealing (SA), 304
Single-crystal fiber growth technique, 202, 203*f*
Single-objective optimization, 302
Single-walled (SW) carbon nanotubes, 261
Sisal fibers, 217, 220*f*, 221*t*, 230*t*
Si-Ti-C-O fiber system, 193
Si-Zr-C-O fiber system, 193
Slurry spinning technique, 263–264
Spherical particulate systems
  Boyd (CHU) model, 17–18
  Chantler model, 17–18
  Gold model, 18–19
  Guth model, 18–19
  Halpin-Tsai model, 15–16
  Hu model, 17–18
  Lewis-Nielsen model, 16–17, 18*f*
  S-combining rule, 17, 18*f*
Spinning method, 128
Spray-up technique, 64, 65*f*
Starch-gpoly(methyl acrylate) (S-g-PMA), 244
Stiffness matrix, 10
Stochastic optimization methods, 303
Strength failure theories
  orthotropic lamina, 37–38
  orthotropic materials, 33–36
  properties and stress-strain relations, 33
Stress-strain relations, 34–36
  lamina, arbitrary orientation, 34–36
Structural reaction injection molding (SRIM), 69–70

T

Technora, 153–154, 156*t*
Terephthaloyl dichloride (TDC), 153–154
Thermoplastics, 117–119
Thermoplastic starch (TPS), 242–243
Topology optimization, 306–311

U

Ultrahigh-molecular-weight polyethylenes (UHMWPE), 163
UV treatment, 85–86

V

Vacuum assisted resin transfer molding (VARTM), 61–63, 65–66, 147, 287–288
Vacuum infusion technique, 64, 65*f*
Vapor-grown carbon nanofibers (VGCNFs), 261
VARTM. *See* Vacuum assisted resin transfer molding (VARTM)
Vinylester, 145

W

Woven fabric composites, 22–25
  constitutive equations, 22–25
Woven fabrics, 143

This page intentionally left blank

WOODHEAD PUBLISHING SERIES IN COMPOSITES SCIENCE AND ENGINEERING

As material technologies develop, composite materials are becoming more and more important in a range of applications such as transportation, construction, electronic, and sporting goods, the defense industry, and other areas of research. Access to information on fiber technology for composites has previously been limited but this book provides a comprehensive review on fiber-reinforced composites and their manufacturing techniques.

After the introduction to fiber technology, subsequent chapters will discuss the mechanics of fiber composites as well as the different types of surface modification. Several types of fibers are then discussed in detail, including glass, carbon, aramid, basalt, ceramic, and natural fibers. The closing chapters analyze the use of biotechnology for green composites, nanofibers for fiber-reinforced composites, and design and optimization of fiber composites. The final chapter is an overview on the future outlook of fiber technology for fiber-reinforced composites.

Fiber Technology for Fiber-Reinforced Composites focuses on a broad range of different fiber types used in composite manufacturing and includes contributions from leading experts working in both industry and academia.

M. Özgür Seydibeyoğlu is an Associate Professor in Materials Science and Engineering Department at the Izmir Katip Çelebi University, Turkey and has more than 50 international publications on composites and fibers including peer review journals, chapters, and conference publications.

Amar K. Mohanty is a world renowned Professor and Premier's Research Chair in Biomaterials and Transportation in the area of biocomposites, bio-based materials, and composite materials working in the Department of Plant Agriculture and School of Engineering at the University of Guelph, Canada. He has more than 700 publications so far in his career in the form of peer-reviewed papers, patents, books, book chapters, conference presentations, etc. Among several awards, he has received the "Lifetime Achievement Award," the highest recognition from BioEnvironmental Polymer Society (BEPS) in 2015.

Manjusri Misra is a world leading professor in the area of composite materials, biocomposites, nano-enhanced composites, electrospinning, and 3D printing and is currently working in the School of Engineering and cross appointed in the Department of Plant Agriculture at the University of Guelph, Canada. To date, she has contributed to her field of study through more than 600 publications in several different platforms including peer-reviewed journal papers, patents, books, book chapters, conference papers, etc. In 2012, Manjusri Misra received the prestigious "Jim Hammer Memorial Award" from the BEPS.

ISBN 978-0-08-101871-2

9 780081 018712

ELSEVIER

WP
WOODHEAD PUBLISHING
An imprint of Elsevier
elsevier.com/books-and-journals